

University of New England, Armidale, Australia

Understanding factors affecting the synthesis of protoporphyrin IX in the shell gland of laying hens

A dissertation submitted by

SAMIULLAH, DVM, MRURSC

For the award of **Doctor of Philosophy**

June 2017

Certification of Dissertation

I certify that the content of this dissertation has not been submitted for any degree and is not currently being submitted for any other degree or qualification. I also certify that, to the best of my knowledge, any assistance received in preparing this dissertation, and all sources used, have been properly acknowledged. I further certify that, to the best of my knowledge, this work contains no material previously published or written by another person, except where proper reference has been made in the text.



SAMIULLAH Date 09/06/2017

Preface

This dissertation has been written and structured in journal article format. I have tried to minimise duplication and repetition of content. Nevertheless, there is unavoidable repetition particularly in materials and methods and references sections of individual experimental chapters.

Table of Contents

List of Contents……...v

List of Tables…….xiii

List of Figures…….....xvii

Acknowledgements……...xxi

Abbreviations……xxii

List of Publications……..xxiv

Abstract……xxvi

General Introduction…….xxviii

Appendices……311

List of Contents

Chapter 1 Review of literature 1

1.1 Abstract 1

1.2 Introduction 1

1.3 Methods of calculating eggshell colour 3

1.4 Protoporphyrin IX in the brown eggshell and shell gland 5

1.5 Metabolic pathway of protoporphyrin IX 6

1.5.1 Evidence for synthesis of protoporphyrin IX from RBCs 6

1.5.2 Evidence for synthesis of protoporphyrin IX in the shell gland 7

1.6 Housing system, nutrition and eggshell colour 10

1.7 Genetics of the eggshell colour 11

1.8 Hen strain, age and eggshell colour 12

1.9 Infectious bronchitis virus and eggshell colour 13

1.10 Stress and eggshell colour 14

1.11 Nicarbazin and eggshell colour 15

1.12 Shell colour and egg quality 15

1.13 Conclusions and future research 16

1.14 References 16

Chapter 2 Effect of production system and flock age on eggshell and egg internal quality measurements 29

2.1 Abstract 29

2.2 Introduction 30

2.3 Materials and Methods 32

2.3.1 Eggshell and egg internal quality measurements 33

2.3.2 Microscopic observations of the shell mammillary layer ultrastructure 34

2.3.3 Cuticle cover estimation 35

2.3.4 Protoporphyrin IX quantification from eggshell with and without cuticle 35

2.3.5 Standard curve construction and calculation of protoporphyrin IX per gram of shell 38

2.4 Statistical analysis 38

2.5 Results 39
2.5.1 Eggshell and egg internal quality measurements 39
2.5.2 Microscopic observations of the shell mammillary layer ultrastructure 42
2.5.3 Cuticle cover estimation 46
2.5.4 Shell reflectivity and L*a*b* measurements 48
2.5.5 Protoporphyrin IX quantification from shell with and without cuticle 50
2.6 Discussion 53
2.6.1 Eggshell and egg internal quality measurements 53
2.6.2 Microscopic observations of the shell mammillary layer ultrastructure 54
2.6.3 Cuticle cover estimation 59
2.6.4 Shell reflectivity and L*a*b* measurements 59
2.6.5 Protoporphyrin IX quantification from shell with and without cuticle 60
2.7 Conclusions 60
2.8 References 61
Chapter 3 Oviposition time, flock age and egg position in clutch in relation to brown eggshell colour in laying hens 69
3.1 Abstract 69
3.2 Introduction 70
3.3 Materials and Methods 71
3.3.1 Effect of oviposition time and flock age on brown eggshell colour- Experiment 1 71
3.3.2 Effect of egg position in-clutch on brown eggshell colour- Experiment 2 71
3.4 Processing of samples 72
3.4.1 Egg weight, shell reflectivity and shell colour measurements 72
3.4.2 Protoporphyrin IX quantification from shell 72
3.5 Statistical analysis 73
3.6 Results 73
3.6.1 Effect of oviposition time and flock age on brown eggshell colour- Experiment 1 73
3.6.2 Effect of egg position in-clutch on brown eggshell colour- Experiment 2 78
3.7 Discussion 79

3.7.1 Effect of oviposition time and flock age on brown eggshell colour- Experiment 1 79
3.7.2 Effect of egg position in-clutch on brown eggshell colour- Experiment 2 81
3.8 Conclusions 81
3.8.1 References 82
Chapter 4 The Australian strains of infectious bronchitis virus affect brown eggshell colour in commercial laying hens differently 87
4.1 Abstract 87
4.2 Introduction 88
4.3 Materials and Methods 89
4.3.1 Experiment 1 89
4.3.2 Experiment 2 91
4.3.3 Measurement of shell reflectivity and shell colour 91
4.3.4 PP IX quantification from eggshells 92
4.3.5 Standard curve construction 92
4.4 Statistical analysis 92
4.5 Results 93
4.5.1 Experiment 1 93
4.5.2 Experiment 2 96
4.6 Discussion 98
4.7 References 104
Chapter 5 Reference gene selection for the shell gland of laying hens in response to time-points of eggshell formation and nicarbazin ... 109
5.1 Abstract 109
5.2 Introduction 110
5.3 Materials and Methods 114
5.3.1 Selection of reference genes and primer design 114
5.3.2 Laying hens and tissue sampling 117
5.3.2.1 Effect of time-points on stability of reference gene expression (Experiment 1) 117
5.3.2.2 Effect of time-points and nicarbazin on stability of reference gene expression (Experiment 2) 118

5.3.3 Total RNA extraction and purification 119
5.3.4 Quantitative PCR 120
5.4 Statistical analysis 120
5.5 Results 122
5.5.1 Primers specificity and efficiency 122
5.5.2 Effect of time-points on stability of reference gene expression (Experiment 1) 124
5.5.3 Effect of time-points and nicarbazin treatment on stability of reference gene expression (Experiment 2) 127
5.5.4 Expression of candidate target genes using most stable and least stable reference genes 131
5.6 Discussion 134
5.7 Conclusions 137
5.8 Acknowledgements 137
5.9 Competing interests 137
5.10 Financial competing interests 138
5.11 Authors' contributions 138
5.12 References 138
Chapter 6 Downregulation of *ALAS1* by nicarbazin treatment underlies the reduced synthesis of protoporphyrin IX in shell gland of laying hens 147
6.1 Abstract 147
6.2 Introduction 147
6.3 Results 152
6.3.1 Mitochondrial count per cell and PP IX synthesis genes 152
6.3.2 Measurement of PP IX in shell gland tissue 156
6.3.3 Measurement of PP IX in eggshell 156
6.4 Discussion 157
6.5 Methods 161
6.5.1 Ethics statement and rearing of laying hens 161

6.5.2 Experiment 1: Effect of time-points on mitochondrial count and expression of protoporphyrin IX synthesis genes 162
6.5.3 Experiment 2: Effect of time-points and nicarbazin treatment on mitochondrial count and expression of protoporphyrin IX synthesis genes 163
6.5.4 Shell gland tissue collection 164
6.5.5 Total RNA and DNA extraction 165
6.5.6 Primer design for oligonucleotides 166
6.5.7 Mitochondrial DNA quantification 167
6.5.7.1 DNA cloning 167
6.5.7.2 Standard curve construction 168
6.5.7.3 Mitochondrial DNA copy number quantification by qPCR 169
6.5.7.4 Calculation of mitochondria per cell 169
6.5.8 Gene expression analysis by qPCR 170
6.5.9 Measurement of protoporphyrin IX in tissue and eggshell 170
6.6 Statistical analysis 171
6.7 Acknowledgements 173
6.8 Authors' contributions 173
6.9 Competing interests 173
6.10 Competing financial interests 173
6.11 References 173
Chapter 7 Reference gene selection for gene expression study in shell gland and spleen of laying hens challenged with infectious bronchitis virus 185
7.1 Abstract 185
7.2 Introduction 186
7.3 Results 189
7.3.1 Efficiency and specificity of primers 189
7.3.2 Reference gene expression stability in shell gland and spleen 192
7.3.3 Reference gene validation in shell gland and spleen 195
7.4 Discussion 197
7.5 Methods 199

7.5.1 Ethics statement 199
7.5.2 Rearing of IBV free laying hens and virus challenge 200
7.5.3 Selection of primers sequence and validation 201
7.5.4 Tissue collection for RNA extraction 203
7.5.5 Total RNA extraction and purification 203
7.5.6 Quantitative PCR 204
7.6 Statistical analysis 204
7.7 Acknowledgements 205
7.8 Authors' contributions 205
7.9 Competing interests 205
7.10 Competing financial interests 205
7.11 References 206
Chapter 8 RNA-Sequencing analysis of shell gland of laying hens in relation to time-points of eggshell formation and infectious bronchitis virus challenge 217
8.1 Abstract 217
8.2 Background 218
8.3 Materials and Methods 220
8.3.1 Ethics statement 220
8.3.2 Rearing of IBV free laying hens and virus challenge 220
8.3.3 Tissue collection 221
8.3.4 Total RNA extraction and purification 222
8.3.5 RNA-Sequencing of selected shell gland samples 222
8.3.5.1 cDNA libraries preparation 222
8.3.5.2 Sequence quality control and sequence data evaluation 223
8.3.5.3 Reads mapping and raw gene counts 224
8.3.5.4 Reference guided transcript assembly 224
8.3.6 Differential gene expression data analysis 224
8.3.7 Hierarchical clustering analysis 224
8.3.8 Functional annotation of DEGs 225
8.3.9 Primers sequence for candidate genes and validation 225

8.3.10 Validation of RNA-Seq results by qPCR 228
8.3.11 Viral quantification from shell gland of challenged hens 228
8.4 Statistical analysis 229
8.5 Results 229
8.5.1 IBV detection in shell gland of challenged laying hens 229
8.5.2 Global gene response to virus challenge and differential gene expression at different stages of eggshell formation 230
8.5.3 DEGs analysis for hypothetical functions 235
8.5.4 Functional annotation of DEGs 237
8.5.5 Hierarchical clustering analysis 239
8.5.6 Validation of RNA-Seq data by qPCR 240
8.6 Discussion 242
8.7 Conclusions 247
8.8 References 247
Chapter 9 Mitochondrial count in oviduct of laying hens challenged with infectious bronchitis virus 259
9.1 Abstract 259
9.2 Introduction 260
9.3 Materials and Methods 263
9.3.1 Rearing of IBV free laying hens and IBV challenge 263
9.3.2 Oviduct tissue collection 264
9.3.3 Total DNA extraction 265
9.3.4 Total RNA extraction and purification 265
9.3.5 Primer design for oligonucleotides 266
9.3.6 Mitochondrial DNA quantification 268
9.3.6.1 DNA cloning 268
9.3.6.2 Mitochondrial DNA copy number quantification by qPCR 269
9.3.6.3 Calculation of mitochondria per cell 269
9.3.7 Gene expression analysis by qPCR 270
9.4 Statistical analysis 270
9.5 Results 270

9.5.1 Mitochondrial count per cell 271
9.5.2 Effect of IBV and time-point on gene expression in the shell gland tissue 273
9.6 Discussion 274
9.7 References 277
Chapter 10 Histological and immunohistological observations of shell gland of laying hens in relation to time-points of eggshell formation and nicarbazin treatment 289
10.1 Abstract 289
10.2 Introduction 289
10.3 Materials and Methods 292
10.3.1 Preparation of frozen sections for immunofluorescence 292
10.3.2 Western Blotting 293
10.3.2.1 Total protein extraction from shell gland tissue 293
10.3.2.2 Total protein determination 294
10.3.2.3 SDS PAGE 294
10.3.2.4 Western Blotting (electro-transfer of the protein onto a membrane). 295
10.3.2.5 Immuno-detection of protein 295
10.3.3 Paraffin embedded tissue preparation for histology 296
10.4 Statistical analysis 297
10.5 Results 297
10.5.1 Immunofluorescence microscopy of the shell gland tissue 297
10.5.2 Western blotting 298
10.5.3 Histology of the shell gland tissue 300
10.6 Discussion 302
10.7 Conclusions 302
10.8 References 302
Chapter 11 General conclusions 307

List of Tables

Table 2.1 Effect of production system and flock age on eggshell and egg internal quality variables 40

Table 2.2 Eggshell and egg internal quality variables for cage and barn production systems at 68 weeks of age 42

Table 2.3 Effect of production system and flock age on ultrastructural variables of shell mammillary layer.....44

Table 2.4 Shell reflectivity (%) and L*a*b* values as affected by production system and flock age 49

Table 2.5 Shell reflectivity (%) and L* values as affected by production systems at 68 week of flock age 50

Table 2.6 The amount of protoporphyrin IX in 1 g of shell with, without and in cuticle as affected by production system and flock age.....52

Table 3.1 Hen oviposition time in relation to egg and eggshell quality variables.75

Table 3.2 Effect of flock age on egg and eggshell quality variables 77

Table 3.3 Multiple regression analysis of effect of category of oviposition time and flock age on egg and eggshell quality variables.....78

Table 3.4 Linear regression analysis of egg position in-clutch on egg and eggshell quality variables 79

Table 3.5 Regression analysis of shell quality variables against category of clutch length (day) 79

Table 4.1 Effect of infectious bronchitis virus challenge strains on eggshell colour variables (Experiment 1) 94

Table 4.2 Effect of day post inoculation with different infectious bronchitis virus strains on eggshell colour variables (Experiment 1) 95

Table 4.3 Effect of day p.i. on shell colour variables following challenge with different infectious bronchitis virus strains (Experiment 2).....97

Table 4.4 Effect of vaccination status on eggshell colour of hens challenged with infectious bronchitis virus strains (Experiment 2) 98

Table 5.1 Functional annotation of the reference genes used in the current study 115

Table 5.2 Forward (F) and reverse (R) primers sequence of the selected candidate reference and target genes 116

Table 5.3 Eggshell colour (L*) and egg weight of the hens selected for reference gene study optimisation at different time-points.....118

Table 5.4 Eggshell colour (L*) and egg weight of the hens selected for reference gene optimisation with nicarbazin treatment at different time-points 119

Table 5.5 Stability values of reference genes affected by four different time-points performed in Experiment 1 125

Table 5.6 Overall stability values of reference genes affected by time-points and nicarbazin treatment 128

Table 5.7 Stability values of reference genes affected by time-points 129

Table 5.8 Stability values of reference genes affected by nicarbazin treatment (nicarbazin group only) 130

Table 6.1 Relative expression levels of candidate target genes involved in the synthesis of protoporphyrin IX and/or heme at different time-points of eggshell formation in the shell gland of laying hens.....154

Table 6.2 Relative expression levels of candidate target genes involved in the synthesis of protoporphyrin IX and/or heme at different time-points of eggshell formation in the shell gland of laying hens treated with nicarbazin 155

Table 6.3 Mean values (±S.E.) of egg quality variables measured before dividing hens into different groups.....163

Table 6.4 Mean values (±S.E.) of egg quality variables measured before dividing hens into different groups (time-points and nicarbazin treatment) ...164

Table 6.5 Forward (F) and reverse (R) sequence of the primers used in the study 172

Table 7.1 Overall stability values of reference genes in the combined data set of shell gland and spleen affected by IBV T and Vic S strain challenge.....194

Table 7.2 Grouping of laying hens for tissues collection for reference genes study 201

Table 7.3 Candidate reference and target genes in expression studies by qPCR in the shell gland and spleen of laying hens challenged with infectious bronchitis virus T and Vic S strains 202

Table 8.1 Candidate target and reference* genes in expression studies by qPCR in the shell gland of laying hens challenged with infectious bronchitis virus T strain.....227

Table 8.2 Summary statistics of sequence quality and alignment information of 12 shell gland samples in four groups (G1-G4) 231

Table 8.3 Top 30 DEGs in G2 (5 hr time-point) vs G4 (15 hr time-point).....233

Table 8.4 Top 30 DEGs in G4 (15 hr time-point) vs G2 (5 hr time-point).....234

Table 8.5 Putative functions of mRNA sequences that did not annotate to any known gene functions during alignment 236

Table 8.6 Comparison of the gene expression changes between G2 (5 hr time-point) vs G4 (15 hr time-point).....242

Table 9.1 Allocation of birds into various groups for IBV challenge study in the oviduct of laying hens 264

Table 9.2 Forward (F) and reverse (R) sequence of the primers used in the study 267

Table 9.3 Relative expression stabilities of genes in the shell gland of laying hens challenged with IBV.....273

Table 10.1 Morphometric measurements (µm) of various layers of shell gland tissue 301

List of Figures

Figure 1.1 The protoporphyrin IX biosynthesis pathway presumed to be in the shell gland of brown-egg laying hen.....9
Figure 2.1 Longitudinal half of the eggshell soaked in EDTA.....37
Figure 2.2 Eggshell with and without cuticle layer.....37
Figure 2.3 Interaction between flock age and production system (P < 0.0001).....41
Figure 2.4 Interaction of flock age and production system (P < 0.0001) 41
Figure 2.5 Interaction between production system and flock age (P=0.0056).....45
Figure 2.6 Interaction between production system and flock age (P=0.0002).....45
Figure 2.7 Interaction between production system and flock age (P<0.0001).....46
Figure 2.8 Effect of production system on cuticle cover (P=0.0057) 47
Figure 2.9 Effect of flock age (week) on cuticle cover (P=0.0003).....47
Figure 2.10 Good caps cover with confluence.....57
Figure 2.11 Variable cap size with poor caps 57
Figure 2.12 Extensive B bodies with some changed membrane.....58
Figure 2.13 Extensive aragonite in the shell mammillary layer.....58
Figure 3.1 Number of eggs laid in 5 categories of oviposition time (all hen ages combined).....74
Figure 4.1 Effect of IBV on eggshell reflectivity with and without cuticle (P < 0.05) 101
Figure 4.2 Effect of IBV on L* of eggshells with and without cuticle (P < 0.0001).....101
Figure 4.3 Mean values of PP IX in eggshells with and without cuticle from eggs collected from hens that had been inoculated with IBV (P < 0.05) ..103
Figure 4.4 Mean values of PP IX in the cuticle of eggs collected from hens that had been inoculated with IBV (P = 0.0005) 103
Figure 5.1 Amplification of the gene fragments from the eggshell gland tissue of laying hens to assess the specificities of the primers used in the current study 122

Figure 5.2 Melting curves of the amplicons from 10 candidate reference genes showing that the amplifications were specific and no primer dimers were present.....124

Figure 5.3 Effect of time-points and combination of time-points and nicarbazin treatment on the expression stability of reference genes in the shell gland of laying hens 126

Figure 5.4 Comparison of the relative expression stability of 10 candidate reference genes analysed by geNorm, NormFinder and BestKeeper 131

Figure 5.5 Validation of the expression level of four candidate target genes affected by three different time-points of eggshell formation 133

Figure 6.1 Schematic representation of protoporphyrin IX biosynthetic pathway in the shell gland of brown-egg laying hens.....150

Figure 6.2 Mitochondria per cell and PP IX per gram of shell gland tissue affected by time-points of eggshell formation and nicarbazin treatment.....153

Figure 6.3 Eggshell quality variables measured in control and nicarbazin treated laying hens affected by day effect.....157

Figure 6.4 Amplification of the genes fragments from the shell gland tissue of a chicken to assess the specificities of the primers used in the current study 167

Figure 6.5 Schematic diagram of single-insert plasmid pCR^{TM} 4-TOPO (3956 nucleotides) 168

Figure 7.1 Amplification of the genes fragments from the shell gland tissue of chicken to assess the specificities of the primers used in the current study 190

Figure 7.2 Melting curves of 10 reference genes in the shell gland samples.....191

Figure 7.3 Effect of IBV challenge on the expression stability of 10 reference genes in the shell gland and spleen 193

Figure 7.4 Relative expression levels of the candidate target genes affected by IBV T challenge in the shell gland and spleen of laying hens 196

Figure 8.1 Schematic diagram explaining the selection of samples for RNA-Sequencing and DEGs data analysis 223

Figure 8.2 Antibody titre of the control and challenged hens on days 9-10 post-infection.....230

Figure 8.3 Ven diagram of differentially expressed genes between different groups.....232

Figure 8.4 Functional map of differentially expressed genes (adjusted P value <0.05; fold change >1.5) enriched for GO biological process, cellular component and molecular functions terms.....238

Figure 8.5 GO terms that were common between 5 and 15 hrs time-points.....239

Figure 8.6 Hierarchical clustering analysis of the top 50 DEGs.....240

Figure 8.7 DNA gel electrophoresis of the qPCR products showing that the primers were specific in amplification.....241

Figure 9.1 Amplification of the genes fragments to assess the specificities of the primers.....271

Figure 9.2 Mean mitochondrial count per cell in different segments of oviduct of laying hens challenged with IBV T and Vic S strains.....272

Figure 9.3 Relative expression levels of nuclear DNA encoded genes involved in mitochondrial biogenesis and fission.....274

Figure 10.1 Histological structure of the cross section of shell gland tissue fixed in 4% paraformaldehyde.....290

Figure 10.2 Gel pad preparation for transferring proteins bands from running gel (SDS-PAGE) to PVDF membrane.....295

Figure 10.3 Immunofluorescence of nuclei in the sections of shell gland tissue of laying hens counter stained with DAPI for nuclear staining.....298

Figure 10.4 Total proteins separated on 12% SDS PAGE from shell gland tissue of laying hen.....299

Figure 10.5 Protein immunoblotted from 12% SDS PAGE gel on PVDF membrane.....299

Figure 10.6 Protein bands on PVDF membrane.....300

Acknowledgements

My thanks equally go to my principal supervisor, Associate Professor **Juliet ROBERTS** and the main co-supervisor Associate Professor **Shu-Biao WU** for their continuous help and healthy criticism during the whole period of the study. I highly appreciate the efforts of both of them for sparing an extra time for me from their multifarious activities. Next, I am deeply indebted to the help of my co-supervisor Associate Professor **Kapil CHOUSALKAR** in various experimental design and from time to time guidance. I am acknowledging the help of my co-supervisor **Dr Andrew TALK** for helping me in performing cryo-sections preparation for immunohistochemistry and immunofluorescence work.

I also highly acknowledge the help of Ms **Annette McLEOD** in tissue samples processing for traditional histology. Special thanks go to Associate Professor **Pierre MOEN** who helped and taught me the use of confocal microscope. For teaching me Western Blotting related work, I am highly grateful and thanking Dr **Geerth GEESINK** and Ms **Xuemei HAN**. In last, I highly acknowledge the University of New England for granting me **Australian Postgraduate Award (APA)** scholarship.

Abbreviations

A3	A3 strain of infectious bronchitis virus
AECL	Australian Egg Corporation Limited
ALAD	delta-aminolevulinic acid dehydratase
ALAS1	delta-aminolevulinic acid synthase 1
ANOVA	analysis of variance
bp	base pair
BSN	shell breaking strength in Newtons
cm	centimetre
DAB	3,3'-diaminobenzidine
DAPI	4',6-diamidino-2-phenylindole
DEGs	differentially expressed genes
DEPC	diethyl pyrocarbonate
EDTA	ethylenediaminetetraacetic acid
EID_{50}	embryo infective dose 50
ELISA	enzyme linked immunosorbent assay
FECH	ferrochelatase
g	gram
$\times g$	times gravity
gDNA	genomic DNA
HCl	hydrochloric acid
H&E	hematoxylin & eosin
hr	hour
HRP	horseradish peroxidase
IB	infectious bronchitis
IBV	infectious bronchitis virus
IgG	immunoglobulin G
M	molar

mm	millimeter
mM	millimolar
mtDNA	mitochondrial DNA
µL	micro litre
µm	micrometer
nm	nanometer
N1/88	N1/88 strain of infectious bronchitis virus
nMole	nanomole
RNA-Seq	RNA-sequencing
PBS	phosphate buffered saline
PP IX	protoporphyrin IX
qPCR	quantitative polymerase chain reaction
PVDF	polyvinylidene difluoride
RT-PCR	reverse transcriptase- polymerase chain reaction
RO	reverse osmosis
SD	standard deviation
SDS PAGE	sodium dodecyl sulfate polyacrylamide gel electrophoresis
Sec	second
SE	standard error
SEM	scanning electron microscope
T strain	T strain of infectious bronchitis virus
wk	week
Vic S	Vic S strain of infectious bronchitis virus
V	volt

List of publications (Journal Articles)

Manuscripts published and/or submitted for publication

Samiullah, S., Roberts, J. and Wu, S-B. (2017). Reference gene selection for gene expression study in shell gland and spleen of laying hens challenged with infectious bronchitis virus. **Scientific Reports** (under revision).

Samiullah, S., Roberts, J. and Wu, S-B. Mitochondrial count in oviduct of laying hens challenged with infectious bronchitis virus. **Biology of Reproduction** (in preparation).

Samiullah, S., Roberts, J. and Wu, S-B. RNA-Sequencing of shell gland of laying hens in relation to time-points of eggshell formation and infectious bronchitis virus challenge. **BMC Genomics** (in preparation).

Samiullah, S., Roberts, J. and Wu, S-B. (2017). Downregulation of *ALAS1* by nicarbazin treatment underlies the reduced synthesis of protoporphyrin IX in shell gland of laying hens. **Scientific Reports** 7; 6253.

Samiullah, S., Roberts, J. and Wu, S-B. (2017). Optimisation of reference gene selection in the shell gland of laying hens in response to time-points of eggshell formation and nicarbazin. **PLOS ONE** 12(7):e0180432 .

Samiullah, S., Roberts, J. and Chousalkar, K. (2016). Oviposition time, flock age and egg position in clutch in relation to brown eggshell colour in laying hens. **Poultry Science** 95:2052-2057.

Samiullah, S., Roberts, J. and Chousalkar, K. (2016). Infectious bronchitis virus and brown shell colour: The Australian strains of infectious bronchitis virus affect brown eggshell colour in commercial laying hens differently. **Avian Pathology** 45:552-558.

Samiullah, S., Omar, A.S., Roberts, J. and Chousalkar, K. (2017). Effect of production systems and flocks age on eggshell and egg internal quality measurements. **Poultry Science** 96:246-258.

Samiullah, S., Roberts, J.R. and Chousalkar, K. (2015). The eggshell colour in brown laying hen-a review. **Poultry Science** 94:2566-2575.

Peer reviewed symposium papers

Samiullah, S., Wu, S-B. and Roberts, J.R. (2017). Quantification of mitochondrial count and protoporphyrin ix associated gene expression in relation to different stages of eggshell formation and nicarbazin challenge in the shell gland of laying hen. **Proceedings of the Australian Poultry Science Symposium** 2017. 28: 78-83, February 13-15.

Samiullah, S., Omar, A.S., Roberts, J.R. and Chousalkar, K. (2016). Effect of production system and flock age on egg quality. **Proceedings of the Australian Poultry Science Symposium** 2016. 27: 133-136, February 14-17.

Samiullah, S., Roberts, J.R. and Chousalkar, K. (2015). Quantification of protoporphyrin IX from eggshell of brown egg laying hens challenged with vaccine and wild strains of infectious bronchitis virus. **Proceedings of the Australian Poultry Science Symposium** 2015. 26:44-47, February 9-11.

Samiullah, S., Roberts, J.R. and Chousalkar, K. (2014). Protoporphyrin quantification from eggshells of laying hens challenged with infectious bronchitis virus strains (N1/88 and T Strains). **Proceedings of the Australian Poultry Science Symposium** 2014. 25: 144-147, February 16-19.

Roberts, J.R., Scott, P., Samiullah, S., Fernando, N. and Anwar, A.M. (2014). Maintenance of shell colour in free range laying hens. **Proceedings of the Australian Poultry Science Symposium** 2014. 25: 122-125, February 16-19.

Abstract

Nine experiments were performed to investigate how the synthesis and/or deposition of protoporphyrin IX (PP IX) into eggshell is influenced in brown-egg laying hens. The findings obtained in the first experiment (Chapter 2) showed that flock age and production system affected overall eggshell and egg quality. Egg weight was significantly higher in cage eggs, while albumen height was significantly higher in barn eggs. The mammillary layer ultrastructural variables showed no clear relationship with production system and flock age. Cuticle cover (ΔE*ab) was significantly higher in barn eggs compared with free range and cage eggs and was significantly higher in eggs from the 44 week old flock than for 64 and 73 week old flocks. In 1 gram of eggshell with and without cuticle, there was more PP IX in cage eggs followed by free range and barn eggs. The findings in experiment 2 (Chapter 3) indicate that eggs laid earlier in the day had deeper brown eggshell colour compared with the eggs laid later in the day. Egg position in a clutch had a clearer effect on eggshell quality in long clutches, as compared with medium and short clutches. The findings of the third experiment (Chapter 4) showed that different infectious bronchitis virus (IBV) strains affected the level of PP IX in eggshell differently. In unvaccinated laying hens, the mean PP IX per gram of shell was significantly higher on day 1 post-infection (p.i.) compared to day 7, after which PP IX increased with day p.i. In unvaccinated and vaccinated laying hens, PP IX decreased with increased day p.i. until day 12. The effect on loss of shell colour was more marked in the T strain infected group followed by N1/88, Vic S and A3 strains. Experiment four (Chapter 5) investigated reference gene stability in the shell gland in relation to time-points (time post-oviposition) of eggshell formation and nicarbazin treatment. The two most stable reference genes selected, *HPRT1* and *HMBS*, were used for the normalisation of gene expression data obtained in experiment five (Chapter 6). The findings in experiment five showed that mitochondria per cell did not vary significantly with different time-points of eggshell formation and nicarbazin treatment. Genes involved in the synthesis of PP IX were regulated differentially in relation to time-points of eggshell formation. Feeding nicarbazin caused down-regulation of the *ALAS1* gene that resulted in lower production of PP IX appearing in the shell gland tissue and eggshell.

Experiment six (Chapter 7) investigated reference gene stability in the shell gland and spleen of infectious bronchitis virus (IBV) infected hens. The two most stable reference genes selected, *TBP* and *YWHAZ*, were used for the normalisation of gene expression data obtained in experiments seven and eight (Chapters 8 and 9). The RNA-sequencing findings in experiment seven showed that there were no differentially expressed genes (DEGs) involved in the mucosal immune system and eggshell formation in the shell gland between IBV challenged and control laying hens. However, there were 1608 and 1806 DEGs at 5 and 15 hrs time-points of eggshell formation, respectively. The Gene Ontology (GO) terms and functional gene analysis showed that the DEGs at 5 hr post-oviposition were mainly involved in ion transport and synthetic activities, while the DEGs at 15 hr were involved in energy metabolism and secretory activities, reflecting the peak stage of eggshell formation. The findings in experiment eight (Chapter 9) showed that IBV T infection significantly lowered mitochondrial count per cell in the shell gland region of the oviduct but not in the magnum or isthmus. The expression levels of nuclear DNA encoded genes involved in mitochondrial biogenesis and fission showed no clear correlation with mitochondrial count and were not significantly different between the control and challenged samples. The expression levels of all the genes except for *PGC-1α* were significantly affected by the time-points of eggshell formation. Experiment nine (Chapter 10) attempted to localize ALAS1, ALAD and FECH enzymes in shell gland tissue collected at different time-points (time post-oviposition) and in response to nicarbazin treatment. The findings showed that these antibodies did not recognise their respective proteins, possibly due to their amino acid sequences being derived from humans. PP IX fluorescence was not detected in Zenker Formol fixed tissue sections, stained or unstained, taken at different time-points and with or without nicarbazin treatment. Future work is suggested using chicken specific antibodies to localise cells involved in PP IX synthesis. Taken together, the findings in the current study broaden the understanding of factors affecting the synthesis and deposition of PP IX into eggshells.

General introduction

Among livestock commodities, poultry play a pivotal role throughout the world. Egg quality in laying hens is an important trait that is affected by multiple factors. Among the various production systems, cage, free range and barn are the most widely used production systems in Australia and around the world. However, due to hen welfare concerns (Appleby & Hughes, 1991; Lay *et al.,* 2011; Tactacan et al., 2009), poultry producers in Australia are now changing towards the free range production system. Different production systems have the potential to affect the overall quality of an egg (Abrahamsson & Tauson, 1998; Holt *et al.*, 2011). Among other contributing factors, flock age has been shown to affect egg quality (Roberts *et al.,* 2013; Samiullah *et al.,* 2014; Silversides, 1994; Silversides & Scott, 2001). Egg quality is measured in terms of eggshell quality and egg internal quality. Eggshell quality contributes to preserving the overall integrity of the egg as well as egg internal quality, and thus deformities in the eggshell will result in deteriorated egg internal quality.

Eggshell formation takes place in the shell gland region of the oviduct where various eggshell layers are deposited sequentially upon the eggshell membrane (Bain, 2017). Both the outer and inner shell membranes are synthesised in the isthmus region of the oviduct (Nys *et al.,* 1999). Brown eggshell pigment known as protoporphyrin IX (PP IX) is synthesised in the shell gland tissue and deposited into the eggshell. The amount of PP IX present in an eggshell has been shown to be positively correlated with eggshell quality, percent hatchability, shell thickness and antimicrobial properties (Godfrey, 1947; Ishikawa *et al.,* 2010; Shafey *et al.,* 2002; Shafey *et al.,* 2005). PP IX also serves as an immediate precursor of heme and its synthesis is believed to occur in the shell gland epithelial tissue; however, this claim has not been established scientifically. The synthesis of PP IX takes place in mitochondria and cytosol with the involvement of various enzymatic steps (Ajioka *et al.,* 2006; Khan & Quigley, 2011). It is also not known how PP IX is inhibited from being converted into heme through the action of ferrochelatase enzyme in the shell gland of laying hens.

The studies reported in this dissertation investigated various factors affecting the synthesis and/or deposition of PP IX into eggshells.

In view of the knowledge currently available in the literature about shell colour and the factors that affect it, the hypotheses tested in this dissertation were:

- The synthesis of PP IX in the shell gland and its ultimate deposition into eggshell is affected by flock age and type of poultry production system.
- The eggs laid earlier in the day are darker brown in colour and the amount of PP IX synthesis in the shell gland and/or deposition into eggshell decreases with egg position in-clutch.
- Infectious bronchitis virus (IBV) adversely affects the synthesis and/or deposition of PP IX and this effect varies with strain of IBV.
- Mitochondrial count per cell varies with the stage of egg/eggshell formation.
- The level of synthesis of PP IX depends on mitochondrial count per cell in the shell gland of laying hens.
- Nicarbazin disrupts the mechanism of PP IX synthesis and thus a lower amount of PP IX is synthesised in the shell gland of laying hens fed with nicarbazin.
- The most pathogenic Australian strain of infectious bronchitis virus adversely affects the molecular mechanisms involved in the mucosal immune system and eggshell formation in the shell gland of laying hens.
- The multiplication of infectious bronchitis virus in the oviduct of the laying hen causes mitochondria to degenerate.

Based on the broader objectives, and to test the above hypotheses, different experiments were designed, the findings of which have been reported in individual experimental chapters. This study furthers understanding of the factors involved in the production of PP IX in the shell gland of brown-egg laying hens. Furthermore, the role of various genes involved in the synthesis of PP IX at different stages of eggshell formation has been elucidated. The study has also shown how feeding nicarbazin to laying hens disrupts the biosynthetic model of PP IX synthesis.

The Literature Review and experiments 1-3, outlined in Chapters 1-4, have already been published and details of the publication are included in each chapter. Experiment 5, outlined in Chapter 6 has been published in Scientific Reports. Experiment 4, outlined in Chapter 5 has been published the journal PLOS ONE and Experiment 6, outlined in Chapter 7, is under revision for Scientific Reports. Experiments 7-8, outlined in Chapters 8-9, are presented in the form of manuscripts

ready for submission to journals. Chapter 10 describes experiments the results of which are not suitable for publication.

References

Abrahamsson, P., & Tauson, R. (1998). Performance and egg quality of laying hens in an aviary system. *The Journal of Applied Poultry Research*, 7(3), 225-232.

Ajioka, R. S., Phillips, J. D., & Kushner, J. P. (2006). Biosynthesis of heme in mammals. *Biochimica et Biophysica Acta (BBA)-Molecular Cell Research*, 1763(7), 723-736.

Appleby, M. C., & Hughes, B. O. (1991). Welfare of laying hens in cages and alternative systems: environmental, physical and behavioural aspects. *World's Poultry Science Journal*, 47(02), 109-128.

Bain, M. (2017). Composition and properties of eggshell. In R. Julie (Ed.), Achieving sustainable production of eggs (Vol. 1, pp. 3-23). UK: Burleight Dodds Science Publishing Limited.

Godfrey, G. F. (1947). The relationship of egg shell colour to hatchability in some brown egg laying breeds. *Poultry Science*, 26(4), 381-388.

Holt, P. S., Davies, R. H., Dewulf, J., Gast, R. K., Huwe, J. K., Jones, D. R., Waltman, D., & Willian, K. R. (2011). The impact of different housing systems on egg safety and quality. *Poultry Science*, 90(1), 251-262.

Ishikawa, S.-i., Suzuki, K., Fukuda, E., Arihara, K., Yamamoto, Y., Mukai, T., & Itoh, M. (2010). Photodynamic antimicrobial activity of avian eggshell pigments. *FEBS letters*, 584(4), 770-774.

Khan, A. A., & Quigley, J. G. (2011). Control of intracellular heme levels: heme transporters and heme oxygenases. *Biochimica et Biophysica Acta (BBA)-Molecular Cell Research*, 1813(5), 668-682.

Lay, D. C., Fulton, R. M., Hester, P. Y., Karcher, D. M., Kjaer, J. B., Mench, J. A., Mullens, B. A., Newberry, R. C., Nicol, C. J., & O'Sullivan, N. P. (2011). Hen welfare in different housing systems. *Poultry Science*, 90(1), 278-294.

Nys, Y., Hincke, M. T., Arias, J. L., Garcia-Ruiz, J. M., & Solomon, S. E. (1999). Avian eggshell mineralization. *Poultry and Avian Biology Reviews*, 10(3), 143-166.

Roberts, J. R., Chousalkar, K., & Samiullah. (2013). Egg quality and age of laying hens: implications for product safety. *Animal Production Science*, 53(12), 1291-1297.

Samiullah, Roberts, J. R., & Chousalkar, K. K. (2014). Effect of production system and flock age on egg quality and total bacterial load in commercial laying hens. *The Journal of Applied Poultry Research*, 23(1), 59-70.

Shafey, T., Al-Mohsen, T. H., Al-Sobayel, A. A., Al-Hassan, M. J., & Ghnnam, M. M. (2002). Effects of eggshell pigmentation and egg size on the spectral properties and characteristics of eggshell of meat and layer breeder eggs. *Asian Australasian Journal of Animal Sciences*, 15(2), 297-302.

Shafey, T. M., Al-Batshan, H. A., Ghannam, M. M., & Al-Ayed, M. S. (2005). Effect of intensity of eggshell pigment and illuminated incubation on hatchability of brown eggs. *British Poultry Science*, 46(2), 190-198.

Silversides, F. G. (1994). The Haugh unit correction for egg weight is not adequate for comparing eggs from chickens of different lines and ages. *The Journal of Applied Poultry Research*, 3(2), 120-126.

Silversides, F. G., & Scott, T. A. (2001). Effect of storage and layer age on quality of eggs from two lines of hens. *Poultry Science*, 80(8), 1240-1245.

Tactacan, G. B., Guenter, W., Lewis, N. J., Rodriguez-Lecompte, J. C., & House, J. D. (2009). Performance and welfare of laying hens in conventional and enriched cages. *Poultry Science*, 88(4), 698-707.

Chapter 1 Review of literature

Published as: Samiullah, S., Roberts, J.R. and Chousalkar, K. (2015). The eggshell color in brown laying hen-a review. Poultry Science; 94(10):2566-2575.

1.1 Abstract

The major pigment in eggshells of brown-egg laying hens is protoporphyrin IX, but traces of biliverdin and its zinc chelates are also present. The pigment appears to be synthesized in the shell gland. The protoporphyrin IX synthetic pathway is well defined, but precisely where and how it is synthesized in the shell gland of the brown-egg laying hen is still ambiguous. The pigment is deposited onto all shell layers including the shell membranes, but most of it is concentrated in the outermost layer of the calcareous shell and in the cuticle. Recently, the genes that are involved in pigment synthesis have been identified, but the genetic control of synthesis and deposition of brown pigment in the commercial laying hen is not fully understood. The brown colouration of the shell is an important shell quality parameter, and has a positive influence on consumer preference. The extent of pigment deposition is influenced by housing system, hen age, hen strain, diet, stressors and certain diseases such as infectious bronchitis. In this paper, the physiological and biochemical characteristics of the brown pigment in commercial brown-egg layers are reviewed in relation to its various functions in the poultry industry.

Key words: brown eggs; laying hens; protoporphyrin IX; eggshell quality; stress factors

1.2 Introduction

The eggshell, which is a primary packaging container and also a microbial barrier, is of great importance to poultry producers. The eggshell layers are deposited in a precise order as the egg descends through the highly differentiated parts of the oviduct (Gautron et al., 1997). The hen eggshell is composed of three main layers, each having its own complex morphology: the cysteine-abundant proteinaceous shell membrane, the mineralized hard complex layer and the outer non-mineralized

cuticle (Kodali et al., 2011). The shell membrane is synthesized over a period of 1-2 hr, when the immature egg travels through the proximal isthmus (Nys et al., 2004). The mineralized multilayered complex layer is formed in the distal isthmus and shell gland over an approximately 19-20 hr period of time. The cuticle is deposited onto the eggshell in the uterus 1.5-2.0 hr before oviposition (Nys and Guyot, 2011). The eggshell is composed mainly of calcite, but a thin layer of hydroxyapatite is also present in the inner cuticle (Dennis et al., 1996).

There is an extensive scientific literature regarding eggshell pigmentation of wild birds, but relatively little in relation to eggshell pigment in commercial brown-egg laying hens. The study of eggshell pigments has a long history, and the major pigment extracted from brown eggshells was initially named oorhodeine (Sorby, 1875). The first published report in English describing brown eggshell pigment as protoporphyrin was that of Punnett (1933), although earlier studies had acknowledged its presence in avian eggshells (Fischer and Kogl, 1923; as cited in Kennedy and Vevers, 1973). Later, it was confirmed that the brown pigment is protoporphyrin IX (Kennedy and Vevers, 1973). Protoporphyrin IX belongs to a group of families of biologically active tetrapyrrole compounds. Structurally, protoporphyrin IX is a tetrapyrrole ring containing a highly conjugated planner, and a rigid macrocycle consisting of four pyrrole rings connected by methane groups (Bhosale et al., 2013). The nomenclature of this tetrapyrrole compound often includes a numerical suffix such as IX, which refers to the position of the side chain (Sparks, 2011). In addition to protoporphyrin IX, biliverdin, coproporphyrin and uroporphryin, were also identified from domestic hen eggshell and shell gland (With, 1974; Baird et al., 1975). However, the dominant eggshell pigment in brown-egg laying hens is protoporphyrin IX, with traces of other porphyrins (Lang and Wells, 1987). The complex nature of eggshell colour in laying hens is still under investigation, and the fact that certain hens lay brown eggs, others lay white and some lay even blue shelled eggs, has long indicated a genetic basis for shell colour, possibly involving sex linked genes (Hall, 1944). More recent studies have confirmed the high heritability of shell colour (Forster et al., 1996; Francesch et al., 1997; Zhang et al., 2005). Brown eggshell colour has been positively correlated with some shell characteristics such as shell strength and hatchability (Sekeroglu and Duman, 2011). Apart from quality functions, in the presence of light, brown

pigment has shown bactericidal activity against certain gram positive bacteria (Ishikawa et al., 2010). In this review paper, some important aspects of the brown pigment in the eggshells of the laying hen are discussed.

1.3 Methods of calculating eggshell colour

A traditional scientific method is to use a reflectivity meter for measuring shell colour intensity. Shell reflectivity, expressed as a percentage, is the amount of light that is reflected from the surface of an egg. It is an indication of shell colour lightness – the higher the value, the lighter the colour of the eggshell and vice versa. Shell reflectivity is less time consuming; however, it is not as accurate as other methods for measuring shell colour. The reason could be that the reflectivity meter takes only one reading by targeting a small circular surface area (1cm) of the eggshell. The most commonly used method for eggshell colour quantification is spectrophotometry. One of the recent versions of spectrophotometer is the Konica Minolta hand-held spectrophotometer (CM-2600d) that works on the L*a*b* colour space system, where L* has a maximum of 100 (white) and a minimum of 0 (black) and is the important component for simply measuring shell chromaticity. For a*, green is towards the negative end of the scale and red towards the positive end. For b*, blue is towards the negative end and yellow towards the positive end of the scale (Roberts et al., 2013). The average value appears on the screen, and is read as SCI L*a*b* and SCE L*a*b*. The SCI (specular component included) and SCE (specular component excluded) are very similar to each other and usually SCI values are used for interpretation. The lower the L* value on the scale the darker is the colour of the shell surface and vice versa. One of the problems with spectrophotometer (CM-2600d) is, how to interpret the results of a* and b* individually when the reading is taken on unstained eggshell surface. For the amount of cuticle estimation, L*a*b* values are usually interpreted as single score. The single score, as described by Leleu et al. (2011), measures the L*, a*, and b* values, before and after staining, and calculates a single value, ΔE^*_{ab}:

$$\Delta E^*_{ab} = \sqrt{[(\Delta L^*)^2 + (\Delta a^*)^2 + (\Delta b^*)^2]}$$

A higher ΔE^*_{ab} denotes a higher staining affinity and hence more cuticle coverage (Leleu et al., 2011; Roberts et al., 2013). A Hunter lab calorimeter (working on the

L*a*b* system) has been used for measuring eggshell colour, but the values are less standardized compared to Minolta colourimeter values (Wei and Bitgood, 1990). A Colour Computer Vision machine is an alternative to the Konica Minolta spectrophotometer (L*a*b*). This machine measures the colour of a larger surface area of eggshell and can also detect dirt (Mertens et al., 2005). The Colour Computer Vision machine operates on the same L*a*b* colour space system (Odabasi et al., 2006). Image analysis is another effective tool used for eggshell colour estimation. In this method, a rectangular area, region of interest (ROI), of the shell is selected and the machine calculates the average values of intensity of the pixels in red, green and blue bands (Sezer and Tekelioglu, 2009). The values are then divided by 255 in order to produce a scale ranging from 0 to 1. This method is good for eggshells having numerous colour spots. A High Performance Liquid Chromatography (HPLC) has been previously used to quantify the pigment from eggshell, uterine fluid and parts of the shell gland (Liu et al., 2010). In HPLC, the sample is usually mixed with diluent (e.g. 50% HCl and acetonitrile), centrifuged and read its absorbance in the machine. A shell (0.4 g) without shell membrane is dissolved in 0.08 g of celite and the pigment is then extracted with HCl, acetone and oxalic acid (1:1:1). The extract is glass filtered and its absorbance is read in spectrophotometer at 409-412 nm (Nys et al., 1991). This method seems to be quiet tedious.

In certain cases, eggshell colour is masked by extraneous calcium deposition and thus the intensity of colour is not measured precisely. In addition, the shell colour measurement does not indicate how much pigment (g) is present in different shell layers. In order to confirm the intensity of shell colour, the brown pigment in the eggshell (with and without cuticle) is quantified. Pigment (protoporphyrin IX) quantification is a more accurate way of determining the intensity and amount of pigment present in the shell. A method developed by Poole (1965) and modified by others (Wang et al., 2007, 2009a; Samiullah and Roberts, 2013) may be used for pigment quantification.

1.4 Protoporphyrin IX in the brown eggshell and shell gland

Microscopic examination of cross sections of the eggshell has shown that protoporphyrin is deposited in layers at different depths between the crystals within the eggshell (Tamura and Fujii, 1967a). Samiullah and Roberts (2013) found more protoporphyrin IX in the calcareous shell than in the cuticle. Other reports that most pigment is contained in the cuticle may reflect the methodology used in those studies (Tamura and Fujii, 1967a; Schwartz et al., 1975; Lang and Wells, 1987; Miksik et al., 2007). Protoporphyrin IX is also present in the shell membrane (Tamura et al., 1965). Using a subjective assessment of the extent of hen eggshell cuticle cover, it has been found that there is great variation in cuticle deposition on eggs of different breeds and of individual hens (Bain et al., 2013). A lack of significant genetic correlation has been recorded between the amount of cuticle and shell colour intensity in brown eggs (Bain et al., 2013).

Protoporphyrin IX is primarily present in the surface epithelial cells of the shell gland (Baird et al., 1975), but in Japanese quail the lower isthmus may contribute to pigment production (Baird et al., 1975). The eggshell pigment appears in quail uterine tissue as granular and diffuse colouring in the cytoplasm of apical cells in the epithelium, and its concentration varies inversely with the amount of the pigment deposited into eggshell (Poole, 1967). The hen eggshell gland is considered to be the primary site of pigment production, and it produces twice as much porphyrin from δ-aminolevulinic acid compared to liver cells *in vitro* (Polin, 1957). Various hormones, like oestrogen, progesterone and certain prostaglandins, have been shown to be involved in the pigment production (Soh and Koga, 1994, 1997, 1999). It has not been confirmed where the pigment is synthesized in the brown-egg laying hen. However, enzymatic activity of δ-aminolevulinic acid synthase was detectable in the uterine glandular tissue of Rhode Island hens, but not that of White Leghorn hens (Stevens et al., 1974). The δ-aminolevulinic acid dehydratase activity was higher in the shell gland followed by isthmus and magnum, and the activity was also higher in Rhode Island hens than White Leghorn hens, even in the absence of an egg (Stevens et al., 1974). Pigment granules of porphyrin were detected in apical ciliated cells of the uterine epithelium of Rhode Island Red hen, but were absent in the uterus of White Leghorn hen (Tamura and Fujii, 1967b).

The timing of pigment secretion by shell gland epithelial cells and its deposition into the eggshell varies among species and from bird to bird within a species (Liu and Cheng, 2010). Pigment deposition and its rate of secretion are different in brown, blue and white eggshell hens (Liu et al., 2010). More research has been conducted using Japanese quail rather than the commercial hen, but the histological structure of the uterus of Japanese quail is very similar to the commercial hen (Poole, 1967). The pigment on the surface of quail eggshells is accumulated in the last 3-3.5 hr prior to oviposition (Poole, 1965; Soh et al., 1993). Similarly, the eggshell pigmentation in Dongxiang blue shelled chickens is thought to be secreted mainly in the 2-3 hr before oviposition (Zhao et al., 2006). It is assumed that, in the hen, pigment is deposited onto brown eggs throughout the shell formation process, but 50-74 percent of it is deposited in the last 5 hr before oviposition (Warren and Conrad, 1942). From the presence of the pigment in all shell layers in brown-egg laying hens, it is assumed that pigment deposition follows a similar pattern to that seen in Japanese quail. It is also assumed that the same factors (hormonal, calcium and phosphorus concentrations in shell gland) that are responsible for cuticle completion and termination (Nys et al., 1991; Soh and Koga, 1999) are also responsible for pigment deposition and its ultimate termination in brown-egg laying hen. More work is needed to measure precisely the timing of pigment deposition in the brown-egg laying hen.

1.5 Metabolic pathway of protoporphyrin IX

Early reports suggest that protoporphyrin IX is derived from blood heme, although more recent findings indicate that pigment is synthesized in the tissues of the hen's shell gland.

1.5.1 Evidence for synthesis of protoporphyrin IX from RBCs

Early researchers suggested that eggshell pigments are derived from normal erythrocyte destruction in the mucous layer of the oviduct, transported by special cells which enter the uterine epithelium in the final stages of calcification of shell, and from there deposited into shells (Giersberg 1921; as cited in Kennedy and Vevers, 1973). The protoporphyrin IX in the shell gland is reported to originate

either from free erythrocytes during circulation (Kennedy and Vevers, 1973), or as a metabolite from the heme released from ageing erythrocytes (Wang et al., 2009a). It was suggested that haemoglobin degrades to bile pigments whereas protoporphyrin IX is synthesized from heme via the δ-aminolevulinic acid pathway (Polin, 1957). Support for the synthesis of protoporphyrin IX from red blood cells was based partly on the histological work of Giersberg (1921; as cited in (Kennedy and Vevers, 1973), who linked pigment derivation with the erythrocyte ageing and destruction process.

1.5.2 Evidence for synthesis of protoporphyrin IX in the shell gland

Most authors are of the opinion that protoporphyrin IX is first synthesized in the shell gland, from where it is secreted and deposited into eggshell layers (Baird et al., 1975; Solomon, 2002). This view is supported by evidence that previously free heme, protoporphyrin and biliverdin in sufficient quantity have been quantified from the shell gland of hen (Gorchein et al., 2012). The extraction of precursor enzymes and protoporphyrin IX from the shell gland (Schwartz et al., 1980) suggests that porphyrin synthesis occurs in the shell gland of the hen. A comparison of protoporphyrin IX in different tissues of light and deep brown-egg laying Rhode Island Red hens indicated that eggshell pigment is synthesized in the shell gland and there was a significantly higher gene expression of δ-aminolevulinic acid synthase recorded in the deep brown-egg laying hens compared with hens laying lighter colour eggs (Li et al., 2013). The shell gland tissue of laying hens has the capability of transforming δ-aminolevulinic acid into porphyrin *in vitro* (Polin, 1957) at greater capacity than do tissues from other segments of the oviduct (Polin, 1959). The histological and radiographic study of the shell gland at various stages of shell formation showed red fluorescence and pigment granules, which increased until cuticle deposition (Tamura and Fujii, 1967b; Baird et al., 1975). A higher activity of several porphyrin biochemical enzymes in the shell gland was recorded in Rhode Island Red hens compared to mutant and White Leghorn hens (Schwartz et al., 1980). There is much evidence that protoporphyrin IX is synthesized in the shell gland (Zhao et al., 2006; Wang et al., 2007), but this type of synthesis does not exclude the possibility that the precursors material are derived from blood

(Wang et al., 2009a). The biosynthetic pathway of protoporphyrin IX pigment is well established as shown in Figure 1.1, but the cells involved and precursor origins still need to be investigated. Protoporphyrin IX appears to be an immediate precursor of heme, following the same metabolic pathway. The first step in protoporphyrin IX synthesis is thought to be transportation of glycine from cytosol to mitochondria. Many transporters are presumed to be involved in this pathway in the chicken shell gland and these include some with known functions such as *SLC25A38* and *ABCB6*. In normal heme biosynthesis, the last step is conversion of PP IX into heme catalysed by ferrochelatase enzyme. In the chicken shell gland, it is not clear how PP IX is not transformed into heme by ferrochelatase. *ABCG2* is thought to export PP IX out of the cell; however, it is not clear whether it is located on the mitochondrial outer membrane or on the cell membrane.

The availability of δ-aminolevulinic acid in the shell gland might determine the amount of porphyrin deposited into the eggshell (Polin, 1957). In attempting to clarify whether or not the enzyme catalyse reaction for heme synthesis is the same in erythroid and non-erythroid cells, Riddle et al. (1989) found that at least two separate genes were expressed in erythroid and non-erythroid cells, and the enzymes regulated by the genes also differ widely in biochemical properties. Brown eggshell pigment primarily contains protoporphyrin IX, but other pigments including uroporphyrin, coproporphyrin, biliverdin and its zinc chelates are also present, which led With (1974) to conclude that protoporphyrin is synthesised in the oviduct. The precursor molecule, protoporphyrinogen, is colourless and the brown colour appears when this compound is auto-oxidized into protoporphyrin (Sparks, 2011).

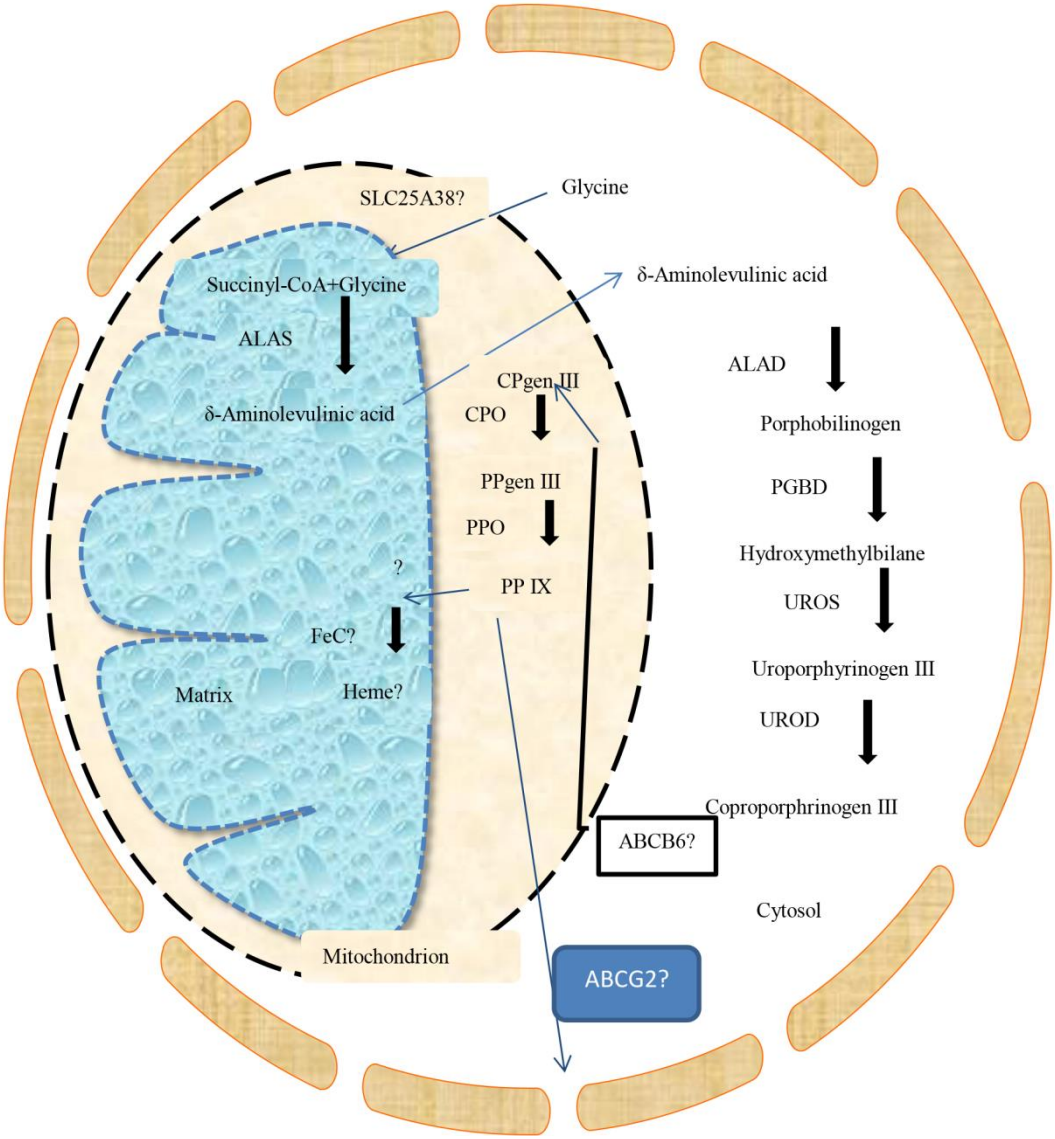

Figure 1.1 The protoporphyrin IX biosynthesis pathway presumed to be in the shell gland of brown-egg laying hen

Figure 1.1 has been partly adapted from Ajioka et al. (2006), Khan and Quigley (2011) and Miller and Kappas (1974). ALAS is delta-aminolevulinic acid synthase; ALAD is aminolevulinic acid dehydratase; PGBD is porphobilinogen deaminase; UROS is uroporphyrinogen III synthase; UROD is uroporphyrinogen decarboxylase; CPgen III is coproporphyrinogen III; CPO is coproporphyrinogen oxidase; PPgen III is protoporphyrinogen III; PPO is protoporphyrinogen oxidase; PP IX is protoporphyrin IX; SLC25A38 is solute carrier family 25, member 38; ABCB6 is ATP-binding cassette, sub-family B, member 6; ABCG2 is ATP-binding cassette, sub-family G, member 2.

1.6 Housing system, nutrition and eggshell colour

With the increase in free range commercial farming in different parts of the world and particularly in Australia, there is interest in investigation of the factors causing pale shell colour and how to improve eggshell colour in hens laying brown shelled eggs. Consumer preference is shifting from quantity to quality with free range eggs gaining popularity due to the perception that it is a natural production system (Wang et al., 2009b). Egg colour is generally maintained well in cage flocks, but there is anecdotal evidence that maintenance of shell colour can be more challenging in free range flocks (Sekeroglu et al., 2010). It has been reported that eggs from free range flocks may be lighter in colour compared to those from cage systems (Samiullah et al., 2014).

Hen nutrition is an area that needs to be tested in relation to eggshell colour. Hooge (2007) reported that certain probiotics improved shell colour in hens laying brown shelled eggs. Feeding *Bacillus subtilis* supplemented feed to 63 week Lohman Brown hens improved the intensity of brown shell colour in the following two weeks of production. The mode of action of *Bacillus subtilis* is not clear and needs further investigation. However, a possible mechanism of action could be due to amino acid residues such as His183 and Glu264 in *Bacillus subtilis* ferrochelatase facilitating the insertion of metal ion into protoporphyrin (Hansson et al., 2007). Some elements like Fe, Cu, Mn and Zn function as chelating carriers at the central position of porphyrin molecules (Solomon, 1987). Feed supplemented with Fe soy proteinate significantly improved eggshell colour in brown laying hens (Seo et al., 2010).

Vanadium is usually found in commercial poultry feed at very low inclusion level (Miles and Henry, 2004). Vanadium in poultry feed has a detrimental effect on shell colour (Sutly et al., 2001), which can be overcome by feeding vitamin C at various levels depending the level of vanadium in the feed (Odabasi et al., 2006). The exact mechanism of vanadium toxicosis is not clear. The suggestion that loss of shell colour in free range laying hens could be due to elevated levels of vitamin D, was tested in a study that found that vitamin D had no significant effect on shell colour (Roberts et al., 2014).

1.7 Genetics of the eggshell colour

The molecular basis of brown pigment synthesis and its possible metabolic pathway in brown-egg laying hens need further exploration in order to determine the genes involved (Wang et al., 2013). The colour of the eggshell is assumed to be controlled by several genes that encode proteins and enzymes, thereby regulating the production and deposition of pigment into the shell (Van Brummelen and Bissbort, 1993; Liu and Cheng, 2010), but the responsible genes in brown-egg laying hens are yet to be identified. The higher δ-aminolevulinic acid synthase activity in brown-egg laying hens compared to white egg laying hens suggests that the trait is purely controlled by genes (Schwartz et al., 1980). Brown eggshell colour is due to a dominant gene that is epistatic to the recessive white shell colour gene (Punnett and Bailey, 1920). However, the phenotypic heritability calculations for dams (s^2=0.9135) for eggshell colour in brown shelled eggs showed some dominance over sire (s^2=0.3035) (Blow et al., 1950). Similarly, measuring the heritability estimates of sire and dams for shell colour in a Light Sussex flock, the dam heritability was higher than the sire, indicating the existence of a dominance effect (Hunton, 1962). Genetically, the quantitative trait loci (QTL) region on chromosomes 2, 4, 5, 6 and 11 influences eggshell colour (Wardecka et al., 2002; Sasaki et al., 2004; Schreiweis et al., 2006). The genes coding for delta-aminolevulinic acid synthase and ferrochelatase are thought to be located in chromosome 1 (Schwartz et al., 1980). Based on the phenotypic observations, when white and brown-egg laying chickens are crossed, a co-dominance effect is created with an intermediate eggshell colour (Hall, 1944; Blow et al., 1950). However, when comparing the sire effects, pullets sired by the White Leghorn male produced eggs with less pigment than the pullets sired by the Rhode Island Red male, suggesting the involvement of sex linked genes (Hall, 1944). Based on the available information, it is still unclear which genes are responsible for brown pigment synthesis in the shell gland.

The heritability of eggshell colour in a brown-egg laying breed was closer to 0.50 (Francesch et al., 1997). The analysis of brown-egg laying strains and its crosses has shown a higher variance value for dam than sire (Blow et al., 1950; Hunton, 1962). A protein haplotype of ovocalyxin-32 has been shown to affect eggshell

colour (Fulton et al., 2012). A gene which can reduce protoporphyrin has some value in breeding for eliminating the tinted eggshell problems occurring sometimes in white egg laying hens (Shoffner et al., 1982). Recent molecular work has established that the expression of *SLCO1A2* and *SLCO1C1* genes in the shell gland of a brown-egg laying hen was associated with brown eggshell colour (Zheng et al., 2014). In the heritability measurements, a low genetic correlation of eggshell colour with quality traits suggests that eggshell colour affects other shell traits at a very low level (Zhang et al., 2005). Summarizing the genetic work conducted, it can be concluded that the genetics of the brown eggshell colour in the laying hen has not been studied sufficiently to understand the process of shell pigment synthesis in the shell gland. Dunn (2011) offers the opinion that traditional methods of selection for shell colour may prove more useful than molecular methods.

1.8 Hen strain, age and eggshell colour

Production of uniform dark brown coloured eggshells through selective breeding is the goal of poultry breeders of brown-egg laying hens. Significant differences in shell colour have been recorded among breeds laying eggs with brown shells (Grover et al., 1980). The amount of brown and blue pigments is higher in the shell gland and eggshell of brown and blue eggs when compared to white shelled eggs, which indicates that pigment is breed specific (Liu et al., 2010). Hens that lay lighter coloured eggs at the start of lay also lay lighter coloured eggs in the late laying period (Odabasi et al., 2007).

Generally, the eggshell gets paler as the hen ages (Odabasi et al., 2007). It is not clear how this happens, but increase in egg size with hen age is considered one of the main factors (Hunton, 1962; Grover et al., 1980; Odabasi et al., 2007). In a longitudinal study of the effect of hen age on brown eggshell colour, there was no significant difference between the eggshell colour at 35 to 75 week, but the 25 week eggshell colour was significantly darker than all other age groups (Samiullah et al., 2014). Following the same flock at different ages (longitudinal study), or different ages of different brown-egg laying flocks (horizontal study), eggshell colour gets lighter as the flocks get older (Samiullah, 2012).The amount of protoporphyrin IX in 1g of whole eggshell in 33, 50 and 67 week old HyLine Brown flocks was not

significantly different (Samiullah and Roberts, 2013). However, the amount of protoporphyrin IX measured in the cuticle itself was significantly higher at 50 week compared with 33 and 67 week eggs, which suggests that shell colour gets lighter with flock age and the amount of cuticle present on eggshell surface has positive influence on pigment present in the shell. It can be concluded that eggshell colour generally gets lighter as the hen ages.

1.9 Infectious bronchitis virus and eggshell colour

Infectious bronchitis virus (IBV) is a coronavirus of economic importance to the poultry industry around the world. IBV can infect chickens of all ages and has the capability to multiply in various epithelial tissues including trachea, lungs, kidney, ovaries and oviduct (Ignjatovic et al., 2002). The incubation period of IBV in fully susceptible hen is about 18-36 hr (Sevoian and Levine, 1957). Many IBV strains affect egg production and cause paleness of eggshell colour in brown-egg laying hens (Chousalkar and Roberts, 2007). Previous studies show that IBV strains differentially affect the epithelial tissues in the shell forming regions of the oviduct in brown-egg laying hens (Chousalkar et al., 2007). The Australian IBV strains are mainly respiratory and nephropathogenic with variation in pathogenicity, but they are also capable of infecting the oviduct (Ignjatovic et al., 2002). There was no significant difference in the histopathology induced by two strains of IBV (T and N1/88) in the oviduct of vaccinated and unvaccinated birds (Chousalkar et al., 2007). Comparing the histopathological severity of the different strains in the oviduct, T strain was more virulent followed by N1/88 and then the vaccine strains, Vic S and A3. All strains caused paler colouration of brown shelled eggs (Chousalkar and Roberts, 2009; Chousalkar et al., 2009). The mechanism of action of IBV strains on pigment synthesis is not clear, but pathology induced in the oviduct by IBV may disrupt the cellular mechanisms responsible for the secretion and subsequent deposition of pigment onto the eggshell. Further research is needed to explore the mechanism of action of IBV on pigment secretion and deposition. IBV strains have been shown to cause disorder of eggshell formation by disrupting isthmus gene expression of collagen type I and calcium binding protein 28kDa (CaBP-D28K) in the uterus (Nii et al., 2014). The viral antigen localizes only in the

epithelial cells lining the oviduct (Crinion and Hofstad, 1972). Different strains differentially reduce the beating of epithelial cilia (Raj and Jones, 1996). Other diseases, which cause deterioration of brown shell colour are *Mycoplasma spp.* (Gole et al., 2012), Newcastle disease and egg drop syndrome 76 (Higashihara et al., 1987), but their mechanism of action are also not known. Some parasitic diseases (e.g. *Leucocytozoon caulleryi*) which cause damage to the oviduct (Nakamura et al., 2001) may result in the production of paler shelled eggs.

1.10 Stress and eggshell colour

One of the major problems in the assessment of poultry welfare is measurement of stress. Handling and relocation stress for about 4.5 hr prior to subsequent oviposition has been shown to delay hen oviposition time by about 3 hr (Reynard and Savory, 1999). Hens become unable to lay, if the level and duration of stress exceeds a certain level (Reynard and Savory, 1999). Molting stress has been shown to severely affect eggshell colour once the hen starts laying again, with the extent of the response being different among individual hens (Aygun, 2013). Hens kept at high densities in cages, are more stressed compared to hens in individual cages or those at low stocking densities (Mills et al., 1987). Stress factors, such as cage design, high cage density, fear and frequent disturbance can cause brown-egg laying hens to lay lighter coloured eggshells (Walker and Hughes, 1998). Shell abnormalities, such as pale colouration or extraneous calcium may be caused by exposure of hens to environmental disturbances (Hughes et al., 1986), larger group size (Mills et al., 1987), certain drug infusions (e.g. adrenaline, nicarbazin, sulphonamides) and management failure. If such disturbances occur shortly prior to oviposition, the egg is retained in the shell gland and extra calcium coating takes place, which masks the brown shell colour (Hughes et al., 1986). Physical stress, such as experimental removal of feathers and high environmental temperature, has a detrimental effect on pigment deposition into the shell (Tangkere et al., 2001). An intrauterine injection of prostaglandin F2α can cause the secretion of pigment and induce quick oviposition with paler shells (Soh and Koga, 1999). A drug, indomethacin, administered by intrauterine injection, has been shown to completely inhibit the secretion of pigment in the shell gland (Soh and Koga, 1999).

1.11 Nicarbazin and eggshell colour

The coccidiostat drug nicarbazin, when feed to poultry, resulted in depigmented eggs at various levels within days of its administration (Hughes et al., 1991). The severity and duration of the effect depends on the drug concentration and duration of treatment (Schwartz et al., 1975; Hughes et al., 1991). This drug did not affect porphyrin synthesis in oviduct tissue (Polin, 1959; Schwartz et al., 1975), but how it affects deposition of protoporphyrin into the eggshell is not clear. Similarly, it did not prevent the elevation of erythrocyte protoporphyrin levels in the regenerative phase, following hen bleeding nor did it affect the formation of porphyrin from δ-aminolevulinic acid incubated with homogenates of uterus (Polin, 1959). The effect of the drug is reversible and shell colour is restored usually within 6-8 days, once the drug is withdrawn (Hughes et al., 1991).

In an *in vitro* study, nicarbazin did not prevent tissue porphyrin synthesis from aminolevulinic acid, as tissues from hens fed nicarbazin formed the same level of porphyrin as the control group (Polin, 1959). These findings suggest that there could be another pathway for porphyrin synthesis other than the glycine succinate cycle. The decrease in shell pigment deposition in nicarbazin fed laying hens varied with the amount of nicarbazin fed (Polin, 1959).

1.12 Shell colour and egg quality

Eggshell and egg internal quality are influenced by various factors, such as egg weight, shell weight, specific gravity, shell breaking strength, shell deformation, shell thickness, albumen height and yolk colour. A significant correlation between brown shell colour and shell strength (Yang et al., 2009) may indicate that brown eggshell pigment affects shell quality. A dark brown eggshell colour has been linked to higher eggshell specific gravity which is a shell quality indicator (Joseph et al., 1999). Brown eggshell colour has been positively correlated with some shell characteristics, such as shell strength and hatchability (Sekeroglu and Duman, 2011), while egg internal quality has no correlation with shell colour (Yang et al., 2009). Further, it has been suggested that some shell quality parameters, such as shell strength, shell weight, shell thickness and shell ultrastructure can be assessed

via shell colour because of significant correlations between the shell quality indicator and shell colour (Schreiweis et al., 2006; Yang et al., 2009). However, others have provided conflicting evidence (Joseph et al., 1999; Richards and Deeming, 2001), and thus shell colour cannot be applied reliably as a quality assessment tool.

1.13 Conclusions and future research

It can be concluded that protoporphyrin IX is synthesized in the shell gland, but the mechanism of synthesis is not fully understood. Eggshell colour has some positive correlations with egg quality parameters. The intensity and evenness of the shell colour deposition is affected by multiple factors. Further research is needed to elucidate the metabolic pathway of brown pigment in the shell gland and find out the genes for which overexpression can significantly increase the intensity of the brown shell pigment.

1.14 References

Ajioka, R. S., J. D. Phillips, and J. P. Kushner. 2006. Biosynthesis of heme in mammals. BBA - Mol. Cell Res. 1763(7):723-736.

Aygun, A. 2013. Effects of force molting on eggshell colour, egg production and quality traits in laying hens. Revue Med. Vet. 164(2):46-51.

Bain, M. M., K. Mcdade, R. Burchmore, A. Law, P. W. Wilson, M. Schmutz, R. Preisinger, and I. C. Dunn. 2013. Enhancing the egg's natural defence against bacterial penetration by increasing cuticle deposition. Anim. Genet. 44(6):661-668.

Baird, T., S. E. Solomon, and D. R. Tedstone. 1975. Localization and characterization of eggshell porphyrins in several avian species. Br. Poult. Sci. 16(2):201-208.

Bhosale, S. V., S. V. Bhosale, G. V. Shitre, S. R. Bobe, and A. Gupta. 2013. Supramolecular chemistry of protoporphyrin IX and its derivatives. Eur. J. Org. Chem. 2013(19):3939-3954.

Blow, W. L., C. H. Bostian, and E. W. Glazener. 1950. The inheritance of eggshell colour. Poult. Sci. 29(3):381-385.

Chousalkar, K. K., and J. R. Roberts. 2009. Effects of Australian strains of infectious bronchitis virus on internal and external quality of hen eggs. Anim. Prod. Sci. 49(2):162-169.

Chousalkar, K. K., B. F. Cheetham, and J. R. Roberts. 2009. Effects of infectious bronchitis virus vaccine on the oviduct of hens. Vaccine 27(10):1485-1489.

Chousalkar, K. K., and J. R. Roberts. 2007. Pathogenesis of two strains of infectious bronchitis virus for the oviduct of unvaccinated laying hens. Proc. Aust. Poult. Sci. Symp. 19:211-214.

Chousalkar, K. K., J. R. Roberts, and R. Reece. 2007. Histopathology of two serotypes of infectious bronchitis virus in laying hens vaccinated in the rearing phase. Poult. Sci. 86(1):59-62.

Crinion, R. A. P., and M. S. Hofstad. 1972. Pathogenicity of four serotypes of avian infectious bronchitis virus for the ovidct of young chickens of various ages. Avian Dis. 16(2):351-363.

Dennis, J. E., S. Q. Xiao, M. Agarwal, D. J. Fink, A. H. Heuer, and A. I. Caplan. 1996. Microstructure of matrix and mineral components of eggshells from White Leghorn chickens (*Gallus gallus*). J. Morphol. 228(3):287-306.

Dunn, I. 2011. Poultry breeding for egg quality: traditional and modern genetic approaches. Pages 245-260 in Improving the safety and quality of eggs and egg products. Volume 1: Egg chemistry, production and consumption. Y. Nys, M. Bain, F. van Immerseel, ed. Woodhead Publishing, Cambridge, U.K.

Forster, A., D. Jaenecke, M. Wittmann, D. K. Flock, and M. Kreuzer. 1996. Use of photometrically determined shell colour parameters as selection criteria for marketable brown shelled eggs. Archiv für Geflugelkunde 60(1):1-6.

Francesch, A., J. Estany, L. Alfonso, and M. Iglesias. 1997. Genetic parameters for egg number, egg weight, and eggshell colour in three Catalan poultry breeds. Poult. Sci. 76(12):1627-1631.

Fulton, J. E., M. Soller, A. R. Lund, J. Arango, and E. Lipkin. 2012. Variation in the ovocalyxin-32 gene in commercial egg-laying chickens and its relationship with egg production and egg quality traits. Anim. Genet. 43(1):102-113.

Gautron, J., M. T. Hincke, and Y. Nys. 1997. Precursor matrix proteins in the uterine fluid change with stages of eggshell formation in hens. Connect. Tissue Res. 36(3):195-210.

Gole, V. C., K. K. Chousalkar, and J. R. Roberts. 2012. Prevalence of antibodies to Mycoplasma synoviae in laying hens and possible effects on eggshell quality. Prev. Vet. Med. 106(1):75-78.

Gorchein, A., G. Lord, and C. K. Lim. 2012. Isolation and characterization of free heme from the shell gland of quail and hen. Biomed. Chromatogr. 26(3):355-357.

Grover, R. M., D. L. Erson, and R. A. Damon. 1980. The correlation between eggshell colour and specific gravity as a measure of shell strength. Poult. Sci. 59(6):1335-1336.

Hall, G. O. 1944. Eggshell colour in crosses between white and brown egg breeds. Poult. Sci. 23(4):259-265.

Hansson, M. D., T. Karlberg, M. A. Rahardja, S. Al-Karadaghi, and S. Hansson. 2007. Amino acid residues His183 and Glu264 in *Bacillus subtili*s ferrochelatase direct and facilitate the insertion of metal ion into protoporphyrin IX. Biochem. 46(1):87-94.

Higashihara, M., M. Hiruma, T. Houdatsu, S. Takai, and M. Matumoto. 1987. Experimental infection of laying chickens with egg-drop syndrome 1976 virus. Avian Dis. 31(1):193-196.

Hooge, D. M. 2007. *Bacillus subtilis* spores improve brown egg colour. World Poult. 23(3):14-15.

Hughes, B. L., J. E. Jones, J. Toler, J. Solis, and D. J. Castaldo. 1991. Effects of exposing broiler breeders to nicarbazin contaminated feed. Poult. Sci. 70(3):476-482.

Hughes, B. O., A. B. Gilbert, and M. F. Brown. 1986. Categorisation and causes of abnormal eggshells: Relationship with stress. Br. Poult. Sci. 27(2):325-337.

Hunton, P. 1962. Genetics of eggshell colour in a light sussex flock. Br. Poult. Sci. 3(3):189-193.

Ignjatovic, J., D. F. Ashton, R. Reece, P. Scott, and P. Hooper. 2002. Pathogenicity of Australian strains of avian infectious bronchitis virus. J. Comp. Pathol. 126(2-3):115-123.

Ishikawa, S. I., K. Suzuki, E. Fukuda, K. Arihara, Y. Yamamoto, T. Mukai, and M. Itoh. 2010. Photodynamic antimicrobial activity of avian eggshell pigments. FEBS Lett. 584(4):770-774.

Joseph, N. S., N. A. Robinson, R. A. Renema, and F. E. Robinson. 1999. Shell quality and colour variation in broiler breeder eggs. J. Appl. Poultry Res. 8(1):70-74.

Kennedy, G. Y., and H. G. Vevers. 1973. Eggshell pigments of the Araucano fowl. Comp. Biochem. Physiol. B: 44(1):11-25.

Khan, A. A., and Quigley, J. G. 2011. Control of intracellular heme levels: Heme transporters and heme oxygenases. BBA-Mol. Cell Res. 1813(5):668-682.

Kodali, V. K., S. A. Gannon, S. Paramasivam, S. Raje, T. Polenova, and C. Thorpe. 2011. A novel disulfide-rich protein motif from avian eggshell membranes. PLoS ONE 6(3):e18187.

Lang, M. R., and J. W. Wells. 1987. A Review of eggshell pigmentation. World's Poult. Sci. J. 43(3):238-246.

Leleu, S., W. Messens, K. De Reu, S. De Preter, S. Herman, M. Heyndrickx, J. De Baerdemaeker, C. W. Michiels, and M. Bain. 2011. Effect of egg washing on the cuticle quality of brown and white table eggs. J. Food Protect. 74(10):1649-1654.

Li, G., S. Chen, Z. Duan, L. Qu, G. Xu, and N. Yang. 2013. Comparison of protoporphyrin IX content and related gene expression in the tissues of chickens laying brown shelled eggs. Poult. Sci. 92(12):3120-3124.

Liu, H. C., and W. T. K. Cheng. 2010. Eggshell pigmentation. J. Chin. Soc. Anim. Sci. 39(2):75-89.

Liu, H. C., M. C. Hsiao, Y. H. Hu, S. R. Lee, and W. T. K. Cheng. 2010. Eggshell pigmentation study in blue shelled and white shelled ducks. Asian Austral. J. Anim. Sci. 23(2):162-168.

Mertens, K., B. De-Ketelaere, B. Kamers, F. R. Bamelis, B. J. Kemps, E. M. Verhoelst, J. G. De-Baerdemaeker, and E. M. Decuypere. 2005. Dirt detection on brown eggs by means of colour computer vision. Poult. Sci. 84(10):1653-1659.

Miksik, I., A. Eckhardt, P. Sedlakova, and K. Mikulikova. 2007. Proteins of insoluble matrix of avian (*Gallus gallus*) eggshell. Connect. Tissue Res. 48(1):1-8.

Miles, R. D., and P. R. Henry. 2004. Effect of time and storage conditions on albumen quality of eggs from hens fed vanadium. J. Appl. Poultry Res. 13(4):619-627.

Miller, L. K., and A. Kappas. 1974. The effect of progesterone on activities of δ-aminolevulinic acid synthase and δ-aminolevulinic acid dehydratase in estrogen-primed avian oviduct. Gen. Comp. Endocrinol. 22(2):238-244.

Mills, A. D., M. Marche, and J. M. Faure. 1987. Extraneous eggshell calcification as a measure of stress in poultry. Br. Poult. Sci. 28(1):177-181.

Nakamura, K., M. Ogiso, T. Shibahara, H. Kasuga, and T. Isobe. 2001. Pathogenicity of *Leucocytozoon caulleryi* for specific pathogen free laying hens. J. Parasitol. 87(5):1202-1204.

Nii, T., N. Isobe, and Y. Yoshimura. 2014. Effects of avian infectious bronchitis virus antigen on eggshell formation and immunoreaction in hen oviduct. Theriogenology 81(8):1129-1138.

Nys, Y., and N. Guyot. (2011). Egg formation and chemistry. In Yves Nys, Maureen Bain and Filip Van Immerseel (Eds.). Improving the safety and quality of eggs and egg products. Woodhead Publishing Limited, Cambridge UK, Volume 1:83-132.

Nys, Y., J. Gautron, J. M. Garcia-Ruiz, and M. T. Hincke. 2004. Avian eggshell mineralization: biochemical and functional characterization of matrix proteins. C. R. Palevol. 3(6-7):549-562.

Nys, Y., J. Zawadzki, J. Gautron, and A. D. Mills. 1991. Whitening of brown shelled eggs: Mineral composition of uterine fluid and rate of protoporphyrin deposition. Poult. Sci. 70(5):1236-1245.

Odabasi, A. Z., R. D. Miles, M. O. Balaban, and K. M. Portier. 2007. Changes in brown eggshell colour as the hen ages. Poult. Sci. 86(2):356-363.

Odabasi, A. Z., R. D. Miles, M. O. Balaban, K. M. Portier, and V. Sampath. 2006. Vitamin C overcomes the detrimental effect of vanadium on brown eggshell pigmentation. J. Appl. Poultry Res. 15(3):425-432.

Polin, D. 1957. Formation of porphyrin from delta-aminolevulenic acid by uterine and liver tissue from laying hens. Exp. Biol. Med. 94(2):276-279.

Polin, D. 1959. Porphyrin formation by tissues from laying hens fed nicarbazin. Exp. Biol. Med. 100(4):695-698.

Poole, H. K. 1965. Spectrophotometric identification of eggshell pigments and timing of superficial pigment deposition in the Japanese quail. Exp. Biol. Med. 119(2):547-551.

Poole, H. K. 1967. A microscopic study of uterine eggshell pigment in Japanese quail. J. Hered. 58(4):200-203.

Punnett, C. 1933. Genetic studies in poultry. J. Genet. 27(3):465-470.

Punnett, R. C., and P. G. Bailey. 1920. Genetic studies in poultry. II Inheritance of egg colour and broodiness. J. Genet. 10(4):277-292.

Raj, G. D., and R. C. Jones. 1996. An *in vitro* comparison of the virulence of seven strains of infectious bronchitis virus using tracheal and oviduct organ cultures. Avian Pathol. 25(4):649-662.

Reynard, M., and C. J. Savory. 1999. Stress-induced oviposition delays in laying hens: Duration and consequences for eggshell quality. Br. Poult. Sci. 40(5):585-591.

Richards, P. D. G., and D. C. Deeming. 2001. Correlation between shell colour and ultrastructure in pheasant eggs. Br. Poult. Sci. 42(3):338-343.

Riddle, R. D., M. Yamamoto, and J. D. Engel. 1989. Expression of delta-aminolevulinate synthase in avian cells: separate genes encode erythroid-specific and nonspecific isozymes. Proc. Natl. Acad. Sci. U.S.A. 86(3):792-796.

Roberts, J. R., K. Chousalkar, and Samiullah. 2013. Egg quality and age of laying hens: implications for product safety. Anim. Prod. Sci. 53(12):1291-1297.

Roberts, J. R., P. Scott, S. Samiullah, N. Fernando, and A. M. Anwar. 2014. Maintenance of shell colour in free range laying hens. Proc. Aust. Poult. Sci. Symp. 25:122-125.

Samiullah, S. 2012. The eggshell quality of table eggs and how this affects food safety. Master Thesis. University of New England of New England Armidale Australia. Accessed Nov. 2014. https://e-publications.une.edu.au/vital/access/manager/Repository/une:13681

Samiullah, S., and J. R. Roberts. 2013. The location of protoporphyrin in the eggshell of brown-shelled eggs. Poult. Sci. 92(10):2783-2788.

Samiullah, J. R. Roberts, and K. K. Chousalkar. 2014. Effect of production system and flock age on egg quality and total bacterial load in commercial laying hens. J. Appl. Poultry Res. 23(1):59-70.

Sasaki, O., S. Odawara, H. Takahashi, K. Nirasawa, Y. Oyamada, R. Yamamoto, K. Ishii, Y. Nagamine, H. Takeda, E. Kobayashi, and T. Furukawa. 2004. Genetic mapping of quantitative trait loci affecting body weight, egg character and egg production in F2 intercross chickens. Anim. Genet. 35(3):188-194.

Schreiweis, M. A., P. Y. Hester, P. Settar, and D. E. Moody. 2006. Identification of quantitative trait loci associated with egg quality, egg production, and body weight in an F2 resource population of chickens. Anim. Genet. 37(2):106-112.

Schwartz, S., W. A. Raux, B. A. Schacter, B. D. Stephenson, and R. N. Shoffner. 1980. Loss of hereditary uterine protoporphyria through chromosomal rearrangement in mutant Rhode Island Red hens. Int. J. Biochem. 12(5-6):935-940.

Schwartz, S., B. D. Stephenson, D. H. Sarkar, and M. R. Bracho. 1975. Red, white, and blue eggs as models of porphyrin and heme metabolism. Ann. NY Acad. Sci. 244(1):570-588.

Sekeroglu, A., and M. Duman. 2011. Effect of eggshell colour of broiler parent stocks on hatching results, chickens performance, carcass characteristics, internal organ weights and some stress indicators. Kafkas Uni. Vet. Fak. 17(5):837-842.

Sekeroglu, A., M. Sarica, E. Demir, Z. Ulutas, M. Tilki , M. Saatci, and H. Omed. 2010. Effects of different housing systems on some performance traits and egg qualities of laying hens. J. Anim. Vet. Advan. 9(12):1739-1744.

Seo, Y. M., K. S. Shin, A. R. Rhee, Y. S. Chi, J. Han, and I. K. Paik. 2010. Effects of dietary Fe-soy proteinate and MgO on egg production and quality of eggshell in laying hens. Asian Aust. J. Anim. Sci. 23(8):1043-1048.

Sevoian, M., and P. P. Levine. 1957. Effects of infectious bronchitis on the reproductive tracts, egg production, and egg quality of laying chickens. Avian Dis. 1(2):136-164.

Sezer, M., and O. Tekelioglu. 2009. Quantification of Japanese quail eggshell colour by image analysis. Biol. Res. 42(1):99-105.

Shoffner, R. N., R. Shuman, J. S. Otis, J. J. Bitgood, V. Garwood, and P. Lowe. 1982. The effect of a protoporphyrin mutant on some economic traits of the chicken. Poult. Sci. 61(5):817-820.

Soh, T., N. Fujihara, and O. Koga. 1993. Observations of pigment accumulation in the epithelium of the shell gland and superficial pigmentation on the eggshell in Japanese quail. J. Fac. Agr. Kyushu U. 38(1):73-80.

Soh, T., and O. Koga. 1994. The effects of sex steroid hormones on the pigment accumulation in the shell gland of Japanese quail. Poult. Sci. 73(1):179-185.

Soh, T., and O. Koga. 1997. The effect of progesterone and estradiol-17 β on the pigment accumulation of the shell gland in Japanese quail pretreated with aminoglutethimide. J. Fac. Agr. Kyushu U. 42(1-2):147-150.

Soh, T., and O. Koga. 1999. Effects of phosphate, prostaglandins, arachidonic acid and arginine vasotocin on oviposition and pigment secretion from the shell gland in Japanese quail. Br. Poult. Sci. 40(1):131-134.

Solomon, S. E. 1987. Eggshell pigmentation. In R. G. Wells and C. G. Belyavin (Eds.), Egg quality: current problems and recent advances: Butterworths, London, U.K. (pp. 147-157).

Solomon, S. E. 2002. The oviduct in chaos. World's Poult. Sci. J. 58(1):41-48.

Sorby, H. C. 1875. On the colouring matters of the shells of birds eggs. P. Zool. Soc. Lond. 43(1):351-365.

Sparks, N. H. C. 2011. Eggshell pigments - from formation to deposition. Avian Biol. Res. 4(4):162-167.

Stevens, E. V., L. K. Miller, S. Weinstein, and A. Kappas. 1974. Biosynthesis of δ-aminolevulinic acid and porphobilinogen in the domestic fowl (*Gallus domesticus*). Comp. Biochem. Physiol. B: 47(4):779-786.

Sutly, J. P., R. D. Miles, C. W. Comer, and M. O. Balaban. 2001. The influence of vanadium on pigmentation of brown shelled eggs. Poult. Sci. 80(1):1039 (Abst).

Tamura, T., and S. Fujii. 1967a. Comparative observations on the distribution of fluorescent pigments (porphyrins) in the egg coverings of chicken and quail. Journal of the Faculty of Fisheries and Animal, Husbandry Hiroshima University, 7:35-41.

Tamura, T., and S. Fujii. 1967b. Comparative observations on the distribution of fluorescent pigments (porphyrins) in the chicken and quail uteri. Journal of the Faculty of Fisheries and Animal Husbandry, Hiroshima University, 7:43-49.

Tamura, T., S. Fujii, H. Kunisaki, and M. Yamane. 1965. Histological observations on the quail oviduct; with reference to pigment (porphyrin) in the uterus. Journal of Faculty of Fisheries and Animal Husbandry, Hiroshima University, 6:37-57.

Tangkere, E. S., B. Bhandari, and J. G. Dingle. 2001. Eggshell quality of caged laying hens in different ambient temperatures given drinking water of different temperatures. Proc. Aust. Poult. Sci. Symp. 13:224-227.

Van Brummelen, R., and S. Bissbort. 1993. Chicken eggshell porphyrins and the glyoxalase pathway: Its possible physiological role. Comp. Biochem. Physiol. B: 104(4):657-662.

Walker, A. W., and B. O. Hughes. 1998. Eggshell colour is affected by laying cage design. Br. Poult. Sci. 39(5):696-699.

Wang, X. T., X. M. Deng, C. J. Zhao, J. Y. Li, G. Y. Xu, L. S. Lian, and C. X. Wu. 2007. Study of the deposition process of eggshell pigments using an improved dissolution method. Poult. Sci. 86(10):2236-2238.

Wang, X. T., C. J. Zhao, J. Y. Li, G. Y. Xu, L. S. Lian, C. X. Wu, and X. M. Deng. 2009a. Comparison of the total amount of eggshell pigments in Dongxiang brown-shelled eggs and Dongxiang blue-shelled eggs. Poult. Sci. 88(8):1735-1739.

Wang, X. L., J. X. Zheng, Z. H. Ning, L. J. Qu, G. Y. Xu, and N. Yang. 2009b. Laying performance and egg quality of blue-shelled layers as affected by different housing systems. Poult. Sci. 88(7):1485-1492.

Wang, Z., R. Liu, and A. Wang. 2013. Comparison of HMOX1 expression and enzyme activity in blue-shelled chickens and brown-shelled chickens. Genet. Mol. Biol. 36:282-286.

Wardecka, B., R. Olszewski, K. Jaszczak, G. Zieba, M. Pierzchala, and K. Wicinska. 2002. Relationship between microsatellite marker alleles on chromosomes 1-5 originating from the Rhode Island Red and Green-legged Partrigenous breeds and egg production and quality traits in F2 mapping population. J. Appl. Genet. 43(3):319-329.

Warren, D. C., and R. M. Conrad. 1942. Time of pigment deposition in brown shelled hen eggs and in turkey eggs. Poult. Sci. 21(6):515-520.

Wei, R., and J. J. Bitgood. 1990. A new objective measurement of eggshell colour. 1. A test for potential usefulness of two colour measuring devices. Poult. Sci. 69(10):1775-1780.

With, T. K. 1974. Porphyrins in eggshells. Biochem. J. 137(3):597-598.

Yang, H. M., Z. Y. Wang, and J. Lu. 2009. Study on the relationship between eggshell colour and egg quality as well as shell ultrastructure in Yangzhou chicken. Afr. J. Biotechnol. 8(12):2898-2902.

Zhang, L. C., Z. H. Ning, G. Y. Xu, Z. C. Hou, and N. Yang. 2005. Heritabilities and genetic and phenotypic correlations of egg quality traits in brown-egg dwarf layers. Poult. Sci. 84(8):1209-1213.

Zhao, R., G. Y. Xu, Z. Z. Liu, J. Y. Li, and N. Yang. 2006. A study on eggshell pigmentation: biliverdin in blue-shelled chickens. Poult. Sci. 85(3):546-549.

Zheng, C., Z. Li, N. Yang, and Z. Ning. 2014. Quantitative expression of candidate genes affecting eggshell colour. Anim. Sci. J. 85(5):506-510.

Higher Degree Research Thesis by Publication
University of New England

STATEMENT OF AUTHORS' CONTRIBUTION

(To appear at the end of each thesis chapter submitted as an article/paper)

We, the Research Master/PhD candidate and the candidate's Principal Supervisor, certify that all co-authors have consented to their work being included in the thesis and they have accepted the candidate's contribution as indicated in the *Statement of Originality*.

	Author's Name (please print clearly)	% of contribution
Candidate	**Sami Samiullah**	65
Other Authors	**Juliet Roberts**	30
	Kapil Chousalkar	5

Name of Candidate: **Samiullah**

Name/title of Principal Supervisor: **Associate Professor Juliet Roberts**



Candidate Date 09/06/2017



Principal Supervisor Date 09/06/2017

Higher Degree Research Thesis by Publication
University of New England

STATEMENT OF ORIGINALITY

(To appear at the end of each thesis chapter submitted as an article/paper)

We, the Research Master/PhD candidate and the candidate's Principal Supervisor, certify that the following text, figures and diagrams are the candidate's original work.

Type of work	**Page number/s**
Figure 1.1	9
Text	1-25

Name of Candidate: **Samiullah**

Name/title of Principal Supervisor: **Associate Professor Juliet Roberts**

[redacted]

Candidate Date 09/06/2017

[redacted]

Principal Supervisor Date 09/06/2017

Chapter 2 Effect of production system and flock age on eggshell and egg internal quality measurements

Published as: Samiullah, S., Omar, A.S., Roberts, J. and Chousalkar, K. (2017). Effect of production systems and flocks age on eggshell and egg internal quality measurements. Poultry Science; 96 (1): 246-258.

2.1 Abstract

Egg quality was measured in eggs from different flocks that were reared together and then allocated to different production systems. Eggs were processed for measurements of eggshell and egg internal quality variables, scoring of ultrastructural mammillary layer features, completeness of cuticle cover and protoporphyrin IX (PP IX) quantification. There was a significant main effect ($P < 0.05$) of production system on shell reflectivity, egg weight and egg internal quality and significant effects of flock age on most measurements. The mammillary layer ultrastructural variables showed no clear relationship with production system and flock age. However, there was a significant interaction between production system and flock age for mammillary cap, early and late fusions. Cuticle cover (ΔE^*_{ab}), was significantly higher in barn eggs (19.20), followed by free range (17.57) and cage eggs (15.99). Completeness of cuticle cover was significantly higher in eggs from the 44 week old flock than for 64 week and 73 week old flocks. For eggshells with cuticle intact, there was a significant main effect of both production system and flock age, and significant interaction between the two, for shell reflectivity, L*a*b* values and amount of PP IX. For PP IX, when this difference was calculated for the cuticle alone, there were no statistically significant differences. In 1 g of shell with and without cuticle, there was more PP IX in cage eggs (9.49×10^{-8}, 7.90×10^{-8} mM) followed by free range (8.24×10^{-8}, 6.90×10^{-8} mM) and barn eggs (8.64×10^{-8}, 7.28×10^{-8} mM). Similar trends were recorded for the amount of PP IX in 1 g of cuticle, but the difference was not statistically significant. The amount of PP IX decreased significantly with increasing flock age. Comparing the cage and barn production systems at 68 week of flock age, there was no difference for the amount of PP IX in shell with or without cuticle, or in the cuticle alone. Eggs from the cage

production system were darker in colour and contained more PP IX mainly within the calcareous part of the shell. For the barn production system, the completeness of cuticle cover was higher and egg weight generally lower.

Key words: Brown-egg laying hen, eggshell quality, protoporphyrin IX, cuticle, mammillary layer ultrastructure

2.2 Introduction

Eggs are a cheap and nutritionally balanced source for human nutrition (Mine and Kovacs-Nolan, 2004). In many countries, conventional cages are a common production system for table eggs (Sorensen et al., 2006). However, there are some hen welfare concerns about conventional cages and thus European countries have replaced conventional cages with alternative systems where hens have more free space available (Appleby, 2003). With the increasing trend in the commercialization of non-cage systems, there is an increased consumption of eggs from these production systems (Anderson and Koelkebeck, 2007; Anderson, 2009). Different commercial egg production systems have their own advantages and disadvantages which is why all three production systems (cage, barn, free range) exist in Australia and many other countries. In Australia, the cage production system is the most efficient and cost effective and accounts for approximately 53% of the total table egg production (AECL, 2014). Modern cage production systems typically consist of multiple tiers of cages installed in environmentally controlled poultry houses. According to the current Australian Model Code of Practice (Primary Industries Standing Committee, 2002), a minimum floor space allowance of 550 cm^2 per hen must be provided for 3 or more birds per cage where the birds weigh less than 2.4 kg. The barn system offers access to a deep litter system, automated feeding and drinking systems, perches, and stepping rails to automated egg collection nest boxes. The barn egg production system's average contribution to total eggs produced in Australia is about 8% (AECL, 2014). Free range production is increasing in Australia, reported as being 38% of total egg production in the latest report published by Australian Egg Corporation Limited (AECL, 2014). In a typical free range production system, nest boxes, perches, feed and water are

available in the house which is often very similar to the barn production system but birds also have access to a grassed outdoor free range area.

The eggshell is a thin mineralized structure that forms in the acellular medium of the shell gland over an approximately 18 hr period of time. The quality of an eggshell is measured in terms of shell strength and shell thickness. A stronger eggshell protects the internal contents from microbial spoilage and transportation shock. The four major layers of the eggshell are mammillary layer, palisade layer, surface crystal layer and cuticle.

The mammillary layer comprises about one third to one fifth of the total thickness of the shell (Hodges, 1974). It consists of numerous irregular conical knobs, the mammillae, whose apices are embedded in the outer shell membrane and whose irregular bases are fused together to form the foundation of palisade layer (Fernandez et al., 2003, Rose and Hincke, 2009). The formation of the mammillary layer of the eggshell occurs once the calcite crystals begin to be deposited onto the outer shell membranes in the distal part of the isthmus and shell gland of the oviduct (Parsons, 1982; Arias et al., 1993; Nys et al., 2004). The mammillary layer acquires cone-like structures with special features that affect its thickness, strength and attachment to shell membranes (Nys et al., 1999). The mammillary layer contributes to the overall strength of the shell.

The cuticle is a proteinaceous layer that is synthesized in the shell gland during a 1.5-2.0 hr period prior to oviposition (Hincke et al., 2011). The egg cuticle acts as a gaseous exchange controller and a first line of defence against microbial penetration. There is always natural variation in the amount of cuticle present on eggshell and its thickness is affected by various factors such as hen breed, strain, age, production system and management (Solomon et al., 1994; Messens et al., 2005; Samiullah et al., 2014).

The colour of an eggshell in commercial laying hens is determined primarily by the genotype of the hen. Apart from playing a role in consumer preference, brown eggshell pigment correlates positively with shell breaking strength, shell thickness and hatchability (Curtis et al., 1985; Jones et al., 2010; Mertens et al., 2010). Recently, brown pigment has been shown to have photodynamic dependent gram positive bactericidal function (Ishikawa et al., 2010). Protoporphyrin IX has been

identified as the main eggshell pigment in brown eggshells of laying hens, in addition to traces of biliverdin (With, 1973; Kennedy and Vevers, 1973; Miksik et al., 1996).

As hens age, eggshell colour deteriorates in strains of hens that lay brown shelled eggs. In addition, eggs laid even by young flocks are sometimes lighter in colour and anecdotal evidence provided by Australian egg industry members indicates that this can be a particular problem in some free range flocks. Testing for the effect of production system on shell colour at different flock ages can be difficult owing to the many other variables involved. For example, rearing conditions are known to be of vital importance to the subsequent performance of layer flocks (Faure, 1991). The opportunity arose for the researchers to sample eggs from four different rearing flocks of birds, at different ages, where pullets were reared together and then placed into different large scale commercial production systems.

Therefore, the main objective of the present study was to compare the performance of flocks of different ages where pullets were reared together and then placed into three commercial production systems (cage, barn, free range), as indicated by traditional egg quality measurements, scoring of mammillary layer ultrastructural features, cuticle estimation and protoporphyrin IX quantification from shell.

2.3 Materials and Methods

Hy-Line brown-egg laying flocks were housed in conventional cage, barn and free range commercial production systems. For three flocks that were sampled at one of 44, 64 and 73 weeks of age, pullets were reared together and then allocated to one of cage, barn or free range commercial production systems. For one flock, which was sampled at 68 weeks of age, pullets were reared together and then allocated to either a cage or barn commercial production system. For each of the flocks, birds were reared together in cages (at a density of a maximum of 40 kg per cage at 16 weeks of age) until 16 weeks of age, under the same environmental and husbandry conditions. During rearing, all flocks received locally formulated feed containing wheat (or wheat plus sorghum), soybean meal, meat meal, vegetable oil, limestone and yolk colour pigment as major components, with feed formulated according to Hy-Line Brown Breeder Company recommendations for intensive production

systems (Hy-Line Australia, 2016). In the environmentally controlled cage system, in each conventional expanded cage, 6 hens were reared at a maximum density of 550 cm^2/hen, with total flock size ranging from 84,000 to 120,000 hens. Stocking density for hens in the barn system was a maximum of 30 kg /m^2, and flock size ranged from 14,000 to 20,000 hens. The barn systems were fully slatted with nest boxes and perches but no dust bath facilities. The feed for the barn production system was the same as for the cage production system. The free range system provided a maximum density of 1500 hens/hectare on the range and 12 hens/m^2 of floor space in the sheds. For each free range flock, there were between 20,000 and 25,000 hens and birds were fed a diet formulated to Hy-Line Brown specifications for extensive production systems (Hy-Line Australia, 2016). From each age of flock, in each production system, eggs were collected at random from the cage fronts and processed for the measurement of traditional eggshell and egg internal quality variables (30 eggs per flock per production system), estimation of the completeness of cuticle cover (30 eggs per flock per production system) and the amount of protoporphyrin IX present in the shell (30 eggs per flock per production system). From the 30 eggshells per flock per production system used for traditional quality measurements, 10 eggshells from each age group in each production system (a total of 110 samples) were randomly selected and processed for the scoring of eggshell mammillary layer ultrastructural features using a scanning electron microscope.

2.3.1 Eggshell and egg internal quality measurements

Eggshell and egg internal quality parameters were measured by TSS (Technical Services and Supplies, Dunnington, York, UK) equipment. Briefly, egg weight was measured on a top pan balance. Shell breaking strength and shell deformation were measured by quasi-static compression using TSS QC-SPA (50 N load cell) equipment. Individual eggs were placed horizontally in the egg holder before being compressed by the shell breaking strength machine. The peak force required to break the shell was recorded. Shell weight was measured on shells that had been washed and dried thoroughly, using a Quintix513-1S balance (Sartorius Lab Instruments GmbH & Co. KG Goettingen, Germany). Shell thickness was

measured by a custom-built gauge, based on a Mitutoyo Dial Comparator Gauge Model 2109–10 (Kawasaki, Japan). For shell thickness, three pieces of eggshell with intact shell membranes were taken from around the equator of the shell. Percentage shell was calculated as a shell weight to egg weight ratio. For the egg internal quality variables; albumen height, Haugh unit, and yolk colour were measured using the TSS QCE-QCM equipment. The yolk colour scoring system used in the TSS QCE-QCM is based on the 1 to 15 scale of the DSM (previously Roche) yolk colour fan scoring system.

2.3.2 Microscopic observations of the shell mammillary layer ultrastructure

The ultrastructural features of the shell mammillary layer were scored using a JCM-5000 Neoscope benchtop scanning electron microscope (SEM). Briefly, pieces of shell approximately 1 cm^2 were cut from around the equator of the eggshell using a Dremel tool (Dremel High Speed rotary tool, 300 series, Robert Bosch Tool Corporation, Gerlingen, Germany), and soaked overnight in tap water. Shell membranes were peeled off manually, and pieces of shell allowed to dry thoroughly. Following the method of Reid (1983), the dried pieces were plasma etched for 4 hours in a BioRAD RF Plasma Barrel Etcher PT 7150 to remove the outer shell membrane. Individual shell pieces were air dusted and mounted on a 9 mm diameter aluminum stub using aqueous conductive silver liquid SEM adhesive (I005–ProSciTech, Townsville, QLD, Australia), sputter coated in a Neocoater (Nikon, Tokyo, Japan) for 8 minutes, and viewed under the SEM at magnifications of approximately 22 to 500. Mammillary ultrastructural variables were scored following the method of Solomon (1991).

A total of sixteen different ultrastructural variables were viewed in the mammillary layer of individual eggshells. Mammillary cap size was scored as 1 (similar), 2 (variable), 3 (highly variable). Mammillary caps were scored according to their quality which was assessed as both the size of the cap in relation to its cone and the degree of membrane attachment from 1 (best) to 5 (worst). Other variables like confluence, early fusion, late fusion, alignment, Type A bodies, Type B bodies,

aragonite, cubics, cubic cone formations, changed membrane, cuffing, depressions, erosion, and holes were each ranked for incidence from 1 (none) to 4 (extensive).

2.3.3 Cuticle cover estimation

For the cuticle cover estimation, shell colour (L*a*b*) was measured on eggs before staining, using a hand-held Konica Minolta spectrophotometer (CM-2600d Ramsey, NJ, USA). The spectrophotometer was calibrated against a reference white tile and the reflectance reading of individual eggs was taken 3 times at three equidistant points around the equator, and an average value recorded used for analysis. The Konica Minolta spectrophotometer used in the current study functions on the L*a*b* space system, where L* represents the grading between black (0) and white (100). The higher the value for L*, the lighter is the shell colour. The value for chromatic component a* indicates the colour grading between green and red, where green is towards the negative end of the scale and red towards the positive end. The b* component is the grading between yellow and blue, where blue is towards the negative end and yellow towards the positive end of the scale. Next, eggs were soaked in MST cuticle blue stain (MS Technologies, Europe Ltd, Kettering, Northamptonshire, UK) for 1 minute, and rinsed in tap water to remove excess stain. Shell colour (L*a*b*) was measured again on stained eggs as mentioned earlier. The amount of cuticle was estimated following the method of Leleu et al. (2011a) by converting the L*a*b* values into a single score. The single score, measures the L*, a*, and b* values, before and after staining, and calculates a single value as ΔE^*_{ab}:

$$\Delta E^*_{ab} = \sqrt{[(\Delta L^*)^2 + (\Delta a^*)^2 + (\Delta b^*)^2]}$$

A higher ΔE^*_{ab} denotes a higher staining affinity and hence more cuticle coverage (Leleu et al., 2011a; Roberts et al., 2013).

2.3.4 Protoporphyrin IX quantification from eggshell with and without cuticle

Shell reflectivity and shell colour (L*a*b*) were measured on eggs before and after removal of the cuticle layer. The method described by Poole (1965), and modified

by Samiullah and Roberts (2013), was used for the amount of protoporphyrin IX quantification. Briefly, the cuticle layer was removed following the method described by Leleu et al. (2011b) and modified by Samiullah and Roberts (2013). Egg internal contents were removed by making a small hole at the blunt end of individual eggs using a rotary Dremel tool. Eggs were washed to remove any adherent albumen, and another hole was made at the pointed end to pass a thin stick across the eggshell. Each egg, individually, was soaked in an EDTA solution (0.34 M, pH 7.5) for 5 minutes (Figure 2.1), and the cuticle of the soaked longitudinal half side of the shell was carefully scrubbed off using a soft brush in running tap water (Figure 2.2). Individual shells were cut longitudinally into two halves (with and without cuticle). Shell membrane was removed manually and shells were allowed to dry thoroughly. Shell reflectivity and L*a*b* were measured again on the shells with cuticle removed. From the equator of each shell, a 0.25 g sample was weighed into a 10 mL plastic centrifuge tube into which 4 mL of methanol - concentrated HCl (2:1) solvent was added. For each flock age, 30 tubes were prepared with whole eggshells (shells with intact cuticle), and 30 tubes from the shells without cuticle, thus a total of 660 tubes were prepared for the eleven different age groups. The tubes were stored in a refrigerator for 3 hours to allow the shell pieces to digest completely. The tubes were centrifuged at 800 ×*g* at 4°C for 0.5 hour, the supernatant solution was decanted into a 4 mL acrylic cuvettes, and the absorbance of the supernatant read at 412 nm in a spectrophotometer (UV-1201, Shimadzu, Kyoto, Japan).



Figure 2.1 Longitudinal half of the eggshell soaked in EDTA

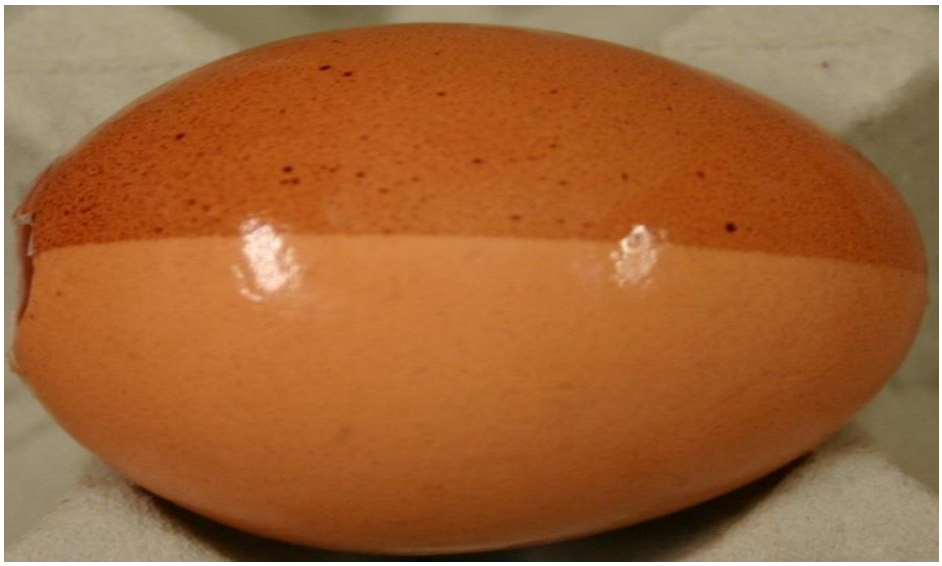

Figure 2.2 Eggshell with and without cuticle layer

2.3.5 Standard curve construction and calculation of protoporphyrin IX per gram of shell

A standard solution was prepared by dissolving 0.0060 g of powder protoporphyrin IX disodium salt (Sigma Aldrich, Castle Hill, NSW, Australia) in 90 mL methanol - concentrated HCl (2:1) solvent. Serial dilutions from the standard stock solution were prepared until a 1:128 dilution was reached. A standard curve was constructed using the absorbance at 412 nm of concentrations of protoporphyrin standards from 0 mM to 6.87×10^{-6} mM. The absorbance values from the analysed samples were converted into concentration of protoporphyrin IX in 1 g of eggshell (with and without cuticle present). For determination of the amount of protoporphyrin IX in the cuticle, the values of the eggshell samples without cuticle were subtracted from the values of the eggshell samples with the cuticle.

2.4 Statistical analysis

Eggs from birds originating from each rearing flock were compared among the production systems to test for any differences. Although each age of flock was essentially a separate experiment, data from the different aged flocks were compared to test for any differences based on age of flock. Data were subjected to one-way and two-way analysis of variance (ANOVA) and General Linear Model (GLM) Procedures (SAS 2004) to test the probability of significant differences between the means values. For flocks at the age of 44, 64 and 73 weeks, data were analyzed by taking flock age and production system as independent variables and the eggshell and egg internal quality measurements as dependent variables. An interaction between the flock age and the production system was also recorded for some variables measured. The data for the 68 weeks old flocks in cage and barn production systems were analyzed by taking production system as the independent variable. The Level of Significance was assumed at 95% confidence ($P < 0.05$).

2.5 Results

2.5.1 Eggshell and egg internal quality measurements

For eggshell quality measurements, there was a significant difference among production systems for shell reflectivity and egg weight; however, there was no statistically significant difference ($P > 0.05$) in the other parameters (shell weight, shell percentage, shell thickness, shell breaking strength and deformation unit) as shown in Table 2.1. Eggs from the barn system had the highest percentage of shell reflectivity (29.74%) and the lowest egg weight (58.63 g) as compared to cage and free range systems. The egg internal quality was significantly affected ($P < 0.0001$) by production system. The highest values for albumen height and Haugh unit (7.45 mm and 85.56, respectively) were recorded for the free range system. The hens kept in cage and barn production systems laid eggs of darker yolk colour as compared with the free range system.

The eggshell quality measurements indicated that flock age had a significant effect on all variables measured, except shell weight and deformation unit. Shell reflectivity and egg weight significantly increased as hen age increased (Table 2.1). The 44 week of age hens had highest values for shell thickness (414.95 µm) and shell breaking strength (44.10 N). Haugh unit significantly decreased with increasing age of laying hens. The 44 week flock had significantly higher values for albumen height (7.12 mm). The intensity of yolk colour was lowest in the 73 week old birds. A statistically significant interaction between production system and flock age was observed only for shell reflectivity and yolk colour (Figures 2.3 and 2.4). For the 68 week old flock, there was no significant difference between cage and barn production systems for eggshell and egg internal quality variables (Table 2.2). However, the eggs produced in the cage production system had higher numerical values than the barn system for egg weight, albumen height, Haugh unit and shell breaking strength.

Table 2.1 Effect of production system and flock age on eggshell and egg internal quality variables

Variable	Production System			Flock Age (week)			P value	
	Cage	Barn	Free range	44	64	73	P	A
Shell reflectivity (%)	25.24±0.46^{c}	29.74±0.66^{a}	27.36±0.62^{b}	24.34±41^{c}	27.33±0.48^{b}	30.75±0.72^{a}	<0.0001	<0.0001
Egg weight (g)	60.66±048^{a}	58.63±0.41^{b}	61.26±0.54^{a}	59.14±0.39^{a}	60.01±0.52^{b}	61.43±0.53^{a}	0.0003	0.0031
Shell weight (g)	5.57±0.05	5.51±0.07	5.71±0.04	5.64±0.04	5.63±0.07	5.52±0.06	0.0765	0.3585
Shell percentage	9.22±0.09	9.39±0.09	9.24±0.08	9.55±0.07^{a}	9.22±0.1b	9.07±0.09^{b}	0.2652	0.0002
Shell thickness (µm)	406.55±2.8	408.80±3.6	408.25±3.2	414.95±2.6^{a}	405.50±3.5^{b}	403.09±3.4^{b}	0.8780	0.0221
Shell breaking strength (N)	40.51±0.88	41.79±1.02	40.07±0.89	44.10±0.72^{a}	38.45±0.99^{b}	38.87±0.91^{b}	0.3705	<0.0001
Deformation unit (µm)	262.89±4.07	279.44±10.3	274.96±8.69	284.11±3.71	265.01±8.79	267.95±10.38	0.3293	0.2030
Albumen height (mm)	6.16±0.14^{b}	6.19±0.15^{b}	7.45±0.15^{a}	7.12±0.15^{a}	6.47±0.15^{b}	6.19.±0.17^{b}	<0.0001	<0.0001
Haugh unit	76.92±1.04^{b}	77.42±1.2^{b}	85.56±1.43^{a}	83.9±0.98^{a}	79.43±1.03^{b}	76.45±1.75^{c}	<0.0001	<0.0001
Yolk colour	10.83±0.11^{a}	10.63±0.09^{a}	9.98±0.19^{b}	10.74±0.11^{a}	10.84±0.08^{a}	9.84±0.18^{b}	<0.0001	<0.0001

P = production system; A = flock age; Values are Mean±S.E.

^{a,b,c} Across a row, values with different superscripts among different production systems and age groups are significantly different ($P < 0.05$)

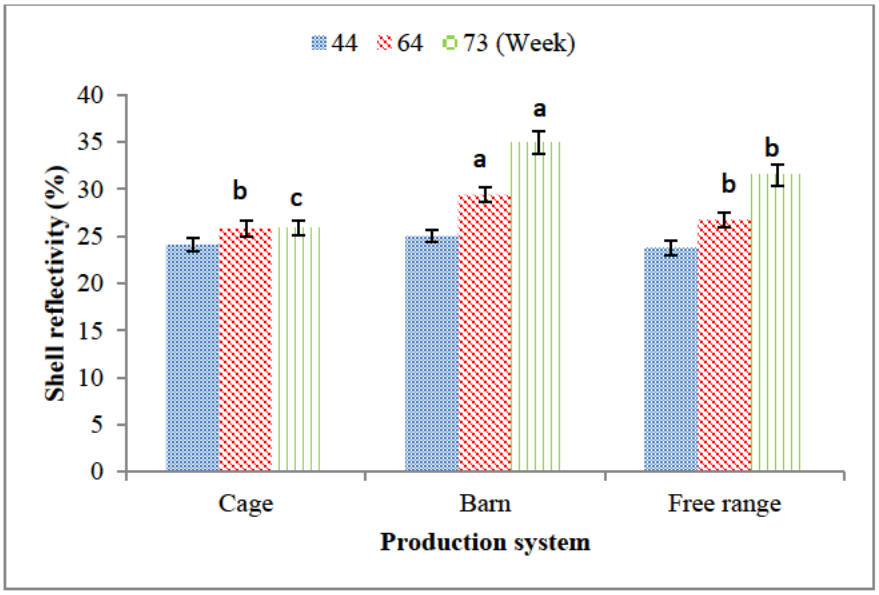

Figure 2.3 Interaction between flock age and production system (P < 0.0001)

Different superscripts show significant difference for the same age among production systems; Bars represent S.E.

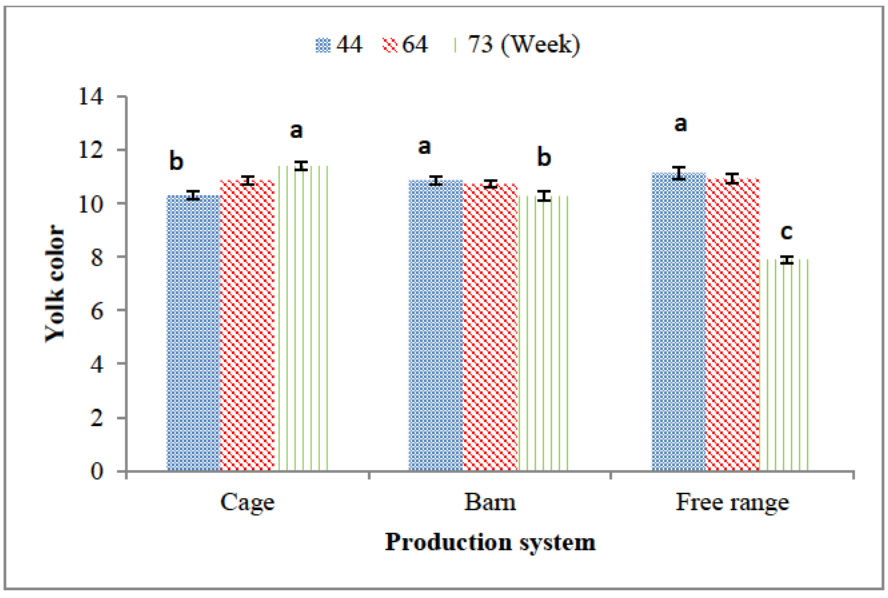

Figure 2.4 Interaction of flock age and production system (P < 0.0001)

Different superscripts show significant difference for the same age among production systems; Bars represent S.E.

Table 2.2 Eggshell and egg internal quality variables for cage and barn production systems at 68 weeks of age

Variable	Production system		P value
	Cage	Barn	
Shell reflectivity (%)	27.24±0.93	26.8±1.1	0.7573
Egg weight (g)	62.13±0.95	61.45±1.1	0.6468
Shell weight (g)	5.69±0.11	5.75±0.10	0.6684
Shell percentage	9.16±0.13	9.40±0.15	0.2149
Shell thickness (µm)	405.25±5.2	413.50±5.1	0.2647
Shell breaking strength (N)	321.72±8.40	263.67±8.13	0.2385
Deformation unit (µm)	10.76±0.26	10.83±0.17	0.8065
Albumen height (mm)	6.64±0.32	6.00±0.24	0.1141
Haugh unit	79.21±2.38	75.28±2.07	0.2165
Yolk colour	10.76±0.26	10.83±0.17	0.8065

Values are Mean±S.E.

2.5.2 Microscopic observations of the shell mammillary layer ultrastructure

For all the sixteen ultrastructural variables of mammillary layer observed, there was a significant main effect ($P < 0.05$) of production system on the variability of mammillary cap size, amount of confluence, incidence of early fusion, changed membrane and erosion (Table 2.3). Flock age significantly affected the incidence of early fusion and changed membrane. The interaction between production system and flock age was only significant for mammillary cap size, early and late fusion (Table 2.3). The cage eggs showed a significantly higher variability in the mammillary cap size compared with other production systems. The variability of the mammillary cap size increased with increased flock age. A significant interaction between production system and flock age was recorded for mammillary cap size, early fusion and late fusion (Figures 2.5-2.7). The amount of confluence was significantly higher in cage eggs compared with barn and free range eggs. The incidence of alignment was not significantly different among production systems and its values were closer to "isolated" on the measuring scale (Table 2.3). Other variables like type A bodies, type B bodies, aragonite, cubic, depression and erosion varied with production system and flock age. The incidence of cubic cone formation was higher in cage eggs compared with barn and free range production systems. There was significantly higher incidence of changed membrane in cage eggs with higher values at 64 week of flock age. The mean incidence of depression was higher

in barn eggs with a significantly higher level of incidence in 64 week flock eggs. The incidence of erosion was higher in cage eggs with no significant change with flock age. Cuffing and holes were not observed in any samples (Table 2.3). At 68 week of flock age, none of the mammillary layer ultrastructural variables was significantly affected by cage and barn production systems.

Table 2.3 Effect of production system and flock age on ultrastructural variables of shell mammillary layer

Variable	Production system			Flock age (week)			P value	
	Cage	Barn	Free range	44	64	73	P	A
Mammillary cap size	2.80±0.07[a]	2.53±0.09[b]	2.43±0.09[b]	2.60±0.09	2.63±0.08	2.53±0.09	0.0065	0.6807
Confluence	1.43±0.12[b]	2.03±0.20[a]	1.83±0.17[ab]	1.80±0.16	1.63±0.16	1.86±0.19	0.0480	0.6155
Cap quality	3.5±0.14[a]	2.9±0.11[b]	3.43±0.16[a]	3.23±0.11	3.33±0.14	3.26±0.17	0.0073	0.8824
Early fusion	2.26±0.13	2.10±0.15	2.23±0.13	2.53±0.11[a]	2.00±0.15[b]	2.06±0.12[b]	0.5918	0.0047
Late fusion	3.00±0.12	3.20±0.12	2.90±0.11	2.86±0.11	3.10±0.13	3.13±0.10	0.1243	0.1509
Alignment	1.36±0.14	1.13±0.06	1.43±0.14	1.30±0.11	1.40±0.14	1.23±0.11	0.2075	0.6362
Type A body	1.40±0.10	1.60±0.09	1.56±0.10	1.33±0.08	1.66±0.10	1.56±0.10	0.3134	0.0553
Type B body	2.56±0.14	2.56±0.14	2.43±0.13	2.30±0.10	2.60±0.14	2.66±0.16	0.7543	0.1684
Aragonite	1.13±0.06	1.30±0.11	1.13±0.06	1.20±0.11	1.06±0.04	1.30±0.08	0.2820	0.1557
Cubic	1.26±0.09	1.23±0.09	1.23±0.07	1.23±0.07	1.36±0.11	1.13±0.06	0.9538	0.1798
Cubic cone formation	1.63±0.12	1.30±0.09	1.36±0.11	1.40±0.11	1.53±0.11	1.36±0.11	0.0766	0.5180
Cuffing	1.00±0.00	1.00±0.00	1.00±0.00	1.00±0.00	1.00±0.00	1.00±0.00	0.9500	0.9500
Changed membrane	2.23±0.19[a]	1.60±0.14[b]	1.53±0.15[b]	1.50±0.16[b]	2.10±0.15[a]	1.76±0.17[b]	0.0031	0.0273
Depression	1.06±0.04	1.20±0.07	1.06±0.04	1.03±0.03	1.20±0.07	1.10±0.05	0.1570	0.1119
Erosion	1.33±0.10	1.23±0.07	1.03±0.03	1.26±0.09	1.13±0.06	1.20±0.07	0.0245	0.4804
Hole	1.00±0.00	1.00±0.00	1.00±0.00	1.00±0.00	1.00±0.00	1.00±0.00	0.9500	0.9500

P- Production system; A- Age; Values are Mean±S.E.

[a,b] Across a row, within each category, values with different superscripts are significantly different ($P < 0.05$)

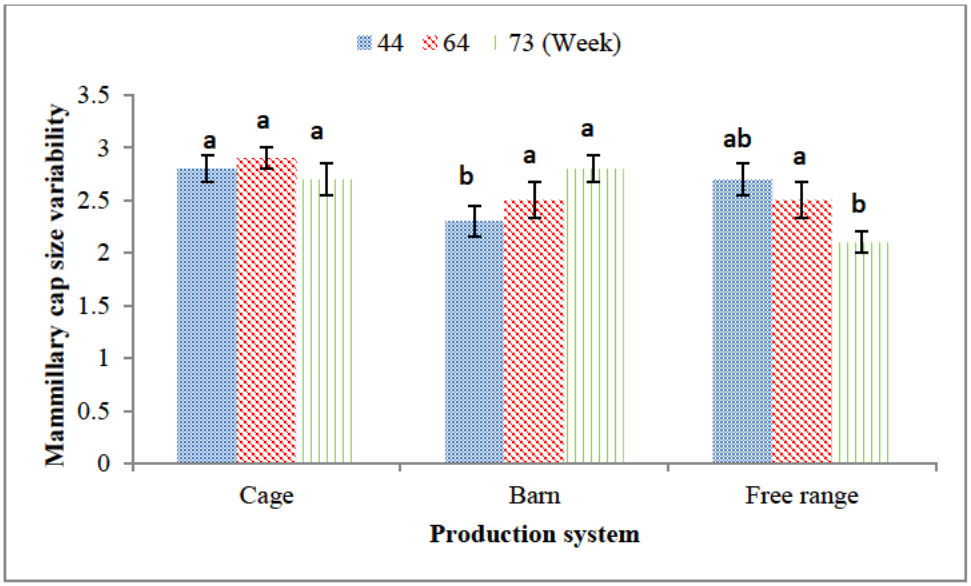

Figure 2.5 Interaction between production system and flock age (P=0.0056)

Different superscripts show significant difference for the same age among production systems; Bars represent S.E.

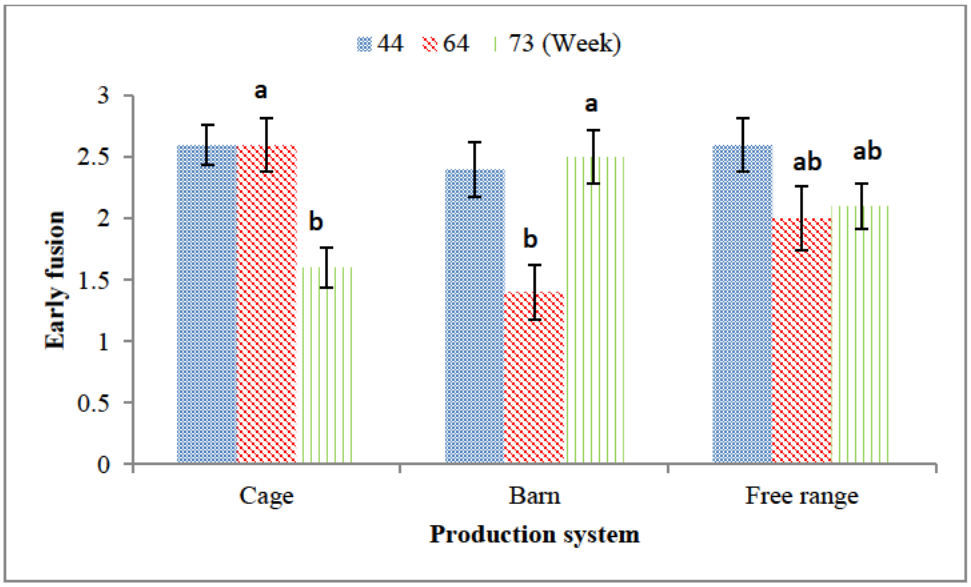

Figure 2.6 Interaction between production system and flock age (P=0.0002)

Different superscripts show significant difference for the same age among production systems; Bars represent S.E.

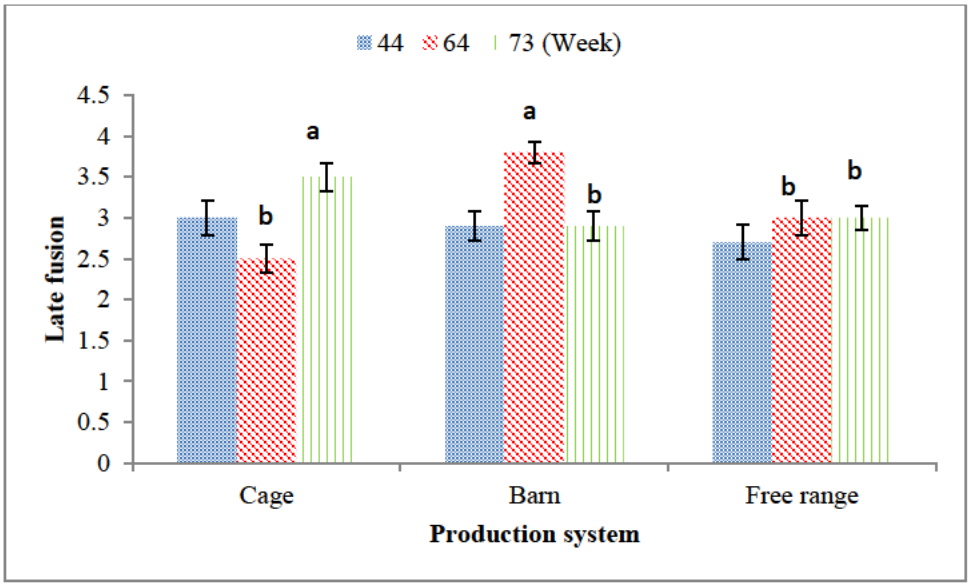

Figure 2.7 Interaction between production system and flock age (P<0.0001)

Different superscripts show significant difference for the same age among production systems; Bars represent S.E.

2.5.3 Cuticle cover estimation

When the completeness of cuticle cover was estimated by the single score value (ΔE^*_{ab}), the barn production system showed a significantly higher amount of cuticle cover compared with cage eggs (Figure 2.8). There was no significant interaction between production system and flock age for the amount of cuticle present on the eggshell surface. Comparing the three flock ages, the 44 week flock eggs had a significantly higher amount of cuticle followed by 73, whereas, 64 and 73 week were not significantly different (Figure 2.9). Comparing the cage and barn production systems at 68 week of age for the cuticle cover, there were no statistically significant differences.

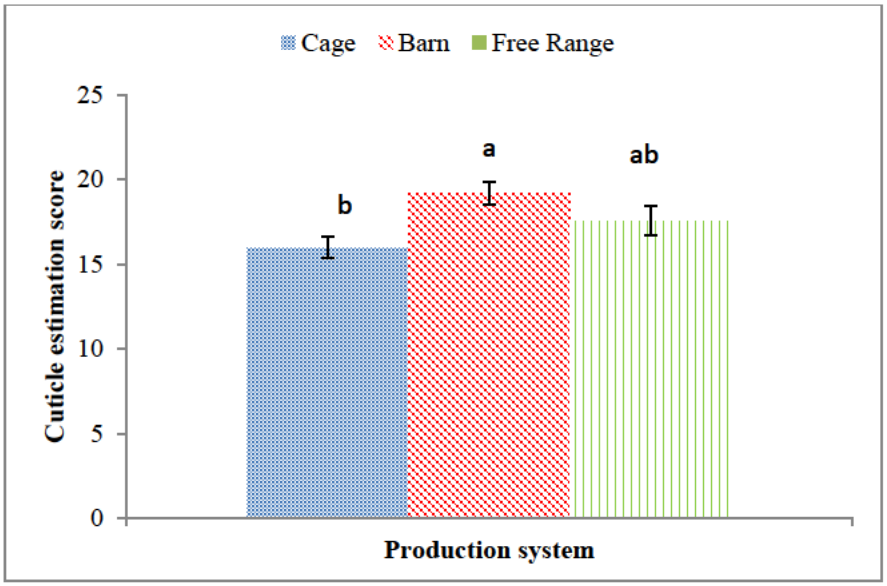

Figure 2.8 Effect of production system on cuticle cover (P=0.0057)

Different superscripts show significant difference among production systems; Bars represent S.E.

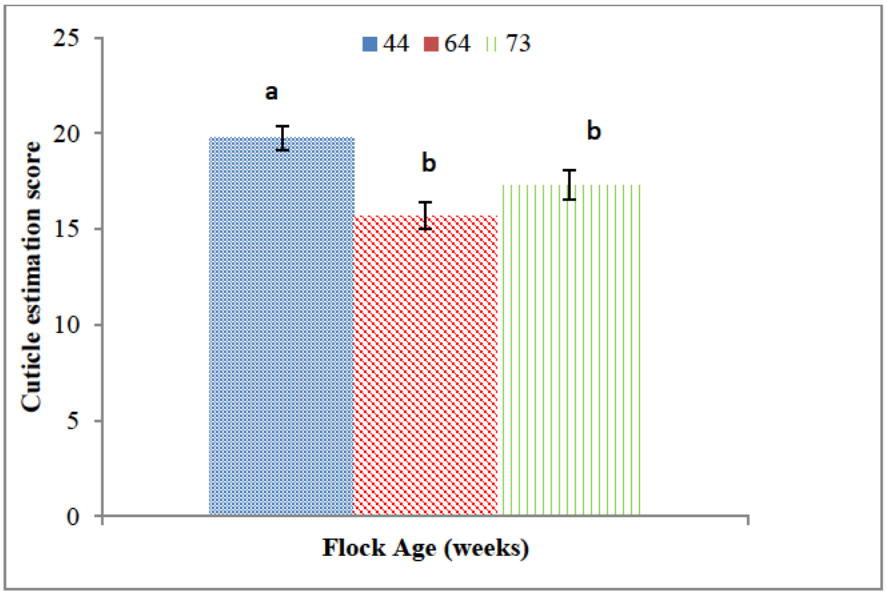

Figure 2.9 Effect of flock age (week) on cuticle cover (P=0.0003)

Different superscripts show significant difference among different ages; Bars represent S.E.

2.5.4 Shell reflectivity and L*a*b* measurements

There was a significant effect of production system and flock age on shell reflectivity and L* values measured on shells with and without cuticle (Table 2.4). When the values of shell reflectivity and L* were compared among different age groups, the 44 week flock eggs had significantly lower values, and the values increased linearly with increasing flock age. A similar pattern was observed for shells from which cuticle layer had been removed (Table 2.4). The a* values for eggshells with and without cuticle and the difference between the two were significantly affected by production system, flock age and interaction between them (Table 2.4). The a* for eggshells with and without cuticle was significantly higher in cage eggs, followed by free range. The a* for eggshells with and without cuticle decreased significantly with increasing flock age (Table 2.4). The difference for a* was only significant between barn and free range systems and between 64 and 73 week flocks age. The b* values for eggshell with and without cuticle were significantly affected by production system and flock age; however, the interaction was only significant for eggshells without cuticle. The difference between the two was only significantly affected by flock age and interaction between production system and flock age (Table 2.4). For b* with cuticle, the barn system was significantly different from cage and free range systems and 73 week flock age was different from 44 and 64 week flocks. The value for b* without cuticle, was significantly different only between barn and cage systems and was significantly different among all flock age groups. The value for b* with and without cuticle was only significantly different for the 44 week flock as compared with the 64 and 73 week flocks. For the 68 week old flock, there were differences between the cage and barn production systems only for reflectivity of shell with cuticle, the difference in reflectivity with and without cuticle and the difference in L* with and without cuticle (Table 2.5).

Table 2.4 Shell reflectivity (%) and L*a*b* values as affected by production system and flock age

Variable	Production system			Flock age (week)			P value	
	Cage	Barn	Free range	44	64	73	P	A
Reflectivity with cuticle	25.28±0.45^{c}	29.86±0.63^{a}	27.59±0.64^{b}	24.98±0.36^{c}	27.27±.52^{b}	30.48±0.75^{a}	<0.0001	<0.0001
Reflectivity without cuticle	32.86±0.55^{b}	36.30±0.62^{a}	34.24±0.60^{b}	31.50±0.42^{c}	34.23±0.51^{b}	37.67±0.68^{a}	<0.0001	<0.0001
Difference	**7.58±0.35^{a}**	**6.44±0.35^{b}**	**6.66±0.37^{ab}**	**6.52±0.33**	**6.97±0.39**	**7.19±0.73**	**0.0578**	**0.4020**
L* with cuticle	62.03±0.41^{c}	65.89±0.56^{a}	63.71±0.57^{b}	61.49±0.33^{c}	63.42±0.48^{b}	66.71±0.62^{a}	<0.0001	<0.0001
L* without cuticle	68.55±0.43^{c}	71.54±0.48^{a}	70.00±0.47^{b}	67.69±0.36^{c}	69.99±0.39^{b}	72.41±0.52^{a}	<0.0001	<0.0001
Difference	**6.51±0.27**	**5.65±0.26**	**6.29±0.38**	**6.19±0.29**	**6.57±0.35**	**5.69±0.28**	**0.1118**	**0.1211**
a* with cuticle	17.02±0.23^{a}	14.65±0.33^{c}	16.19±0.34^{b}	17.57±0.17^{a}	16.27±0.27^{b}	14.02±0.36^{c}	<0.0001	<0.0001
a* without cuticle	14.48±0.25^{a}	12.38±0.28^{c}	13.38±0.27^{b}	14.99±0.19^{a}	13.48±0.23^{b}	11.76±0.31^{c}	<0.0001	<0.0001
Difference	**2.53±0.13^{ab}**	**2.27±0.13^{b}**	**2.80±0.19^{a}**	**2.57±0.13^{ab}**	**2.78±0.18^{a}**	**2.25±0.13^{b}**	**0.0311**	**0.0288**
b* with cuticle	29.11±0.23^{a}	27.96±0.24^{b}	28.67±0.23^{a}	29.14±0.20^{a}	28.78±0.22^{a}	27.82±0.28^{b}	0.0026	0.0002
b* without cuticle	27.30±0.27^{a}	26.23±0.30^{b}	26.70±0.25^{ab}	27.98±0.19^{a}	26.80±0.27^{b}	25.44±0.30^{c}	0.0096	<0.0001
Difference	**1.80±0.27**	**1.73±0.17**	**1.97±0.21**	**1.15±0.22^{b}**	**1.98±0.23^{a}**	**2.37±0.18^{a}**	**0.6975**	**0.0001**

Values are Mean±S.E.; ^{a,b,c} Across the row, in each category, indicate significant difference

Table 2.5 Shell reflectivity (%) and L* values as affected by production systems at 68 week of flock age

Variable	Production system		P value
	Cage	Barn	
Reflectivity with cuticle	24.17±1.83[a]	27.00±0.81[b]	0.0302
Reflectivity without cuticle	33.27±1.00	32.70±0.81	0.6617
Difference	**9.10±0.68[a]**	**5.70±0.49[b]**	**0.0001**
L* with cuticle	61.38±1.00	63.60 ±0.73	0.0811
L* without cuticle	69.19 ±0.76	68.41± 0.67	0.4451
Difference	**7.80±0.64[a]**	**4.81±0.41[b]**	**0.0002**
a* with cuticle	17.18±0.63	16.26±0.43	0.2384
a* without cuticle	14.32±0.53	13.86±0.36	0.4733
Difference	**2.85±0.33**	**2.41±0.23**	**0.2739**
b* with cuticle	28.91±0.53	27.87±0.42	0.1388
b* without cuticle	26.57±0.56	26.27±0.50	0.6873
Difference	**2.32±0.36**	**1.60±0.31**	**0.1350**

Values are Mean±S.E.

[a,b] Across the row, indicate significant difference among different production systems

2.5.5 Protoporphyrin IX quantification from shell with and without cuticle

There was a significant main effect ($P < 0.05$) of production system and flock age, but no significant interaction between the two, on the amount of protoporphyrin IX (PP IX) in 1 g of whole eggshell and eggshell from which the cuticle layer had been removed (Table 2.6). When the amount of PP IX was calculated in the cuticle layer of 1 g of eggshell, neither the production system nor the flock age, nor interaction between the two was statistically significant (Table 2.6). Comparing the three production systems together, eggs from the cage production system showed significantly higher amount of PP IX in 1 g of whole eggshell and shell without cuticle. However, the difference was not significant between barn and free range eggs although free range eggs had a slightly higher mean amount of PP IX. The amount of PP IX in the cuticle layer of 1 g of eggshell was not different among the three commercial layer production systems (Table 2.6). The amount of PP IX in 1 g of whole eggshell tended to be higher in eggs from the 44 week flock, followed by the 64 and 73 week old flocks. At 68 week of flock age, between cage and barn

production systems, the amount of PP IX in 1 g of eggshell (with, without cuticle and in the cuticle layer) was not significantly different although there was a slightly higher amount of PP IX in cage eggs (Table 2.6).

Table 2.6 The amount of protoporphyrin IX in 1 g of shell with, without and in cuticle as affected by production system and flock age

Variable	Production system			Flock age (week)			P value	
	Cage	Barn	Free range	44	64	73	P	A
PP IX in whole shell	$^{a}9.49\times10^{-8}$	$^{b}8.24\times10^{-8}$	$^{b}8.64\times10^{-8}$	$^{a}9.35\times10^{-8}$	$^{b}8.74\times10^{-8}$	$^{b}8.26\times10^{-8}$	<0.0001	<0.0001
PP IX in shell without cuticle	$^{a}7.90\times10^{-8}$	$^{b}6.90\times10^{-8}$	$^{b}7.28\times10^{-8}$	$^{a}7.84\times10^{-8}$	$^{b}7.36\times10^{-8}$	$^{c}6.88\times10^{-8}$	<0.0001	<0.0001
PP IX in cuticle	1.60×10^{-8}	1.35×10^{-8}	1.36×10^{-8}	1.51×10^{-8}	1.38×10^{-8}	1.42×10^{-8}	0.1603	0.6284

Variable	Cage system at 68 week of age	Barn system at 68 week of age	P value (production system)
PP IX in whole shell	9.94×10^{-8}	9.28×10^{-8}	0.0761
PP IX in shell without cuticle	8.36×10^{-8}	7.98×10^{-8}	0.3066
PP IX in cuticle	1.58×10^{-8}	1.30×10^{-8}	0.3050

PP IX is protoporphyrin IX measured in mMoles; Values are Mean

^{a,b,c} Across a row, indicate significant difference among different production systems and age groups

P- Production system; A- Age

2.6 Discussion

2.6.1 Eggshell and egg internal quality measurements

In the current study, shell reflectivity (%) was significantly ($P < 0.0001$) affected by production system, flock age and the interaction between the two (Table 2.1). Lower shell reflectivity values for cage eggs indicated that these eggs were more brown than barn and free range eggs. A higher shell reflectivity values for the 73 week old flock indicated that these eggs were lighter in colour compared with the other age groups. A decrease in brown eggshell colour with flock age has previously been reported (Sekeroglu et al., 2010; Samiullah et al., 2014). Egg weight is an important trait that influences egg quality as well as grading and is determined without breaking the egg. A significantly higher egg weight for free range production system indicates that egg weight is not always higher for cage production systems. No previous study has compared directly eggs from birds reared together and then allocated to three different production systems. The variation among reports on the effects of production system could be due to multiple factors, such as flock age at sample collection, environmental temperature, feed, and hen strain (Van Den Brand et al., 2004; Hidalgo et al., 2008; Varguez-Montero et al., 2012; Lolli et al., 2013; Samiullah et al., 2014). Generally, egg weight increases with increasing flock age and a similar trend was observed in the present study. Similar to egg weight, shell weight is also an important egg quality parameter. In the present study, shell weight was not different among production systems and flock ages. Percentage shell, which is the ratio of shell weight to egg weight, decreased with increasing flock age but was not affected by the production systems and similar results were obtained by Sekeroglu et al. (2010) and Samiullah et al. (2014). However, Hidalgo et al. (2008) recorded a higher percentage shell for cage eggs and other researchers (Van- Den Brand et al., 2004; Wang et al., 2009) reported higher percentage shell for a free range system. Different strains of laying hens and diets could account for the variability in reported results. A desirable shell should be thick enough to resist transportation and handling shock. A linear decrease in shell thickness values with increasing flock age may indicate that the hen either accumulated less calcium during each shell formation cycle or the same

amount of calcium was distributed over a relatively larger surface area of the shell (Table 2.1).

Shell breaking strength (BSN) and shell deformation (µm) assess the ability of the shell to withstand a certain amount of force. A higher shell breaking strength and shell deformation indicate that the shell is strong enough to withstand to a certain amount of force and are more resistant to breaking during handling and transportation. Shell breaking strength and shell deformation were not affected by production system (Table 2.1). Previously, a higher shell breaking strength has been recorded for cage eggs compared with other egg production systems (Mertens et al., 2006). However, age significantly affected the shell breaking strength and the values decreased with increasing flock age.

Freshness, which is mainly evaluated by albumen height and Haugh unit, is the main determinant of table egg internal quality. A significantly higher albumen height and Haugh unit in the free range system indicated that these eggs were better in internal quality compared with the other two production systems. However, the difference between cage and barn eggs was not statistically significant. Previous reports (Silversides and Scott, 2001; Van Den Brand et al., 2004; Hidalgo et al., 2008; Kucukyilmaz et al., 2012; Roberts and Chousalkar, 2012) on albumen height and Haugh unit varied in methodology, flock age and experimental design and none of them can be directly compared with the results of our current study. A darker yolk colour is highly desirable by consumers in many countries including Australia (Roberts, 2004). The yolk colour depends mainly on the amount of xanthophyll added to the feed. In the present study, lower yolk colour values for free range might indicate that the amount of xanthophyll consumed by free range hens was less than the cage and barn system hens perhaps the hens were foraging and thus eating less of the provided diet. The yolk colour was significantly affected by flock age, with a higher intensity of yolk colour observed for the 64 week hens.

2.6.2 Microscopic observations of the shell mammillary layer ultrastructure

The mammillary layer ultrastructural variables are usually observed to determine their level of incidence and variability in individual eggshells. Ultrastructural features, such as lower variability of mammillary cap size, higher incidence of

confluence, completeness of cap cover, a higher incidence of early fusion and cuffing increases mammillary layer strength by enhancing the attachment of shell membrane into the mammillary cone layer. Other variables when present in higher incidence lay a poor foundation for the remaining layers and also decrease the shell membrane attachment and thus reduce shell quality. These variables are; higher incidence of late fusion, alignment, type A bodies, type B bodies, cubics, aragonite, depression, erosion and hole. In the present study, none of the eggshells showed identical mammillary layer features which indicates that the mammillary layer is highly variable despite being constructed of the same basic material, calcite.

The mammillary caps arise from the deposition of calcium carbonate into the shell membrane fibres (Figure 2.10). There was a significant greater variability in mammillary cap size in cage eggs compared with barn and free range eggs, suggesting that the attachment of cap to shell membrane was less consistent in cage eggs as previously recorded (Samiullah et al., 2014). Shell quality decreases with increasing flock age (Nascimento et al., 1992). An average size of the mammillary cones is reported to positively influence mammillary layer thickness (Liao et al., 2013). Cap quality is evaluated by the ratio of the cap size that covers the overall surface of the underlying mammillary cone (Figures 2.10 and 2.11). A cone evenly covered by the cap indicates a firm attachment of the mammillary cone into the shell membrane. In the present study, significantly lower cap values for barn eggs suggests that these eggs had good mammillary cap size with firm attachment to the shell membrane (Table 2.3). A high incidence of early fusion increases the bonding strength between mammillary cones and has a positive effect on mammillary layer strength (Parsons, 1982). A significantly higher incidence of early fusion in the 44 week old flock indicates that growth of the palisade column commenced earlier during shell formation in the youngest flock. Unlike early fusion, late fusion slows the commencement of growth of the palisade columns and reduces the effective thickness of the shell (Solomon, 2010). In the present study, a higher incidence of late fusion observed in barn eggs might suggests that the growth of the palisade columns was slower during shell formation. Alignment arises where there is a hair like marked line passing across adjacent cones. A higher incidence of alignment has a negative effect on shell strength. Alignment is considered to facilitate crack propagation, and is more easily observed (if present) when shell samples are viewed at lower magnifications (e.g. x22). In the present study, neither the production

system nor the flock age significantly affected the incidence of alignment; however, the values were slightly higher for free range eggs (Table 2.3). The overall low incidence of alignment in the present study indicates that the eggshells were less prone to micro-cracks. The type A and type B bodies, aragonite and cubics arise when the crystallized calcium fails to deposit into proper cone structures (Figures 2.12 and 2.13). The exact mechanism of the formation behind these structures is not known; however, stress is believed to play a role in their formation. The higher incidence of these bodies in the mammillary layer increases the gap between true cones. However, our microscopic observations showed no significant difference in the incidence of these bodies among production systems at different flock ages. Also, the overall incidence was closer to "isolated" on the measuring scale, indicating that such crystallized bodies were rarely observed during scanning of the shell surface. A higher incidence of cubic cone formation might result in a firm bonding of the cone to the shell membrane and also provides a solid foundation for the initiation of palisade layer. The higher incidence of cubic cone formation in cage eggs might indicates that the cone to membrane attachment was better compared with barn and free range eggs. The effect of flock age was not clear, as there was no significant difference among age groups for the incidence of cubic cone formation. A slightly higher incidence of erosion observed in cage eggs might explain the poor mammillary layer quality in these eggs; however, the overall incidence was nearer to "isolated" on the measuring scale, which shows these variables were rarely observed.

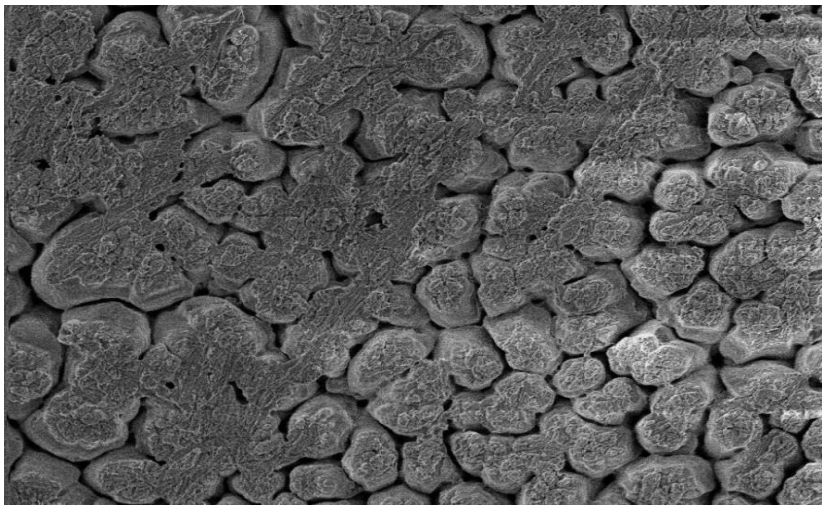

Figure 2.10 Good caps cover with confluence

(Magnification x150, Scale bar 200 µm)

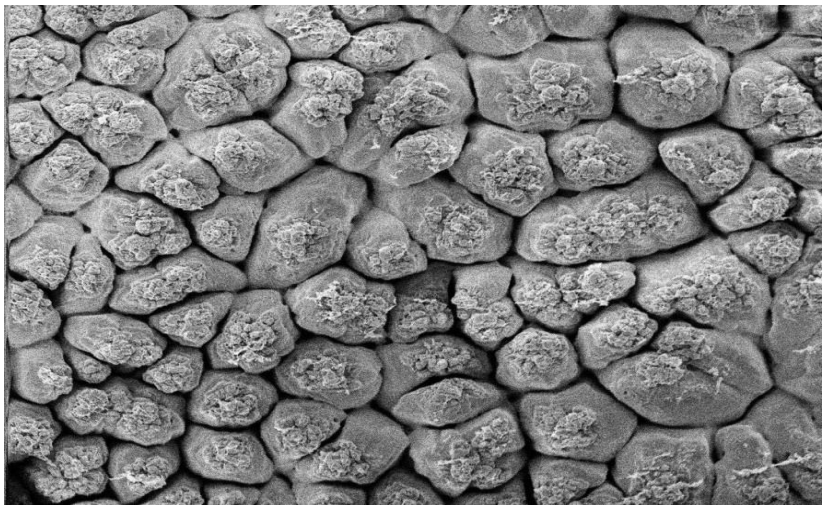

Figure 2.11 Variable cap size with poor caps

(Magnification x150, Scale bar 200 µm)

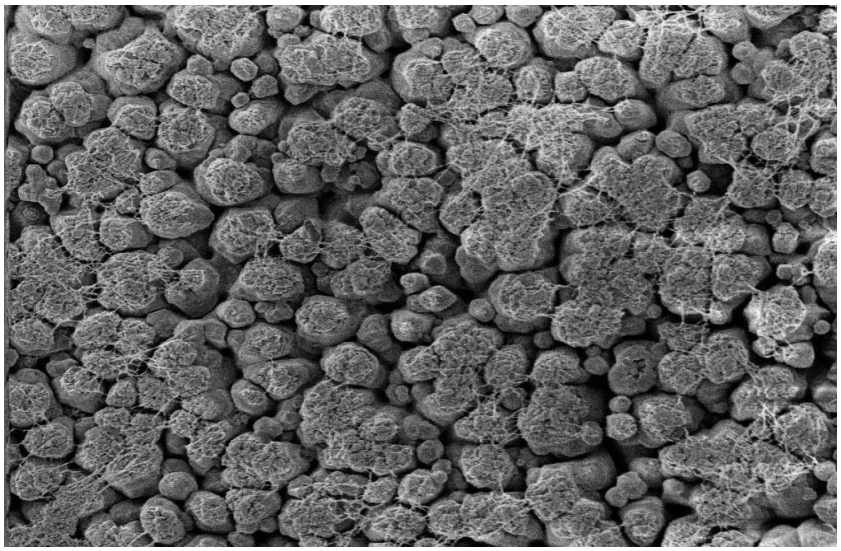

Figure 2.12 Extensive B bodies with some changed membrane

(Magnification x150, Scale bar 200 µm)

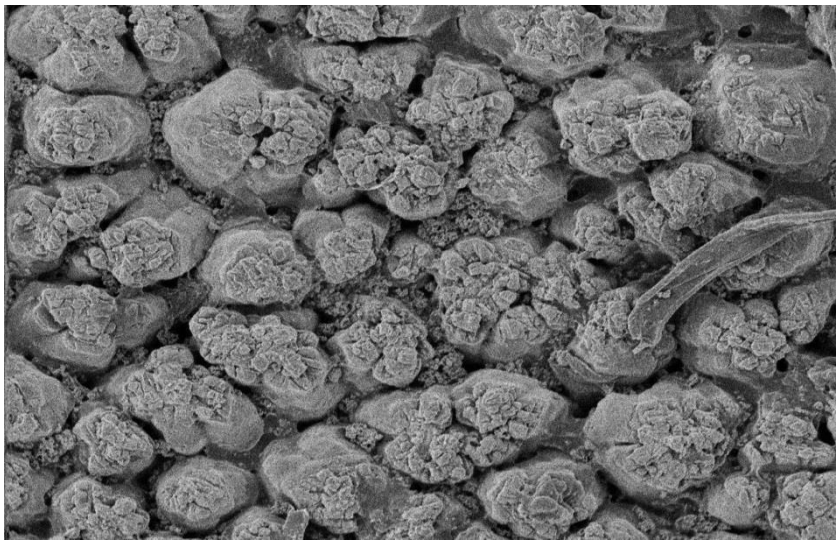

Figure 2.13 Extensive aragonite in the shell mammillary layer

(Magnification x240, Scale bar 100 µm)

Summarizing the results of mammillary layer ultrastructure, none of the production systems were consistently higher or lower for all the sixteen variables microscopically observed and similar pattern was observed for flock age. Based on either a higher or lower incidence of a single variable, it is difficult to make a definitive statement that a particular shell is either strong or weak. It seems that the

mammillary layer ultrastructure is affected by multiple factors possibly including production system and flock age.

2.6.3 Cuticle cover estimation

A significantly higher completeness of cuticle cover in eggs from the barn production system, followed by eggs from the free range production system, indicate that cage eggs do not always have more cuticle cover as previously reported (Samiullah et al., 2014). It is not known how the various management systems affect the cuticle deposition onto the palisade layer in the last stage of shell formation in hen shell gland. A contributory factor to the variation of cuticle cover among different commercial production systems could be selection pressure, which has been removed due to artificial incubation and handling in commercial poultry (Bain et al., 2013). The MST cuticle blue dye used for cuticle estimation in this study has previously been tested to be a reliable indicator of the amount of cuticle present on the egg surface (Samiullah and Roberts, 2013), thus higher ΔE^*_{ab} values for the barn system showed good cuticle cover (Figure 2.8). Fluctuation of the cuticle cover with flock age again indicates that there is an effect of flock age on cuticle cover.

2.6.4 Shell reflectivity and L*a*b* measurements

The main objective of measuring the shell reflectivity and L* of eggshells before and after removing the cuticle cover was to evaluate the location of pigment in the calcareous eggshell and cuticle. Similar to our previous report (Samiullah and Roberts, 2013), we found that, after removing the cuticle cover completely without damaging the underlying structure, there was still a significant amount of pigment remaining as shown by the difference in values in Table 2.4. An increase in shell reflectivity and L* values with increasing flock age that shell colour decreased with increasing flock age (Table 2.4). It is not clear how the amount of pigment synthesized and deposited into the shell is affected by flock age. A slightly different pattern in L* from shell reflectivity could be due to the a* and b* hue components of L* or from the effect of shell surface roughness on shell reflectivity (rougher shells have lower reflectivity). Brown eggshell colour does appear not to be affected by egg size as, in this study, we found no correlation (R^2=0.001) between egg weight and L* values for eggs with cuticle intact. Similarly, the correlation between

egg weight and shell reflectivity was R^2=0.002. Odabasi et al. (2007) have proposed increase in egg size as a possible factor for lighter eggshell colour towards the end of production cycle, speculating that the same amount of protoporphyrin IX is deposited onto a larger surface area of the eggshell.

2.6.5 Protoporphyrin IX quantification from shell with and without cuticle

A statistically higher amount of protoporphyrin IX (PP IX) present in 1 g of shell in cage eggs shows that the production systems does significantly affect eggshell colour with cage eggs being more brown compared with other production systems. The higher amount of PP IX in 1 g of whole eggshell compared with the same amount in 1 g of cuticle indicates that there is more pigment in the underlying calcareous shell than in the cuticle alone. Our previous study (Samiullah and Roberts, 2013) found a similar result of more pigment in the calcareous shell than in the cuticle. The greater amount of PP IX in the calcareous eggshell raises the possibility that the deposition of pigment onto the shell layers may start with the formation of individual shell layers and that pigment synthesis and its related gene expression may occur as the shell is passing through the magnum of the oviduct. A significantly higher amount of cuticle cover and lower amount of PP IX in 1g of shell in barn eggs provides evidence that the amount of pigment is independent of the cuticle cover. Further work is needed to quantify the pattern of pigment synthesis and the related gene expression in the shell gland, in relation to shell formation.

2.7 Conclusions

In conclusion, when birds reared together were allocated to different production systems prior to the onset of lay, there were relatively few differences among production systems for egg quality measurements. Eggs from the cage production system were darker in colour and contained more protoporphyrin mainly within the calcareous part of the shell. For the barn production system, the completeness of cuticle cover was higher and egg weight generally lower. The differences in egg quality in relation to flock age are similar to those reported previously.

2.8 References

AECL, 2014. Australian Egg Corporation Limited Annual Report. Online Retrieved From: https://www.aecl.org/assets/Uploads/Annual-Reports/AECL-Annual-Report-2014.pdf

Anderson, K. E. 2009. Overview of natural and organic egg production: Looking back to the future. J. Appl. Poultry Res. 18:348-354.

Anderson, K. E., and K. W. Koelkebeck. 2007. Realistic views concerning poultry welfare. Poult. Sci. 86:1251-1252.

Appleby, M. C. 2003. The European Union ban on conventional cages for laying hens: history and prospects. J. Appl. Anim. Welf. Sci. 6:103-121.

Arias, J. L, D. J. Fink, S. Q. Xiao, A. H. Heuer, and A. I. Caplan. 1993. Biomineralization and eggshells: cell-mediated acellular compartments of mineralized extracellular matrix. Int. Rev. Cytol. 45:217-250.

Bain, M. M., K. Mcdade, R. Burchmore, A. Law, P. W. Wilson, M. Schmutz, R. Preisinger, and I. C. Dunn. 2013. Enhancing the egg's natural defence against bacterial penetration by increasing cuticle deposition. Anim. Genet. 44:661-668.

Curtis, P. A., F. A. Gardner, and D. B. Mellor. 1985. A comparison of selected quality and compositional characteristics of brown and white shell eggs. II. Interior quality. Poult. Sci. 64:302-306.

Faure, J. M. Rearing conditions and needs for space and litter in laying hens 1991. Appl. Anim. Behav. Sci. 31:111-117.

Fernandez, M. S., C. Escobar, I. Lavelin, M. Pines, and J. L. Arias. 2003. Localization of osteopontin in oviduct tissue and eggshell during different stages of the avian egg laying cycle. J. Struct. Biol. 143:171-180.

Hidalgo, A., M. Rossi, F. Clerici, and S. Ratti. 2008. A market study on the quality characteristics of eggs from different housing systems. Food Chem. 106:1031-1038.

Hincke, M. T., J. Gautron, Y. Nys, A. B. Rodriguez-Navarro, and M. D. McKee. 2011. The eggshell: structure and productive function, in: Nys, Y., Bain, M. & Immerseel, F.V. (Eds) Improving the safety and quality of eggs and egg products, Vol. 1, pp. 151-182 (Woodhead Publishing Limited).

Hodges, R. D. 1974. The histology of the fowl. Academic Press Inc. London.

Hy-Line Australia. 2016. Hy-Line Brown Commercial Layers - Australia. Accessed March 24 2016: http://Hy-Line.specialisedbreeders.com.au/wp-content/uploads/2016/03/BRN-COM-AUS.pdf

Ishikawa, S., K. Suzuki, E. Fukuda, K. Arihara, Y. Yamamoto, T. Mukai, and M. Itoh. 2010. Photodynamic antimicrobial activity of avian eggshell pigments. FEBS Lett. 584:770-774.

Jones, D. R., M. T. Musgrove, K. E. Anderson, and H. S. Thesmar. 2010. Physical quality and composition of retail shell eggs. Poult. Sci. 89:582-587.

Kennedy, G. Y., and H. G. Vevers. 1973. Eggshell pigments of the Araucano fowl. Comp. Biochem. Physiol., B: Comp. Biochem. 44:11-25.

Kucukyilmaz, K., M. Bozkurt, E. N. Herken, M. Cinar, A. U. Cath, E. Bintas, and F. Coven. 2012. Effects of rearing systems on performance, egg characteristics and immune response in two layer hen genotype. Asian-Australas. J. Anim. Sci. 25:559-568.

Leleu, S., W. Messens, K. De Reu, S. De Preter, L. Herman, M. Heyndrickx, J. De Baerdemaeker, C. W. Michiels, and M. Bain. 2011a. Effect of egg washing on the cuticle quality of brown and white table eggs. J. Food Protect. 74:1649-1654.

Leleu, S., M. Bain, L. Herman, M. Heyndrickx, J. De Baerdemaeker, C. W. Michiels, C. Perianu, and W. Messens. 2011b. The effect of micro cracks and the presence of the cuticle on trans-shell penetration of table eggs by *Salmonella* Enteritidis. Proceedings of Egg Meat Symposia Leipzig, Germany, September 4-8.

Liao, B., H. G. Qiao, X. Y. Zhao, M. Bao, L. Liu, C. W. Zheng, C. F. Li, and Z. H. Ning. 2013. Influence of eggshell ultrastructural organization on hatchability. Poult. Sci. 92:2236-2239.

Lolli, S., A. Hidalgo, C. Alamprese, V. Ferrante, and M. Rossi. 2013. Layer performances, eggshell characteristics and bone strength in three different housing systems. Biotech. Anim. Husbandry 29:591-606.

Mertens, K., I. Vaesen, J. loffel, B. Kemps, B. Kamers, C. Perianu, J. Zoons, P. Darius, E. Decuypere, J. De Baerdemaeker, and B. De Ketelaere. 2010. The transmission colour value: A novel egg quality measure for recording shell colour used for monitoring the stress and health status of a brown layer flock. Poult. Sci. 89:609-617.

Mertens, K., F. Bamelis, B. Kemps, B. Kamers, E. Verhoelst, B. De Ketelaere, M. Bain, E. Decuypere, and J. De Baerdemaeker. 2006. Monitoring of eggshell breakage and eggshell strength in different production chains of consumption eggs. Poult. Sci. 85:1670-1677.

Messens, W., K. Grijspeerdt, and L. Herman. 2005. Eggshell characteristics and penetration by *Salmonella enterica* serovar Enteritidis through the production period of a layer flock. Br. Poult. Sci. 46:694-700.

Mine, Y., and J. Kovacs-Nolan. 2004. Biologically active hen egg components in human health and disease. J. Poult. Sci. 41:1-29.

Miksik, I., V. Holan, and Z. Deyl. 1996. Avian eggshell pigments and their variability. Comp. Biochem. Physiol., Part B: Biochem. Mol. Biol. 113:607-612.

Nascimento, V. P., S. Cranstoun, and S. E. Solomon. 1992. Relationship between shell structure and moment of *Salmonella* Enteritidis across the eggshell wall. Br. Poult. Sci. 33:37-48.

Nys, Y., J. Gautron, J. M. Garcia-Ruiz, and M. T. Hincke. 2004. Avian eggshell mineralization: biochemical and functional characterization of matrix proteins. C. R. Palevol. 3:549-562.

Nys, Y., M. T. Hincke, J. L. Arias, J. M. Garcia-Ruiz, and S. Solomon. 1999. Avian eggshell mineralization. Poult. Avian Biol. Rev. 10:143-166.

Odabasi, A. Z., R. D. Miles, M. O. Balaban, and K. M. Porier. 2007. Changes in brown eggshell colour as the hen ages. Poult. Sci. 86:356-363.

Parsons, A. H. 1982. Structure of the eggshell. Poult. Sci. 61:2013-2021.

Poole, H. K. 1965. Spectrophotometric identification of eggshell pigments and timing of superficial pigment deposition in the Japanese quail. Proc. Soc. Exp. Biol. Med. 119:547-551.

Primary Industries Standing Committee 2002. Model Code of Practice for the Welfare of Animals, Domestic Poultry 4th Edition. CSIRO Publishing, Collingwood, Victoria, Australia.

Reid, J. 1983. The use of the plasma chemistry unit as an aid to the scanning electron microscope study of avian eggshell structure. Br. Poult. Sci. 24:233-235.

Roberts, J. R., K. Chousalkar, and Samiullah. 2013. Egg quality and age of laying hens: implications for product safety. Anim. Prod. Sci. 53:1291-1297.

Roberts, J. R., and K. K. Chousalkar. 2012. Egg quality and food safety of table eggs: egg quality and age of flock – a horizontal study. Proc. Aust. Poult. Sci. Symp. 23:241-244.

Roberts, J. R. 2004. Factors affecting egg internal quality and egg shell quality of laying hens. J. Poult. Sci. 41:161-177.

Rose, M. L. H., and M. T. Hincke. 2009. Protein constituents of the eggshell: eggshell-specific matrix proteins. Cell. Mol. Life Sci. 66:2707-2719.

Samiullah, J. R. Roberts, and K. K. Chousalkar. 2014. Effect of production system and flock age on egg quality and total bacterial load in commercial laying hens. J. Appl. Poultry Res. 23:59-70.

Samiullah, S., and J. R. Roberts. 2013. The location of protoporphyrin in the eggshell of brown-shelled eggs. Poult. Sci. 92:2783-2788.

SAS Institute. 2004. SAS User's Guide: Statistics. Edition 9.1 . SAS Institute Inc., Cary, NC.

Sekeroglu, A., M. Sarica, E. Demir, Z. Ulutas, M. Tilki, M. Saatci, and H. Omed. 2010. Effects of different housing systems on some performance traits and egg qualities of laying hens. J. Anim. Vet. Adv. 9:1739-1744.

Silversides, F. G., and T. A. Scott. 2001. Effect of storage and layer age on quality of eggs from two lines of hens. Poult. Sci. 80:1240-1245.

Solomon, S. E. 2010. The eggshell: strength, structure and function. Br. Poult. Sci. 51:52-59.

Solomon, S. E., M. M. Bain, S. Cranstoun, and V. Nascimento. 1994. Hen's eggshell structure and function. In: Board RG, Fuller R, editors. Microbiology of the Avian Egg: Springer US. pp. 1-24.

Solomon, S. E. 1991. Egg and shell quality. Published by Wolfe publishing ltd. England. P. 149.

Sorensen, J. T., S. Edwards, J. Noordhuizen, and S. Gunnarsson. 2006. Animal production systems in the industrialized world. Rev. Sci. Off. Tech. Int. Epiz. 25:493-503.

Van Den Brand, H., H. K. Parmentier, and B. Kemp. 2004. Effects of housing system (outdoor vs cages) and age of laying hens on egg characteristics. Br. Poult. Sci. 45:745-752.

Varguez-Montero, G., L. Sarmiento-Franco, R. San- tos-Ricalde, and J. Segura-Correa. 2012. Egg production and quality under three housings in the tropics. Trop. Anim. Health Prod. 44:201-204.

Wang, X. L., J. X. Zheng, Z. H. Ning, L. J. Qu, G. Y. Xu, and N. Yang. 2009. Laying hen performance and egg quality of blue-shelled layers as affected by different housing systems. Poult. Sci. 88:1485-1492.

With, T. K. 1973. Porphyrin in eggshell. Biochem. J. 137:597-598.

Higher Degree Research Thesis by Publication
University of New England

STATEMENT OF AUTHORS' CONTRIBUTION

(To appear at the end of each thesis chapter submitted as an article/paper)

We, the Research Master/PhD candidate and the candidate's Principal Supervisor, certify that all co-authors have consented to their work being included in the thesis and they have accepted the candidate's contribution as indicated in the *Statement of Originality*.

	Author's Name (please print clearly)	% of contribution
Candidate	**Sami Samiullah**	60
Other Authors	**Amal Saleh Omar**	20
	Juliet Roberts	15
	Kapil Chousalkar	5

Name of Candidate: **Samiullah**

Name/title of Principal Supervisor: **Associate Professor Juliet Roberts**

[redacted]
Candidate Date 09/06/2017

[redacted]
Principal Supervisor Date 09/06/2017

Higher Degree Research Thesis by Publication
University of New England

STATEMENT OF ORIGINALITY

(To appear at the end of each thesis chapter submitted as an article/paper)

We, the Research Master/PhD candidate and the candidate's Principal Supervisor, certify that the following text, figures and diagrams are the candidate's original work.

Type of work	**Page number/s**
Figures 1, 2 and 3	37, 37 and 41, respectively
Figures 4, 5 and 6	41, 45 and 45, respectively
Figures 7, 8 and 9	46, 47, and 47, respectively
Figures 10, 11 and 12	57, 57 and 58, respectively
Figure 13	58
Text and tables	29-65

Name of Candidate: **Samiullah**

Name/title of Principal Supervisor: **Associate Professor Juliet Roberts**

[redacted]

Candidate Date 09/06/2017

[redacted]

Principal Supervisor Date 09/06/2017

Chapter 3 Oviposition time, flock age and egg position in clutch in relation to brown eggshell colour in laying hens

Published as: Samiullah, S., Roberts, J. and Chousalkar, K. (2016). Oviposition time, flock age and egg position in clutch in relation to brown eggshell color in laying hens. Poultry Science; 95(9):2052-2057.

3.1 Abstract

In Australia and other parts of the world, table eggs with uniform brown eggshell colour are well regarded by consumers. Brown eggshell colour has been positively correlated with certain egg characteristics, such as shell strength and egg specific gravity, along with specific antibacterial functions. In the current study, the effect of hen oviposition time, flock age and egg position in-clutch on the intensity of brown eggshell colour was studied in commercial laying hens. The collected eggs were processed to measure egg weight, shell reflectivity, shell colour (L*a*b*), quantification of protoporphyrin IX (PP IX) and shell thickness. Hen oviposition time had a statistically significant effect ($P < 0.05$) on egg weight, L*a*b*, amount of PP IX and shell thickness. L* increased from 59.72 in the first half hour after lights on to 61.67 6 hours later, and PP IX per gram of eggshell decreased from 1.32×10^{-7} mM to 1.26×10^{-7} mM. Flock age had a significant effect on egg weight, L*a*b*, shell reflectivity, PP IX and shell thickness. The mean egg weight increased from 55.4 g at 25 wk of flock age to 63.3 g at 75 wk of flock age. PP IX per gram of eggshell was 1.45×10^{-7} mM at 25 wk and declined to 1.31×10^{-7} mM at 75 wk of flock age. Individual hen clutch length was highly variable, ranging from 22 to 123 eggs in a single clutch. Egg position in a clutch had a significant effect on all egg quality variables measured; however, the R^2 values for each variable measured were low. The eggshell colour declined to a greater extent with increasing position in a clutch for long clutches compared with short and medium clutches. In conclusion, hen oviposition time affected brown eggshell colour with darker brown eggs laid early in the day and lighter coloured brown eggs laid later in the morning. The

intensity of brown colour decreased with flock age, and egg position in-clutch had relatively little effect on brown eggshell colour.

Key words: brown egg, egg weight, eggshell quality, L*a*b*, protoporphyrin IX

3.2 Introduction

Eggshell formation in domestic hens takes a major proportion of the time (18 hr) during a single egg formation cycle (24 hr). In the shell gland, the deposition of calcite onto the shell membranes is usually slow for the first 3 to 4 hrs, then increases rapidly and becomes linear until oviposition (Talbot and Tyler, 1974). Oviposition intervals are studied to understand the effects of duration of shell formation on eggshell quality (Nys, 1986). In domestic hens, an egg clutch refers to the number of eggs laid between two successive pause periods. Determination of the length of a clutch plays an important role in calculating the laying life of a hen. In laying hens, long clutches are a desirable production trait as genetic increases in mean clutch length result in a significant increase in total egg production (Nestor et al., 1980). Oviposition time is reported to affect egg quality, egg composition and egg production (Choi et al., 1981; Arafa et al., 1982; Brake, 1985; Lee and Choi, 1985; Hashiguchi, 1996; Miyoshi et al., 1997).

Oviposition time and position of an egg in a clutch have been reported to influence egg characteristics, fertility, embryo viability, embryo weight and hatchability in broiler breeder flocks (Robinson et al., 1991; Novo et al., 1997; Gumulka et al., 2010). However, there is no published information about eggshell colour and egg position in-clutch. It is reported that the lapse between the oviposition of the terminal egg of one clutch and the oviposition of the first egg of the successive clutch is about 40 hrs (Robinson et al., 1991). The scientific explanation for the termination of a clutch is presumed to be the failure of release of luteinizing hormone from the adenohypophysis, and thus the largest follicle remains in the ovary for an extra 15 to 18 hrs (Robinson et al., 1991). Eggshell colour is determined primarily by the genotype of the hen. Apart from playing a role in consumer preference, brown eggshell pigment correlates positively with shell breaking strength, shell thickness and hatchability (Campo and Escudero, 1984; Curtis et al., 1985; Jones et al., 2010; Mertens et al., 2010). Brown pigment has been shown to have photodynamic-dependent antibacterial functions against some

gram-positive bacteria, such as *Staphylococcus aureus* and *Bacillus cereus* (Ishikawa et al., 2010). The main brown eggshell pigment is protoporphyrin IX (PP IX), although traces of biliverdin and its zinc chelates are also present (Kennedy and Vevers, 1973; With, 1973; Miksik et al., 1996). The intensity of brown eggshell is affected by various factors, such as hen age, strain, nutrition, and disease. The objective of the current study was to investigate the effect of oviposition time, flock age and egg position in a clutch on the intensity of brown eggshell colour in commercial laying hens. The hypotheses tested were that brown eggshell colour intensity decreases with increasing egg position in a clutch and increased age of hens, and that eggs laid early in the morning have a darker brown colour, compared with eggs laid later in the day.

3.3 Materials and Methods

A total of 150 Lohmann brown-egg laying hens were reared in individual conventional cages from 20 to 80 wk of age. Food and water were provided *ad libitum*, feed being commercial layer mash with wheat as the major component. The flock was on a 16 hr lighting regime with lights on at 04:00 and off at 20:00 hr Australian Eastern Standard Time (AEST).

3.3.1 Effect of oviposition time and flock age on brown eggshell colour- Experiment 1

From the flock of 150 hens, eggs were collected twice a wk at 25, 35, 45, 55, 65, and 75 wk of flock age (Experiment 1). The oviposition time of each individual hen was recorded, from 04:30 to 12:00 hr AEST, at 0.5 hr intervals. For the purpose of data analysis, oviposition time was divided into 5 photoperiod categories commencing with lights on: C1 (0.5 to 2 hr), C2 (2 to 3.5 hr), C3 (3.5 to 5 hr), C4 (5 to 6.5 hr), and C5 (6.5 to 8 hr).

3.3.2 Effect of egg position in-clutch on brown eggshell colour- Experiment 2

Out of the 150 laying hens, 14 hens (28 to 51 wk old) were selected for determination of egg position in-clutch (Experiment 2). For recording a single

clutch, individual hens were monitored until each hen missed a day, and then all eggs laid were collected until the same hen missed another day. The same procedure was followed for all 14 hens in the experiment with one clutch per hen analyzed.

3.4 Processing of samples

For both experiments 1 and 2, all eggs collected were processed for measurement of egg weight, shell reflectivity, shell colour, and quantification of PP IX from eggshell.

3.4.1 Egg weight, shell reflectivity and shell colour measurements

Immediately after collection, individual eggs were weighed using an analytical weighing balance Quintix513-1S (Sartorius Lab Instruments GmbH & Co. KG Goettingen, Germany). Eggs were further processed to measure shell reflectivity (%) and shell colour (L*a*b*) using a Reflectivity Meter (Technical Services and Supplies, Dunnington, York, UK) and Spectrophotometer (Konica Minolta CM-2600d Ramsey, NJ), respectively. The Konica Minolta spectrophotometer used in the current study functions on the L*a*b* space system, where L* represents the grading between black (0) and white (100). The higher the value for L*, the lighter is the shell colour. In the L*a*b* colour system, a∗ measures the grading between red and green where an a* value towards the positive end indicates red and a value towards the negative end indicates green. Similarly, b* measures the colour grading between blue and yellow with yellow being towards the positive end and blue towards the negative end of the measuring scale.

3.4.2 Protoporphyrin IX quantification from shell

All eggs collected were further processed for quantification of the amount of PP IX per gram of the whole eggshell. A small hole (1 cm^2) was made at the blunt pole of each individual egg using a Dremel tool (Dremel High Speed rotary tool, 300 series, Robert Bosch Tool Corporation, Gerlingen, Germany). The egg contents were emptied and the internal walls were washed in running tap water in order to remove any adherent albumen. Using the same Dremel tool, each eggshell was cut longitudinally into two equal halves. Shell membrane from the wet shells was

removed manually, and the shells were allowed to dry thoroughly. The shell thickness (without shell membranes) was measured on eggshells from experiment 1 only, using a Mitutoyo Dial Comparator Gauge Model 2109–10 (Kawasaki, Japan). For PP IX quantification from each individual shell, the method described by Samiullah and Roberts (2013) was followed. The amount of PP IX was measured in eggshell with intact cuticle.

3.5 Statistical analysis

Experiment 1: Data were analyzed by factorial ANOVA (Statview Software, SAS Institute Inc., Version 5.0.1.0) taking the category of hen oviposition time and flock age as independent variables and egg weight, L*a*b*, shell reflectivity, PP IX, and shell thickness as dependent variables. The level of significance was indicated by probability of equal to or less than 5%. The Fishers protected least significant difference (PLSD) test was used to differentiate levels of significance between mean values. The data were further subjected to multivariable regression to analyze the effects of category of oviposition time and flock age on all egg quality variables measured.

Experiment 2: Linear regression was used to determine the relationship between egg position in a clutch and shell colour of both individual hens and all hens combined (Statview Software, SAS Institute Inc., Version 5.0.1.0) taking the egg weight, L*a*b*, shell reflectivity and PP IX as dependent variables. The slope intercept, R^2, and P values were recorded for all variables measured. For the purpose of data analysis for egg position in-clutch, hens were divided into 3 categories:

Short clutch, 1 to 50 eggs in a single clutch. Medium clutch, 51 to 100 eggs in a single clutch. Long clutch, 101 to 123 eggs in a single clutch.

3.6 Results

3.6.1 Effect of oviposition time and flock age on brown eggshell colour-Experiment 1

For all flock ages combined, the C2 category of oviposition time (2-3.5 hr) had the highest number of eggs (35.13%) followed by C1 (0.5-2 hr, 34.29%) and C3 (3.5-

5 hr, 22.38%), while C4 (5-6.5 hr, 4.63%) and C5 (6.5-8 hr, 3.55%) had the least number of eggs recorded (Figure 3.1).

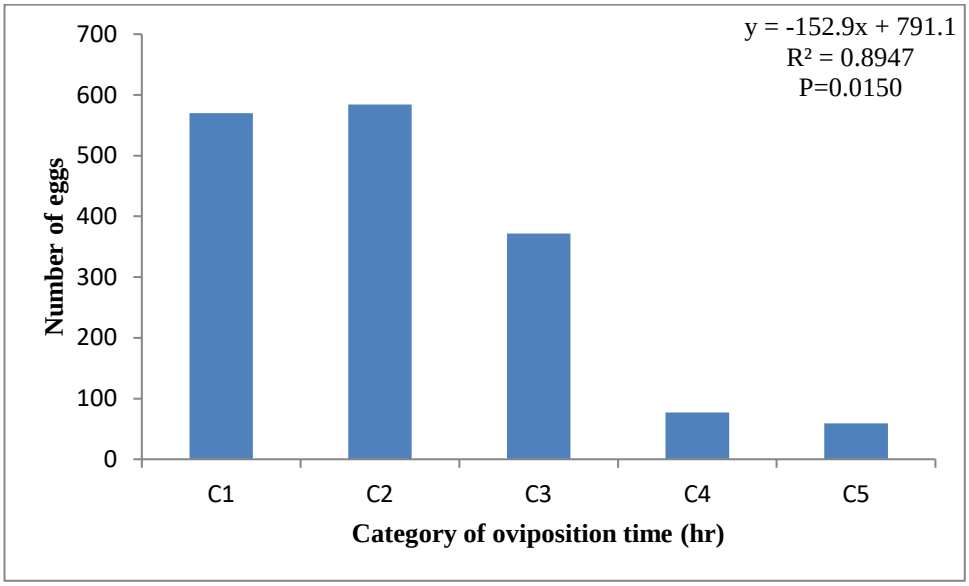

Figure 3.1 Number of eggs laid in 5 categories of oviposition time (all hen ages combined) C1 is oviposition time from 0.5 to 2 hr; C2 is oviposition time from 2.0 to 3.5 hr. C3 is oviposition time from 3.5 to 5 hr; C4 is oviposition time from 5.0 to 6.5 hr; C5 is oviposition time from 6.5 to 8.0 hr

There was a significant main effect ($P < 0.05$) of category of hen oviposition time on all egg quality variables measured except egg weight (Table 3.1). However, egg weight tended to be higher in C1, C2 and C3 compared with C4 and C5. The L* value was lower for C1 and C3 than for all other categories, whereas the a* value was lowest between 6.5 and 8 hr. The b* value was significantly higher for C3 compared with all other categories. The pattern of shell reflectivity was similar to that for L* (Table 3.1). The amount of PP IX per gram of whole eggshell was highest in C1 and C3 and lowest in C2 and C5. Shell thickness generally decreased as hen oviposition time increased from C1 to C5 (Table 3.1).

Table 3.1 Hen oviposition time in relation to egg and eggshell quality variables

Variable	Category of oviposition time (hour)					P value
	C1	C2	C3	C4	C5	
Egg weight (g)	61.97±0.23	62.32±0.23	61.72±0.32	60.82±0.65	60.76±0.73	0.0771
L* (0-100)	59.72±0.15^{b}	60.69±0.14^{a}	60.07±0.20^{b}	61.37±0.49^{a}	61.67±0.45^{a}	<.0001
a* (+red, -green)	17.53±0.08^{a}	17.09±0.08^{b}	17.28±0.12^{ab}	16.35±0.30^{c}	15.97±0.22^{c}	<.0001
b* (+yellow, -blue)	28.52±0.09^{cd}	28.95±0.08^{bc}	29.01±0.10^{a}	28.32±0.25^{d}	28.45±0.38^{cd}	0.0005
Shell reflectivity (%)	23.53±0.14^{b}	23.70±0.14^{b}	23.00±0.18^{c}	24.67±0.46^{a}	24.11±0.45^{ab}	0.0006
PP IX $\times 10^{-7}$ (mM/g of shell)	1.32±0.08^{a}	1.29±0.08^{b}	1.33±0.10^{a}	1.29±0.27^{ab}	1.26±0.30^{b}	0.0143
Shell thickness (μm)	382.8±1.1^{a}	377.8±1.0^{b}	374.5±1.4^{bc}	371.1±3.3^{c}	374.3±3.3^{bc}	<.0001

^{a,b,c} Means within the same row with different superscripts significantly different from each other.

C1 is oviposition time from 0.5 to 2 hr; C2 is oviposition time from 2.0 to 3.5 hr; C3 is oviposition time from 3.5 to 5 hr; C4 is oviposition time from 5.0 to 6.5 hr; C5 is oviposition time from 6.5 to 8.0 hr.

Values are Mean ± S.E.; PP IX is protoporphyrin IX.

There was a statistically significant main effect ($P < 0.0001$) of flock age on all egg quality variables measured (Table 3.2). Egg weight increased to 45 wk and then remained relatively constant (Table 3.2). The L* value increased until 65 wk of flock age and then decreased at 75 weeks. The a* value decreased with increasing flock age, while the b* value fluctuated but was lowest in the older flocks. Shell reflectivity was slightly different from the L* trend, being highest at 45 to 65 wk before decreasing at 75 wk (Table 3.2). The amount of PP IX per gram of whole eggshell decreased until 65 wk of age and was significantly higher at 75 wk compared with 65 wk of flock age. The shell thickness was highest at 35 wk and decreased at 65 to 75 wk of flock age. The multivariable regression analysis of category of hen oviposition time and flock age versus egg quality variables measured is shown in Table 3.3.

Table 3.2 Effect of flock age on egg and eggshell quality variables

Variable	Flock age (week)						P value
	25	35	45	55	65	75	
Egg weight (g)	55.4±0.29^{d}	61.6±0.26^{c}	64.3±0.29^{a}	63.1±0.28^{b}	64.2±0.32^{a}	63.3±0.30^{b}	<0.0001
L* (0-100)	57.2±0.18^{d}	58.1±0.15^{c}	60.6±0.19^{b}	62.1±0.18^{a}	62.3±0.21^{a}	61.8±0.22^{a}	<0.0001
a* (+red, -green)	19.3±0.10^{a}	18.2±0.07^{b}	17.1±0.10^{c}	16.9±0.10^{c}	15.9±0.11^{d}	15.6±0.11^{d}	<0.0001
b* (+yellow, -blue)	29.3±0.16^{a}	28.5±0.10^{b}	28.8±0.13^{b}	29.5±0.10^{a}	28.1±0.14^{b}	28.1±0.12^{b}	<0.0001
Shell reflectivity (%)	21.5±0.19^{d}	22.6±0.16^{c}	24.8±0.21^{a}	24.6±0.20^{a}	24.5±0.23^{a}	23.4±0.21^{b}	<0.0001
PP IX (mM/g shell, $\times 10^{-7}$)	1.45±0.01^{a}	1.32±0.01^{b}	1.29±0.01^{c}	1.24±0.01^{d}	1.25±0.01^{d}	1.31±0.01^{bc}	<0.0001
Shell thickness (µm)	379.8±1.6^{bc}	388.2±1.2^{a}	382.8±1.5^{b}	376.4±1.4^{c}	371.7±1.8^{d}	369.6±1.7^{d}	<0.0001

$^{a–d}$Means within the same row with different superscripts significantly different from each other. Values are Mean ± S.E.; PP IX is protoporphyrin IX

Table 3.3 Multiple regression analysis of effect of category of oviposition time and flock age on egg and eggshell quality variables

Variable	R^2 value	Intercept	P value
Egg weight (g)	0.174	56.55	<0.0001
L* (0-100)	0.230	55.15	<0.0001
a* (+red, -green)	0.339	20.85	<0.0001
b* (+yellow, -blue)	0.023	29.45	<0.0001
Shell reflectivity (%)	0.044	21.61	<0.0001
Protoporphyrin IX	0.054	1.438×10^{-7}	<0.0001
Shell thickness (µm)	0.045	396.22	<0.0001

Protoporphyrin IX was measured in mM in 1 g of whole eggshell

3.6.2 Effect of egg position in-clutch on brown eggshell colour- Experiment 2

The individual hen clutch lengths were highly variable, ranging from 22 to 123 eggs per clutch. There was an overall significant correlation ($P < 0.0001$) between egg position in a clutch and egg weight, L*, a*, shell reflectivity and PP IX, but the R^2 values were very low (Table 3.4). When the correlation between egg position in-clutch and egg weight was analyzed on a clutch length basis, there was a weak positive correlation, which was better the longer the clutch length (Table 3.5). There was no significant correlation between L∗ and clutch length for hens with short and medium clutch lengths, whereas, for hens with long clutches, the correlation was highly significant, but weak (Table 3.5). The L* values ($P < 0.0001$) for long clutch lengths showed that eggs became lighter in colour towards the end of the clutch. The pattern for shell reflectivity was slightly different from L*, showing a negative correlation for medium clutches and a positive correlation for short and long clutches (Table 3.5). Consistent with L* and shell reflectivity, there was no significant correlation observed between the amount of PP IX and clutch length for all 3 categories of clutch combined; however, for short and long clutches, there was a weak negative correlation (R^2=0.0164 and 0.0004, respectively).

Table 3.4 Linear regression analysis of egg position in-clutch on egg and eggshell quality variables

Variable	Position of egg in-clutch (all hens combined)		
	R^2 value	Intercept	P value
Egg weight (g)	0.024	61.205	<0.0001
L* (0-100)	0.090	59.111	<0.0001
a* (+red, -green)	0.066	17.936	<0.0001
b* (+yellow, -blue)	0.00001	27.900	0.9710
Shell reflectivity (%)	0.047	23.483	<0.0001
Protoporphyrin IX	0.028	9.56×10^{-8}	<0.0001

Protoporphyrin IX was measured in mM in 1 g of whole eggshell

Table 3.5 Regression analysis of shell quality variables against category of clutch length (day)

Variable	Short clutch (0-50 day)			Medium clutch (51-100 day)			Long clutch (101-123 day)		
	R^2	Intercept	P value	R^2	Intercept	P value	R^2	Intercept	P value
Egg weight (g)	0.0416	59.81	0.0397	0.0134	62.291	0.0224	0.0794	60.145	0.6246
L* (0-100)	0.0002	58.59	0.9648	0.0012	59.17	0.4891	0.076	60.33	<0.0001
a* (+red, -blue)	0.0029	18.299	0.5931	0.0115	17.761	0.0344	0.1355	17.37	<0.0001
b* (+blue, -yellow)	0.0024	28.771	0.6275	0.0023	27.371	0.3534	0.0006	28.003	0.9643
Shell reflectivity	0.0001	23.03	0.9035	0.0002	23.36	0.8081	0.0291	24.76	<0.0001
PP IX[A]	0.0164	1×10^{-7}	0.1992	0.0004	1×10^{-7}	0.8081	0.0004	9×10^{-8}	0.6246

[A]Protoporphyrin IX was measured in mM in 1 g of whole eggshell

3.7 Discussion

3.7.1 Effect of oviposition time and flock age on brown eggshell colour-Experiment 1

Most eggs (51%) were laid between 0.5 and 3.5 hr after lights on (C1, C2) which indicates that, in commercial brown-egg laying hens with consistent daylight cycle (i.e., 16L:8D), most of the eggs can be collected early in the morning. In the current study, hen oviposition time was relatively narrow and the accuracy of oviposition time recorded was high as individual eggs were recorded at the time they were laid. Egg weight was affected by hen oviposition time with the heaviest eggs being laid early in the day (Table 3.1). These results differ from those of previous studies (Arafa et al., 1982; Brake, 1985, Tumova and Ledvinka, 2009; Campo et al., 2015)

although these other authors used different collection times. However, another study found no significant effect of hen oviposition time on egg weight (Choi et al., 1981). Statistically higher L* values in the C4 and C5 groups indicate that the darkest eggshell colour was found in the eggs laid early in the morning (Table 3.1). Eggshells became less red in colour the later in the day that they were laid and were most yellow at 3.5 to 5 hr after lights on. The pattern for shell reflectivity was slightly different from the L* value, although both variables indicate the degree of brownness of shell colour. This slight difference might reflect the importance of the a* and b* components that describe the red-green and yellow-blue colour of the eggshells in the L*a*b* colour space system. Shell reflectivity values may be less reliable than L* values as reflectivity is also affected by the nature of the surface of the eggshell (i.e., how rough the surface is). However, the high correlation coefficient between L* and shell reflectivity (0.867) indicates that the two measurements are giving similar but not necessarily the same results. The values for PPIX in the eggshell were broadly inverse to the measurements for reflectivity and L∗ indicating that there was less PPIX in the lighter coloured shells (Table 3.1). Shell thickness was greatest in eggs laid early in the morning (Table 3.1), although the physiological mechanism behind this difference has not been investigated. A similar result was reported in a previous study (Arafa et al., 1982). The reduction in shell thickness in eggs laid later in the morning indicates that eggs remaining in the shell gland for a longer time do not necessarily acquire extra calcite.

Egg weight generally increases with increasing flock age (Silversides and Scott, 2001; Samiullah et al., 2014). However, in the current study, egg weight was less consistent in relation to flock age (Table 3.2). A weak correlation (0.089) between egg weight and L* values indicates that shell colour was not affected as the egg weight increased with increasing flock age. This argument was further supported by calculating the correlation (0.05) between egg weight and shell reflectivity. The purpose of PP IX quantification was to observe how much pigment is present per gram of whole eggshell and whether L* and reflectivity values are consistent with PP IX values. A negative correlation between PP IX and L* (0.531) and between PP IX and shell reflectivity (0.577) indicates that eggshells with higher L* and shell reflectivity values have a lower amount of PP IX.

3.7.2 Effect of egg position in-clutch on brown eggshell colour- Experiment 2

The results of this study constitute the first thorough investigation of egg position in-clutch and pattern of change in brown eggshell colour in commercial laying hens. Clutch length varied from 22 to 123 eggs, with an average of 76 eggs, which reflects the high production of commercial laying hens.

There was an overall trend for individual hens to lay eggs of a similar colour throughout the clutch, but the intensity of eggshell colour was highly variable among hens of the same flock at the same age. A weak correlation between position in-clutch and egg weight indicated that the egg weight did not change consistently as the egg position in clutch advanced (Table 3.4). However, when this correlation was calculated on a clutch length basis, there was a stronger positive correlation for long clutches compared with short or medium clutches (Table 3.5). The clutch size in the present study was variable but relatively long, whereas, in earlier studies, egg weight decreased linearly with egg position in-clutch, but the maximum clutch size recorded was 9 eggs (Miyoshi et al., 1997). A weak positive correlation between L* and position in-clutch suggests that there is a small effect of position in-clutch on eggshell colour. Similar to the egg weight and clutch length correlation, other variables measured showed better correlation for long clutches compared with short and medium clutches. The better correlation for long clutches might indicate that shell colour variables such as L*a*b*, shell reflectivity, and PP IX do change with increasing clutch length and this difference is clearer for long clutch lengths.

3.8 Conclusions

From the current study, it can be concluded that there was an overall significant effect of oviposition time on egg quality variables measured. Eggs laid closer to the onset of the photoperiod were darker in eggshell colour. The intensity of eggshell colour decreased with flock age. The egg position in a clutch more clearly affected egg quality variables in long clutches compared with medium and short clutches. Hen age had a greater effect on shell colour than either oviposition time or position of an egg in a clutch. However, it should be noted that these relatively small

differences in shell colour may not be visible to the naked human eye. Further investigation is needed to study the physiological mechanisms involved in the relationship between oviposition time and position in-clutch and pigment synthesis and deposition on eggshells in the shell gland of laying hens.

3.8.1 References

Arafa, A. S., R. H. Harms, R. D. Miles, R. B. Christmas, and J. H. Choi. 1982. Quality characteristics of eggs from different strains of hens as related to time of oviposition. Poult. Sci. 61:842-847.

Brake, J. 1985. Relationship of egg weight, specific gravity and shell weight to time of oviposition and feeding in broiler breeders. Poult. Sci. 64:2037-2040.

Campo, J. L., F. Cigarroa, and O. Torres. 2015. Effect of oviposition time on egg quality characteristics. World's Poult. Sci. J. 71:106.

Campo, J. L., and J. Escudero. 1984. Relationship between eggshell colour and two measurements of shell strength in the Vasca breed. Br. Poult. Sci. 25:467-476.

Choi, J. H., R. D. Miles, A. S. Arafa, and R. H. Harms. 1981. The influence of oviposition time on egg weight, shell quality, and blood phosphorus. Poult. Sci. 60:824-828.

Curtis, P. A., F. A. Gardner, and D. B. Mellor. 1985. A comparison of selected quality and compositional characteristics of brown and white shell eggs. II. Interior quality. Poult. Sci. 64:302-306.

Gumulka, M., E. Kapkowska, and D. Maj. 2010. Laying pattern parameters in broiler breeder hens and intrasequence changes in egg composition. Czech J. Anim. Sci. 55:428-435.

Hashiguchi, M. 1996. Relationship of position of egg in sequence to eggshell quality in laying hen. Jpn. Poult. Sci. 33:230-234.

Ishikawa, S., K. Suzuki, E. Fukuda, K. Arihara, Y. Yamamoto, T. Mukai, and M. Itoh. 2010. Photodynamic antimicrobial activity of avian eggshell pigments. FEBS Lett. 584:770-774.

Jones, D. R., M. T. Musgrove, K. E. Anderson, and H. S. Thesmar. 2010. Physical quality and composition of retail shell eggs. Poult. Sci. 89:582-587.

Kennedy, G. Y., and H. G. Vevers. 1973. Eggshell pigments of the Araucano fowl. Comp. Biochem. Physiol., B: Comp. Biochem. 44:11-25.

Lee, K. D., and J. H. Choi. 1985. Interrelationships among time of oviposition, egg weight, shell weight, and rate of egg production of laying hens. Poult. Sci. 64:2256-2258.

Mertens, K., I. Vaesen, J. Loffel, B. Kemps, B. Kamers, C. Perianu, J. Zoons, P. Darius, E. Decuypere, J. De Baerdemaeker, and B. De Ketelaere. 2010. The transmission colour value: A novel egg quality measure for recording shell colour used for monitoring the stress and health status of a brown layer flock. Poult. Sci. 89:609-617.

Miksik, I., V. Holan, and Z. Deyl. 1996. Avian eggshell pigments and their variability. Comp. Biochem. Physiol., Part B: Biochem. Mol. Biol. 113:607-612.

Miyoshi, S., K. Inoue, K. M. Luc, K. Kuchida, and T. Mitsumoto. 1997. Intra-clutch changes in egg composition and shell quality in laying hens. Jpn. Poult. Sci. 34:273-281.

Nestor, K. E., W. L. Bacon, and P. A. Renner. 1980. The influence of genetic changes in total egg production, clutch length, broodiness and body weight on ovarian follicular development in Turkeys. Poult. Sci. 59:1694-1699.

Novo, R. P., L. T. Gama, and M. C. Soares. 1997. Effects of oviposition time, hen age and extra dietary calcium on egg characteristics and hatchability. J. Appl. Poultry Res. 6:335-343.

Nys, Y. 1986. Relationships between age, shell quality and individual rate and duration of shell formation in domestic hens, Br. Poult. Sci. 27:253-259.

Robinson, F. E., R. T. Hardin, N. A. Robinson, and B. J. Williams. 1991. The influence of egg sequence position on fertility, embryo viability, and embryo weight in broiler breeders. Poult. Sci. 70:760-765.

Samiullah, J. R. Roberts, and K. K. Chousalkar. 2014. Effect of production system and flock age on egg quality and total bacterial load in commercial laying hens. J. Appl. Poultry Res. 23:59-70.

Samiullah, S., and J. R. Roberts. 2013. The location of protoporphyrin in the eggshell of brown-shelled eggs. Poult. Sci. 92:2783-2788.

Silversides, F. G., and T. A. Scott. 2001. Effect of storage and layer age on quality of eggs from two lines of hens. Poult. Sci. 80:1240-1245.

Talbot, C. J., and C. Tyler. 1974. A study of the progressive deposition of shell in the shell gland of the domestic hen. Br. Poult. Sci. 15:217-224.

Tumova, E., and Z. Ledvinka. 2009. The effect of time of oviposition and age on egg weight, egg components weight and eggshell quality. Arch. Geflugelk. 73:110-115.

With, T. K. 1973. Porphyrin in eggshell. Biochem. J. 137:597-598.

Higher Degree Research Thesis by Publication
University of New England

STATEMENT OF AUTHORS' CONTRIBUTION

(To appear at the end of each thesis chapter submitted as an article/paper)

We, the Research Master/PhD candidate and the candidate's Principal Supervisor, certify that all co-authors have consented to their work being included in the thesis and they have accepted the candidate's contribution as indicated in the *Statement of Originality*.

	Author's Name (please print clearly)	**% of contribution**
Candidate	**Sami Samiullah**	75
Other Authors	**Juliet Roberts**	20
	Kapil Chousalkar	5

Name of Candidate: **Samiullah**

Name/title of Principal Supervisor: **Associate Professor Juliet Roberts**

[redacted]
Candidate Date 09/06/2017

[redacted]
Principal Supervisor Date 09/06/2017

Higher Degree Research Thesis by Publication
University of New England

STATEMENT OF ORIGINALITY

(To appear at the end of each thesis chapter submitted as an article/paper)

We, the Research Master/PhD candidate and the candidate's Principal Supervisor, certify that the following text, figures and diagrams are the candidate's original work.

Type of work	**Page number/s**
Figure 3.1	74
Text and tables	69-84

Name of Candidate: **Samiullah**

Name/title of Principal Supervisor: **Associate Professor Juliet Roberts**



Candidate Date 09/06/2017



Principal Supervisor Date 09/06/2017

Chapter 4 The Australian strains of infectious bronchitis virus affect brown eggshell colour in commercial laying hens differently

Published as: Samiullah, S., Roberts, J. and Chousalkar, K. (2016). Infectious bronchitis virus and brown shell colour: The Australian strains of infectious bronchitis virus affect brown eggshell colour in commercial laying hens differently. Avian Pathology; 45(5):552-558.

4.1 Abstract

The aim of the current study was to assess any effect of wild and vaccine Australian infectious bronchitis virus (IBV) strains on shell colour in brown shelled eggs. In Experiment 1, eggs were collected from day 1 to day 13 post-inoculation (p.i.) from unvaccinated laying hens challenged with IBV wild strains T and N1/88 and from a negative control group of hens. In Experiment 2, eggs were collected from 2 to 22 days p.i. from unvaccinated and vaccinated laying hens challenged with either a wild or a vaccine strain of IBV. In Experiment 1, there was a significant effect ($P < 0.05$) of day p.i. and of viral strain on shell reflectivity, L* and protoporphyrin IX (PP IX) in eggshells, with and without cuticle. The mean PP IX/g of shell with and without cuticle was significantly higher on day 1 p.i. compared to day 7, after which PP IX increased with day p.i. In Experiment 2, shell reflectivity and L* increased and PP IX decreased with increased day p.i. until day 12. Shell reflectivity and L* decreased slightly after day 12 and increased again towards day 22. Shell reflectivity, L* and PP IX were not significantly different for eggshells from unvaccinated and vaccinated laying hens in the intact eggshell, but were significantly different in shells from which cuticle had been removed. In conclusion, the IBV strains reduced the intensity of brown shell colour to different extents with a lower amount of PP IX in eggshells.

Keywords: Infectious bronchitis; virus strains; shell colour; L*; protoporphyrin IX; vaccine

4.2 Introduction

Infectious bronchitis (IB) is a highly contagious disease caused by a group 3 gammacoronavirus that affects both broiler and layer poultry production worldwide (Balestrin et al., 2014; Hewson et al., 2014). The incubation period of infectious bronchitis virus (IBV) in fully susceptible hens is 18-36 hours (Sevoian & Levine, 1957). IBV can infect chickens of all ages and has the capability of multiplying in various epithelial tissues including trachea, lung, kidney, ovary, oviduct and intestine (Uenaka et al., 1998; Ignjatovic et al., 2002). In brown-egg laying hens, IBV is one of the factors responsible for eggshell deterioration and for the production of lighter shell colour (Chousalkar & Roberts, 2009). The Australian strains of IBV have the ability to multiply in the shell gland of vaccinated and unvaccinated Isa Brown laying hens (Chousalkar & Roberts, 2007a). The T strain of IBV is mainly nephropathogenic, but also results in the production of lighter colour shells (Chousalkar & Roberts, 2009). The N1/88, Vic S and A3 strains also infect the oviduct in laying hens, causing the production of lighter coloured shells (Chousalkar & Roberts, 2009). Other IBV isolates have also been shown to affect the intensity of brown eggshell colour (Cook & Huggins, 1986). The decline in egg production in an IBV-infected flock depends upon many factors such as flock age, flock strain and IBV strain virulence (Sevoian & Levine, 1957; McMartin, 1968; Ignjatovic & Sapats, 2000). IBV strains have been shown to cause disorder of eggshell formation by disrupting isthmus gene expression of collagen type I and calcium binding protein 28 kDa (CaBP-D28 K) in the uterus (Nii et al., 2014). The viral antigen localizes only in the epithelial cells lining the oviduct (Crinion & Hofstad, 1972).

A uniform deep brown eggshell colour is considered an important trait for external egg quality. The eggshell colour of brown eggs is a quality aspect for consumers (Curtis et al., 1985). Shell colour has been linked to egg quality parameters in brown eggs (Jones et al., 2010) and with antimicrobial properties (Ishikawa et al., 2010). Pale or unevenly coloured eggs may be rejected by consumers, and egg producers in many countries including Australia aim to keep eggshell colour uniform. Commercial brown egg lines have been selected for attractive and uniform deep brown eggshell colour for many years. Besides hen strain, the intensity of eggshell

colour is affected by various factors such as flock age and certain diseases including IB. Recently, Hy-Line International has developed a shell colour guide for measuring the intensity of brown colour on a scale from 70 to 110. Protoporphyrin IX (PP IX) is the main eggshell pigment (Kennedy & Vevers, 1976) and has been shown to be correlated with shell quality parameters such as shell strength, shell weight, shell thickness and shell ultrastructure (Yang et al., 2009). However, there is no mention in the literature of the effect of IBV infection on the amount of PP IX in eggshells.

The main objective of the present study was to measure shell colour and quantify the amount of PP IX from the cuticle and calcareous shell in brown shelled eggs of Isa Brown laying hens challenged with two wild (N1/88 and T) and two vaccine (Vic S and A3) strains of IBV, as compared with a control group of hens, and to establish the effectiveness of vaccination in protecting against changes in shell colour. The eggshells processed in this study were collected and stored from previous IBV challenge studies in brown-egg laying hens (Chousalkar et al., 2007, 2009a, b, 2010). Hens, either unvaccinated and challenged with two different strains of IBV, or vaccinated and challenged with four different strains of IBV, were kept in isolation sheds under strict biosecurity. All challenged hens were positive for IBV antibody at 5 and 10 weeks post inoculation (p.i.) and the virus was detected in the oviduct (Chousalkar et al., 2007, 2009a, b, 2010).

4.3 Materials and Methods

The eggshells used in these experiments were collected during two previous studies from which other data have already been published. Experiment 1 was approved by the University of New England (UNE), Armidale, NSW, Australia, Animal Ethics Committee under Authority No. AEC05/082 and Experiment 2 under Authority No. AEC06/166. For both experiments, the day-old chicks were raised free from exposure to IBV in isolation sheds at the UNE to 30 weeks of age.

4.3.1 Experiment 1

Day-old chicks (Isa Brown layers) were reared in chicken isolation sheds with strict biosecurity. Food and water were provided *ad libitum*. At 30 weeks of age, hens

were divided into three groups: a control group (n=48), a group challenged with N1/88 strain IBV (n=52) and a group (n=52) challenged with T (now N1/62) strain of IBV. Each bird was inoculated by the intraocular route with 2×10^5 median embryo infective doses (EID_{50}) of IBV. A negative control group of hens was sham inoculated with normal saline (Chousalkar & Roberts, 2007a, b, 2009). From all groups, eggs were collected between 3 January and 22 March 2006, daily for one week before challenge, daily for five weeks immediately following challenge and then weekly until 10 weeks p.i. (Chousalkar & Roberts, 2009). After processing of eggs in the earlier experiments, the eggshells were washed, labelled and stored in the dark until September 2012, at cool ambient temperature (20–25°C) under dry conditions on egg fillers inside cardboard boxes. Therefore, the eggshells were stored as described above for 6–7 years prior to examination in this study. From the collected eggshells, those collected at days 1, 3, 5, 7, 9, 11 and 13 p.i. were used in the current study. From each group, 45 eggshells were processed on each day of collection. The shells were processed for measurement of shell reflectivity (%), shell colour (L* component of L*a*b* colour space system) and quantification of PP IX from shells with and without the cuticle layer. Shell reflectivity was measured again on these eggshells in order to understand the level of reflectivity difference between whole eggshells and shells from which the cuticle layer had been removed (calcareous part of shell). In order to determine the effects of long term storage on the possible deterioration of PP IX in eggshells, a pilot experiment was conducted using the eggshells stored in the dark from another experiment. The data on the PP IX content in these eggshells previously measured (referred to as fresh eggshells) were published earlier (Samiullah & Roberts, 2013). Eggshells tested during the pilot experiment were stored in the dark for more than 4 years at ambient temperature. These eggshells (referred to as stored eggshells) were processed again for PP IX quantification from whole eggshells, the calcareous part of the shells and in cuticle alone. The PP IX values from fresh eggshells and stored eggshells were compared.

4.3.2 Experiment 2

This experiment used both unvaccinated and vaccinated groups of birds reared from day-old. The unvaccinated group of birds (n=160) was maintained free from exposure to IBV, whereas the birds in the vaccinated group (n=230) were vaccinated by the intraocular route with Vic S at day 1, A3 at 4 weeks and Vic S at 12 weeks of age and then maintained free from further exposure to IBV. Both unvaccinated and vaccinated groups of laying hens were challenged at 30 weeks of age with T, N1/88, Vic S or A3 strains of IBV. The inoculation dose and route were the same as that used in Experiment 1. A control group was included for both the unvaccinated and vaccinated birds (Chousalkar et al., 2007, 2009a, b, 2010). The number of hens in each group was as follows: unvaccinated and vaccinated control (30 hens each), unvaccinated or vaccinated and challenged with Vic S and A3 strains (50 hens each), unvaccinated and challenged with N1/88 and T strains (15 hens each) and vaccinated and challenged with N1/88 and T strains (50 hens each). Eggs from all the groups were collected daily before and after the challenge. From the collected eggs, eggshells were processed at days 2, 4, 6 to 22 p.i. from all groups. Eggshells were stored as described for Experiment 1. From each group on each day p.i., 10 eggshells randomly selected were processed for the same parameters as in Experiment 1. The eggshells tested in this experiment had been collected between 13 April 2007 and 8 July 2007 and stored for approximately 6 years as described above until examined between September 2012 and April 2013.

4.3.3 Measurement of shell reflectivity and shell colour

In both experiments, shell reflectivity and shell colour (L*) were measured with cuticle intact using a reflectivity metre and a Konica Minolta spectrophotometer (CM-2600d Ramsey, NJ, USA), respectively. Shell reflectivity, expressed as a percentage, is an indicator of shell colour lightness – the higher the value, the lighter the colour of the eggshell. In the L*a*b* colour space system, L* represents the grading between white (100) and black (0). The higher the value for L*, the lighter the shell colour. The value for a* represents the grading between red and green, with red towards the positive end of the measuring scale and green towards the negative end. The value for b* indicates the difference between blue and yellow,

with yellow towards the positive end of the measuring scale and blue towards the negative end. Only the data for L* are presented in this study. Next, each eggshell was individually soaked in EDTA solution (pH 7.5, 0.34 M) for 5 min and the cuticle was scrubbed off in running tap water using a soft brush. Shell reflectivity and L* were measured as described earlier on the eggshells with cuticle removed.

4.3.4 PP IX quantification from eggshells

Eggshells were further processed in order to measure the amount of PP IX in 1 g of whole eggshell with and without cuticle. The dried shells were soaked for 2 hrs in water, the shell membrane was removed manually and the shells were allowed to dry thoroughly. From each individual shell, a 250 mg sample was weighed (to an accuracy of 1 mg using an electronic balance) into a 10 mL centrifuge tube into which 4 mL of methanol-concentrated HCl (2:1) solvent was added. All tubes were placed in a refrigerator for 3 hrs, avoiding exposure to light. The samples were centrifuged at 800 ×*g* at 4°C for 30 min. After centrifugation, the supernatant solution was decanted into a 4 mL spectrophotometer acrylic cuvette and the absorbance of the supernatant was read at 412 nm (UV-1201, Shimadzu, Kyoto, Japan). The spectrophotometer was blanked with reverse osmosis water before reading the samples.

4.3.5 Standard curve construction

A standard curve was constructed from solutions of PP IX (Sigma Aldrich, Castle Hill NSW 1765, Australia) ranging from 0 to 6.87×10^{-6} mM and used to calculate the amount of PP IX in 1 g of eggshell (with and without cuticle). For the determination of the amount of PP IX in the cuticle, the values of the eggshell samples without cuticle were subtracted from the values of the eggshell samples with cuticle.

4.4 Statistical analysis

Data were analysed using Statview Software (SAS Insti-tute Inc., Version 5.0.1.0, 1992–1998). A two-way analysis of variance (ANOVA) was conducted taking day

p.i. and group as independent variables and shell reflectivity, L* and amount of PP IX in shell with, without and in cuticle alone as dependent variables. Level of significance was indicated by probability of less than 5%. Fisher's PLSD test was used to differentiate levels of significance between mean values.

4.5 Results

Results from the pilot experiment indicated that the storage conditions had no deleterious effects on PP IX level in the eggshells. There was no significant difference in PP IX levels between the whole eggshells of fresh and stored eggshells. Similarly, the differences in PP IX levels in the calcareous part of eggshells and in the cuticle alone were also non-significant (data not shown).

4.5.1 Experiment 1

There was a significant effect ($P < 0.0001$) of challenge virus strain, day p.i. and interaction between the two on shell reflectivity, L* and PP IX for shells with and without cuticle. There was no significant effect of challenge virus strain, day p.i. or interaction between the two on the amount of PP IX in 1 g of cuticle (Tables 4.1 and 4.2). Shell reflectivity and L* for the control eggs were significantly lower ($P < 0.0001$) compared to those from hens challenged with each strain of IBV and were also significantly lower on day 1 compared to the value on day 5 p.i. (Table 4.1). The mean PP IX/g of shells with and without cuticle was significantly higher on day 1 compared with that on day 5 p.i. After day 5, the mean PP IX increased again with increasing day p.i. The amount of PP IX in the shells decreased with increasing time post infection for the IBV groups. The amount of PP IX in whole eggshells was highest for the control group and lowest for the T strain group, with the N1/88 group being intermediate (Table 4.1). However, the amount of PP IX calculated in the cuticle of 1 g of eggshell alone tended to be highest in eggshells from the N1/88 strain infected hens, but the values were not statistically significantly different among the three groups (Table 4.1).

Table 4.1 Effect of infectious bronchitis virus challenge strains on eggshell colour variables (Experiment 1)

Variable	Control	T strain	N1/88 strain	P value
Shell reflectivity with cuticle	[b]27.86±4.0[C]	31.13±5.0[A]	29.59±5.2[B]	<0.0001
Shell reflectivity without cuticle	34.11±5.2[C]	38.29±5.0[A]	36.44±5.1[B]	<0.0001
L* with cuticle	62.46±3.6[C]	65.45±3.6[A]	63.86±3.8[B]	<0.0001
L* without cuticle	67.85±3.9[C]	70.94±3.7[A]	69.54±4.0[B]	<0.0001
[a]PP IX in whole eggshell ($\times 10^{-8}$)	9.96±1.9[A]	8.84±1.7[C]	9.55±1.8[B]	<0.0001
PP IX in shell without cuticle ($\times 10^{-8}$)	7.97±1.8[A]	6.89±1.5[C]	7.49±1.5[B]	<0.0001
PP IX in cuticle ($\times 10^{-8}$)	1.99±1.1	1.95±1.2	2.06±1.2	0.5202

[a]protoporphyrin IX measured in mM per gram of eggshell.

[b]Mean±SD.

[A,B,C] Across a row, values with different superscripts are significantly different from each other.

Table 4.2 Effect of day post inoculation with different infectious bronchitis virus strains on eggshell colour variables (Experiment 1)

Day p.i.	Shell reflectivity with cuticle	Shell reflectivity without cuticle	L* of shell with cuticle	L* of shell without cuticle	[a]PP IX in whole eggshell ($\times 10^{-8}$)	PP IX in shell without cuticle ($\times 10^{-8}$)	PP IX in cuticle ($\times 10^{-8}$)
1	[b]30.89±4.0^{B}	35.68±4.6^{B}	62.59±3.7^{C}	66.63±3.5^{C}	10.0±1.8^{A}	8.13±1.6^{A}	1.92±1.1^{C}
3	32.67±4.8^{A}	39.19±5.1^{A}	64.04±4.1^{AB}	69.57±3.8^{B}	8.07±1.3^{BC}	6.51±1.3^{B}	1.56±1.0^{C}
5	33.14±5.2^{A}	40.04±5.4^{A}	64.83±4.2^{A}	70.58±3.8^{A}	8.71±1.7^{BC}	6.99±1.5^{B}	1.71±1.2^{C}
7	29.11±4.7^{C}	36.25±5.2^{B}	64.56±3.9^{AB}	70.08±3.9^{AB}	9.43±1.9^{B}	7.42±1.6^{B}	2.01±1.2^{BC}
9	28.86±4.5^{C}	36.67±4.9^{B}	64.29±3.7^{AB}	70.31±3.6^{AB}	9.45±1.8^{B}	7.32±1.6^{B}	2.12±1.1^{ABC}
11	26.82±4.1^{D}	34.33±5.0^{C}	63.94±3.5^{BC}	70.29±4.0^{AB}	9.73±1.8^{C}	7.44±1.7^{C}	2.29±1.1^{AB}
13	25.94±4.0^{D}	32.86±4.7^{C}	63.63±3.6^{C}	69.65±4.0^{B}	9.97±1.8^{C}	7.76±1.7^{C}	2.22±1.1^{A}
P value	**<0.0001**	**<0.0001**	**<0.0001**	**<0.0001**	**<0.0001**	**<0.0001**	**<0.0001**

[a]Protoporphyrin IX measured in mM per gram of eggshell.

[b]Mean±SD.

[A,B,C,D] Across a column, values with different superscripts is significantly different from each other.

4.5.2 Experiment 2

There was a statistically significant main effect ($P < 0.0001$) of day p.i. and challenge strain (control, N1/88, T, Vic S and A3 strains), but no significant interaction between the two ($P > 0.05$) for shell reflectivity (%) and L* measured on eggshells with and without cuticle (Table 4.3, Figures 4.1–4.4). The shell reflectivity and L* increased with day p.i. until day 12, and then decreased slightly up to day 22, indicating that the amount of pigment first decreased and then increased slightly with day p.i. (Table 4.3). The eggshells of hens infected with wild strains of IBV were lighter in colour compared with those from hens infected with the vaccine strains. The shell reflectivity, L* and PP IX values were not significantly different between unvaccinated and vaccinated hens for whole eggshells, but the difference was significant when values were measured on shells without cuticle and for the cuticle alone (Table 4.4). Eggshells from the control group and A3 strain infected hens were significantly different from that of the other groups with lower shell reflectivity and L*, and higher PP IX.

Table 4.3 Effect of day p.i. on shell colour variables following challenge with different infectious bronchitis virus strains (Experiment 2)

Day p.i.	Shell reflectivity with cuticle	Shell reflectivity without cuticle	L* with cuticle	L* without cuticle	[a]PP IX in whole eggshell ($\times 10^{-8}$)	PP IX in shell without cuticle ($\times 10^{-8}$)	PP IX in cuticle ($\times 10^{-8}$)
2	[b]31.18±4.0^{C}	37.48±4.3^{AB}	62.95±3.3^{D}	68.19±3.7^{BCD}	10.03±1.5^{A}	8.06±1.4^{A}	2.27±1.2
4	32.41±4.3^{B}	38.18±4.8^{AC}	64.22±3.5^{ABC}	69.30±3.3^{A}	9.68±1.9^{BC}	7.57±1.6^{BCD}	2.10±1.4
6	32.79±4.8^{A}	38.76±5.5^{A}	64.92±3.8^{A}	69.67±4.0^{A}	9.24±1.9^{C}	7.46±1.7^{CD}	1.78±1.1
8	32.61±4.6^{AB}	38.46±4.8^{AB}	64.38±3.5^{AB}	69.30±3.6^{A}	9.28±1.8^{C}	7.31±1.6^{D}	1.97±1.1
10	31.30±5.1^{C}	37.45±4.9^{BCD}	63.88±4.0^{BCD}	68.38±3.7^{AB}	9.75±1.9^{BC}	7.60±1.5^{BCD}	2.15±1.2
12	31.74±4.8^{ABC}	36.85±4.9^{DE}	64.13±3.8^{ABC}	68.32±3.8^{BCD}	9.98±1.7^{AB}	7.83±1.5^{ABC}	2.14±1.2
14	30.78±4.2^{C}	36.20±4.5^{DE}	62.31±3.7^{D}	67.54±3.5^{D}	10.01±1.8^{AB}	7.96±1.5^{AB}	2.19±1.2
16	31.15±4.8^{C}	36.89±4.5^{CD}	63.33±3.9^{CD}	68.22±3.5^{BCD}	9.84±1.8^{AB}	7.81±1.5^{ABC}	2.03±1.1
18	30.86±5.0^{C}	36.09±4.8^{E}	63.23±4.0^{CD}	67.66±3.8^{CD}	10.02±1.8^{AB}	8.17±1.4^{A}	2.09±1.2
20	31.50±4.4^{BC}	37.27±4.8^{E}	63.82±3.6^{BCD}	68.61±3.7^{ABC}	9.88±1.5^{AB}	7.84±1.5^{ABC}	2.04±1.2
22	30.85±4.3^{C}	36.89±4.4^{CDE}	63.45±3.5^{BCD}	68.20±3.2^{BCD}	9.98±1.7^{AB}	7.88±1.7^{ABC}	2.10±1.2
P value	**0.0017**	**0.0002**	**0.0003**	**<0.0001**	**<0.0001**	**0.0036**	**0.3566**

[a]Protoporphyrin IX expressed in mM per gram of eggshell.

[b]Mean±SD.

[A,B,C,D,E] Across a column, values with different superscripts are significantly different from each other.

For a 1 g piece of eggshell, there was more PP IX in the shell with cuticle intact, as compared with a piece of shell from the same eggshell with cuticle removed. The total amount of PP IX in 1 g of shell both with and without cuticle was significantly higher at day 2 p.i. compared to the other days p.i. up until day 22 (Table 4.3). Among the treatment groups, for shells with and without cuticle, control group eggshells had the most PP IX, T strain the lowest, with the N1/88, Vic S and A groups having intermediate (Figure 4.3).

Table 4.4 Effect of vaccination status on eggshell colour of hens challenged with infectious bronchitis virus strains (Experiment 2)

Variable	Laying hens status		P value
	Unvaccinated	Vaccinated	
Shell reflectivity with cuticle	31.63±4.5[b]	31.44±4.8	0.4789
Shell reflectivity without cuticle	37.79±4.5[A]	36.86±5.1[B]	0.0010
L* with cuticle	63.89±3.5	63.57±3.9	0.1416
L* without cuticle	68.91±3.3[A]	68.15±3.9[B]	0.0004
[a]PP IX in whole eggshell ($\times 10^{-8}$)	9.77±1.7	9.95±1.9	0.0947
PP IX in eggshell without cuticle ($\times 10^{-8}$)	7.59±1.4[B]	7.96±1.7[A]	0.0001
PP IX in cuticle ($\times 10^{-8}$)	2.18±1.2[A]	1.99±1.2[B]	0.0105

[a]Protoporphyrin IX expressed in mM per gram of eggshell. [b]Mean±SD.

[A,B] Across a column, values with different superscripts are significantly different from each other

4.6 Discussion

The pilot experiment suggested that storage under the conditions described here had no effect on the PP IX levels in eggshells. The shell reflectivity results for the whole eggshells and for the calcareous part of the shells also indicated that the storage conditions did not significantly affect the amount of PP IX present in the eggshells. The results of shell reflectivity measured again on the whole eggshells were very similar to the results published by Chousalkar and Roberts (2009). The

measurements of shell reflectivity in eggshells without cuticle generated a new data set and these data were compared with L* and PP IX results in order to gain an insight into the correlation between these variables.

Experiment 1 was conducted to investigate the effects of two wild IBV strains (T and N1/88) on the loss of brown eggshell colour and how quickly the colour was restored compared with a control group of hens. Significantly, lower values for shell reflectivity and L* for eggshells with cuticle on day 1 p.i. showed that the shell colour was lighter following exposure of the hens to IBV. The changing pattern in shell reflectivity with day p.i. was not consistent with the change occurring in L*. The results of L* may be more accurate than shell reflectivity as during measurement of L*, the spectrophotometer takes three readings in each of three locations around the eggshell and calculates an average. In addition, reflectivity may be affected by the smoothness of the surface of the eggshell. The results of PP IX concentrations confirmed that the loss of shell colour resulting from IBV challenge correlates with a smaller amount of the pigment PP IX being deposited into the eggshell during eggshell formation in the shell gland of the brown laying hen. A slightly different trend in the values of shell reflectivity and L* for shells without cuticle indicates the importance of the cuticle layer. A positive correlation (0.7049) between shell reflectivity and L* confirmed that the two methods gave consistent values, although they were slightly different from each other. The reduction in shell colour resulting from the challenge of unvaccinated hens with the N1/88 and T strains of IBV has been reported previously (Chousalkar & Roberts, 2009). There was no significant difference in egg production ($P > 0.05$) between the control and IBV-infected groups (Chousalkar & Roberts, 2007a). The virus was detected in the shell gland of unvaccinated laying hens on day 6 p.i. (Chousalkar et al., 2009b, 2010). All hens were negative for IBV antibodies before challenge and there was a significant rise in ELISA antibody titres in treatment groups measured before challenge and 5 and 10 weeks p.i. (Chousalkar & Roberts, 2007b). The antibody titres were significantly higher in T as compared with N1/88 strain infected hens (Chousalkar & Roberts, 2007b). The correlation between L* and PP IX for shells with cuticle confirmed that, in lighter coloured eggshells, there was always a lower amount of PP IX in 1 g of shell.

A significant effect of day p.i. on shell reflectivity and L* with and without cuticle, as well as PP IX in shells with and without cuticle and in cuticle alone, indicated that IBV strains affected the pigment synthesis and/or deposition during the different stages of eggshell formation. The purpose of removing cuticle from individual eggshells and remeasuring shell reflectivity, L* and PP IX was to examine any possible effect of IBV infection on cuticle synthesis and/or deposition onto shells. From Tables 4.2 and 4.3, it can be seen that IBV-infected hens laid eggs with the cuticle layer present and thus the viral strains significantly affected the PP IX synthesis and/or deposition rather than the formation of the cuticle layer itself. However, this is a tentative conclusion as the amount of cuticle on the surface of the eggshells was not directly measured in the current study. Also, the cuticle layer on the eggshell surface varies between eggs from the same hen and eggs from different hens of the same flock.

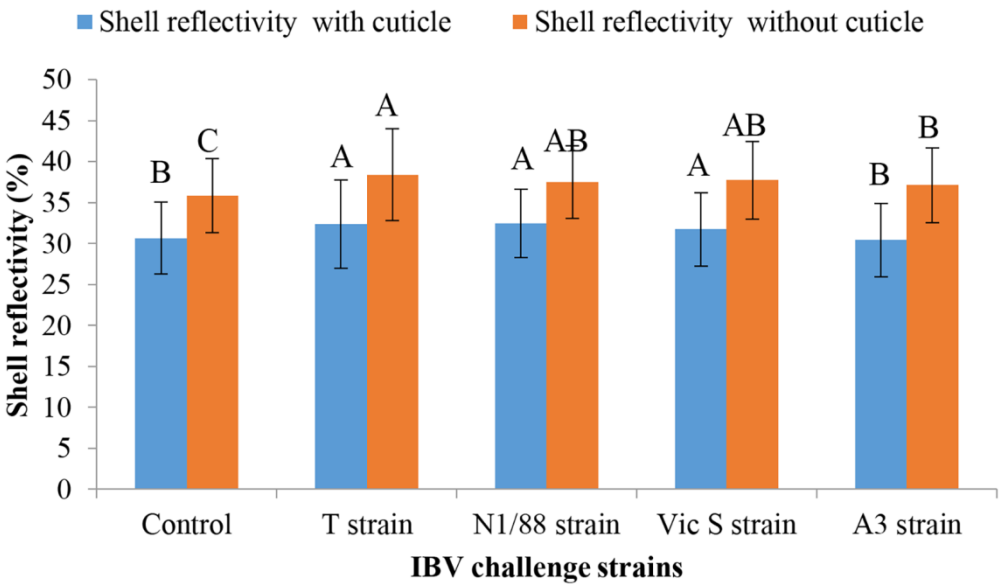

Figure 4.1 Effect of IBV on eggshell reflectivity with and without cuticle ($P < 0.05$)

Bars represent standard deviation. In each category, values with different superscripts are significantly different from each other.

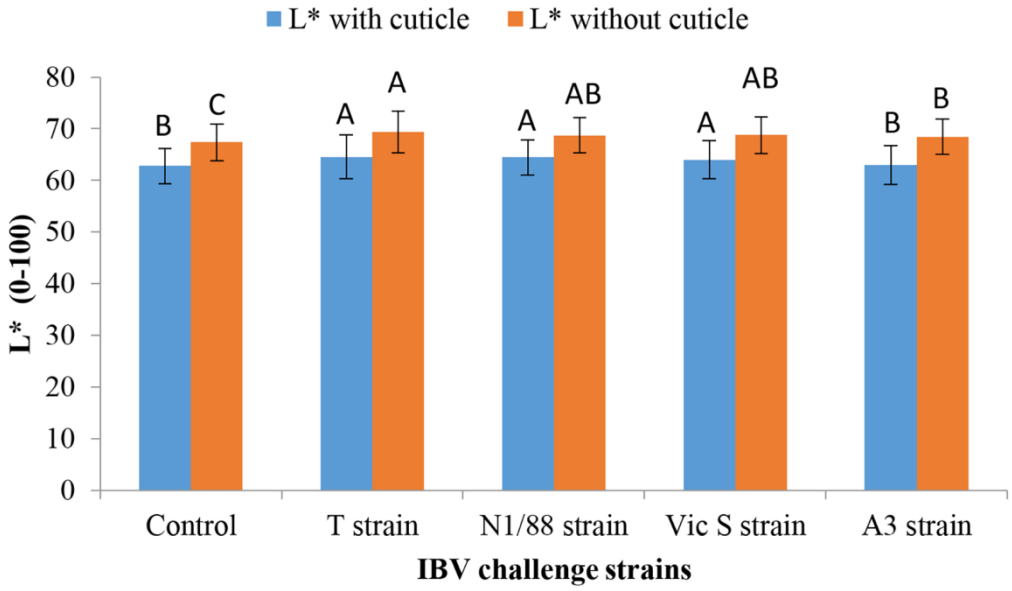

Figure 4.2 Effect of IBV on L* of eggshells with and without cuticle ($P < 0.0001$)

Bars represent standard deviation. In each category, values with different superscripts are significantly different from each other.

Experiment 2 also showed that different IBV strains affected the intensity of brown eggshell colour in laying hens differently. In unvaccinated laying hens, a higher amount of PP IX in cuticle alone might indicate that the cuticle layer was more complete on eggs laid by these hens. The non-significant difference between unvaccinated and vaccinated hen eggshell values for shell reflectivity, L* and PP IX suggests that the vaccination had little or no protective effect against the effects of IBV infection on the secretion and/or deposition pattern of PP IX in the shell gland. Eggshells from the control group and A3 strain infected hens were significantly different from the other groups with lower shell reflectivity, L* values and higher PP IX values, which means that these hens deposited a higher amount of PP IX onto the shells.

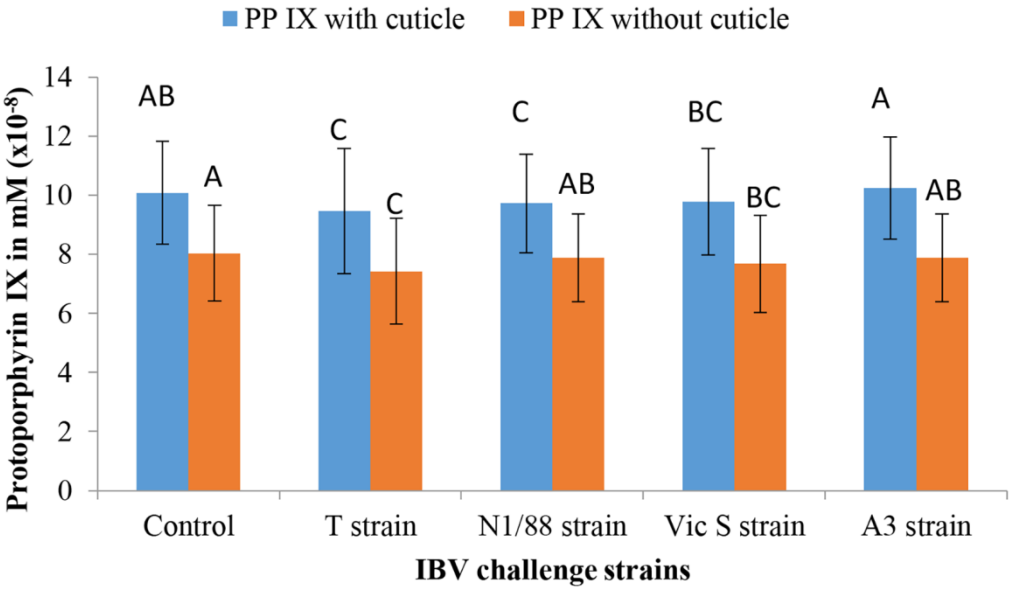

Figure 4.3 Mean values of PP IX in eggshells with and without cuticle from eggs collected from hens that had been inoculated with IBV ($P < 0.05$)

Bars represent standard deviation. In each category, values with different superscripts are significantly different from each other.

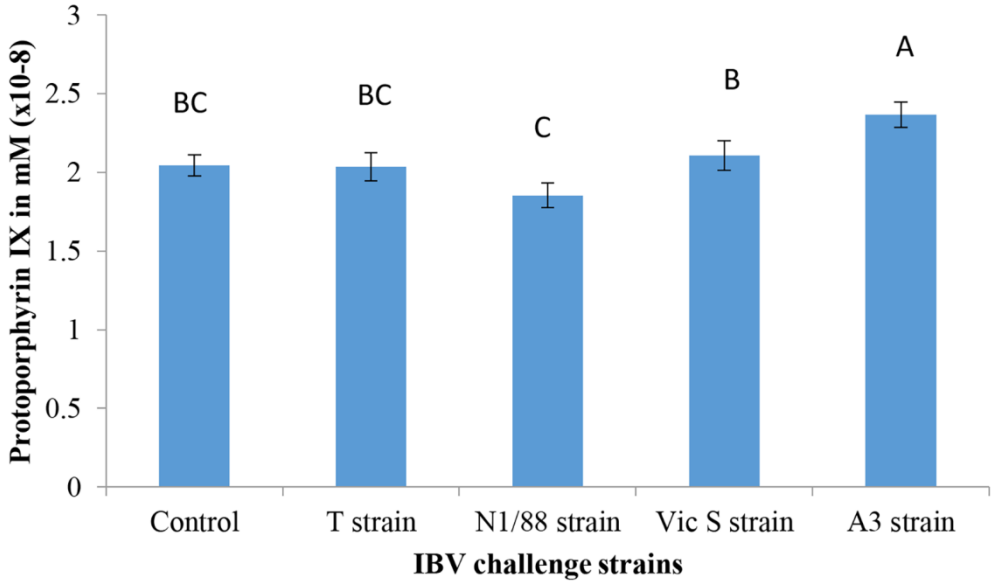

Figure 4.4 Mean values of PP IX in the cuticle of eggs collected from hens that had been inoculated with IBV ($P = 0.0005$)

Bars represent standard deviation. Values with different superscripts are significantly different from each other.

The mechanism of action of IBV strains on pigment synthesis is not clear, but pathology induced in the oviduct by IBV may disrupt the cellular mechanisms responsible for the synthesis and subsequent deposition of pigment onto the eggshell. The present study showed that all four strains of IBV investigated in this study caused loss of brown colour in the eggshells and that this loss of colour correlated with a lower amount of PP IX in the shells. The mean egg production was not significantly different among the treatment groups (Chousalkar et al., 2009a). The T and N1/88 strains of IBV were detected in the shell gland of vaccinated and unvaccinated laying hens at day 6 p.i. (Chousalkar et al., 2009b, 2010). In the group of hens vaccinated and challenged with the Vic S strain, the virus was not detected in the shell gland until day 12 p.i. (Chousalkar et al., 2009a). Hens from unvaccinated control groups were negative for IBV antibodies (Chousalkar et al., 2009a). The ELISA antibody titres measured before the challenge and at 5 and 10 weeks p.i. were significantly higher following vaccination and challenge with IBV strains Vic S and A (Chousalkar et al., 2009a). Antibody titres in the vaccinated but uninfected control group remained constant at 5 and 10 weeks p.i. (Chousalkar et al., 2009a). In conclusion, inoculation with the IBV strains used in this study reduced the intensity of brown shell colour to different extents. Furthermore, the lower PP IX values for the T strain challenged group showed that this strain had a more severe effect, compared with N1/88, on pigment synthesis and/or deposition in the shell gland of brown-egg laying hens. Similar to the results of Experiment 1, in Experiment 2, different IBV strains affected brown eggshell colour to different extents, with a non-significantly higher amount of PP IX in eggshells from vaccinated hens compared with unvaccinated hens. Further research is needed to explore the mechanism of action of IBV on pigment secretion and deposition.

4.7 References

Balestrin, E., Fraga, A. P., Ikuta, N., Canal, C. W., Fonseca, A. S. K. & Lunge, V. R. (2014). Infectious bronchitis virus in different avian physiological systems-A field study in Brazilian poultry flocks. Poultry Science, 93, 1922-1929.

Chousalkar, K. K., Cheetham, B. F. & Roberts, J. R. (2009a). Effects of infectious bronchitis virus vaccine on the oviduct of hens. Vaccine, 27, 1485-1489.

Chousalkar, K. K., Cheetham, B. F. & Roberts, J. R. (2009b). LNA probe-based real-time RT-PCR for the detection of infectious bronchitis virus from the oviduct of unvaccinated and vaccinated laying hens. Journal of Virological Methods, 155, 67-71.

Chousalkar, K. K., Cheetham, B. F. & Roberts, J. R. (2010). Detection of infectious bronchitis virus strain N1/88 from the oviduct and feces of experimentally infected vaccinated and unvaccinated hens. Poultry Science, 89, 1603-1608.

Chousalkar, K. K. & Roberts, J. R. (2007a). Ultrastructural observations on effects of infectious bronchitis virus in eggshell-forming regions of the oviduct of the commercial laying hen. Poultry Science, 86, 1915-1919.

Chousalkar, K. K. & Roberts, J. R. (2007b). Ultrastructural study of infectious bronchitis virus infection in infundibulum and magnum of commercial laying hens. Veterinary Microbiology, 122, 223-236.

Chousalkar, K. K. & Roberts, J. R. (2009). Effects of Australian strains of infectious bronchitis virus on internal and external quality of hen eggs. Animal Production Science, 49, 162-169.

Chousalkar, K. K., Roberts, J. R. & Reece, R. (2007). Histopathology of two serotypes of infectious bronchitis virus in laying hens vaccinated in the rearing phase. Poultry Science, 86, 59-62.

Cook, J. K. A. & Huggins, M. B. (1986). Newly isolated serotypes of infectious bronchitis virus: their role in disease. Avian Pathology, 15, 129-138.

Crinion, R. A. P. & Hofstad, M. S. (1972). Pathogenicity of four serotypes of avian infectious bronchitis virus for the oviduct of young chickens of various ages. Avian Diseases, 16, 351-363.

Curtis, P. A., Gardner, F. A. & Mellor, D. B. (1985). A comparison of selected quality and compositional characteristics of brown and white shell eggs. II. Interior quality. Poultry Science, 64, 302-306.

Hewson, K. A., Tobertson, T., Steer, P. A., Devlin, J. M., Noormohammadi, A. H. & Ignjatovic, J. (2014). Assessment of the potential relationship between egg quality and infectious bronchitis virus infection in Australian layer flocks. Australian Veterinary Journal, 92, 132-138.

Ignjatovic, J., Ashton, D. F., Reece, R., Scott, P. & Hooper, P. (2002). Pathogenicity of Australian strains of avian infectious bronchitis virus. Journal of Comparative Pathology, 126, 115-123.

Ignjatovic, J. & Sapats, S. (2000). Avian infectious bronchitis virus. Revue Scientifique et Technique de l'OIE, 19, 493-508.

Ishikawa, S., Suzuki, K., Fukuda, E., Arihara, K., Yamamoto, Y., Mukai, T. & Itoh, M. (2010). Photodynamic antimicrobial activity of avian eggshell pigments. FEBS Letters, 584, 770-774.

Jones, D. R., Musgrove, M. T., Anderson, K. E. & Thesmar, H. S. (2010). Physical quality and composition of retail shell eggs. Poultry Science, 89, 582-587.

Kennedy, G. Y. & Vevers, H. G. (1976). A survey of avian eggshell pigments. Comparative Biochemistry and Physiology Part B: Comparative Biochemistry, 55, 117-123.

McMartin, D. A. (1968). The pathogenicity of an infectious bronchitis virus for laying hens, with observations on pathogenesis. British Veterinary Journal, 124, 576-581.

Nii, T., Isobe, N. & Yoshimura, Y. (2014). Effects of avian infectious bronchitis virus antigen on eggshell formation and immunoreaction in hen oviduct. Theriogenology, 81, 1129-1138.

Samiullah, S. & Roberts, J. R. (2013). The location of protoporphyrin in the eggshell of brown-shelled eggs. Poultry Science, 92, 2783-2788.

Sevoian, M. & Levine, P. P. (1957). Effects of infectious bron-chitis on the reproductive tracts, egg production, and egg quality of laying chickens. Avian Diseases, 1, 136-164.

Uenaka, T., Kishimoto, I., Sato, S., Animas, S. B., Ito, T., Otsuki, K. & Cook, J. K. A. (1998). Intracloacal infection with avian infectious bronchitis virus. Avian Pathology, 27, 309-312.

Yang, H. M., Wang, Z. Y. & Lu, J. (2009). Study on the relationship between eggshell colour and egg quality as well as shell ultrastructure in Yangzhou chicken. African Journal of Biotechnology, 8, 2898-2902.

Higher Degree Research Thesis by Publication
University of New England

STATEMENT OF AUTHORS' CONTRIBUTION

(To appear at the end of each thesis chapter submitted as an article/paper)

We, the Research Master/PhD candidate and the candidate's Principal Supervisor, certify that all co-authors have consented to their work being included in the thesis and they have accepted the candidate's contribution as indicated in the *Statement of Originality*.

	Author's Name (please print clearly)	% of contribution
Candidate	**Sami Samiullah**	60
Other Authors	**Juliet Roberts**	20
	Kapil Chousalkar	20

Name of Candidate: **Samiullah**

Name/title of Principal Supervisor: **Associate Professor Juliet Roberts**



Candidate Date 09/06/2017



Principal Supervisor Date 09/06/2017

Higher Degree Research Thesis by Publication
University of New England

STATEMENT OF ORIGINALITY

(To appear at the end of each thesis chapter submitted as an article/paper)

We, the Research Master/PhD candidate and the candidate's Principal Supervisor, certify that the following text, figures and diagrams are the candidate's original work.

Type of work	**Page number/s**
Figure 4.1	101
Figure 4.2	101
Figure 4.3	103
Figure 4.4	103
Text and tables	87-106

Name of Candidate: **Samiullah**

Name/title of Principal Supervisor: **Associate Professor Juliet Roberts**

[redacted]

Candidate Date 09/06/2017

[redacted]

Principal Supervisor Date 09/06/2017

Chapter 5 Reference gene selection for the shell gland of laying hens in response to time-points of eggshell formation and nicarbazin

Published as: Samiullah S, Roberts J, Wu S-B (2017). Reference gene selection for the shell gland of laying hens in response to time-points of eggshellformation and nicarbazin. PLoS ONE 12(7):e0180432

5.1 Abstract

Ten reference genes were investigated for normalization of gene expression data in the shell gland of laying hens. Analyses performed with geNorm revealed that hypoxanthine phosphoribosyltransferase 1 (*HPRT1*) and hydroxymethylbilane synthase (*HMBS*) were the two most stable reference genes in response to post-oviposition time alone (POT) or with nicarbazin treatment (POT+N) of laying hens. NormFinder analyses showed that the two most stable reference genes in response to POT and POT+N were 18S ribosomal RNA (*18S rRNA*), ribosomal protein L4 (*RPL4*) and *HMBS*, *RPL4*, respectively. BestKeeper analyses showed that *18S rRNA*, *RPL4* and *HPRT1*, *HMBS* were the two most stable reference genes for POT, and POT+N, respectively. Of the ten reference genes, all except *B2M* showed geNorm M <0.5, suggesting that they were stably expressed in the shell gland tissue. Consensus from these three programs suggested *HPRT1* and *HMBS* could be used as the two most stable reference genes in the present study. Expression analyses of four candidate target genes with the two most and the two least stable genes showed that a combination of stable reference genes leads to more discriminable quantification of expression levels of target genes, while the least stable genes failed to do so. Therefore, *HMBS* and *HPRT1* are recommended as the two most stable reference genes for the normalization of gene expression data at different stages of eggshell formation in brown-egg laying hens. Available statistical programs for reference gene ranking should include more robust analysis capability to analyse the gene expression data generated from factorial design experiments.

5.2 Introduction

The chicken reproductive tract is divided into five histologically distinct parts, the ovary, infundibulum, magnum, isthmus, and shell gland (uterus). The shell gland is an expanded pouch-like part of the oviduct where an egg remains for approximately 18-20 hours, during which shell formation takes place [1]. The next ovulation occurs 0.5 hour after the preceding oviposition [2]. Calcification of the eggshell is associated with stimuli initiated by ovulation or by neuroendocrine factors that control and coordinate both ovulation and calcium secretion [3]. The eggshell is a highly ordered bio-ceramic (about 5 g calcium) of fused calcite crystalline cones, formed on a protein skeleton with distinct layers and regular pores [4]. Like other epithelial cells, the shell gland epithelium provides antimicrobial protection for both hen and egg; thus, it is a rich source of anti-microbial proteins [5].

Approximately 437 peptides and ion transporters have been identified as being involved in the formation of three distinct layers of the eggshell [6, 7]. However, the mechanisms of egg and eggshell biogenesis in relation to the origin and flow of the precursors at various stages of egg formation are not fully understood. The biosynthetic pathway of protoporphyrin IX (PP IX) is important in the formation of the eggshell as it contributes to the shell colour. PP IX is an immediate precursor of heme and a major component of brown eggshell pigment. To date, there is little information about the origin of its precursors and how PP IX is inhibited from converting into heme through the enzymatic activity of ferrochelatase in the shell gland of laying hens. Furthermore, it is not clear how many genes are involved in the PP IX synthesis, ultimate transportation across cell membranes and subsequent deposition into distinct eggshell layers. In the shell gland, hundreds of genes that are differentially expressed between juvenile and mature laying hens have been identified [8]. It is assumed that some genes express differentially in relation to the formation of distinct layers of the eggshell. Furthermore, the expression of genes associated with epithelial differentiation and tissue remodelling may vary with different levels of estrogen secretion in the presence or absence of an egg [9].

Nicarbazin is one of the various factors that causes lower production and/or deposition of PP IX into eggshell, when fed at recommended dosages (50-125

mg/kg of feed) to brown-egg laying hens [10, 11]. It is a chemically produced drug composed of a complex equimolar amount of 4,40-dinitrocarbanilide (DNC) and 2-hydroxy-4,6-dimethylpyrimidine (HDP) and is registered for use in poultry fattening and for treating coccidiosis [10, 12]. It is used either in pure or combined forms as a feed additive in poultry production [13]. Its effects on eggshell colour, which are dosage and time dependent, are reversible [14]. The pharmacodynamics of nicarbazin in the shell gland are not yet known, and the way it acts at the molecular level to alter the synthesis and/or deposition of PP IX into eggshells at different stages of shell formation needs to be further investigated. Therefore, we anticipate that the responses of the genes involved in the PP IX synthesis pathway to nicarbazin will shed some light on its actions in the alteration of eggshell colour deposition. Nicarbazin was used as a model as residues of this drug in feed are still a problem of loss in shell colour particularly in Australia. In addition, investigation of the molecular basis of nicarbazin effects on shell colour may shed light on the mechanisms of shell colour loss in commercial laying flocks from other causes.

The transcriptional profiling in the shell gland is different from other parts of the oviduct, such as the magnum and isthmus [7]. Thus, data on differential gene expression in the shell gland are needed and, therefore, selection of reference genes for gene expression analysis as a normalization approach is paramount. To the best of our knowledge, no studies have been performed to identify suitable reference genes for the normalization of quantitative PCR (qPCR) gene expression data in the shell gland of chickens. Traditionally, the most commonly used housekeeping genes, such as *ACTB*, *TUBB*, and *GAPDH* have been selected as generic reference genes. However, ample evidence has shown that the expression of these genes may not be constant across a range of experimental conditions and tissues under investigation [15-20]. Thus, it is now recommended to use these genes only as reference genes for normalization when prior analysis of their expression stability has been carried out [21], to ensure that cellular expression level of the reference genes is virtually identical under different conditions in the study. It is also recommended that more than one reference gene be employed to achieve more robust, accurate and reliable normalization of gene expression data [22].

Of the available statistical software, three distinct tools have been frequently reported in the literature for ranking the overall expression stabilities of the reference genes as normalizers for gene expression studies. The geNorm module in qbase+ software version 3.0 (Biogazelle, Belgium) calculates the gene expression stability (geNorm M) as the arithmetic mean of the pairwise variation (geNorm V) between all tested genes [22, 23]. The geNorm V for any given two genes is the standard deviation calculated from the $\log_2$ transformed relative quantities between those two genes [22]. Before analysis, qbase+ pre-processes the data for efficiency correction, inter-run calibration, bad replicates removal and conversion to relative quantities [23]. The relative quantities are then converted to either linear or log transformed scale. The current geNorm tool does limit the minimum number of genes to 8, unlike to its previous Excel based version. qbase+ allows easy exchange of data between users, and exports tabulated data for further statistical analysis using dedicated software. The most stably expressed gene produces the lowest geNorm M value. The most stable reference gene is determined by step-wise exclusion of the least stable genes [22]. geNorm eliminates the genes sequentially and thus a differentially expressed gene does not affect the ultimate outcomes from the analysis. Therefore, geNorm is usually less sensitive to differentially expressed genes initially included in the assay. Good reference genes have an $M < 0.5$ and CV (Coefficient of variance) <0.2, while M values up to 1 are acceptable for more difficult samples [23]. The cut-off value for geNorm V is 0.15. geNorm does not consider treatment groups and all samples are treated as being from a single population. NormFinder (GenEx version 6.0.1) calculates the standard deviation (SD) of the genes relative to the mean expression of all the genes in the panel [24]. It calculates a global average expression of all the genes in all the samples, to which the individual genes are compared. Based on this comparison, SD for each reference gene is estimated. Furthermore, if the samples are from different treatment groups, NormFinder separates the variation into an intragroup and an intergroup contribution [24, 25]. Hence, a low stability value reflects low inter- and intra-group variation. Similar to qbase+, GenEx does have an option to highlight bad replicates during data analysis and thus bad replicates can be excluded from the analysis easily. In the GenEx version 6.0.1, the data pre-processing is very similar to that explained in the qbase+ section. In addition, the data in GenEx, can be also

converted to logarithmic scale, such as $\log_2$, $\log_{10}$, 1n and log(X+1). An Excel based BestKeeper (Version 1) software is used to determine the best stable reference genes based on Pearson correlation coefficient (r), coefficient of variance (CV) and standard deviation (SD). Only genes with a high r and low SD values are combined into BestKeeper index (BKI) value using the geometric mean of their Cq values [26]. The BKI is calculated from the geometric mean of the candidates Cq values for each specific sample [26]. The most stable reference genes are the ones with the lowest SD values and highest coefficients of correlation with the BKI [26]. BestKeeper also uses a statistical algorithm wherein the Pearson correlation coefficient for each candidate reference gene pair is calculated along with the probability of correlation significance of the pair [26]. Overall, a generalized opinion from the literature and scientific forums can be summarised: geNorm, NormFinder and BestKeeper basically provide similar outcomes for the overall stability of candidate reference genes.

In the present study, we aimed to select reference genes from ten housekeeping genes to be used for the analysis of gene expression levels at different stages of eggshell formation in the shell gland and in response to nicarbazin feeding of the laying hens. The most stable genes were selected on the basis of the stability of the genes across the three software. Furthermore, four candidate target genes encoding either enzymes or peptide transporter were chosen to compare the outcomes from the data by the two most and the two least stable reference genes. The solute carrier family 25, member 38 (*SLC25A38*), located on mitochondrial membrane, transports glycine into mitochondria for the synthesis of aminolevulinic acid, the first step in the synthesis of PP IX [27]. The delta-aminolevulinate synthase 1 (*ALAS1*) gene encodes a rate limiting non-erythroid enzyme that catalyses the reaction of succinyl co-enzyme A with glycine to form delta-aminolevulinic acid within the mitochondrial matrix [28]. Coproporphyrinogen oxidase (*CPOX*) gene encodes an enzyme in the PP IX biosynthetic pathway that converts coproporphyrinogen III into protoporhyrinogen III [29]. Ferrochelatase (*FECH*) gene encodes *FECH* enzyme, which converts PP IX into heme [30, 31]. The outcome of the study provides a set of reference genes that are expressed in a relatively constant level for all the birds sampled at different time-points of eggshell formation and in response to treatment with nicarbazin.

5.3 Materials and Methods

The experimental setup was approved by the University of New England, Animal Ethics Approval Committee under Authority No. AEC15-022. The protocol was carried out in accordance with the guidelines specified in the Australian Code for the Care and Use of Animals for Scientific Purposes 8th edition 2013.

5.3.1 Selection of reference genes and primer design

In the current study, ten reference genes were selected from the literature published for chickens and other animals (Table 5.1). The primers were either sourced from previously published studies in chickens or designed using NCBI primer tool (Table 5.2). The primer quality was checked in "Beacon Designer" software (http://www.premierbiosoft.com/qOligo/Oligo.jsp?PID=1) for the levels of secondary structures such as primer dimer, sequence repeats and palindrome. To check the sequence specificity, primers were blasted against the NCBI database using BLASTN, Ensembl Chicken Galgal4 and UCSC's Chicken (*Gallus gallus*) Genome Browser Gateway. Prior to qPCR analysis, primer efficiency and specificity for each primer pair were examined with target RNA samples in 10-time serial dilutions. Only primer pairs with specific amplifications and high efficiency were used in the optimisation.

Table 5.1 Functional annotation of the reference genes used in the current study

Gene symbol	Description	Cellular localization	Biological function
18S rRNA	Nuclear ribosomal RNA small subunit	cytoplasm, nucleus	biogenesis and export of the 40S ribosomal subunit
ALB	Albumin	extracellular	stabilizing extracellular fluid volume
ACTB	β-actin	cytoplasm, membranes	cytoskeletal structural protein, nucleotide, and ATP binding
B2M	Beta 2-microglobulin	Golgi membrane, plasma membrane, early endosome membrane, extracellular region	cytoskeletal protein, immune response, protein binding
CA2	Carbonic anhydrase 2	cytoplasm, cell membrane	catalyses reversible hydration of carbon dioxide
CST3	Cystatin C	extracellular	as an inhibitor of cysteine proteinases
GAPDH	Glyceraldehyde 3-phosphate dehydrogenase	plasma membrane	glycolytic enzyme, oxidoreductase in glycolysis and gluconeogenesis
HMBS	Hydroxymethylbilane synthase	cytoplasm	heme synthesis, porphyrin metabolism, transferase activity
HPRT1	Hypoxanthine phosphoribosyltransferase 1	cytoplasm	purine synthesis in salvage pathway
RPL4	Ribosomal protein L4	cytoplasm	component of the 60S subunit and encodes a ribosomal protein

Table 5.2 Forward (F) and reverse (R) primers sequence of the selected candidate reference and target genes

Gene	Primer sequence (5′-3′)	Amplicon size (bp)	Ta (°C)	Accession No.	Reference
18S rRNA	F: TGTGCCGCTAGAGGTGAAATT R: TGGCAAATGCTTTCGCTTT	63	60	AF173612.1	[32]
ALB	F: CCTGGACACCAAGGAAAT R: TGTGGACGCCGATAGAAT	197	60	NM_205261.2	[33]
ACTB	F: CTGTGCCCATCTATGAAGGCTA R: ATTTCTCTCTCGGCTGTGGTG	139	60	NM_205518.1	[33]
B2M	F: CGTCCTCAACTGCTTCGTG R: TCTCGTGCTCCACCTTGC	194	63	NM_001001750.1	[33]
CA2	F: TCAAACCAAGGGGAAACAAGC R: GTAGTCAGGGAGCCAGGGTA	99	63	NM_205317.1	this study
CST3	F: ATGAGAACGACGAGGGCTTG R: ATTCCAGACACGAGCTGCC	130	63	NM_205500.2	this study
GAPDH	F: GAGGGTAGTGAAGGCTGCTG R: CATCAAAGGTGGAGGAATGG	113	63	NM_204305.1	[34]
HMBS	F: GGCTGGGAGAATCGCATAGG R: TCCTGCAGGGCAGATACCAT	131	60	XM_417846.2	[35]
HPRT1	F: ACTGGCTGCTTCTTGTG R: GGTTGGGTTGTGCTGTT	245	63	NM_204848.1	[33]
RPL4	F: TTATGCCATCTGTTCTGCC R: GCGATTCCTCATCTTACCCT	235	60	NM_001007479.1	[32]
SLC25A38*	F: AGACACGGTATGAGAGTGGA R: ATCCCAGAGAAAGGTGCGTC	139	63	XM_418818.3	this study
CPOX*	F: GAGAGGACGGTATGTGGAGT R: TTTGGGATTGCGGAGAAC	187	60	XM_004938236.1	[36]
ALAS1*	F: GGTGGACAGGAAAGGTAAAGA R: ACTGGTCATACTGGAAGGTG	197	60	NM_001018012.1	[36]
FECH*	F: TGCTTTGCCGATCACAT R: CACGGTTCACCACAGACAT	112	60	U68033.1	[36]

*Genes used as candidate target genes for validation of reference genes at three different time-points of eggshell formation

5.3.2 Laying hens and tissue sampling

5.3.2.1 Effect of time-points on stability of reference gene expression (Experiment 1)

Based on the intensity of brown eggshell colour and uniformity in egg weight, 20 hens out of a flock of 63 Hy-Line Brown laying hens were selected. The laying production of the selected hens was 100%. The feed offered was premium top layer mash (Barastock, Australia). At the time of the experiment, hens were 36-37 weeks old. From the selected 20 hens, eggshell colour (L*) and egg weight (g) were measured using a Spectrophotometer (Konica CM-2600d Ramsey, NJ, USA) [37] and analytical weighing balance Quintix513-1S (Sartorius Lab Instruments GmbH & Co. KG Goettingen, Germany), respectively. The hens were divided into four groups in such a way that the average L* values and egg weight were not significantly different among the selected groups (Table 5.3). Individual hen oviposition time was monitored using a video camera at the time of sampling. Four groups of hens were sampled based on time-points (post-oviposition time 2, 5, 15 and 23.5 hrs). The hens were euthanized by CO_2 and the shell gland tissue was excised within 2 minutes of the euthanization. Approximately 500 mg tissue was taken from the centre of the shell gland after opening the shell gland from the anterior-ventral position and transferred directly to RNALater (Sigma Aldrich, Australia). The samples were stored at -20°C until further processing for total RNA extraction.

Table 5.3 Eggshell colour (L*) and egg weight of the hens selected for reference gene study optimisation at different time-points

Variable	Time-point (hr)				P value
	2 (5 hens)	5 (5 hens)	15 (5 hens)	23.5 (5 hens)	
L* value	56.24±0.99	54.38±0.98	54.19±0.89	54.36±0.28	0.2982
Egg weight (g)	62.81±3.51	63.95±2.31	62.96±1.66	65.65±1.77	0.8326

Values are mean±S.E.

The eggs were collected and analysed before dividing the experimental hens into various groups. On the basis of eggshell variables, hens were divided into groups in such a way that the variables were not significantly different among groups.

5.3.2.2 Effect of time-points and nicarbazin on stability of reference gene expression (Experiment 2)

A total of 30 hens having 100% laying efficiency were selected based on the intensity of eggshell colour (L*) and egg weight from the remaining flock of 43 Hy-Line Brown laying hens (Table 5.4). Rearing conditions were the same as described previously. At the time of the experiment, hens were 42-45 weeks old and were divided into groups with a 2×3 factorial design (Table 5.4). The hens were divided into groups in such a way that the average L* values and egg weight (g) were not significantly different among groups. Out of 30 hens, 15 hens were fed nicarbazin at a rate of 100mg/kg of commercial layer diet while the control hens were fed only commercial layer diet. Nicarbazin was fed to each group at a time in order to allow time for the processing of the treated hens without intoxicating them. The eggshell colour (L*) and egg weight were recorded for all the hens from prior to treatment until the tissue collection. Procedures for tissue collection and handling were the same as mentioned previously.

Table 5.4 Eggshell colour (L*) and egg weight of the hens selected for reference gene optimisation with nicarbazin treatment at different time-points

Variable	Group							
	Control (15 hens)				Nicarbazin (15 hens)			
	Time-point (hr)			P value	Time-point (hr)			P value
	5 (5hens)	15 (5hens)	23.5 (5hens)		5 (5hens)	15 (5hens)	23.5 (5hens)	
L* value	58.69±0.59	59.54±0.89	59.39±0.63	0.6827	58.46±0.67	58.89±0.52	59.06±0 51	0.7548
Egg weight (g)	63.73±1.77	63.29±1.58	63.87±1 58	0.6969	58.74±1.69	60.93±1.41	62.65±1 19	0.2019

Values are mean±S.E.

The eggs were collected and analysed before dividing the experimental hens into various groups. On the basis of eggshell variables, hens were divided into groups in such a way that the variables were not significantly different among groups.

5.3.3 Total RNA extraction and purification

Total RNA was extracted using TRIsure (Bioline, Australia), according to the manufacturer's instructions. Briefly, an approximately 50 mg of tissue (wet weight) was homogenized in 1 mL of TRIsure using an IKA T10 basic Homogenizer (Wilmington, NC, USA). After the RNA pellet was washed with 1.5 mL ethanol (75%) and subsequently air-dried for 10-15 minutes, 50 µL of UltraPure™ DEPC-treated water (Ambion, USA) was used to dissolve RNA pellets. The total RNA was further purified using RNeasy Mini Kit (Qiagen, GmbH, Hilden, Germany) as per the manufacturer's instructions. The elution of RNA from the spin column with 50 µL of RNase-free water was repeated twice and the eluted RNA solutions were mixed thoroughly. The purified RNA was analysed in a NANODROP-8000 spectrophotometer (ThermoFisher Scientific, Wilmington, DE, USA) to measure its quantity and purity. RNA integrity was examined using 1.5% agarose gel electrophoresis in 1× UltraPure™ TAE Buffer (ThermoFisher Scientific, Australia) solution. The 0.1-2 Kb RNA Ladder (Ambion™, Australia) was used as a marker. A 1:1000 Lonza GelStar™ Nucleic Acid Gel Stain in Orange G loading dye was used to stain RNA and the gel was viewed and photographed using a camera. Only RNA showing two distinct 28S and 18S bands without smear was regarded integrate and used in downstream qPCR assay.

5.3.4 Quantitative PCR

qPCR was performed with the SensiFAST SYBR® Lo-ROX One-Step RT-PCR Kit (Bioline, Australia). Master mix was prepared as per the manufacturer's protocol and 4 µL of RNA template from 1:100 dilutions with the exception of *18S rRNA* (that was in 10^{-4} dilutions) was added to the reaction wells using Corbett CAS1200 robotics (Corbett Life Science, Sydney, Australia). The reaction was run in triplicates of 20 µL in a Rotor-Gene Disc 100 (Qiagen, Sydney, Australia) with a Rotor-Gene 6000 thermocycler (Corbett Research, Sydney, Australia). No template control (NTC) and no reverse transcriptase (-RT) control were also included to detect possible contamination. Thermocycling conditions for a 2-step PCR were: reverse transcription at 45°C for 10 minutes, first denaturation at 95°C for 2 minutes, then 40 cycles of denaturation at 95°C for 5s and annealing at 60°C or 63°C for 20s.The fluorescent data were acquired at the end of each annealing step during PCR cycles. A melting step was conducted to assess the specificity of PCR amplification. The PCR products were examined on Agilent 2100 Bioanalyzer (Agilent Technologies, Waldbronn, Germany) gel using Agilent DNA 1000 Kit per the manufacturer's instructions to estimate the size of the amplicons for specificity. PCR amplification efficiencies and correlation coefficients (R^2) were determined with the amplifications of a series of six 10-fold dilutions. The qPCR data of the genes were processed further when the PCR amplification efficiency was in a range of 90 to 105%, and linear correlation coefficient $R^2 > 0.980$ were considered of high standard [38].

5.4 Statistical analysis

The eggshell colour (L*) and egg weight data were analysed by Statview software (SAS Institute Inc., Version 5.0.1.0). A two-way analysis of variance (ANOVA) was conducted taking time-point and nicarbazin treatment as independent and L* and egg weight as dependent variables. Level of significance was indicated by probability of less than 5%. The Fishers LSD test was used to differentiate levels of significance between mean values.

To determine the expression stability of 10 different reference genes, the geNorm module in qbase+ software version 3.0 (Biogazelle, Belgium) was used to calculate the gene expression stability measure (geNorm M) [22, 23]. The input data for qbase+ were generated using the relative quantities based on comparative quantification cycle (Cq). To be consistent, the Cq values for *18S rRNA*, which were from 10^{-4} dilutions, were adjusted according to 1:100 dilutions. Any triplicate reaction with difference more than 0.5 cycle was excluded from the analysis. To select the most stable genes, geNorm re-calculates the M stability measures after removing the least stable genes and repeats the process until the one most stable gene remains [22, 23]. To test the minimum number of reference genes, geNorm calculates a pairwise variation (geNorm V) based on $V_{n/n+1}$ and a higher value indicates a significant effect of additional gene on data normalization. Normally, the benefit of using an extra $(n+1)^{th}$ reference gene is limited as soon as the $V_{n/n+1}$ value drops below the 0.15 threshold. Due to its sequential elimination of less stable genes so as to produce less bias on the output of analysis, this program was used as the primary base for the selection of the reference genes.

In addition, another two programs, i.e., NormFinder [24, 25] and BestKeeper [26], were used to analyse the stability of gene expression as complementary measures to safeguard the output generated from geNorm. The raw Cq values were exported and analysed in NormFinder for reference gene expression stabilities. An Excel based BestKeeper (Version 1) software was also used to determine the best stable reference genes based on Pearson correlation coefficient (r), coefficient of variance (CV) and standard deviation (SD). The most stable genes were selected on the basis of the stability of the genes across the three software.

Data for the candidate target gene expression using the two most stable and the two least stable reference genes were analysed in qbase+ by scaling the average relative quantities across all unknown samples per target gene [23, 39]. Effect of time-points on the relative expression levels of the candidate target genes was analysed using one-way ANOVA. Tukey-Kramer method was used to correct the P-value results (corrected P value < 0.05) for the pairwise group comparisons in the ANOVA test [23].

5.5 Results

5.5.1 Primers specificity and efficiency

All of the primer pairs were specific in amplifications by showing a single band on the Agilent 2100 Bioanalyzer gel (Figure 5.1). The melting curve analyses of all primer pairs are depicted in Figure 5.2. The amplification efficiency of all ten candidate reference genes was between 93% and 101%. The amplification efficiencies were 100% for *18S rRNA*, 98% for *ACTB*, 101% for *ALB*, 93% for *B2M*, 94% for *CA2*, 100% for *CST3* and *GAPDH*, 94% for *HMBS*, 98% for *HPRT1* and 94% for *RPL4*. The overall expression pattern (Cq values) for these ten reference genes is shown in Figure 5.3A. Most of the reference genes were highly expressed, with average Cq values between 12 and 22 cycles, except *ALB*, which showed average Cq values around 28 cycles (Figure 5.3A). The expression pattern of all ten reference genes was calculated in the combined dataset of four different time-points (2, 5, 15, 23.5 hr, post-oviposition times).

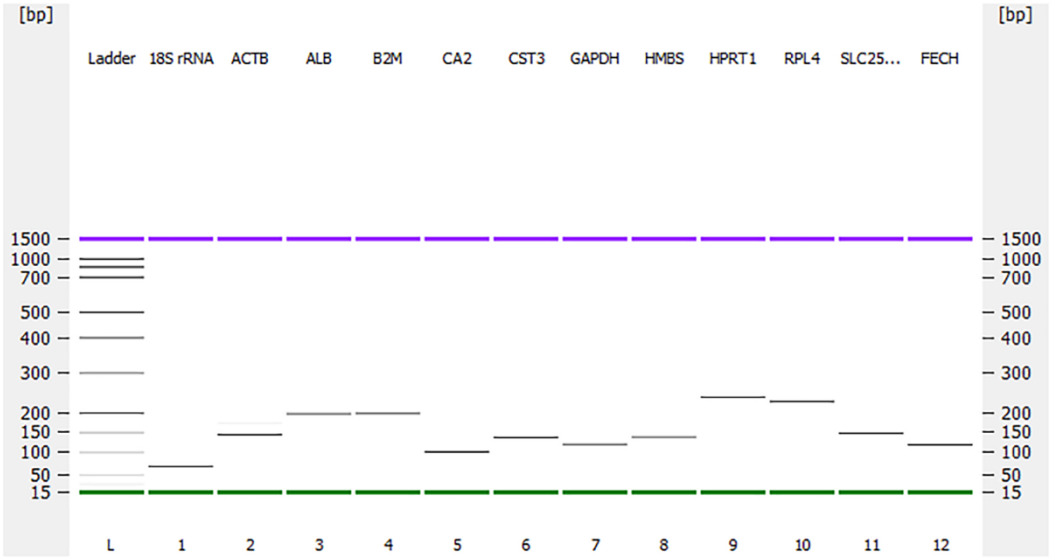

Figure 5.1 Amplification of the gene fragments from the eggshell gland tissue of laying hens to assess the specificities of the primers used in the current study

L, DNA ladder; **1**. *18S rRNA* (63 bp); **2**. *ACTB* (139 bp); **3**. *ALB* (197 bp); **4**. *B2M* (194 bp); **5**. *CA2* (99 bp); **6**. *CST3* (130 bp); **7**. *GAPDH* (113 bp); **8**. *HMBS* (131 bp); **9**. *HPRT1* (245 bp); **10**. *RPL4* (235); **11**. *SLC25A38* (139 bp); **12**. *FECH* (112 bp). All the amplified products were in accordance to the expected sizes. The amplified products were run on Agilent 2100 Bioanalyzer using Agilent DNA 1000 Kit as per the manufacturer's instructions. The upper

(purple) and lower (green) markers act as internal standards and are used to align the ladder analysis with the individual DNA sample analysis. The standard curve (plotting migration time against DNA amplicon size), in conjunction with the markers, is then used to calculate DNA fragment sizes for each well from the migration times measured (for more detail see Agilent 2100 Bioanalyzer Users Guide for Molecular Assays).

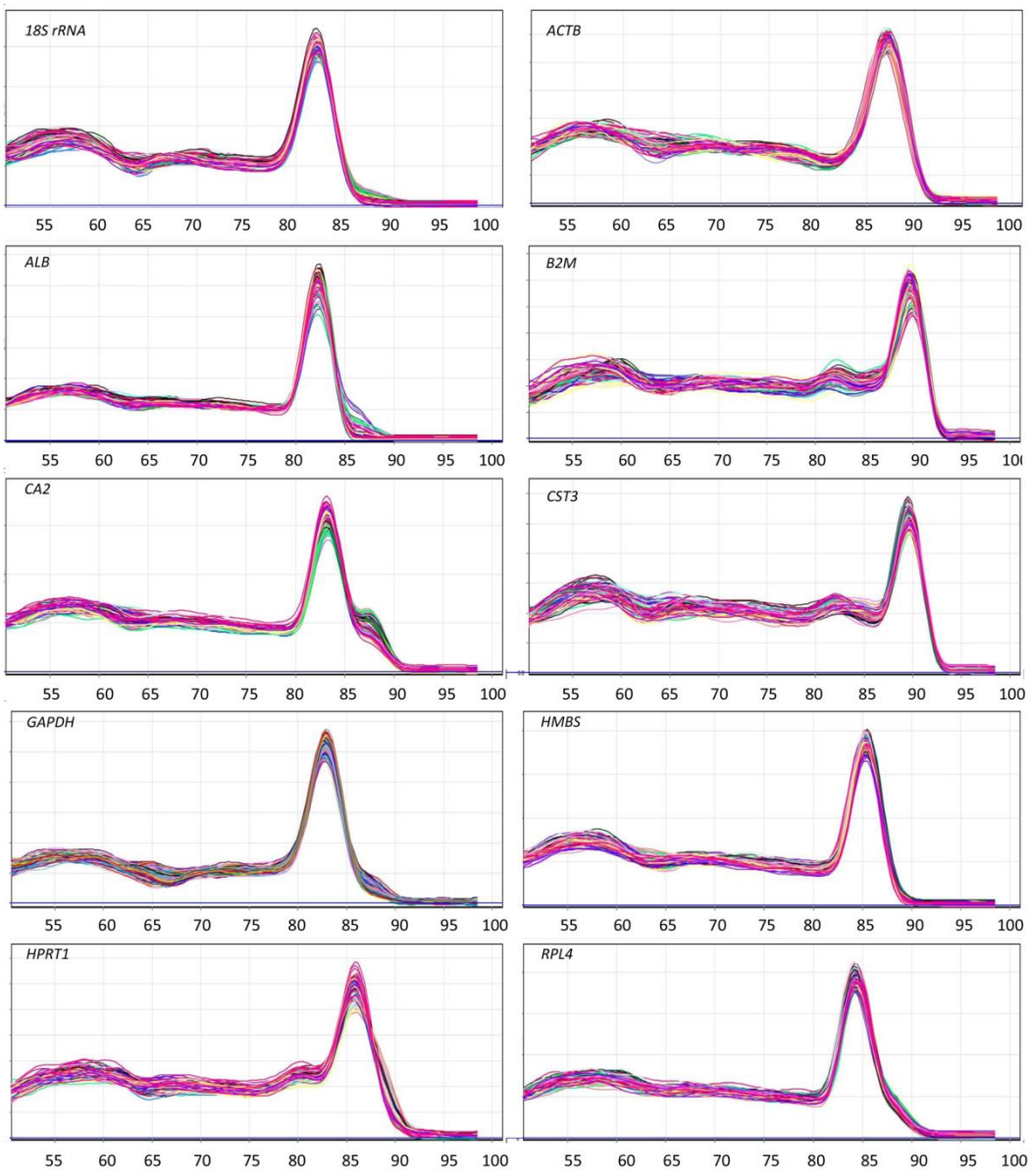

Figure 5.2 Melting curves of the amplicons from 10 candidate reference genes showing that the amplifications were specific and no primer dimers were present

All of the amplicons showed a single peak in melting curve analysis. After qPCR cycles, a melting phase at a ramp from 50°C to 99°C at 1°C increment was conducted to assess the specificity of PCR amplification.

5.5.2 Effect of time-points on stability of reference gene expression (Experiment 1)

Based on the expression stability (geNorm M), *HPRT1* and *HMBS* were the two most stable genes. The average expression stabilities (geNorm M) of the ten

reference genes were within the acceptable range (<0.50) that varied from 0.252 (*HPRT1*) to 0.482 (*ACTB*) (Table 5.5). The pairwise variation (geNorm V) also chose *HPRT1* and *HMBS* as the best set of genes to be used for expression data analysis (Figure 5.3B). The geNorm V value of *HPRT1* and *HMBS*, which was 0.086, indicated that stepwise inclusion of the next most stable reference gene (*18S rRNA*) is not necessary for data normalization. In line with geNorm M results, all ten reference genes showed geNorm V <0.15 (a default cut-off value). The results of NormFinder and BestKeeper analyses were slightly different from those of the geNorm. NormFinder ranked *18S rRNA* and *RPL4* as the two most stable reference genes, while the two most stable reference genes in BestKeeper were *18S rRNA* and *HPRT1* (Table 5.5). Nevertheless, all the genes analysed by NormFinder and BestKeeper had SD < 1.0, showing that these genes were overall stably expressed in the tissue under investigation. The two least stable reference genes across all the three statistical tools were *CA2* and *ACTB* (Table 5.5). The expression data were also analysed in geNorm excluding post-oviposition time 2 hours but this had no significant effect on the ranking of genes (Figure 5.3C).

Table 5.5 Stability values of reference genes affected by four different time-points performed in Experiment 1

Rank	**geNorm**		**NormFinder**		**BestKeeper**	
	Gene	**M value**	**Gene**	**SD**	**Gene**	**SD**
1	*HPRT1*	0.252	*18S rRNA*	0.065	*18S rRNA*	0.190
2	*HMBS*	0.254	*RPL4*	0.178	*HPRT1*	0.220
3	*18S rRNA*	0.264	*CST3*	0.182	*HMBS*	0.230
4	*CST3*	0.284	*HPRT1*	0.261	*CST3*	0.240
5	*RPL4*	0.306	*HMBS*	0.288	*GAPDH*	0.260
6	*ALB*	0.331	*ALB*	0.331	*RPL4*	0.290
7	*GAPDH*	0.352	*GAPDH*	0.388	*ALB*	0.300
8	*B2M*	0.400	*B2M*	0.442	*B2M*	0.370
9	*CA2*	0.440	*CA2*	0.489	*CA2*	0.500
10	*ACTB*	0.482	*ACTB*	0.551	*ACTB*	0.500

Means of relative expression levels of genes at four different time-points (post-oviposition times 2, 5, 15, 23.5 hrs) were used to calculate the expression stability of genes across the three statistical software.

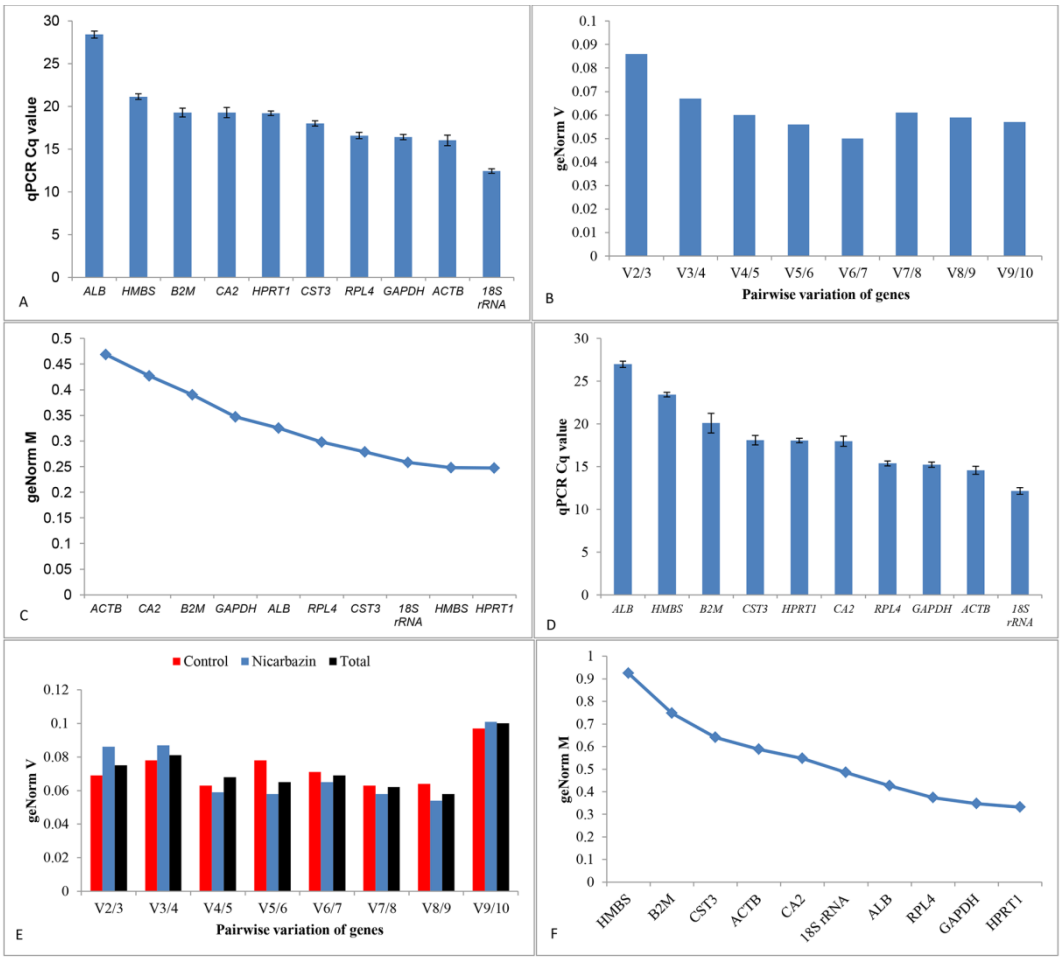

Figure 5.3 Effect of time-points and combination of time-points and nicarbazin treatment on the expression stability of reference genes in the shell gland of laying hens

A). Mean Cq values of 10 reference genes affected by time-points (Experiment 1). Bars represent standard deviation. **B**). Pairwise variation (geNorm V) of the optimal number of reference genes affected by time-points (Experiment 1). Pairwise variation ($V_{n/n+1}$) was analysed between the normalization factors NF_n and NF_{n+1} to determine the optimal number of reference genes. In the geNorm V graph, each bar represents change in normalization accuracy by stepwise inclusion of most to least stable gene. **C**). Average expression stability (geNorm M) values of reference genes excluding time-point 2 (post-oviposition time, 2 hours; Experiment 1). Most stable genes have lower M value. Time-point 2 was excluded to compare it with the control group of the time-points and nicarbazin treatment experiment (Experiment 2). **D**). Mean Cq values of 10 reference genes affected by time-points and nicarbazin treatment (control and nicarbazin groups combined). Bars represent standard deviation. **E**). Pairwise variation (geNorm V) of the optimal number of reference genes

(control, nicarbazin treated and both the groups combined). **F**). Average expression stability (geNorm M) values of reference genes (time-points (Experiment 1) and control hens from the time-points and nicarbazin treated groups (Experiment 2)). Most stable genes have lower M value.

5.5.3 Effect of time-points and nicarbazin treatment on stability of reference gene expression (Experiment 2)

The overall expression pattern (Cq values) of all the ten reference genes is depicted in Figure 5.3D. Calculating the expression stability of the reference genes for both the groups combined (control and nicarbazin treated), geNorm ranked *HMBS* and *HPRT1* as the two most stable genes (Table 5.6). The pairwise variations (geNorm V) for the control, nicarbazin treated and both the groups combined are shown in Figure 5.3E. The geNorm V values of the pairwise variation of the ten reference genes for the control, nicarbazin and both the groups combined were <0.15 (a default cut-off value). In order to gain insight into any difference between the expression data of the time-points experiment (Experiment 1) and the combination of time-points and nicarbazin treatment experiment (Experiment 2), the expression data of time-points and the control hens from time-points and nicarbazin treatment were analysed together with the exclusion of post-oviposition time 2 hours. The gene ranking was reshuffled and *HMBS* was ranked as the least stable gene (Figure 5.3F). NormFinder ranked *HMBS* and *RPL4*, while the BestKeeper showed *HPRT1* and *HMBS* as the two most stable genes (Table 5.6). Categorising all the ten reference genes into most stable, middle order and least stable, the reshuffling in gene ranking was different but relatively consistent for the first four genes across all the three statistical tools. It seems that the genes falling in mid order were more variable in stability when analysed for comparison by the three statistical tools. For the overall ranking obtained by the three algorithms, the two most stable reference genes for the total dataset were *HMBS* and *HPRT1*, while the two least stable genes were *B2M* and *CA2* (Table 5.6).

Table 5.6 Overall stability values of reference genes affected by time-points and nicarbazin treatment

Rank	geNorm		NormFinder		BestKeeper	
	Gene	**M value**	**Gene**	**SD**	**Gene**	**SD**
1	*HMBS*	0.236	*HMBS*	0.182	*HPRT1*	0.210
2	*HPRT1*	0.243	*RPL4*	0.191	*HMBS*	0.220
3	*GAPDH*	0.247	*HPRT1*	0.266	*RPL4*	0.230
4	*RPL4*	0.300	*18S rRNA*	0.291	*GAPDH*	0.270
5	*18S rRNA*	0.331	*GAPDH*	0.296	*ALB*	0.320
6	*ALB*	0.369	*ALB*	0.409	*18S rRNA*	0.330
7	*ACTB*	0.418	*ACTB*	0.446	*ACTB*	0.380
8	*CST3*	0.454	*CST3*	0.475	*CST3*	0.450
9	*CA2*	0.488	*CA2*	0.491	*CA2*	0.480
10	*B2M*	0.601	*B2M*	0.991	*B2M*	0.860

Means of relative expression levels in respective groups at three different time-points (post-oviposition times 5, 15, 23.5 hrs) and with nicarbazin treatments (yes, no) were used to calculate the expression stability of genes in responses to the time points and nicarbazin treatment across the three statistical software.

When the data were normalized in geNorm for each group separately, the control group showed that *HMBS* and *HPRT1* were the most stable reference genes (Table 5.7). In the same group, both NormFinder and BestKeeper ranked *RPL4* and *HMBS* as the two most stable reference genes. However, the overall ranking of the genes falling in middle order was reshuffled following the analyses by all the three statistical software. In the control group, the two least stable genes across all the three applets were *B2M* and *CA2*. The only genes that showed higher M value than the cut-off value in geNorm were *CA2* and *B2M* (Table 5.7).

Table 5.7 Stability values of reference genes affected by time-points

Rank	geNorm		NormFinder		BestKeeper	
	Gene	**M value**	**Gene**	**SD**	**Gene**	**SD**
1	*HMBS*	0.207	*RPL4*	0.138	*RPL4*	0.190
2	*HPRT1*	0.207	*HMBS*	0.172	*HMBS*	0.220
3	*GAPDH*	0.214	*HPRT1*	0.225	*HPRT1*	0.240
4	*RPL4*	0.274	*18S rRNA*	0.300	*GAPDH*	0.260
5	*18S rRNA*	0.305	*GAPDH*	0.309	*18S rRNA*	0.290
6	*ACTB*	0.373	*CST3*	0.455	*ALB*	0.340
7	*CST3*	0.424	*ACTB*	0.459	*ACTB*	0.400
8	*ALB*	0.461	*ALB*	0.499	*CST3*	0.450
9	*CA2*	0.503	*CA2*	0.544	*CA2*	0.480
10	*B2M*	0.609	*B2M*	0.963	*B2M*	0.710

Means of relative expression levels of the genes in the control group at three different time-points (post-oviposition times 5, 15, 23.5 hrs) were used to calculate the expression stability of genes across the three statistical software.

The reference genes ranking in the nicarbazin treatment group was slightly different from the control group. The geNorm ranked *HMBS* and *GAPDH* as the two most stable genes followed by *HPRT1* (Table 5.8). NormFinder showed *HMBS* and *ALB*, while the BestKeeper showed *HPRT1* and *HMBS* as the two most stable reference genes (Table 5.8). The two least stable genes across all the three applets were *B2M* and *CST3* (Table 5.8). The stability values of *B2M* were slightly higher than the cut-off value (geNorm M < 0.5; SD < 1.0) when the data were analysed both in the geNorm and NormFinder.

Table 5.8 Stability values of reference genes affected by nicarbazin treatment (nicarbazin group only)

Rank	geNorm		NormFinder		BestKeeper	
	Gene	**M value**	**Gene**	**SD**	**Gene**	**SD**
1	*HMBS*	0.262	*HMBS*	0.199	*HPRT1*	0.190
2	*GAPDH*	0.273	*ALB*	0.226	*HMBS*	0.230
3	*HPRT1*	0.278	*RPL4*	0.231	*GAPDH*	0.260
4	*ALB*	0.329	*HPRT1*	0.284	*RPL4*	0.280
5	*RPL4*	0.340	*GAPDH*	0.289	*ALB*	0.280
6	*18S rRNA*	0.360	*18S rRNA*	0.297	*ACTB*	0.300
7	*ACTB*	0.403	*CA2*	0.427	*18S rRNA*	0.340
8	*CA2*	0.435	*ACTB*	0.435	*CA2*	0.460
9	*CST3*	0.463	*CST3*	0.513	*CST3*	0.490
10	*B2M*	0.583	*B2M*	1.008	*B2M*	0.860

Means of relative expression levels of the genes in the nicarbazin group at three different time-points (post-oviposition times 5, 15, 23.5 hrs) were used to calculate the expression stability of genes across the three statistical software.

In order to determine the consistency of the stabilities of the reference genes analysed by geNorm, NormFinder and BestKeeper, the relative expressions of the ten genes were compared as shown in Figure 5.4. The results showed that the expression stability of the genes was consistent from the analyses performed by the three programs except *B2M* when the birds were treated with nicarbazin at three time-points of egg shell formation (birds age 42-45 weeks).

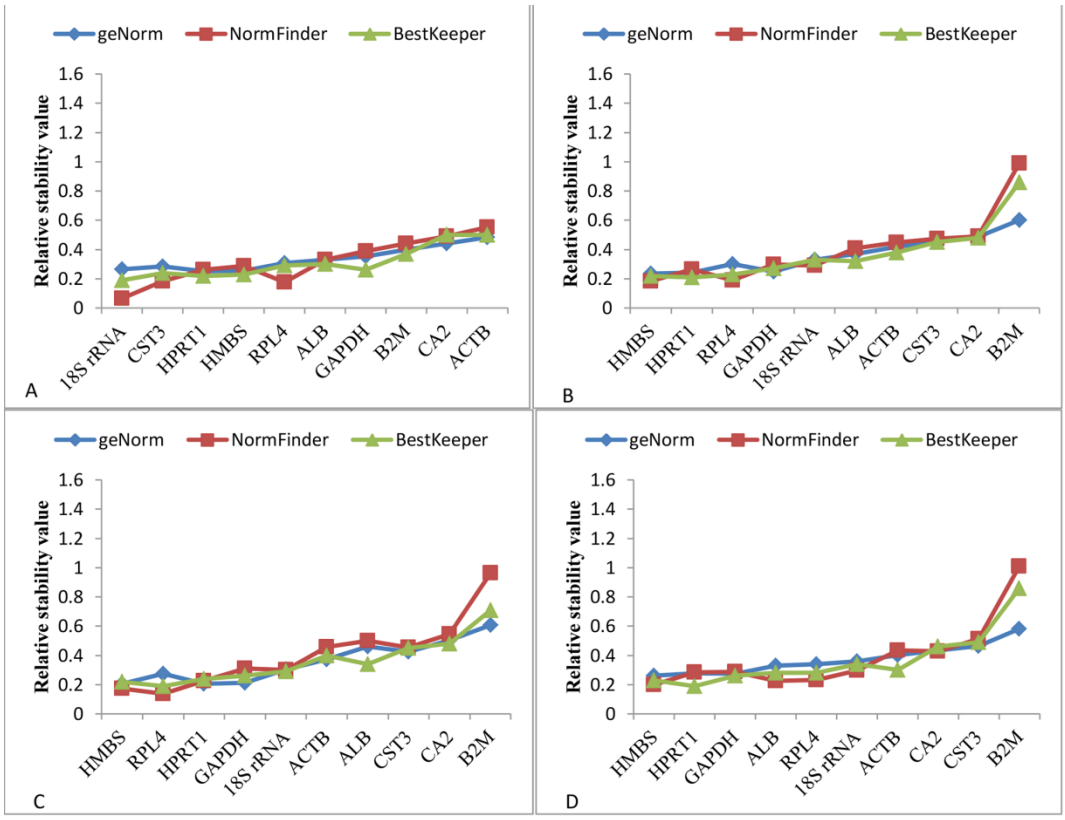

Figure 5.4 Comparison of the relative expression stability of 10 candidate reference genes analysed by geNorm, NormFinder and BestKeeper

The geNorm M and SD values of 10 reference genes were graphed to assess the ranking pattern of the genes assigned by three different software. **A**). Four different time-points (2, 5, 15, 23.5 hrs) post-oviposition in the birds at age of 36-37 weeks. **B**). Groups treated with or without nicarbazin at three different time-points (5, 15, 23.5 hrs) post-oviposition of birds at 42-45 weeks. **C**). Three different time-points (5, 15, 23.5 hrs) post-oviposition times of the birds without nicarbazin treatment at age of 42-45 weeks. **D**). Three different time-points (5, 15, 23.5 hrs) post-oviposition of the birds with nicarbazin treatment at age of 42-45 weeks.

5.5.4 Expression of candidate target genes using most stable and least stable reference genes

The level of significance (P value) changed for all four candidate target genes when the relative expression data were normalized with the two most stable (*HMBS*, *HPRT1*) and the two least stable reference genes (*B2M*, *CA2*) (Figure 5.5). The P value increased when the data were normalized with the two least stable reference genes. The relative expression level of *SLC25A38* was significantly different (P

value $4.8E^{-10}$) among different time-points when the data were normalized with the two most stable reference genes (*HMBS* and *HPRT1*) (Figure 5.5A). However, for the same candidate target gene, the level of significance decreased (P value 0.0847) among different time-points when the data were normalized with the two least stable reference genes, *B2M* and *CA2* (Figure 5.5A). The expression levels of *ALAS1, CPOX* and *FECH* were changed in terms of the P values when the data were normalized with the two most stable and the two least stable reference genes. The P value of *ALAS1* changed from $3.2E^{-12}$ when two most stable reference genes were used, to 0.0111 when the two least stable reference genes were used (Figure 5.5B). The P value of *CPOX* changed from 0.0700 to 0.6134 when the data were normalized with the two least stable reference genes (Figure 5.5C). The P value of *FECH* changed from $4.6E^{-16}$ to $9.9E^{-05}$ when the data were normalized with the two least stable reference genes (Figure 5.5D).

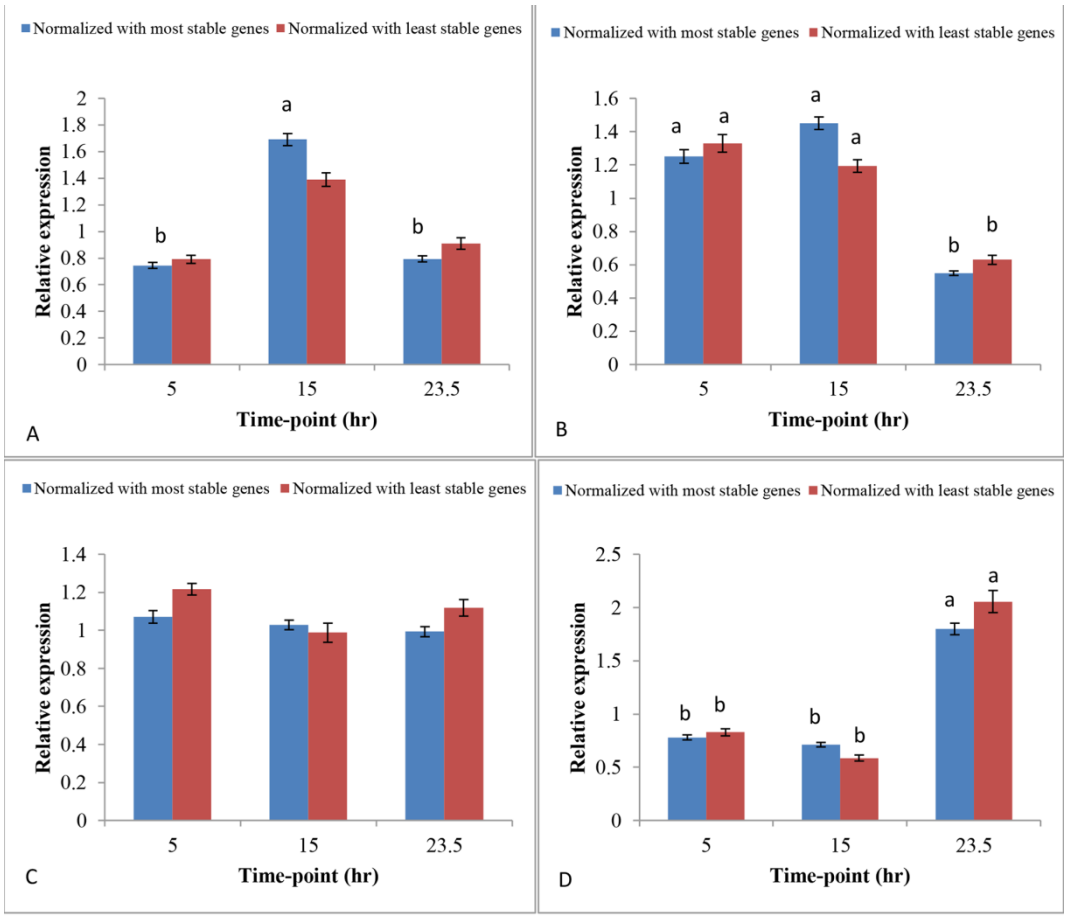

Figure 5.5 Validation of the expression level of four candidate target genes affected by three different time-points of eggshell formation

The candidate target genes were normalized with the two most stable (*HMBS* and *HPRT1*) and the two least stable reference genes (*B2M* and *CA2*). **A**). *SLC25A38* normalized with the two most stable genes (P=4.8E^{-10}); *SLC25A38* normalized with the two least stable genes (P=0.0847). **B**) *ALAS1* normalized with the two most stable genes (P=3.2E^{-12}); *ALAS1* normalized with the two least stable genes (P=0.0111). **C**). *CPOX* normalized with the two most stable genes (P=0.0700); *CPOX* normalized with the two least stable genes (P=0.6134). **D**). *FECH* normalized with the two most stable genes (P=4.6E^{-16}); *FECH* normalized with the two least stable genes (P=9.9E^{-05}). For the same gene in the same treatment, ^{a,b} across the bars indicate significant differences. For the four candidate target genes, normalized relative quantities were calculated in qbase+ based on ($2^{\wedge\text{-}\Delta\Delta Cq}$) [40] using gene specific amplification efficiencies [41], to show the relative expression of Cq levels in folds to the mean Cq of all samples of the genes.

5.6 Discussion

We investigated the stability of ten reference genes in the shell gland region of the oviduct in relation to different stages of eggshell formation and nicarbazin treatment. The data analysed by the three different statistical software indicated that the overall stability of the reference genes was affected by different time-points (post-oviposition time) and nicarbazin treatment, and differences in the ranking of reference genes analysed using three statistical software were observed. The current study provides information on the expression stability of these candidate reference genes and most stably expressed reference genes are suggested for the normalization of gene expression data in the chicken shell gland.

The higher stability of *HPRT1* and *HMBS* across all the three software indicated that these two genes can be used as reference genes for the normalization of expression data in the shell gland of the brown-egg laying hen. In fact, most of the ten reference genes tested in the current study were in the acceptable range as reference genes with geNorm M value <0.5 and SD <1.0. *B2M* was the only exception that showed slightly higher geNorm M value in the time-points and nicarbazin treatment study. Taking time-points separately, or together with the nicarbazin treatment, the pairwise variation (geNorm V) showed that the variation between the first two most stable genes was under the cut-off value (<0.15). In qbase+, geNorm V indicates level of variation in the average values of reference gene stability with the sequential inclusion of the next stable reference gene to the equation Vn/n+1 (for calculation of the normalization factor). The analysis starts with the two most stably expressed genes being compared to the pair including the third (V2/3), and the process continues until the least stable gene is added (for example, V9/10). Generally, if a geNorm V (V2/3) of 0.300 is achieved using two most stable genes and a geNorm V (V3/4) of 0.14 is achieved with three most stable reference genes, then the average of the most stable three genes would be the optimal normalization factor for further data analysis. In the current study, the first two most stable reference genes were under the cut-off value (<0.15) of geNorm V and thus adding the third most stable reference gene for expression data normalization was not necessary. However, as indicated by the geNorm V, all of the genes (V2/3 to V9/10) showed pairwise variation <0.15 and thus all could be

used for accurate data normalization. Based on the geNorm V results, this demonstrates that all the genes analysed had relatively high stability in the shell gland tissue in response to nicarbazin treatment of chickens as well as to the cyclic changes in shell gland tissue during the egg lying cycle. Based on geNorm M results, *B2M* showed low expression stability in response to the stages of egg formation in the nicarbazin treatment experiment and therefore should be ruled out from being used in the normalisation of expression data while different stages of egg formation are involved in the study.

Furthermore, the difference in stability values of *B2M* during the egg formation stages may also be dependent on the age of the birds. It appears that it is more stable in response to the time-points when birds are younger (36-37 week vs 42-45 week of age). Nevertheless, consensus from the analyses performed by these three programs was that *HMBS* and *HPRT1* were the two most stable housekeeping genes and thus were chosen as reference genes in the current study and recommended for similar studies in the shell gland of laying hens.

To validate whether most stable reference genes identified in the study would result in more accurate assessment of target gene expression, the data obtained in time-points and nicarbazin treatment experiment for four candidate target genes were normalized with the two most stable (*HPRT1*, *HMBS*) and the two least stable reference genes (*B2M*, *CA2*). Results showed that normalizing candidate target gene expression data with the two least reference stable genes is not as accurate when compared with the data normalized with the two most stable reference genes. Therefore, the most stable genes can produce more robust and accurate results for gene expression data as recommended by the optimisation outcomes achieved in the current study.

To the best of our knowledge, no validated reference genes have been used for the normalization of expression data in the shell gland of avian species under various treatments. Thus, this is the first study to establish a set of stably expressed reference genes in the shell gland and can be used in chickens and possibly in other avian species. In different species, different reference genes under different treatments have been validated in other tissues of the reproductive system. For example, in geese, *HPRT1* and *GAPDH* were ranked as the two most stable

reference genes in the ovary [42]. In bovine, the two most stable reference genes in the uterus were *YWHAZ* and *GAPDH* in relation to developmental stages of an embryo [43]. Similarly, under various toxicological treatments, in the ovary of mouse, the two most stable reference genes were *RPL13a* and *GAPDH* [44]. Based on limited studies already being performed, it appears *HPRT1* may be more stable in the reproductive system of avian species while *GAPDH* is more stable in mammalian species [40]. However, further studies are required to accumulate the information required to reach a more generalised conclusion.

The present study has demonstrated that the rankings of the expression stability of the 10 candidate reference genes had similar trends but discrepancies were observed among three different statistical programs, geNorm, NormFinder and BestKeeper. Similar discrepancies have been observed elsewhere with different species and treatments [42, 45, 46]. So far, there is no consensus as to which software is more powerful in the ranking of expression stability of candidate reference genes and researchers have given the same weight to all three programs. We have shown in this study a comparison in the consistency of the ranking of candidate reference genes among all the three software used in both experiments, indicating that all of them gave similar results and can be used for the analysis of expression data. As has been stated previously, the stability of all the chosen reference genes was in the acceptable range for reference genes. Therefore, the stability levels of these genes are essentially very close. With different algorithms in different programs, slight change of their stability orders can be expected by the analyses using these programs.

It is worth noting; however, that these three programs do not have an option for analysing the reference gene expression data generated from a factorial design, but can only perform analysis based on individual group as independent treatment. To the best of our knowledge, the optimisation of reference genes has not been performed in such a factorial design so far. Therefore, it is questionable whether the programs possess the capacity to generate a reliable ranking for an experiment designed in a factorial fashion. The gene expression stability analysis of reference genes has been reported in experiments exploring the roles of multiple factors; for example, geographical locations and ventilation in new born lambs [47], multiple

stress conditions and different developmental tissues in pear millet [48] and different developmental stages and hormonal stimuli on leaves of tea [49]. However, multiple factors have not been considered as independent effects in the analysis of stability of reference gene expression or for their interactions. We suggest these programs should add such a capacity or new programs should be available for the analyses of data produced from factorial design experiments. This would permit the role of treatments in the expression stability of the reference genes to be more robustly investigated and their interactions explored. Such investigations are warranted to provide a more powerful statistical analysis protocol.

5.7 Conclusions

In summary, we have performed optimisation of reference genes in the samples collected at different time-points of egg/eggshell formation and with nicarbazin treatment in laying hens. All of the reference genes except *B2M* were stably expressed according to the cut-off values of the programs, and two most stably expressed genes, *HMBS* and *HPRT1* are recommended for the normalization of gene expression data in the shell gland of chickens while different shell formation stages and nicarbazin treatment are involved in the experiment. It is anticipated that these reference genes may be used for the study of reproductive system in other avian species.

5.8 Acknowledgements

This study was funded by Australian Egg Corporation Limited, Australia under grant number AECL 1UN121. We thank Kapil Chousalkar at The University of Adelaide, SA, Australia for his technical support in the design of this experiment.

5.9 Competing interests

The authors declare that they have no competing interests.

5.10 Financial competing interests

The authors declare no financial competing interests.

5.11 Authors' contributions

S.S. developed the hypotheses, designed and performed the experiments, analysed and interpreted data, and drafted the manuscript; J.R. oversaw the animal trials, administrated the overall research project, assisted with the experiments, analysis and interpretation of data and critically revised the manuscript; S-B.W. designed gene expression experiments, analysed and interpreted the data, and drafted the manuscript.

5.12 References

1. Nys Y. Relationships between age, shell quality and individual rate and duration of shell formation in domestic hens. Br Poult Sci. 1986;27: 253-259.
2. Melek O, Morris TR, Jennings RC. The time factor in egg formation for hens exposed to ahemeral light ‐ dark cycles. Br Poult Sci. 1973;14: 493-498.
3. Johnson AL. *Reproduction in the female* in Sturkie's Avian Physiology. 6th ed. CC S, editor. USA: Academic Press; 2015.
4. Arias JL, Fink DJ, Xiao S-Q, Heuer AH, Caplan AI. Biomineralization and eggshells: cell-mediated acellular compartments of mineralized extracellular matrix. Int Rev Cytol. 1993;145: 217-250.
5. Wellman-Labadie O, Picman J, Hincke MT. Avian antimicrobial proteins: structure, distribution and activity. Worlds Poult Sci J. 2007;63: 421-438.

6. Liu Z, Zheng Q, Zhang X, Lu L. Microarray analysis of genes involved with shell strength in layer shell gland at the early stage of active calcification. Asian Austral J Anim. 2013;26: 609-624.

7. Jonchère V, Réhault-Godbert S, Hennequet-Antier C, Cabau C, Sibut V, Cogburn LA, et al. Gene expression profiling to identify eggshell proteins involved in physical defense of the chicken egg. BMC Genomics. 2010;11: 57.

8. Dunn IC, Wilson PW, Lu Z, Bain MM, Crossan CL, Talbot RT, et al. New hypotheses on the function of the avian shell gland derived from microarray analysis comparing tissue from juvenile and sexually mature hens. Gen Comp Endocrinol. 2009;163: 225-232.

9. Song G, Seo HW, Choi JW, Rengaraj D, Kim TM, Lee BR, et al. Discovery of candidate genes and pathways regulating oviduct development in chickens. Biol Reprod. 2011;85: 306-314.

10. Additives Epo, Products or Substances used in Animal F. Scientific opinion on the safety and efficacy of Koffogran (nicarbazin) as a feed additive for chickens for fattening. EFSA Journal. 2010;8: 1551.

11. Hughes BL, Jones JE, Toler JE, Solis J, Castaldo DJ. Effects of exposing broiler breeders to nicarbazin contaminated feed. Poult Sci. 1991;70: 476-482.

12. Dorne JLCM, Fernández-Cruz ML, Bertelsen U, Renshaw DW, Peltonen K, Anadon A, et al. Risk assessment of coccidostatics during feed cross-contamination: animal and human health aspects. Toxicol Appl Pharmacol. 2013;270: 196-208.

13. Bilandžić N, Dolenc J, Gačnik KŠ, Varenina I, Kolanović BS. Feed additives diclazuril and nicarbazin in egg and liver samples from Croatian farms. Food Addit Contam B. 2013;6: 90-97.

14. Leeson S, Caston LJ, Summers JD. The effect of graded levels of nicarbazin on reproductive performance of laying hens. Can J Anim Sci. 1989;69: 757-764.

15. Thellin O, Zorzi W, Lakaye B, De Borman B, Coumans B, Hennen G, et al. Housekeeping genes as internal standards: use and limits. J Biotechnol. 1999;75: 291-295.

16. Lee PD, Sladek R, Greenwood CM, Hudson TJ. Control genes and variability: absence of ubiquitous reference transcripts in diverse mammalian expression studies. Genome Res. 2002;12: 292-297.

17. Greer S, Honeywell R, Geletu M, Arulanandam R, Raptis L. Housekeeping genes; expression levels may change with density of cultured cells. J Immunol Methods. 2010;355: 76-79.

18. Uddin MJ, Cinar MU, Tesfaye D, Looft C, Tholen E, Schellander K. Age-related changes in relative expression stability of commonly used housekeeping genes in selected porcine tissues. BMC Res Notes. 2011;4: 441.

19. Cinar MU, Islam MA, Uddin MJ, Tholen E, Tesfaye D, Looft C, et al. Evaluation of suitable reference genes for gene expression studies in porcine alveolar macrophages in response to LPS and LTA. BMC Res Notes. 2012;5: 107.

20. Beekman L, Tohver T, Dardari R, Léguillette R. Evaluation of suitable reference genes for gene expression studies in bronchoalveolar lavage cells from horses with inflammatory airway disease. BMC Mol Biol. 2011;12: 5.

21. Petriccione M, Mastrobuoni F, Zampella L, Scortichini M. Reference gene selection for normalization of RT-qPCR gene expression data from *Actinidia deliciosa* leaves infected with *Pseudomonas syringae pv. actinidiae*. Sci Rep. 2015;5: 16961.

22. Vandesompele J, De Preter K, Pattyn F, Poppe B, Van Roy N, De Paepe A, et al. Accurate normalization of real-time quantitative RT-PCR data by geometric averaging of multiple internal control genes. Genome Biol. 2002;3: research0034. 0031.

23. qbase+ version 3.0. https://www.qbaseplus.com/.

24. GenEx version 6.0.1. http://genex.gene-quantification.info/.

25. Andersen CL, Jensen JL, Ørntoft TF. Normalization of real-time quantitative reverse transcription-PCR data: a model-based variance

estimation approach to identify genes suited for normalization, applied to bladder and colon cancer data sets. Cancer Res. 2004;64: 5245-5250.

26. Pfaffl MW, Tichopad A, Prgomet C, Neuvians TP. Determination of stable housekeeping genes, differentially regulated target genes and sample integrity: BestKeeper–Excel-based tool using pair-wise correlations. Biotechnol Lett. 2004;26: 509-515.

27. Guernsey DL, Jiang H, Campagna DR, Evans SC, Ferguson M, Kellogg MD, et al. Mutations in mitochondrial carrier family gene SLC25A38 cause nonsyndromic autosomal recessive congenital sideroblastic anemia. Nat Genet. 2009;41: 651-653.

28. May BK, Dogra SC, Sadlon TJ, Bhasker CR, Cox TC, Bottomley SS. Molecular regulation of heme biosynthesis in higher vertebrates. Prog Nucleic Acid Res Mol Biol. 1995;51: 1-51.

29. Takahashi S, Taketani S, Akasaka J-e, Kobayashi A, Hayashi N, Yamamoto M, et al. Differential regulation of *coproporphyrinogen oxidase* gene between erythroid and nonerythroid cells. Blood. 1998;92: 3436-3444.

30. Day AL, Parsons BM, Dailey HA. Cloning and characterization of Gallus and Xenopus ferrochelatases: Presence of the [2Fe-2S] cluster in nonmammalian ferrochelatase. Arch Biochem Biophys. 1998;359: 160-169.

31. Harbin BM, Dailey HA. Orientation of ferrochelatase in bovine liver mitochondria. Biochemistry (Mosc). 1985;24: 366-370.

32. Kuchipudi SV, Tellabati M, Sebastian S, Londt BZ, Jansen C, Vervelde L, et al. Highly pathogenic avian influenza virus infection in chickens but not ducks is associated with elevated host immune and pro-inflammatory responses. Vet Res. 2014;45: 118.

33. Yang F, Lei X, Rodriguez-Palacios A, Tang C, Yue H. Selection of reference genes for quantitative real-time PCR analysis in chicken embryo fibroblasts infected with avian leukosis virus subgroup J. BMC Res Notes. 2013;6: 402.

34. Dalgaard TS, Skovgaard K, Norup LR, Pleidrup J, Permin A, Schou TW, et al. Immune gene expression in the spleen of chickens experimentally

infected with *Ascaridia galli*. Vet Immunol Immunopathol. 2015;164: 79-86.

35. Yin R, Liu X, Liu C, Ding Z, Zhang X, Tian F, et al. Systematic selection of housekeeping genes for gene expression normalization in chicken embryo fibroblasts infected with Newcastle disease virus. Biochem Biophys Res Commun. 2011;413: 537-540.

36. Li G, Chen S, Duan Z, Qu L, Xu G, Yang N. Comparison of protoporphyrin IX content and related gene expression in the tissues of chickens laying brown-shelled eggs. Poult Sci. 2013;92: 3120-3124.

37. Samiullah S, Roberts JR. The location of protoporphyrin in the eggshell of brown-shelled eggs. Poult Sci. 2013;92: 2783-2788.

38. Bio-Rad Application User Guide. (2006) Available at: http://www.bio-rad.com/webroot/web/pdf/lsr/literature/Bulletin_5279.pdf. (Accessed: 4th June 2016).

39. Hellemans J, Mortier G, De Paepe A, Speleman F, Vandesompele J. qBase relative quantification framework and software for management and automated analysis of real-time quantitative PCR data. Genome Biol. 2007;8: R19.

40. Radonić A, Thulke S, Bae H-G, Müller MA, Siegert W, Nitsche A. Reference gene selection for quantitative real-time PCR analysis in virus infected cells: SARS corona virus, Yellow fever virus, Human Herpesvirus-6, Camelpox virus and Cytomegalovirus infections. Virol J. 2005;2: 7.

41. Pfaffl MW. A new mathematical model for relative quantification in real-time RT–PCR. Nucleic Acids Res. 2001;29: e45.

42. Ji H, Wang J, Liu J, Guo J, Wang Z, Zhang X, et al. Selection of reliable reference genes for real-time qRT-PCR analysis of Zi geese (*Anser anser domestica*) gene expression. Asian Austral J Anim. 2013;26: 423-432.

43. Goossens K, Van Poucke M, Van Soom A, Vandesompele J, Van Zeveren A, Peelman LJ. Selection of reference genes for quantitative real-time PCR in bovine preimplantation embryos. BMC Dev Biol. 2005;5: 27.

44. Svingen T, Letting H, Hadrup N, Hass U, Vinggaard AM. Selection of reference genes for quantitative RT-PCR (RT-qPCR) analysis of rat tissues under physiological and toxicological conditions. PeerJ. 2015;3: e855.

45. Nascimento CS, Barbosa LT, Brito C, Fernandes RP, Mann RS, Pinto APG, et al. Identification of suitable reference genes for real time quantitative polymerase chain reaction assays on Pectoralis major muscle in chicken (*Gallus gallus*). PloS ONE. 2015;10: e0127935.

46. Cinar MU, Islam MA, Pröll M, Kocamis H, Tholen E, Tesfaye D, et al. Evaluation of suitable reference genes for gene expression studies in porcine PBMCs in response to LPS and LTA. BMC Res Notes. 2013;6: 56.

47. Pereira-Fantini PM, Rajapaksa AE, Oakley R, Tingay DG. Selection of reference genes for gene expression studies related to lung injury in a preterm lamb model. Sci Rep. 2016;6: 26476.

48. Shivhare R, Lata C. Selection of suitable reference genes for assessing gene expression in pearl millet under different abiotic stresses and their combinations. Sci Rep. 2016;6: 23036.

49. Wu Z-J, Tian C, Jiang Q, Li X-H, Zhuang J. Selection of suitable reference genes for qRT-PCR normalization during leaf development and hormonal stimuli in tea plant (*Camellia sinensis*). Sci Rep. 2016;6: 19748.

Higher Degree Research Thesis by Publication
University of New England

STATEMENT OF AUTHORS' CONTRIBUTION

(To appear at the end of each thesis chapter submitted as an article/paper)

We, the Research Master/PhD candidate and the candidate's Principal Supervisor, certify that all co-authors have consented to their work being included in the thesis and they have accepted the candidate's contribution as indicated in the *Statement of Originality*.

	Author's Name (please print clearly)	**% of contribution**
Candidate	**Sami Samiullah**	60
Other Authors	**Juliet Roberts**	15
	Shu-Biao Wu	25

Name of Candidate: **Samiullah**

Name/title of Principal Supervisor: **Associate Professor Juliet Roberts**



Candidate Date 09/06/2017



Principal Supervisor Date 09/06/2017

Higher Degree Research Thesis by Publication
University of New England

STATEMENT OF ORIGINALITY

(To appear at the end of each thesis chapter submitted as an article/paper)

We, the Research Master/PhD candidate and the candidate's Principal Supervisor, certify that the following text, figures and diagrams are the candidate's original work.

Type of work	**Page number/s**
Figure 5.1	122
Figure 5.2	124
Figure 5.3	126
Figure 5.4	131
Figure 5.5	133
Text and tables	109-143

Name of Candidate: **Samiullah**

Name/title of Principal Supervisor: **Associate Professor Juliet Roberts**

[redacted]

Candidate Date 09/06/2017

[redacted]

Principal Supervisor Date..09/06/2017

Chapter 6 Downregulation of *ALAS1* by nicarbazin treatment underlies the reduced synthesis of protoporphyrin IX in shell gland of laying hens

Published as: Sami Samiullah, Juliet Roberts and Shu-Biao Wu (2017). Downregulation of *ALAS1* by nicarbazin treatment underlies the reduced synthesis of protoporphyrin IX in shell gland of laying hens. Scientific Reports, 7; 6253.

6.1 Abstract

Shell colour is an important trait for eggs and an understanding of pigment deposition will assist potential management of egg shell colour loss. We demonstrated that nicarbazin feeding down-regulated *ALAS1* and reduced protoporphyrin IX (PP IX) in both shell gland and eggshell, indicating the role of nicarbazin in inhibiting the synthesis of PP IX. Additionally, the expression levels of the genes did not show sequential upregulation in the same order of diurnal time-points (TP) during egg formation. The gene *SLC25A38*, responsible for transporting glycine from cytoplasm to mitochondria, and the gene *ALAS1*, encoding rate-limiting enzyme (delta-aminolevulinic acid synthase 1), had higher expression at 15 hr, as compared with 2, 5 and 23.5 hrs postoviposition. Interestingly, *ABCB6*, a gene encoding an enzyme responsible for transporting coproporphyrinogen III, showed higher expression level at 2 and 5 hrs. However, the expression of *CPOX* that converts coproporphyrinogen III to protoporphyrinogen III, and *ABCG2* that transports PP IX out from mitochondria did not alter. Nevertheless, mitochondrial count per cell did not show consistent change in response to time-points postoviposition and nicarbazin feeding. The information obtained in the study sheds light on how nicarbazin disrupts the synthesis of PP IX.

6.2 Introduction

The oviduct in laying hens is divided into five distinguishable regions: infundibulum (10 cm), magnum (35 cm), isthmus (8 cm), shell gland (10 cm) and vagina (4 cm)[1,2]. The formation of the egg takes about 24 hrs during which it

sequentially passes through various parts of the oviduct. The release of the next ovum is precisely synchronized, occurring an average of 24 minutes post-oviposition under a 24 hr light-dark cycle[3]. The ovum remains in the infundibulum for about 0.5 hr, in the magnum for about 3 hrs, in the isthmus for 1-2 hrs, and in the shell gland for about 18-20 hrs[2,4,5]. The eggshell comprises both organic and inorganic components that are synthesised in the isthmus and shell gland[6-9]. The eggshell is composed of shell membranes, mammillary layer, palisade layer, surface crystal layer and cuticle[10,11]. The brown eggshell colour in laying hens is due mainly to the deposition of a pigment known as protoporphyrin IX (PP IX) during eggshell formation in the shell gland. The presence of PP IX in various shell layers has been reported[12-14] although most of the pigment is deposited into the outmost layers of the palisade layer (80-87%) with a smaller amount in the cuticle (13-20%)[15]. Shell deposition increases regularly 12-23 hrs post-oviposition and reaches a plateau 1.5 hrs before oviposition[16], which coincides with the deposition of cuticle (1-1.5 hrs)[17]. PP IX deposition increases greatly during the last 20-24 hrs post-oviposition[18].

It is assumed that regular egg formation may change the energy metabolism of key organs such as the oviduct, liver and adipose tissue. At the cellular level, alterations of nutrient and energy requirements coincide with changes in the mitochondria, the main site of production of ATP in cells[19]. The mitochondrial genome has multiple copies per cell and the number of mitochondria varies depending on energy demands of a cell, the age and sex of an organism, the organ and patho-physiological conditions[20-22]. Certain drugs are nucleoside analogs that block the progression of polymerase γ[23], which leads to the inhibition of mitochondrial biogenesis. The mitochondrial DNA (mtDNA) copies decrease with age, as shown in mice and humans[24]. However, mtDNA copies increased from early to late lactation in the mammillary glands of cows[25]. The mtDNA replication is independent of the cell cycle and is controlled by the nuclear DNA encoded polymerase γ[26,27] and mitochondrial transcription factor A[28].

Chicken (*Gallus gallus*) mtDNA is circular in shape with about 16758 bp, containing 37 identified genes encoding 13 polypeptides, 2 rRNAs, 22 tRNAs and 1 non coding control D-loop region[29,30]. This small genome has been shown to contain around 15% of repetitive DNA organized as short tandem repeats, such as telomeric and centromeric tandem repeats[31]. Determination of mtDNA content is

important for understanding many cellular processes[32]. An essential component of mitochondrial biogenesis is the regulation of mitochondrial morphology and number within healthy cells with a dynamic balance of fission and fusion events. The number of mtDNA copies is highly dynamic and regulates in a cell-specific manner by mechanisms that are not completely understood[33,34].

In the epithelial cells of the chicken shell gland, mitochondria are of particular interest, owing to the high demand for energy used in the biogenesis of the eggshell. Mitochondrial biogenesis in these cells also allows them to meet changing energy loads for production of various components of the eggshell, including eggshell pigment. Nicarbazin is one of the various factors that has been shown to cause reduced synthesis and/or deposition of protoporphyrin into eggshells, when fed to brown-egg laying hens at recommended dosages (50–125 mg/kg of feed)[35,36]. Nicarbazin produces reversible pharmacological effects by causing decolouration of brown egg pigment, which is dosage dependent[37,38]. Thus, this model can be easily reproduced in studies to investigate effects of nicarbazin on eggshell formation in laying hens. Understanding the molecular basis for the effect of nicarbazin may also provide an understanding of the mechanisms by which shell colour decreases in response to other factors which have been less well-defined.

The biosynthetic pathway of PP IX is well established; however, the origin of its precursors and the mechanism of deposition are still not known. The pigment is believed to be synthesized in the mucosal epithelial cells of the shell gland where the whole process takes place in the mitochondria and cytoplasm with the involvement of various enzymes. Briefly, as illustrated in Figure 6.1, the solute carrier family 25, member 38 (*SLC25A38*) gene, functions to facilitate delta-aminolevulinic acid production by transporting glycine into the mitochondrial matrix from the cytosol[39]. The delta-aminolevulinic acid synthase 1 (*ALAS1*) gene encodes a rate limiting non-erythroid enzyme that catalyses the reaction of succinyl coenzyme A with glycine to form delta-aminolevulinic acid within the mitochondrial matrix[40,41]. Cell surface ATP-binding cassette (ABC) transporters serve to efflux a variety of compounds[42] and are also involved in the transport of substances across mitochondrial membranes[43]. The gene *ABCB6* is part of the ATP-binding cassette family and is located on the mitochondrial membrane[44]. This gene encodes a transporter that has been demonstrated to play a role in transporting

coproporphyrinogen III back to the mitochondria from the cytosol[45]. The coproporphyrinogen oxidase (*CPOX*) gene encodes an enzyme that converts coproporphyrinogen III into protoporphyrinogen III and this gene is located in the mitochondria[46]. *ABCG2* is also part of the ATP-binding cassette family but plays a role in the export of PP IX out of the cell[47,48]. The feline leukemia virus subgroup C cellular receptor 1 (*FLVCR1*) gene is located on the cell membrane that encodes an enzyme that transports heme/PP IX out of the cell[45]. This gene is highly conserved throughout evolution with orthologs present in plants, bacteria and animals, suggesting its importance in cell biology[49]. The ferrochelatase gene (*FECH*) encodes the enzyme that catalyses the final step in converting PP IX into heme[50,51].

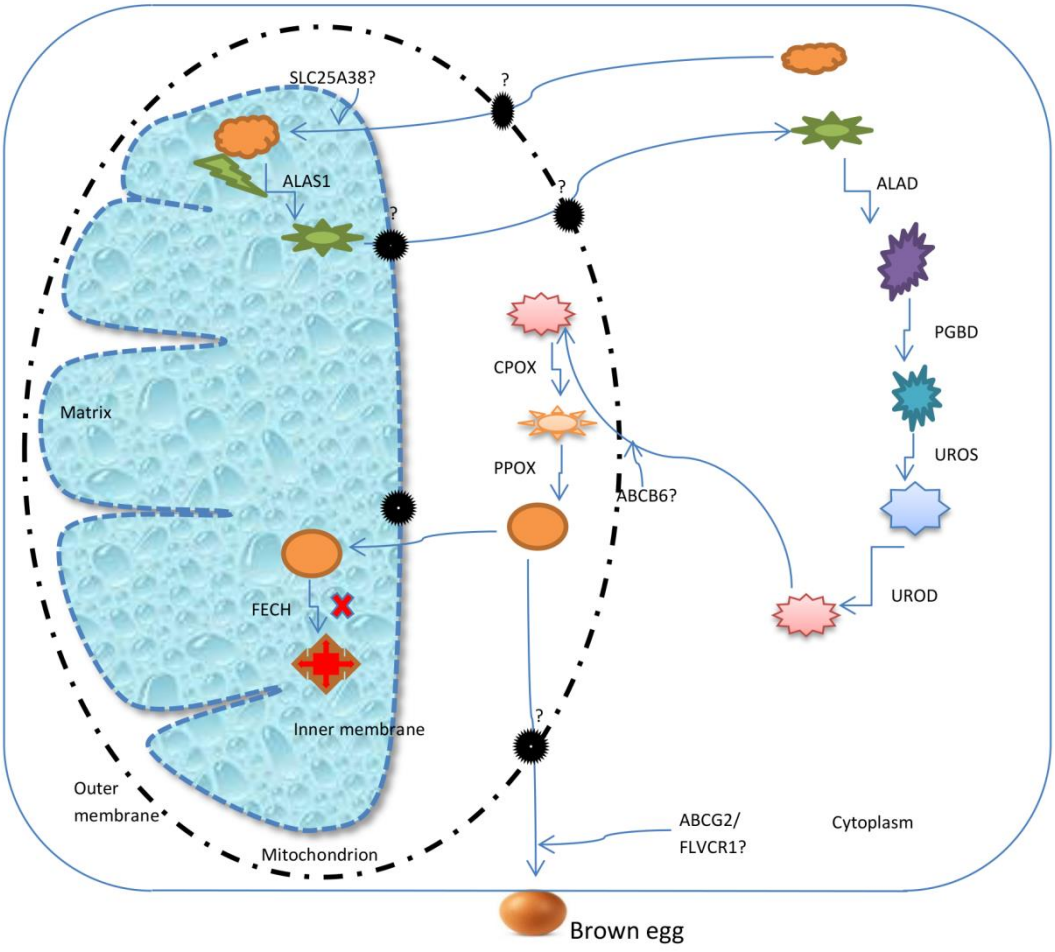

Figure 6.1 Schematic representation of protoporphyrin IX biosynthetic pathway in the shell gland of brown-egg laying hens

Glycine ( ) is transported from the cytosol to the matrix of mitochondria through the possible transporter SLC25A38. Succinyl CoA ( ) and glycine are oxidized by delta-

aminolevulinic acid synthase 1 (*ALAS1*) to delta-aminolevulinic acid (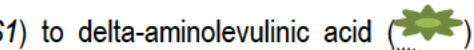), which is transported back to the cytosol through unknown transporter/s (). The delta-aminolevulinic acid is converted into porphobilinogen () through the action of aminolevulinic acid dehydratase (ALAD). The porphobilinogen is further reduced into hydroxymethylbilane () through porphobilinogen deaminase (PGBD). In the next two steps, uroporphyrinogen III () and coproporphyrinogen III () are synthesized through the actions of uroporphyrinogen III synthase (UROS) and uroporphyrinogen decarboxylase (UROD), respectively. The coproporphyrinogen III is transported back to mitochondria and is converted to protoporhyrinogen III () through the action of coproporphyrinogen oxidase (CPOX). The protoporhyrinogen III is converted into protoporphyrin IX () through protoporhyrinogen oxidase (PPOX) that deposits into eggshell. It is not known, how the protoporphyrin IX is inhibited from being converted into heme (), a part of haemoglobin.

Based on the active involvement of the avian shell gland in the production of various components of eggshells, we hypothesized that expression levels of the genes involved in the synthesis of PP IX may change according to their roles in the synthesis procedure following a temporal manner and possibly mitochondrial numbers in the cell of shell gland vary with different stages of eggshell formation. To test this hypothesis, we studied the possible variations in the expression of relevant genes and mitochondrial count per cell at different stages of egg/eggshell formation (time-points). We also hypothesized, on the basis of the effects of nicarbazin on production of PP IX, that nicarbazin may disrupt the mechanism involved in PP IX production by either regulating the genes involved in its production or affecting the mitochondrial numbers in the cells, resulting in lower production of PP IX appearing in eggshells of nicarbazin fed brown-egg laying hens. Nicarbazin was used as a model as it has been shown to produce reversible loss of brown eggshell colour[36,37]. Therefore, Experiment 1 was performed to study the expression of genes involved in the synthesis of PP IX at different stages of egg/eggshell formation. In Experiment 2, the mechanism by which nicarbazin disrupts PP IX synthesis at different time-points of eggshell formation was studied. In both the experiments, the mitochondrial count per cell was quantified at different stages of egg/eggshell formation and during nicarbazin treatment, to establish any relationship between mitochondrial copy number and PP IX synthesis. The PP IX level was measured in shell gland tissue and eggshell to understand the effect of

expression levels of genes on the synthesis and deposition of PP IX. Thus, the main objective of the study was to investigate the expression levels of genes involved in the synthesis of PP IX, as well as mitochondrial count, at different stages of egg/eggshell formation and during nicarbazin treatment in brown-egg laying hens.

6.3 Results

6.3.1 Mitochondrial count per cell and PP IX synthesis genes

In Experiment 1, the mean mitochondrial count per cell in the shell gland tissue was not significantly different ($P > 0.05$) among the four different stages of egg/eggshell formation (time-points) (Figure 6.2a). However, the expression levels of the candidate genes were significantly affected ($P < 0.05$) by the time-points except for the *CPOX* and the *ABCG2* (Table 6.1). The expression level of *SLC25A38* gene was significantly higher at 15 hr compared with the 2, 5 and 23.5 hrs post-oviposition times. The expression level of *ALAS1* gene was significantly higher at 5 and 15 hrs compared with 2 and 23.5 hrs post-oviposition. The expression level of *ABCB6* gene was significantly higher at 2, 5 and 15 hrs post-oviposition compared with 23.5 hr. The expression levels of *FECH* and *FLVCR1* genes were significantly higher at 23.5 hr compared with the other post-oviposition times.

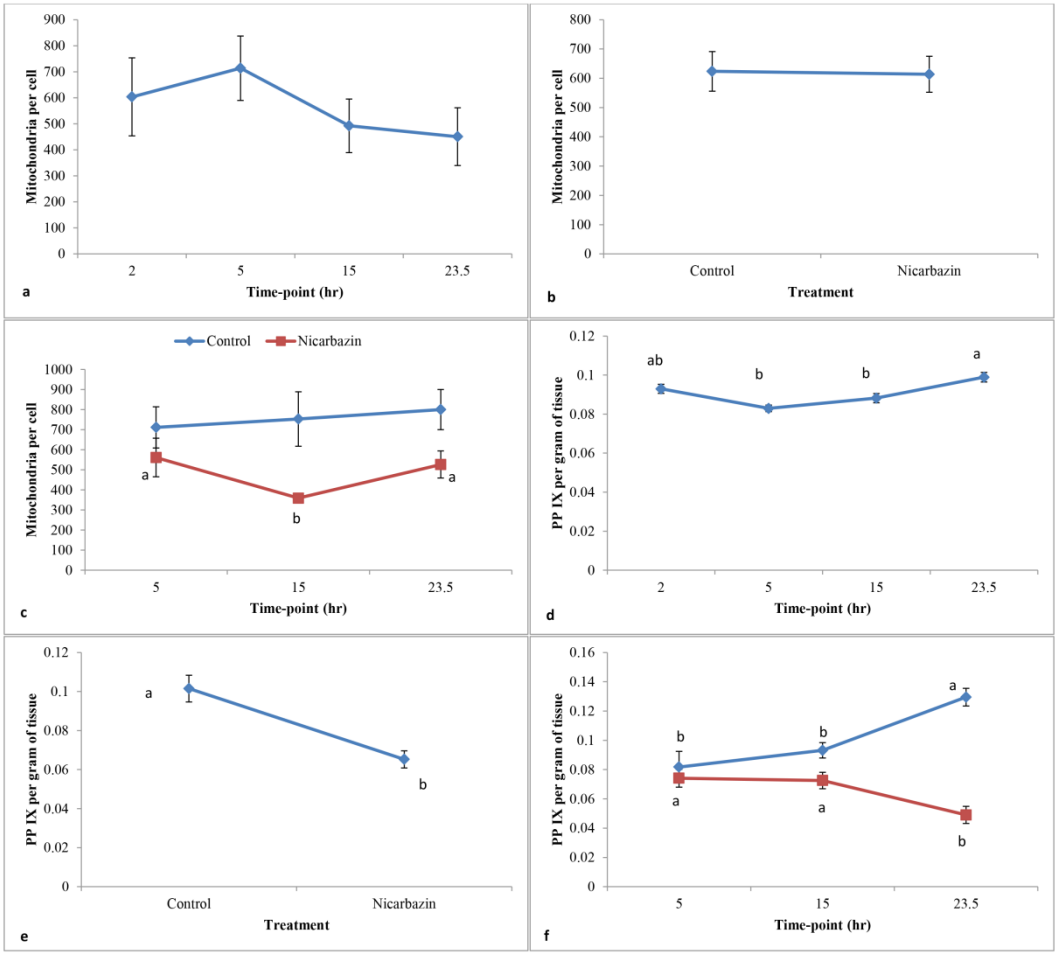

Figure 6.2 Mitochondria per cell and PP IX per gram of shell gland tissue affected by time-points of eggshell formation and nicarbazin treatment

(a) Mitochondria per cell in the shell gland tissue of laying hens affected by four different time-points of eggshell formation. (**b**) Mitochondria per cell in the shell gland tissue between control and nicarbazin treated laying hens. (**c**) Mitochondria per cell affected by interaction between three different time-points and nicarbazin treatment. (**d**) PP IX (in nMoles) per gram of shell gland tissue affected by four different time-points of eggshell formation. (**e**) PP IX (in nMoles) per gram of shell gland tissue between the control and nicarbazin treated hens. (**f**) PP IX (in nMoles) per gram of shell gland tissue affected by three different time-points and nicarbazin treatment. Values are mean and bars represent standard error. Different superscripts $^{(a,b)}$ show significant difference.

Gene	Time-point (hr)				P value
	2	5	15	23.5	
SLC25A38	0.87±0.12^{b}	0.84±0.12^{b}	1.74±0.12^{a}	0.94±0.13^{b}	0.0019
ALAS1	0.79±0.05^{c}	1.32±0.09^{b}	1.69±0.10^{a}	0.59±0.05^{c}	<0.0001
ABCB6	1.23±0.05^{a}	1.25±0.13^{a}	1.06±0.11^{a}	0.67±0.11^{b}	0.0047
CPOX	0.96±0.05	1.03±0.04	1.11±0.09	0.95±0.06	0.3727
ABCG2	1.04±0.08	1.15±0.08	0.87±0.05	1.01±0.06	0.0936
FECH	0.88±0.04^{b}	0.85±0.05^{b}	0.80±0.05^{b}	1.72±0.04^{a}	<0.0001
FLVCR1	0.97±0.04^{b}	0.85±0.05^{b}	1.03±0.07^{ab}	1.23±0.12^{a}	0.0255

Table 6.1 Relative expression levels of candidate target genes involved in the synthesis of protoporphyrin IX and/or heme at different time-points of eggshell formation in the shell gland of laying hens

Values are the mean of normalized relative quantities (NRQ) ± standard error. Relative quantities for individual gene are scaled to the average across all unknown samples per target gene. Different superscript letters $^{(a,b,c)}$ across a row denote significantly different results.

In Experiment 2, no main effect of either time-point or nicarbazin treatment was observed on the mitochondrial count (Figure 6.2b). There was significant interaction ($P < 0.05$) of time-points and nicarbazin treatment for mitochondrial count at 15 hr time-point (Figure 6.2c). The nicarbazin decreased mitochondrial count only at 15 hr post-oviposition but not at other time-points. The expression levels of all the genes except for *CPOX* were significantly affected by time-points, both in the control and nicarbazin treatment groups (Table 6.2). The expression level of *SLC25A38* was significantly higher at 15 hr both in the control and nicarbazin treatment groups (Table 6.2). *ALAS1* expression level was significantly higher at 15 hr compared with the 5 and 23.5 hrs in the control group. However, in the nicarbazin treatment groups, *ALAS1* expression level showed no significant difference between 5 and 15 hrs. *ABCG2* expression level was significantly higher at 5 hr compared with both the 15 and 23.5 hrs time-points in the control and in the nicarbazin treatment groups.

Gene	Time-point (hr)			Treatment		P value		
	5	15	23.5	Control	Nicarbazin	TP	N	TP*N
SLC25A38	0.75 ±0.03[b]	1.71 ±0.07[a]	0.82 ±0.07[b]	1.04 ±0.11	1.14 ±0.13	<0.0001	0.1567	0.3481
ALAS1	1.28 ±0.09[b]	1.47 ±0.08[a]	0 55 ±0.02[c]	1.20 ±0.09[a]	0.99 ±0.06[b]	<0.0001	0.0104	0.2148
ABCB6	1.32 ±0.08[a]	1.02 ±0.06[ab]	0.80 ±0.07[b]	1.06 ±0.06	1.03 ±0.08	0.0002	0.6805	0.7290
CPOX	1.07 ±0.04	1.03 ±0.02	0 93 ±0.04	1.02 ±0.04	1.00 ±0.03	0.0700	0.7199	0.7765
ABCG2	1.34 ±0.09[a]	0.87 ±0.04[b]	0 91 ±0.08[b]	1.04 ±0.05	1.05 ±0.10	0.0002	0.9335	0.1560
FECH	0.78 ±0.02[b]	0.72 ±0.03[b]	1.80 ±0.05[a]	1.07 ±0.13	1.13 ±0.13	<0.0001	0.1467	0.7750
FLVCR1	0.79 ±0.02[c]	1.26 ±0.07[a]	1.05 ±0.09[b]	1.07 ±0.07	1.00 ±0.07	0.0002	0.3850	0.1792

Table 6.2 Relative expression levels of candidate target genes involved in the synthesis of protoporphyrin IX and/or heme at different time-points of eggshell formation in the shell gland of laying hens treated with nicarbazin

The time-point (TP) and nicarbazin treatment (N) columns show main effects on the expression levels of the genes. Values are mean of normalized relative quantities (NRQ) ± standard error. Relative quantities for individual gene are scaled to the average across all unknown samples per target gene. Within each treatment, different superscript letters [(a,b,c)] across a row denote significantly different results. TP is time-point, while N denotes nicarbazin treatment.

The higher expression level of *FECH* was the same in the control and nicarbazin treatment groups, occurring at 23.5 hr. In both the groups, the *FLVCR1* expression level was significantly higher at 15 hr time-point. There was no significant interaction between time-points and nicarbazin treatment for any of the genes expression levels investigated (Table 6.2). The expression levels of all seven genes studied were not significantly different ($P > 0.05$) between the control and nicarbazin treatment hens except for *ALAS1* (Table 6.2). In the control group, the mean relative expression levels (±S.E.) of *ALAS1* at 5, 15 and 23.5 hrs time-points were 1.34±0.06, 1.66±0.07 and 0.60±0.03, respectively. In the nicarbazin treatment group, the mean relative expression levels (±S.E.) of *ALAS1* at 5, 15 and 23.5 hrs time-points were 1.21±0.09, 1.27±0.06 and 0.50±0.01, respectively.

6.3.2 Measurement of PP IX in shell gland tissue

In Experiment 1, the mean values of PP IX measured per gram of shell gland tissue were significantly affected ($P < 0.05$) by time-point (Figure 6.2d). The PP IX level in the shell gland was at the lowest when the egg was not in the shell gland at 5 hr post-oviposition then gradually increased to the highest at 23.5 hr (Figure 6.2d). In Experiment 2, there was a significantly lower amount of PP IX per gram of shell gland tissue in the nicarbazin treated compared with the control groups (Figure 6.2e). A significant interaction between time-point and treatment showed that, in the control groups, the amount of PP IX significantly increased at the 23.5 hr post-oviposition time whereas, in the nicarbazin treatment groups, the amount of PP IX declined (Figure 6.2f).

6.3.3 Measurement of PP IX in eggshell

In Experiment 2, in the eggshells from the control groups, the amount of PP IX and L* values remained constant whereas, in the nicarbazin treatment groups, PP IX decreased linearly with increasing duration of administration (day effect) of the drug, as indicated by the lower amount of PP IX and higher values of L* (Figure 6.3a and b). Egg weight and shell thickness were not significantly different between the control and nicarbazin treated groups (Figure 6.3c and d).

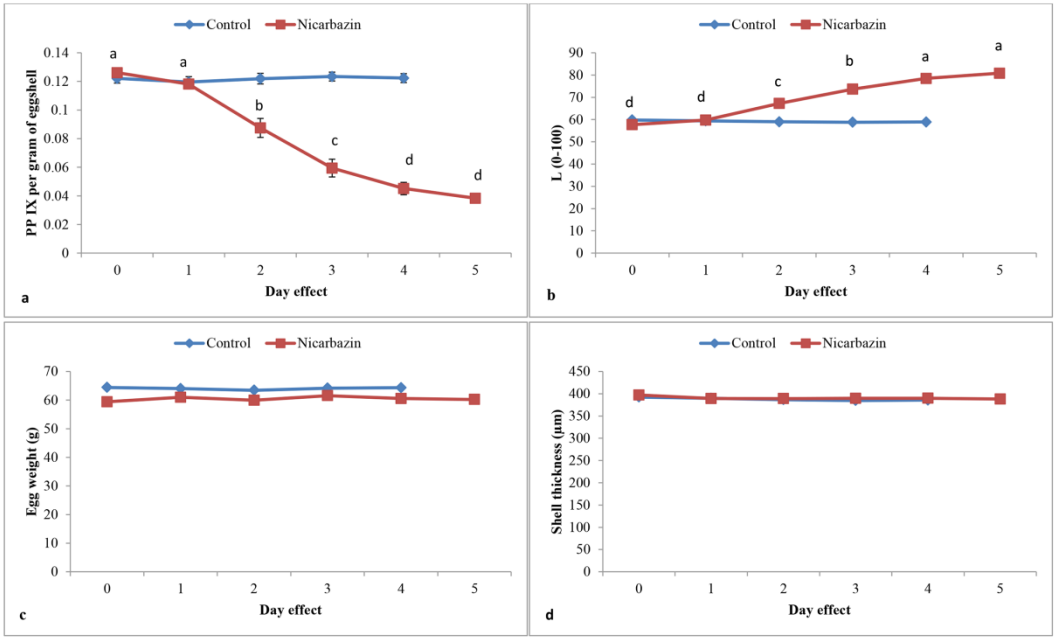

Figure 6.3 Eggshell quality variables measured in control and nicarbazin treated laying hens affected by day effect

(**a**) PP IX per gram of eggshell (nMoles) between the control (P=0.9512) and nicarbazin (P <0.0001) treated hens. (**b**) L* values for eggshells between the control (P=0.7026) and nicarbazin (P <0.0001) treated hens. (**c**) Egg weight between the control (P=0.9683) and nicarbazin (P=0.6414) treated hens. (**d**) Shell thickness of eggshells between the control (P=0.8345) and nicarbazin (P=0.8600) treated hens. Values are mean and bars represent standard error. Different superscripts $^{(a,b,c,d)}$ show significant difference.

6.4 Discussion

The first step in the initiation of PP IX biosynthetic pathway is the transportation of glycine from cell cytoplasm to mitochondria. *SLC25A38* has been shown to be the transporter for glycine, which is located on mitochondrial inner membrane[39]. A significantly higher expression of *SLC25A38* at the 15 hr time-point observed in the current study may indicate that, during this stage, the synthesis of PP IX has already been initiated for the programmed deposition into the shell of the egg to be laid on that day or even the next day. This is further confirmed by the significantly higher expression level of the rate limiting enzyme *ALAS1* at the same time-point of

eggshell formation. The genes that encode proteins involved in the subsequent steps of the PP IX synthesis did not follow the same temporal sequence on the day. For example, *ABCB6* was expressed at significantly higher level at the 5 hr time-point while its role in the PP IX synthetic pathway is at later stage. In the PP IX biosynthetic pathway, it is not clear how the genes involved are co-regulated as the transporters or enzymes. The proteins involved come from different sources and may not necessarily be synthesized at the same level, in the same location of the cell, and in the same duration for their functions.

In the current study, the sampling time-points (time post-oviposition) 2 and 5 hrs were prior to the entry of the forming egg into the shell gland at approximately 5-6 hrs postoviposition. At the 15 hr time-point, the eggshell is undergoing rapid growth of the palisade columns[52]. By the 23.5 hr time-point, mineralisation will have ceased and the cuticle will be forming. Most PP IX is deposited from 21 hours postoviposition to oviposition[18]. Therefore the genes involved in PP IX synthesis may be up-regulated well before the formation of the eggshell. Despite extensive studies on the macromolecules involved in shell formation, the spatio-temporal expression of the genes involved in the sequential synthesis of various layers of the eggshell and PP IX is not clearly established.

In the current study, the expression level of *CPOX* was not significantly changed between the different time-points. The protein encoded by *CPOX* gene is the enzyme that catalyses the sixth step of the PP IX/heme biosynthetic pathway[46]. The encoded enzyme is soluble and found in the intermembrane space of mitochondria[53]. This enzyme catalyses the stepwise oxidative decarboxylation of coproporphyrinogen III to protoporphyrinogen IX, a precursor of PP IX[46,54]. Interestingly, Zheng et al.,[55] observed a correlation between the level of *CPOX* and the level of PP IX synthesis in brown-egg laying hens. This may suggest that sufficient *CPOX* RNA expression is maintained at all the time-points when the data were collected in the current study for the synthesis of PP IX.

The different expression levels of most genes, with the exception of *ABCG2* and *CPOX*, in relation to different time-points, indicate that genes involved in PP IX synthesis expressed differently during eggshell formation. As mentioned earlier, it is not clear how the regulation of various genes is synchronized in a multi-step biosynthetic pathway of PP IX. Therefore, the dynamics of the expression of these

genes including *CPOX* needs to be investigated in a temporal and spatial manner. Based on the effects of time-points on the expression levels of genes, it is assumed that these genes are transcribed and transported at different time-points; however, functionally coordinated for the synthesis of PP IX. Nevertheless, the differential expression of the genes suggests that these genes are essential in the synthesis of PP IX; thus the regulation of the genes may affect the deposition of the pigment into the eggshell.

As mentioned previously, *ALAS1* gene encodes an enzyme that catalyses the rate-limiting step in PP IX/heme biosynthetic pathway[40]. The enzyme encoded by *ALAS1* gene is delta-aminolevulinic acid synthase 1; a separate gene encodes a form of the enzyme (*ALAS2*) that is specific for erythroid tissue[56-58]. The level of the mature encoded protein is regulated by heme: high levels of heme down-regulate the mature enzyme in mitochondria while low heme levels up-regulate[56,59,60]. However, in the shell gland tissue of brown-egg laying hens, the PP IX rather than heme is the final product that deposits into various layers of eggshell. The role of the *FECH* gene in the PP IX biosynthetic pathway, the gene that encodes the enzyme that converts PP IX into heme, is still not clear. In our study, the expression level of *FECH* gene was significantly higher at 23.5 hr, but this could not be aligned in a temporal order with the expression of the other genes studied. Based on studies performed in mammalian[61], bacteria[62] and avian[60] tissues, a negative feedback mechanism exists and the formed heme in turn acts as a regulator of the PP IX biosynthetic pathway. If *FECH* has an active role in the PP IX pathway in the chicken shell gland tissue, the question arises as to how the heme formed in the epithelial cells of the shell gland is transported back to the blood to become a part of the haemoglobin molecule or for degradation. Also, there should be more heme in the shell gland cells rather than PP IX.

The higher expression level of *FLVCR1* at 15 hr can be linked with the expression levels of other genes, also suggesting the initiation of PP IX synthesis around this time-point. A significantly higher expression of the *FLVCR1* gene in the shell gland of laying hens with darker brown eggshells has been reported[63]; however, there are no published reports confirming whether the *FLVCR1* gene is involved in exporting and/or depositing PP IX onto eggshells in the shell gland of laying hens. Further study on its functional role in the PP IX deposition into eggshell is needed.

In the comparison of the expression levels of gene expression data between the control and nicarbazin treatment groups, *ALAS1* was the only gene affected by nicarbazin. It was observed that nicarbazin reduced *ALAS1* expression across all the time-points and thus a lower amount of PP IX was produced in the shell gland. However, the lower expression level of *ALAS1* did not affect the expression levels of the remaining genes studied, as their expression levels were similar between the control and nicarbazin treated hens indicating that no feedback mechanisms exist to such extent for the regulation of the genes involved in the PP IX synthesis pathway. The current study suggests that nicarbazin disrupts PP IX synthesis by affecting the expression level of the *ALAS1* gene. Nicarbazin is a chemically produced drug composed as a complex of an equimolar amount of 4,40-dinitrocarbanilide (DNC) and 2-hydroxy-4,6-dimethylpyrimidine (HDP). The DNC moiety has been shown to inhibit PP IX synthesis[64], but how the DNC moiety inhibits the expression of *ALAS1* gene is not clear. To the best of our knowledge, this is the first observation that nicarbazin regulates PP IX production through regulating *ALAS1* gene expression either directly or indirectly.

The PP IX biosynthetic pathway is well established; however, the origin of precursors and the cells involved in its synthesis in the shell gland of brown-egg laying hens are not yet fully understood (reviewed in Samiullah et al.)[65]. Not all of the enzymes involved in the PP IX/heme biosynthetic pathway are the same between erythroid and non-erythroid cells and differences at their mRNA levels have been reported for ALAS, ALAD and PBGD (reviewed in Ponka)[59]. Similarly, in a mouse model, it has been shown that *CPOX* gene is differentially regulated in erythroid and non-erythroid cells[46]. However, it is not clear whether there is different erythroid and non-erythroid specific regulation of other genes involved in the PP IX/heme biosynthetic pathway. The current study is a preliminary investigation highlighting the role of nicarbazin in disrupting the PP IX biosynthetic pathway without conclusively demonstrating the site of PP IX production in the shell gland tissue of brown-egg laying hens. Due to the lack of conclusive information about the location of genes involved in the pathway and about how nicarbazin affects the biosynthetic pathway of PP IX, we decided to process whole pieces of shell gland tissue for the gene expression study, mitochondrial quantification and quantification of PP IX from the tissue. Nevertheless, the data

presented in the current study have shown that differentially expressed *ALAS1* gene was detectable in response to the nicarbazin treatment. Thus, investigation into the tissue including epithelia and muscle appears to be effective in determining gene expression in the PP IX metabolic pathway.

The fact that there was no difference in egg weight and shell thickness between the control and nicarbazin treatment groups also indicates that nicarbazin does not affect genes involved in eggshell formation including the transport of calcium and phosphorus across the shell gland cells. However, these variables were not measured directly, and the nicarbazin was fed only for a short period. It would be valuable to study the long term effects of nicarbazin on gene expression levels associated with shell matrix formation, as earlier studies have shown a significant deterioration in egg quality when feeding nicarbazin to hens for longer periods[66,67].

Overall, the expression levels of genes involved in the production of PP IX differed in relation to the stages of eggshell formation. Feeding nicarbazin to brown-egg laying hens inhibited the expression level of *ALAS1*, resulting in lower production of PP IX for incorporation into the eggshells. The nicarbazin model could assist in understanding the mechanism of reduced synthesis and/or deposition of PP IX into eggshells due to different factors; however, the mechanism of action of individual factors in lower synthesis of PP IX may not necessarily be the same as for nicarbazin. This study confirmed that mitochondrial count per cell in the shell gland tissue does not vary significantly with different stages of egg/eggshell formation. Nevertheless, further investigation is required to understand the turnover of mitochondria in tissues such as the oviduct of laying hens. This study provides information on the interaction of nicarbazin drug with *ALAS1* gene by reducing its expression in the shell gland of brown-egg laying hens. Furthermore, this study may be used as a base for future studies in which the effect of nicarbazin and other factors on the mechanism of PP IX synthesis can be more broadly investigated.

6.5 Methods

6.5.1 Ethics statement and rearing of laying hens

The following experimental protocol was approved by the Animal Ethics Committee (Authority No.: AEC15-022) of the University of New England,

Armidale, NSW, 2351, Australia. The protocol was carried out in accordance with the guidelines specified in the Australian Code for the Care and Use of Animals for Scientific Purposes 8th edition 2013. Briefly, Hy-Line brown-egg laying hens were reared in individual cages with food and water provided *ad libitum*. The food provided was premium top layer mash (Barastock, Australia), containing crude protein (minimum) 16.5%, crude fat (minimum) 2.5%, crude fibre (maximum) 6%, salt (maximum added) 0.3%, copper (added) 8 mg/kg, selenium (added) 0.3 mg/kg and calcium (minimum) 3.6%. At the time of the experiment, hens were on a 16:8 hour light:dark photoperiod.

6.5.2 Experiment 1: Effect of time-points on mitochondrial count and expression of protoporphyrin IX synthesis genes

The laying hen rearing shed was equipped with a video surveillance camera to precisely record the oviposition time of the hens selected for shell gland tissue collection. Eggs were collected and shell colour (L*) was measured with a spectrophotometer (Konica Minolta CM-2600d Ramsey, NJ, USA) using the L*a*b* colour space system. The L* measurements represent the intensity of brown eggshell colour; the higher the value, the lighter the colour of the eggshell. Egg weight was measured using an analytical balance, and the eggs were further processed for protoporphyrin IX (PP IX) quantification following the method of Samiullah and Roberts[15]. The post-oviposition times (time-points) were 2, 5, 15 and 23.5 hrs for the four groups of hens selected. Of 63 hens (36–37 weeks old), 20 hens were selected and divided in such a way that the mean values of the variables measured were not significantly different among the groups (Table 6.3). As the quantity of PP IX in eggshell may vary from hen to hen, the main purpose of recording these egg quality measurements was to ensure that hens were divided uniformly on the basis of shell weight and colour into the respective groups prior to the experiment.

Variable	Time-point (hr)				P value
	2	5	15	23.5	
Egg weight (g)	62.8±3.50	63.9±2.30	62.9±1.67	65.6±1.76	0.8226
L* (0–100)	56.2±0.98	54.4±0.97	54.2±0.88	54.4±0.27	0.2984
PP IX in whole eggshell	0.14±0.02	0.14±0.03	0.14±0.02	0.14±0.02	0.9896
PP IX in calcareous shell	0.12±0.02	0.11±0.03	0.11±0.02	0.11±0.04	0.7170
PP IX in cuticle	0.02±0.06	0.03±0.04	0.03±0.04	0.03±0.04	0.6708

Table 6.3 Mean values (±S.E.) of egg quality variables measured before dividing hens into different groups

Protoporphyrin IX (PP IX) was measured in nMoles per gram of shell with and without cuticle and in cuticle alone. The eggs were collected before dividing the experimental hens into various groups. On the basis of eggshell variables, hens were divided into groups in such a way that the variables were not significantly different among groups.

6.5.3 Experiment 2: Effect of time-points and nicarbazin treatment on mitochondrial count and expression of protoporphyrin IX synthesis genes

The rearing conditions for the hens were the same as described in Experiment 1. Of 43 hens (42–45 weeks old), 30 hens were selected on the basis of L*, egg weight and PP IX measurements of eggshell and divided equally into two groups, control and nicarbazin treatment (Table 6.4). Based on the results from Experiment 1, it was found that the gene expression values of time-points 2 and 5 hrs were not significantly different for most of the genes. Therefore, time-point 2 hr was omitted in Experiment 2. Time-point 5 hr was chosen because, at this time, the egg is either in the distal magnum and/or isthmus and preparing to move into the shell gland in the subsequent hour or so. Next, each group was subdivided into three groups by post-oviposition time (5, 15 and 23.5 hrs). Therefore, the experimental design was in a 2×3 factorial arrangement. For the control groups, the feed was the same as described earlier. For the nicarbazin treatment groups, each group was offered the same feed supplemented with nicarbazin powder (M.W. 426.38; Sigma Aldrich,

Australia) at a rate of 100 mg/kg of feed. In a pilot experiment, it was determined that feeding nicarbazin at a rate of 100 mg/kg of feed was sufficient to cause complete discolouration of brown eggshell colour without causing any adverse effects on egg formation and feed intake. From the control groups, eggs were collected for analysis at least five days before processing the hens for shell gland tissue collection. From the nicarbazin treatment groups, eggs were collected for analysis at least one day before treatment and continued until the maximum loss in shell colour (>20%) was achieved. Individual hens were processed for shell gland tissue collection at specific time-points postoviposition.

Variable	**Group**							
	Control (15 hens)				**Nicarbazin (15 hens)**			
	Time-point (hr)			**P value**	**Time-point (hr)**			**P value**
	5	**15**	**23.5**		**5**	**15**	**23.5**	
Egg weight (g)	63.7±1.76	63.3±1.60	63.8±1.60	0.7070	59.6±1.70	59.9±1.41	62.6±1.20	0.2102
L* (0-100)	58.7±0.60	59.5±0.90	59.4±0.64	0.6820	58.5±0.68	58.9±0.55	59.1±0.52	0.7652
PP IX	0.12±0.05	0.13±0.06	0.12±0.06	0.7055	0.12±0.05	0.13±0.03	0.13±0.03	0.4532

Table 6.4 Mean values (±S.E.) of egg quality variables measured before dividing hens into different groups (time-points and nicarbazin treatment)

Protoporphyrin IX (PP IX) was measured in nMoles per gram of whole eggshell. The eggs were collected before dividing the experimental hens into various groups. On the basis of eggshell variables, hens were divided into groups in such a way that the variables were not significantly different among groups.

6.5.4 Shell gland tissue collection

For both experiments, individual hen oviposition times were recorded, and each hen was euthanised at a specific post-oviposition time (2, 5, 15, 23.5 hrs and 5, 15, 23.5 hrs for Experiments 1 and 2, respectively). Hens were humanely euthanized with CO_2 gas and the shell gland was aseptically collected through the abdominal incision. The shell gland was opened from the anterior-ventral side and an approximately 500 mg tissue was cut from the centre of the shell gland and

transferred to RNALater (Sigma Aldrich, Australia) in 2 mL Eppendorf tube. The samples were stored at -20°C and were processed for RNA/DNA extraction within one day of collection.

6.5.5 Total RNA and DNA extraction

Total RNA and DNA were extracted from a whole piece of shell gland tissue (all tissue layers) that had been stored in RNALater at -20°C. The TRIsure (Bioline, Australia) protocol was followed with slight modifications. Briefly, approximately 50 mg of tissue (wet weight) was homogenized in 1 mL of TRIsure, using an IKA T10 basic Homogenizer (Wilmington, NC, USA). After chloroform treatment and centrifugation, the upper layer was used for total RNA extraction. RNA was precipitated by adding 0.5 mL chilled iso-propanol (100%) followed by incubation for 10 minutes at room temperature. The precipitated RNA solution was centrifuged at 12000 ×*g* for 10 minutes at 4°C to obtain an RNA pellet. The pellet was washed by adding 1 mL ethanol (75%) and centrifuging at 7500 ×*g* for 5 minutes at 4°C. The resulting RNA pellet was dissolved in 100 µL DEPC-treated water and proceeded to the RNA purification step using an RNeasy Mini Kit (Qiagen, GmbH, Hilden, Germany) as per the manufacturer's instructions. The elution step for RNA from the spin columns with 50 µL of RNase-free water was repeated, and both elutions were mixed together thoroughly. The quantity and purity of purified total RNA were determined using the spectrophotometer NANODROP-8000 (ThermoFisher Scientific, Wilmington, DE, USA). From the original concentration of RNA, 100-fold (1:100) serial dilutions were prepared and stored at -80°C until further processing. RNA integrity was examined in Agilent 2100 Bioanalyzer (Agilent Technologies, Waldbronn, Germany) using Agilent RNA 6000 Nano Kit as per the manufacturer's instructions. The samples with RNA integrity number (RIN) >8.5 were regarded as high integrity and then used in the downstream qPCR assay.

The middle and bottom layers from the homogenized and chloroform separated samples were mixed and processed for total DNA extraction. Briefly, 0.3 mL absolute ethanol was added to precipitate DNA and samples incubated for 3 minutes at room temperature. The precipitated DNA was centrifuged at 2000 ×*g* for 5

minutes at 4°C to obtain a DNA pellet. The pellet was washed with 1 mL of 0.8 M sodium citrate in 10% ethanol and the process was repeated for a total of three times. Next, the pellet was washed with 1.5 mL ethanol (75%) and centrifuged as described earlier. After ethanol removal, the pellet was dissolved in 100 µL TE buffer (10 mM Tris-HCl, 1 mM disodium EDTA, pH 8.0) and centrifuged at 12000 ×*g* for 10 minutes at 4°C to remove any insoluble material. The quantity and purity of total DNA in 2 µL of each sample was determined in a NANODROP-8000 spectrophotometer as described earlier. The pure extracted DNA was stored at -20°C until used for downstream applications.

6.5.6 Primer design for oligonucleotides

The primer sequences were either referenced from literature or designed using NCBI primer and BLAST options (Table 6.5). Primer quality was checked in "Beacon Designer" software (http://www.premierbiosoft.com/qOligo/Oligo.jsp?PID=1) for possible self and cross secondary structures. To check the sequence specificity, primers were aligned against the NCBI database using BLASTN, Ensembl Chicken Galgal4 and UCSC's Chicken (*Gallus gallus*) Genome Browser Gateway. Primers quality for single peak generation during melting curve analysis was also checked in uMelt^{SM} web-based online tool. uMelt^{SM} is used for prediction of DNA melting curves and denaturation profiles of PCR products[68]. Prior to real-time qPCR, the primer amplification efficiency and specificity for each primer pair were analysed by using five 10-fold serial dilutions of the purified total DNA/RNA to construct a standard curve. The amplification efficiency was calculated by the equation[69]: $E = 10^{(1/slope)} - 1$. The primers were synthesized by Invitrogen® (ThermoFisher, Australia). Only the primers specifically amplifying the genes of interest were used in the experiment; those with non-specific amplifications were removed from the study. For example, the primers[63] designed for the *ABCB6* gene were removed due to their amplification of the *UB3* gene. The specificity of the selected primers in amplifications is shown in Figure 6.4. The primers amplified single bands with expected sizes according to their designs based on the sequences of the genes. Furthermore, a single peak of

melting curves of the primers was also confirmed following real-time PCR amplification (Appendix A).

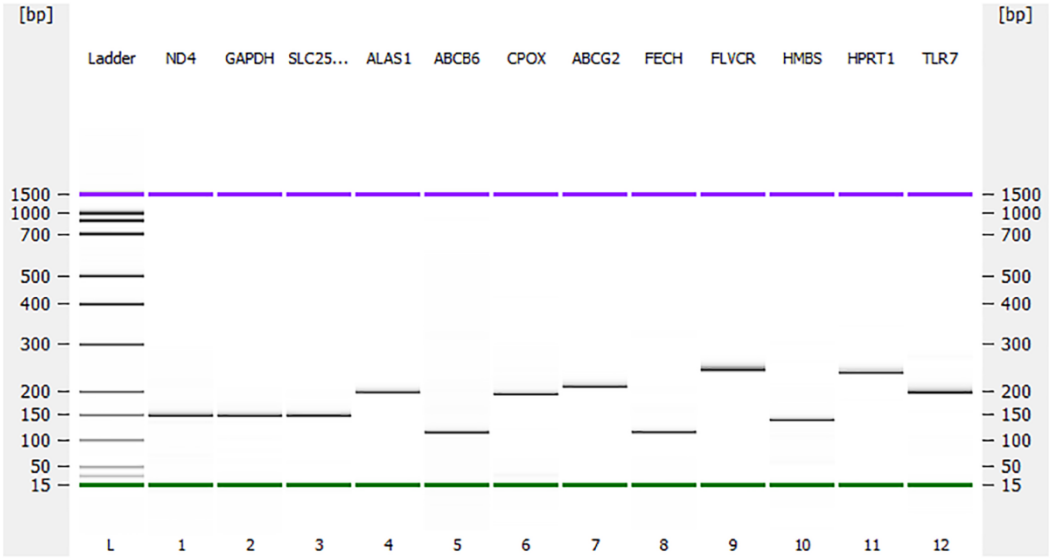

Figure 6.4 Amplification of the genes fragments from the shell gland tissue of a chicken to assess the specificities of the primers used in the current study

L. DNA marker; (**1**) *ND4* (137 bp); (**2**) *GAPDH* (137 bp); (**3**) *SLC25A38* (139 bp); (**4**) *ALAS1* (197 bp); (**5**) *ABCB6* (107 bp); (**6**) *CPOX* (187 bp); (**7**) *ABCG2* (208 bp); (**8**) *FECH* (112 bp); (**9**). *FLVCR1* (239 bp); (**10**) *HMBS* (131 bp); (**11**) *HPRT1* (245 bp); (**12**) TLR7-positive control (200 bp). The upper (purple) and lower (green) markers act as internal standards and are used to align the ladder analysis with the individual DNA sample analysis. The standard curve (plotting migration time against DNA amplicon size), in conjunction with the markers, is then used to calculate DNA fragment sizes for each well from the migration times measured (see Agilent 2100 Bioanalyzer Users Guide for Molecular Assays). The DNA gel in Agilent 2100 Bioanalyzer was performed as per the manufacturer's instructions of Agilent DNA 1000 Kit.

6.5.7 Mitochondrial DNA quantification

6.5.7.1 DNA cloning

In order to quantify the copy number of mtDNA, a recombinant plasmid vector was constructed by cloning 137 bp fragments of each of the *ND4* and *GAPDH* genes (Table 6.5), using TOPO® TA Cloning® Kit for sequencing (ThermoFisher

Scientific, Australia) as per the manufacturer's protocol (Figure 6.5). The recombinant plasmid was transfected into *Escherichia coli* that was grown overnight on Difco™ LB Agar (Bacto Laboratories, Australia) and then a single colony was enriched in LB broth. Recombinant plasmid DNA from overnight cultured *Escherichia coli* in LB broth was extracted using the PureLink® Quick Plasmid Miniprep Kit (ThermoFisher Scientific, Australia). The procedure was as per the manufacturer's protocol with 75 µL pre-heated (65°C) TE buffer used for elution. The eluted recombinant plasmid DNA quality and quantity were checked with the NANODROP-8000 spectrophotometer and stored at -20°C until used for downstream applications.

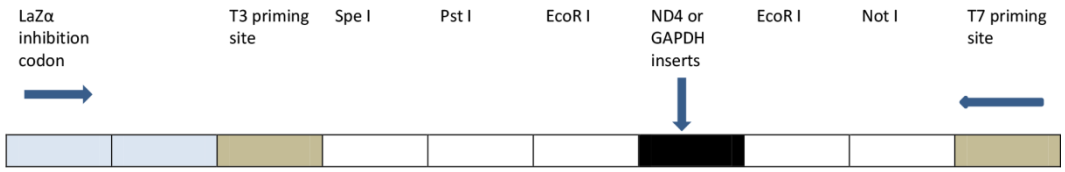

Figure 6.5 Schematic diagram of single-insert plasmid pCR™ 4-TOPO (3956 nucleotides) The diagram shows site into which specific fragments of chicken *ND4* or *GAPDH* genes were inserted. The fragments in the study were flanked by restriction and priming sites.

6.5.7.2 Standard curve construction

qPCR was performed on the recombinant plasmid DNA at six different dilutions (10^{-2}~10^{-6}) in 20 µL reaction to check the cloned chicken mtDNA and gDNA amplification efficiencies alongside plasmid DNA amplification. The master-mix preparation and cycling conditions were as per the protocol of the SensiFAST™ SYBR® No-ROX Kit (Bioline, Australia). To construct a standard curve for analysis, eight 10-fold serial dilutions (10^{-2}~10^{-9}) were prepared from the recombinant plasmid DNA, and qPCR was performed on all the samples as described earlier. The standard curve was constructed by plotting the quantification cycles (Cq) against $\log_{10}$ copy numbers of plasmids. All recombinant plasmid constructs were analysed by qPCR and sequencing (AGRF, Australia)[70] to confirm that accurate cloning of target DNA fragments was executed.

6.5.7.3 Mitochondrial DNA copy number quantification by qPCR

Mitochondria were enumerated by the quantification of their DNA copies in a cell and genomic DNA copies were used to represent cell numbers in the samples[71]. Quantitative PCR to quantify mitochondrial DNA copy numbers in a cell was performed with SYBR green method by using the SensiFAST™ SYBR® No-ROX Kit. qPCR reaction was performed in a total volume of 20 µL with a Rotor-Gene 6000 thermocycler (Corbett Research, Sydney, Australia). The reaction consisted of 10 µL 2× SensiFAST™ SYBR® No-ROX mix, 400 nMoles primers, 6.4 µL RNase-free water and 2 µL of diluted DNA (10^{-2} dilution of extracted DNA samples). Reaction without DNA template was included as a no template control (NTC). Recombinant plasmid DNA dilutions were included in the qPCR runs. qPCR was performed following a 2-step protocol: polymerase activation and DNA denaturation at 95°C for 3 minutes, and 40 cycles of denaturation at 95°C for 5 seconds and annealing and extension at 60°C or 63°C for 30 seconds. Fluorescent signals were acquired at the end of each annealing/extension step during qPCR cycles (40). A melting phase at a ramp from 50ºC to 99ºC at 1ºC increment was conducted to assess the specificity of qPCR amplification. The qPCR products were examined in the Bioanalyzer using Agilent DNA 1000 Kit to determine the amplification specificity by the size of the amplicons estimated. qPCR amplification efficiency was determined as previously described. The qPCR data for the genes were processed further when the qPCR amplification efficiency was in a range of 94% to 105%, and linear correlation coefficient $R^2 > 0.980$ as these were considered of high standard[72].

6.5.7.4 Calculation of mitochondria per cell

The cloned plasmid DNA with *ND4* and *GAPDH* genes inserts were converted into plasmid DNA copies/µL in six different dilutions for analysis. Plasmid copy number was calculated based on the concentration of plasmid DNA and its molecular weight. The cloned plasmid DNA amplification cycle (Cq) values were then used to construct a standard curve to calculate the mtDNA and gDNA copies per diploid cell. The absolute copy number of mtDNA per cell was calculated according to the equation: (copy number of mtDNA)/(copy number of gDNA/2).

6.5.8 Gene expression analysis by qPCR

For the gene expression studies, samples were run in triplicate with the inclusion of NTC and no reverse transcriptase (-RT) controls. Master-mix was prepared as per the manufacturer's protocol using the SensiFAST SYBR® Lo-ROX One-Step RT-PCR Kit (Bioline, Australia). The reaction in a volume of 20 µL contained 10 µL of 2× SensiFAST SYBR low Rox one-step mix, 400 nMoles primers, 0.2 µL of reverse transcriptase, 0.4 µL of RiboSafe RNase inhibitor, 3.8 µL RNase-free water and 4 µL of RNA template (diluted 100 times). Reverse transcription and amplification were conducted following the thermal cycling protocol in Rotor-Gene 6000: reverse transcription at 45°C for 10 minutes, polymerase activation and denaturation at 95°C for 2 minutes, then 40 cycles of denaturation at 95°C for 5 seconds and annealing and extension at 60°C, 63°C or 65°C for 20 seconds. The fluorescent data collection and melting analysis were performed as described previously.

6.5.9 Measurement of protoporphyrin IX in tissue and eggshell

The shell gland that was opened for tissue collection for RNA and DNA extractions was used for protoporphyrin IX (PP IX) measurements. From the right half of the shell gland, a 0.25 g piece (including muscle layers) was weighed with an analytical weighing balance (Quintix513-1S, Göttingen, Germany) and directly transferred into a 10 mL tube containing 4 mL of 3N HCl[73]. The tissue was homogenized (IKA T10 homogenizer) and stored in a refrigerator for 3 hrs. The homogenised tissues were centrifuged at 800 ×g for 30 minutes at 4°C and the absorbance of the supernatant was read in a spectrophotometer (UV-1201, Shimadzu, Kyoto, Japan) at PP IX specific absorbance wavelength of 412 nm. Standard dilutions (0 to 6.87 nMoles) prepared from protoporphyrin IX di-sodium salt (Sigma Aldrich, Australia) were read at the same wavelength in order to construct a standard curve for the calculations of the amount of PP IX per gram of tissue. The quantification of PP IX in the eggshells was performed according to Samiullah and Roberts[15].

6.6 Statistical analysis

In order to determine the mitochondrial count, the mtDNA copies per cell data were analysed in SPSS version 22 (IBM Corporation, Armonk, NY, USA)[74] with the GLM module by taking the time-points and nicarbazin treatment as main effects. Level of significance was indicated by a probability of less than 5%. The Tukey test was used to differentiate levels of significance between mean values.

For the gene expression studies, raw Cq values for all candidate target genes were imported into qbase+ version 3.0 (Biogazelle, Belgium)[75] and analysed against the two reference genes *HMBS* and *HPRT1*, validated in the current study. The qbase+ applies an arithmetic mean method to transform logarithmic Cq value to linear relative quantity using exponential function for relative quantification of genes and the arithmetic mean of average Cq is scaled to a given target sample[76,77]. For data analysis, the basic calculation used in qbase+ was based on $2^{\wedge\text{-}\Delta\Delta Cq}$ method[78] as the amplification efficiencies of the genes were very close to 100%. In qbase+ algorithm, the relative quantity of gene expression level between different samples for a given target gene does not have an absolute scale and is only meaningful in comparison to values obtained for other samples measured for that gene in the same experiment[75]. The result table shows normalized relative quantities (NRQ) values that are calculated across all unknown samples per target gene. The gene expression levels are typically log-normally distributed and all statistical calculations are performed on the $\log_{10}$ transformed NRQ values[75,79]. For easy interpretation of the statistical results, values are re-transformed to linear scale by taking the antilogarithm. Thus, in the current study, the relative expression values for a given gene show fold changes relative to the average expression level across all samples for that particular gene.

To determine the effect of time-points and nicarbazin treatment on expression stability of individual target genes, the NRQ (linear scale) were exported and analysed in SPSS using GLM module. Level of significance was calculated as stated previously. All other parameters data were analysed in SPSS using GLM module unless stated.

Gene name	Gene symbol	Primer sequence (5' –3')	Amplicon size (bp)	Annealing temperature °C	Amplification efficiency (%)	Accession No.	Reference
NADH dehydrogenase subunit 4	*ND4*[a]	F:CGCAGGCTCCATACTACTCG R:TTAGGGCACCTCATAGGGCT	137	60	94	NC_001323.1	this study
Glyceraldehyde-3-phosphate dehydrogenase	*GAPDH*[b]	F: GGTCACCAAGAAGGTGGAGA R: GACAGTGCCCTTGAAGTGTC	137	63	97	NC_006088.3	this study
Solute carrier family 25, member 38	*SLC25A38*	F: AGACACGGTATGAGAGTGGA R: ATCCCAGAGAAAGGTGCGTC	139	63	95	XM_418818.3	this study
delta-aminolevulinic acid synthase 1	*ALAS1*	F: GGTGGACAGGAAAGGTAAAGA R: ACTGGTCATACTGGAAGGTG	197	60	98	NM_001018012.1	Li et al., 2013[63]
ATP binding cassette subfamily C member 6	*ABCB6*	F: CTCAACTGGTTCGGCACCTA R: TTCACTGCATCCTTCACCTCC	107	60	94	XM_015290086.1	this study
Coproporphyrinogen oxidase	*CPOX*	F: GAGAGGACGGTATGTGGAGT R: TTTGGGATTGCGGAGAAC	187	60	95	XM_004938236.1	Li et al., 2013[63]
ATP binding cassette subfamily G member 2	*ABCG2*	F: CCTCCTTGTAAACCTCCCTT R: GTAATCTTCACCAGAGCACCTT	208	65	98	XM_421638.4	Li et al., 2013[63]
Ferrochelatase	*FECH*	F: TGCTTTGCCGATCACAT R: CACGGTTCACCACAGACAT	112	60	96	U68033.1	Li et al., 2013[63]
Feline leukemia virus subgroup C cellular receptor 1	*FLVCR1*	F: CGGGAGTCGTGTTTGAAGAGA R: CCCAGCGTTCACTTCTTCTCC	239	63	99	XM_419425.5	this study
Hydroxymethylbilane synthase	*HMBS*	F: GGCTGGGAGAATCGCATAGG R: TCCTGCAGGGCAGATACCAT	131	60	94	XM_417846.2	Yin et al., 2011[80]
Hypoxanthine phosphoribosyltransferase 1	*HPRT1*	F: ACTGGCTGCTTCTTGTG R: GGTTGGGTTGTGCTGTT	245	63	98	NM_204848.1	Yang et al., 2013[81]

Table 6.5 Forward (F) and reverse (R) sequence of the primers used in the study

[a]Gene was used to amplify fragment of mtDNA; [b]Gene was used to amplify fragment of gDNA.

6.7 Acknowledgements

This study was funded by the Australian Egg Corporation Limited, Australia, grant number AECL 1UN121. We thank Kapil Chousalkar for technical guidance in experimental design and critical reading of the manuscript.

6.8 Authors' contributions

S.S. developed the hypotheses, designed and performed the experiments, analysed and interpreted data, and drafted the manuscript; J.R. oversaw the animal trials, administrated the overall research project, assisted with the experiments, analysis and interpretation of data and critically revised the manuscript; S-B.W. designed mitochondrial quantification experiments, oversaw the assays involved in gene expression and mitochondrial quantification experiments, analysed and interpreted the data, and drafted the manuscript. This study was performed as part of a PhD project of Sami Samiullah funded by AECL.

6.9 Competing interests

The authors declare that they have no competing interests.

6.10 Competing financial interests

The authors declare no competing financial interests.

6.11 References

1 Nys, Y. & Guyot, N. Egg formation and chemistry in *Improving the safety and quality of eggs and egg products* Vol. 1 (ed. Nys, Y., Bain, M. & Van Immerseel, F.) 83-132 (Woodhead Publishing Limited, 2011).

2 Johnson, A. L. Reproduction in the female in *Sturkie avian physiology* (ed. Scanes, C. C.) 635-665 (Academic Press, 2015).

3 Melek, O., Morris, T. R. & Jennings, R. C. The time factor in egg formation for hens exposed to ahemeral light-dark cycles. *Br. Poult. Sci.* **14**, 493-498 (1973).

4 Jonchère, V. *et al.* Gene expression profiling to identify eggshell proteins involved in physical defense of the chicken egg. *BMC Genomics* **11**, 1 (2010).

5 Rose, M. L. & Hincke, M. T. Protein constituents of the eggshell: eggshell-specific matrix proteins. *Cell. Mol. Life Sci.* **66**, 2707-2719 (2009).

6 Baker, J. R. & Balch, D. A. A study of the organic material of hen's-egg shell. *Biochem. J.* **82**, 352-361 (1962).

7 Dennis, J. E. *et al.* Microstructure of matrix and mineral components of eggshells from white leghorn chickens (*Gallus gallus*). *J. Morphol.* **228**, 287-306 (1996).

8 Fernandez, M. S., Araya, M. & Arias, J. L. Eggshells are shaped by a precise spatio-temporal arrangement of sequentially deposited macromolecules. *Matrix Biol.* **16**, 13-20 (1997).

9 Fernandez, M. S., Moya, A., Lopez, L. & Arias, J. L. Secretion pattern, ultrastructural localization and function of extracellular matrix molecules involved in eggshell formation. *Matrix Biol.* **19**, 793-803 (2001).

10 Nys, Y., Hincke, M., Arias, J., Garcia-Ruiz, J. & Solomon, S. Avian eggshell mineralization. *Poult. Avian Biol. Rev.* **10**, 143-166 (1999).

11 Solomon, S. E. *Egg and eggshell quality* (Wolfe Publishing Ltd, 1991).

12 Mikšík, I., Eckhardt, A., Sedláková, P. & Mikulikova, K. Proteins of insoluble matrix of avian (*Gallus gallus*) eggshell. *Connect. Tissue Res.* **48**, 1-8 (2007).

13 Baird, T., Solomon, S. E. & Tedstone, D. R. Localisation and characterisation of egg shell porphyrins in several avian species. *Br. Poult. Sci.* **16**, 201-208 (1975).

14 Sparks, N. H. C. Shell accessory materials: structure and function in *Microbiology of the avian egg* (ed. Board, R. G. & Fuller, R.) 25-42 (Chapman & Hall, 1994).

15 Samiullah, S. & Roberts, J. R. The location of protoporphyrin in the eggshell of brown-shelled eggs. *Poult. Sci.* **92**, 2783-2788 (2013).

16 Nys, Y. Relationships between age, shell quality and individual rate and duration of shell formation in domestic hens. *Br. Poult. Sci.* **27**, 253-259 (1986).

17 Nys, Y., Gautron, J., Garcia-Ruiz, J. M. & Hincke, M. T. Avian eggshell mineralization: biochemical and functional characterization of matrix proteins. *C. R. Palevol* **3**, 549-562 (2004).

18 Nys, Y., Zawadzki, J., Gautron, J. & Mills, A. Whitening of brown-shelled eggs: mineral composition of uterine fluid and rate of protoporphyrin deposition. *Poult. Sci.* **70**, 1236-1245 (1991).

19 Lentz, S. I. *et al.* Mitochondrial DNA (mtDNA) biogenesis: visualization and duel incorporation of BrdU and EdU into newly synthesized mtDNA *in vitro*. *J. Histochem. Cytochem.* **58**, 207-218 (2010).

20 Fuke, S., Kubota-Sakashita, M., Kasahara, T., Shigeyoshi, Y. & Kato, T. Regional variation in mitochondrial DNA copy number in mouse brain. *Biochim. Biophys. Acta, Bioenerg.* **1807**, 270-274 (2011).

21 Guo, W., Jiang, L., Bhasin, S., Khan, S. M. & Swerdlow, R. H. DNA extraction procedures meaningfully influence qPCR-based mtDNA copy number determination. *Mitochondrion* **9**, 261-265 (2009).

22 Phillips, N. R., Sprouse, M. L. & Roby, R. K. Simultaneous quantification of mitochondrial DNA copy number and deletion ratio: a multiplex real-time PCR assay. *Sci. Rep.* **4**, 3887 (2014).

23 Blanche, S. *et al.* Persistent mitochondrial dysfunction and perinatal exposure to antiretroviral nucleoside analogues. *The Lancet* **354**, 1084-1089 (1999).

24 Barazzoni, R., Short, K. R. & Nair, K. S. Effects of aging on mitochondrial DNA copy number and cytochrome c oxidase gene expression in rat skeletal muscle, liver, and heart. *J. Biol. Chem.* **275**, 3343-3347 (2000).

25 Laubenthal, L. *et al.* Mitochondrial DNA copy number and biogenesis in different tissues of early-and late-lactating dairy cows. *J. Dairy Sci.* **99**, 1571-1583 (2016).

26 Bogenhagen, D. & Clayton, D. A. The number of mitochondrial deoxyribonucleic acid genomes in mouse L and human HeLa cells. Quantitative isolation of mitochondrial deoxyribonucleic acid. *J. Biol. Chem.* **249**, 7991-7995 (1974).

27 Copeland, W. C. The mitochondrial DNA polymerase in health and disease in *Genome stability and human diseases* 211-222 (Springer, 2010).

28 Campbell, C. T., Kolesar, J. E. & Kaufman, B. A. Mitochondrial transcription factor A regulates mitochondrial transcription initiation, DNA packaging, and genome copy number. *Biochim. Biophys. Acta, Gene Regul. Mech.* **1819**, 921-929 (2012).

29 Bao, H., Zhao, C., Li, J. & Wu, C. Sequencing and alignment of mitochondrial genomes of Tibetan chicken and two lowland chicken breeds. *Sci. China Ser. C* **51**, 47-51 (2008).

30 Liu, L.-L., Xie, H.-B., Yang, Y.-S., Yu, Q.-F. & He, J.-H. The complete mitochondrial genome of the Xuefeng black-boned chicken. *Mitochondrial DNA Part A* **27**, 30-31 (2016).

31 Soattin, M., Barcaccia, G., Dalvit, C., Cassandro, M. & Bittante, G. Genomic DNA fingerprinting of indigenous chicken breeds with molecular markers designed on interspersed repeats. *Hereditas* **146**, 183-197 (2009).

32 Andreu, A. L., Martinez, R., Marti, R. & García-Arumí, E. Quantification of mitochondrial DNA copy number: pre-analytical factors. *Mitochondrion* **9**, 242-246 (2009).

33 Montier, L. L. C., Deng, J. J. & Bai, Y. Number matters: control of mammalian mitochondrial DNA copy number. *J. Genet. Genomics* **36**, 125-131 (2009).

34 Gianotti, T. F. *et al.* Mitochondrial DNA copy number is modulated by genetic variation in the signal transducer and activator of transcription 3 (STAT3). *Metabolism.* **60**, 1142-1149 (2011).

35 Scientific Opinion on the safety and efficacy of Koffogran (nicarbazin) as a feed additive for chickens for fattening. *EFSA Journal* **8**, 1551 (2010).

36 Hughes, B. L., Jones, J. E., Toler, J. E., Solis, J. & Castaldo, D. J. Effects of exposing broiler breeders to nicarbazin contaminated feed. *Poult. Sci.* **70**, 476-482 (1991).

37 McLoughlin, D. K., Wehr, E. E. & Rubin, R. Egg shell colour and egg production in new hampshire laying hens as affected by nicarbazin medication. *Poult. Sci.* **36**, 880-884 (1957).

38 McClary, C. F. The restriction of ooporphyrin deposition on egg shells by drug feeding. *Poult. Sci.* **34**, 1164-1165 (1955).

39 Guernsey, D. L. *et al.* Mutations in mitochondrial carrier family gene SLC25A38 cause nonsyndromic autosomal recessive congenital sideroblastic anemia. *Nat. Genet.* **41**, 651-653 (2009).

40 May, B. K. *et al.* Molecular regulation of heme biosynthesis in higher vertebrates. *Prog. Nucleic Acid Res. Mol. Biol.* **51**, 1-51 (1995).

41 Laver, W. G., Neuberger, A. & Udenfriend, S. Initial stages in the biosynthesis of porphyrins. 1. The formation of δ-aminolaevulic acid by particles obtained from chicken erythrocytes. *Biochem. J.* **70**, 4-14 (1958).

42 Rees, D. C., Johnson, E. & Lewinson, O. ABC transporters: the power to change. *Nat. Rev. Mol. Cell Biol.* **10**, 218-227 (2009).

43 Zutz, A., Gompf, S., Schägger, H. & Tampé, R. Mitochondrial ABC proteins in health and disease. *Biochim. Biophys. Acta, Bioenerg.* **1787**, 681-690 (2009).

44 Krishnamurthy, P. C. *et al.* Identification of a mammalian mitochondrial porphyrin transporter. *Nature* **443**, 586-589 (2006).

45 Quigley, J. G. *et al.* Identification of a human heme exporter that is essential for erythropoiesis. *Cell* **118**, 757-766 (2004).

46 Takahashi, S. *et al.* Differential regulation of coproporphyrinogen oxidase gene between erythroid and nonerythroid cells. *Blood* **92**, 3436-3444 (1998).

47 Ogino, T. *et al.* Serum-dependent export of protoporphyrin IX by ATP-binding cassette transporter G2 in T24 cells. *Mol. Cell. Biochem.* **358**, 297-307 (2011).

48 Zhou, S. *et al.* Increased expression of the Abcg2 transporter during erythroid maturation plays a role in decreasing cellular protoporphyrin IX levels. *Blood* **105**, 2571-2576 (2005).

49 Lipovich, L., Hughes, A. L., King, M.-C., Abkowitz, J. L. & Quigley, J. G. Genomic structure and evolutionary context of the human feline leukemia virus subgroup C receptor (hFLVCR) gene: evidence for block duplications and de novo gene formation within duplicons of the hFLVCR locus. *Gene* **286**, 203-213 (2002).

50 Harbin, B. M. & Dailey, H. A. Orientation of ferrochelatase in bovine liver mitochondria. *Biochemistry (Mosc.)* **24**, 366-370 (1985).

51 Day, A. L., Parsons, B. M. & Dailey, H. A. Cloning and characterization of Gallus and Xenopus ferrochelatases: Presence of the [2Fe-2S] cluster in nonmammalian ferrochelatase. *Arch. Biochem. Biophys.* **359**, 160-169 (1998).

52 Bain, M. Composition and properties of eggshell in *Achieving sustainable production of eggs* Vol. 1 (ed Roberts J) 3-23 (Burleigh Dodds Science Publishing Limited, 2017).

53 Grandchamp, B., Phung, N. & Nordmann, Y. The mitochondrial localization of coproporphyrinogen III oxidase. *Biochem. J.* **176**, 97-102 (1978).

54 Nilsson, R. *et al.* Discovery of genes essential for heme biosynthesis through large-scale gene expression analysis. *Cell Metab.* **10**, 119-130 (2009).

55 Zheng, C., Li, Z., Yang, N. & Ning, Z. Quantitative expression of candidate genes affecting eggshell colour. *Anim. Sci. J.* **85**, 506-510 (2014).

56 Sassa, S. & Nagai, T. The role of heme in gene expression. *Int. J. Hematol.* **63**, 167-178 (1996).

57 Yamamoto, M. *et al.* Isolation of recombinant cDNAs encoding chicken erythroid delta-aminolevulinate synthase. *Proc. Nat. Acad. Sci. U.S.A.* **82**, 3702-3706 (1985).

58 Riddle, R. D., Yamamoto, M. & Engel, J. D. Expression of delta-aminolevulinate synthase in avian cells: separate genes encode erythroid-

specific and nonspecific isozymes. *Proc. Nat. Acad. Sci. U.S.A.* **86**, 792-796 (1989).

59 Ponka, P. Tissue-specific regulation of iron metabolism and heme synthesis: distinct control mechanisms in erythroid cells. *Blood* **89**, 1-25 (1997).

60 Granick, S. The induction *in vitro* of the synthesis of δ-aminolevulinic acid synthetase in chemical porphyria: A response to certain drugs, sex hormones, and foreign chemicals. *J. Biol. Chem.* **241**, 1359-1375 (1966).

61 Karibian, D. & London, I. M. Control of heme synthesis by feedback inhibition. *Biochem. Biophys. Res. Commun.* **18**, 243-249 (1965).

62 Burnham, B. F. & Lascelles, J. Control of porphyrin biosynthesis through a negative-feedback mechanism. Studies with preparations of δ-aminolaevulate synthetase and δ-aminolaevulate dehydratase from *Rhodopseudomonas spheroides*. *Biochem. J.* **87**, 462-472 (1963).

63 Li, G. *et al.* Comparison of protoporphyrin IX content and related gene expression in the tissues of chickens laying brown-shelled eggs. *Poult. Sci.* **92**, 3120-3124 (2013).

64 Polin, D., Basso, A. J. & O'Neill, R. C. Some compounds in the carbanilide series preventing shell porphyrin deposition. *Poult. Sci.* **38**, 282-284 (1959).

65 Samiullah, S., Roberts, J. R. & Chousalkar, K. Eggshell colour in brown-egg laying hens-a review. *Poult. Sci.* **94**, 2566-2575 (2015).

66 Sherwood, D. H., Milby, T. T. & Higgins, W. A. The effect of nicarbazin on reproduction in White Rock breeder hens. *Poult. Sci.* **35**, 1014-1019 (1956).

67 Weiss, H. S. Further comments on the effect of nicarbazin on the egg. *Poult. Sci.* **36**, 589-591 (1957).

68 Dwight, Z., Palais, R. & Wittwer, C. T. uMELT: prediction of high-resolution melting curves and dynamic melting profiles of PCR products in a rich web application. *Bioinformatics* **27**, 1019-1020 (2011).

69 Peirson, S. N., Butler, J. N. & Foster, R. G. Experimental validation of novel and conventional approaches to quantitative real-time PCR data analysis. *Nucleic Acids Res.* **31**, e73-e73 (2003).

70 Australian Genome Research Facility, North Melbourne, Victoria, 3051, Australia. URL *http://www.agrf.org.au/*.

71 Miller, F. J., Rosenfeldt, F. L., Zhang, C., Linnane, A. W. & Nagley, P. Precise determination of mitochondrial DNA copy number in human skeletal and cardiac muscle by a PCR-based assay: lack of change of copy number with age. *Nucleic Acids Res.* **31**, e61-e61 (2003).

72 "Bio-Rad Laboratories. Real-Time PCR applications guide. URL http://www.bio-rad.com/webroot/web/pdf/lsr/literature/Bulletin_5279.pdf, (2006) (Date of Access: 15/05/2016)"

73 Soh, T., Koga, O. & Tanaka, K. Research Note: Involvement of ovulation mechanism (s) in the accumulation of pigment in the shell gland of the Japanese quail (Coturnix coturnix japonica). *Poult. Sci.* **68**, 1156-1158 (1989).

74 "IBM Corp. team (2013). IBM SPSS statistics for windows, version 22.0. Armonk, NY, USA. ULR https://www.ibm.com/us-en/marketplace/spss-statistics"

75 "Biogazelle team (2015). qbase+ version 3.0, Belgium. URL https://www.qbaseplus.com/"

76 Hellemans, J., Mortier, G., De Paepe, A., Speleman, F. & Vandesompele, J. qBase relative quantification framework and software for management and automated analysis of real-time quantitative PCR data. *Genome Biol.* **8**, 1 (2007).

77 Vandesompele, J. *et al.* Accurate normalization of real-time quantitative RT-PCR data by geometric averaging of multiple internal control genes. *Genome Biol.* **3**, 1 (2002).

78 Livak, K. J. & Schmittgen, T. D. Analysis of relative gene expression data using real-time quantitative PCR and the $2^{-\Delta\Delta CT}$ method. *Methods* **25**, 402-408 (2001).

79 Hellemans, J. & Vandesompele, J. Quantitative PCR data analysis–unlocking the secret to successful results in *PCR troubleshooting and optimization. The essential guide* 140-141 (Caister Academic Press, 2011).

80 Yin, R. *et al.* Systematic selection of housekeeping genes for gene expression normalization in chicken embryo fibroblasts infected with Newcastle disease virus. *Biochem. Biophys. Res. Commun.* **413**, 537-540 (2011).

81 Yang, F., Lei, X., Rodriguez-Palacios, A., Tang, C. & Yue, H. Selection of reference genes for quantitative real-time PCR analysis in chicken embryo fibroblasts infected with avian leukosis virus subgroup J. *BMC Res. Notes* **6**, 1 (2013).

Higher Degree Research Thesis by Publication
University of New England

STATEMENT OF AUTHORS' CONTRIBUTION

(To appear at the end of each thesis chapter submitted as an article/paper)

We, the Research Master/PhD candidate and the candidate's Principal Supervisor, certify that all co-authors have consented to their work being included in the thesis and they have accepted the candidate's contribution as indicated in the *Statement of Originality*.

	Author's Name (please print clearly)	**% of contribution**
Candidate	**Sami Samiullah**	60
Other Authors	**Juliet Roberts**	15
	Shu-Biao Wu	25

Name of Candidate: **Samiullah**

Name/title of Principal Supervisor: **Associate Professor Juliet Roberts**



Candidate Date 09/06/2017



Principal Supervisor Date 09/06/2017

Higher Degree Research Thesis by Publication
University of New England

STATEMENT OF ORIGINALITY

(To appear at the end of each thesis chapter submitted as an article/paper)

We, the Research Master/PhD candidate and the candidate's Principal Supervisor, certify that the following text, figures and diagrams are the candidate's original work.

Type of work	**Page number/s**
Figure 6.1	151
Figure 6.2	153
Figure 6.3	157
Figure 6.4	167
Figure 6.5	168
Text and tables	147-182

Name of Candidate: **Samiullah**

Name/title of Principal Supervisor: **Associate Professor Juliet Roberts**

[redacted]

Candidate Date 09/06/2017

[redacted]

Principal Supervisor Date 09/06/2017

Chapter 7 Reference gene selection for gene expression study in shell gland and spleen of laying hens challenged with infectious bronchitis virus

Sami Samiullah[1], Juliet Roberts[1], Shu-Biao Wu[1]

[1]Animal Science, School of Environmental and Rural Science, University of New England, Armidale, New South Wales, 2351, Australia

Submitted to: Under revision in Scientific Reports

7.1 Abstract

Ten reference genes were investigated for normalisation of gene expression data in the shell gland and spleen of laying hens challenged with two strains of infectious bronchitis virus (IBV). Data were analysed with geNorm, NormFinder, BestKeeper and ΔCq method and a comprehensive ranking was obtained in RefFinder. In the combined data set of IBV challenged shell gland samples, the comprehensive ranking showed *TBP* and *YWHAZ* as the two most stable, and *SDHA* and *ALB* as the two least stable reference genes. In the spleen, the two most stable and the two least stable reference genes in the combined data set of comprehensive ranking were *TBP* and *YWHAZ*, and *RPL4* and *ALB*, respectively. In the combined data set of the shell gland and spleen, the comprehensive ranking showed *TBP* and *GAPDH* the two most stable genes. The two least stable genes in the same data set were *HMBS* and *ALB*. Slight differences in gene rankings obtained with individual tools were observed. Taken together, the results of the genes analysed with individual software and the comprehensive ranking for the shell gland and spleen tissues suggested *TBP* and *YWHAZ* as suitable reference genes for the normalisation of gene expression data in laying hens. Candidate target genes *CALB1*, *ABCB6*, *IFNγ* and *IL7* were were tested for validation of the choice of reference genes. Validation studies showed that the use of the two most stable reference genes produced accurate and more robust gene expression data. The two most and least stable reference genes were

used for candidate target gene expression data normalisation of the shell gland and spleen under IBV infection model.

7.2 Introduction

The five main segments of hen oviduct are ovary, infundibulum, magnum, isthmus and shell gland (uterus). The isthmus is involved mainly in shell membrane formation. The shell gland is involved in the synthesis and secretion of substances for the formation of distinct layers of the eggshell. During the egg formation cycle, an egg remains for approximately 18-20 hours in the shell gland during which shell formation takes place[1]. Calcium ions for shell formation are secreted from the shell gland cells and the calbindin (*CALB1*) gene plays a primary role in Ca^{2+} transportation[2]. Approximately 437 peptides and ion transporters have been identified as being involved in the formation of the eggshell[3,4].

Infectious bronchitis virus (IBV) is a highly contagious mucosal pathogen of both broiler and layer chickens worldwide[5,6]. IBV replicates in cell cytoplasm and contains an un-segmented single stranded positive sense RNA of 27.6 kbp[7-9]. IBV has a short incubation period[6], and viral spread occurs rapidly among chickens by aerosol and mechanical means[10,11]. IBV has the capability to multiply in various epithelial tissues, such as trachea[12,13], kidney[14], intestine[15,16], spleen[17] and oviduct[16,18-20]. The virus is well known for its effects in laying hens, including egg production and quality drops[10,16,21,22]. In Australia, there are two common forms of this virus, respiratory and nephropathogenic. Both types can induce various degrees of pathological changes in the oviduct of adult laying hens[20]. Genes involved in eggshell formation have been shown to be affected by IBV infection[23]. IBV infection induces a wide range of immune responses in chickens. An innate immune response is activated during the initial stages of infection in the mucosal lining of the trachea following binding of IBV virions to receptors on epithelial cells[24]. Activation of the innate immune response may be initiated by Toll-like receptor (*TLR*) signalling upon IBV recognition[25]. Cellular and local immunity play a critical role in the protection of chicks from IBV infection[26]. Studies have shown that systemic immunisation generally fails to elicit strong mucosal immunity[27,28]. However, all ages are susceptible, with very young chicks exhibiting more severe

respiratory signs and much higher mortality than older birds[29,30]. The spleen is a lymphoid organ that plays an important role in the initiation of the immune response against systemically induced antigens[31] and is among the major organs where T and B cells are localized. In birds, the spleen serves as an important secondary immune organ as lymph nodes are not present[31,32].

Quantifying gene expression in various patho-physiological conditions is a common technique in molecular biology. The two most commonly used methods of performing quantitative gene expression include relative and absolute quantification[33]. In relative quantification, qPCR data of candidate target genes of interest are achieved by including two or more most stably expressed internal control genes as an internal calibrator (reference genes)[34]. Selection of a reliable reference gene under the specific conditions is key to quantitative accuracy. The ideal reference gene should be expressed at a constant level in the tissue regardless of tissue nature, cell type, developmental stage and experimental conditions[34,35]. Traditionally, most commonly used housekeeping genes, such as *ACTB, TUBB* and *GAPDH* have been used widely as generic reference genes. However, ample evidence has shown that the expression of these genes may not be constant across a range of experimental conditions and tissues under investigation[36-38]. Thus, it is now recommended to use housekeeping genes as reference genes for normalisation only when prior analysis of their expression stability has been carried out. It is also recommended that more than one reference gene be used to achieve more robust, accurate and reliable normalisation of gene expression data[34].

The programmes geNorm[34,39], NormFinder[40,41], BestKeeper[42] and ΔCq method[43] have been used to analyse the stability of housekeeping gene expression in sample from various sources. More recently, RefFinder[44,45] has been used for selection of most stable genes on the basis of the comprehensive ranking stability of these genes across the four algorithms used. The underlying principle in each software is slightly different from the others and thus the resulting ranking of genes is not always the same. geNorm in qbase+ module version 3.0 (Biogazelle, Belgium) calculates the gene expression stability (geNorm M) as the arithmetic mean of the pairwise variation (geNorm V) between all tested genes[34,39]. The geNorm V for any given two genes is the standard deviation calculated from the $\log_2$ transformed relative quantities between those two genes[34]. geNorm V shows level of variation

in the average values of reference gene stability with the sequential inclusion of the next stable reference gene to the equation Vn/n+1[34,39]. The analysis starts with the two most stably expressed genes being compared to the pair including the third (V2/3), and the process continues until the least stable gene is added (i.e. V9/10)[39]. To select the most stable single gene, geNorm re-calculates geNorm M after removing the least stable gene and repeats the process until the one most stable gene remains[39]. NormFinder calculates both inter- and intra-group variations and then combines the two to produce a stability value (SD), which thus represents a practical measure of the systemic error introduced when investigating the gene[40,41]. Hence, a low stability value reflects low inter- and intra-group variation[40,41]. Before data analysis in qbase+ and NormFinder, the data are pre-processed for quality control, such as inter-run calibration, amplification efficiency correction, missing data handling, failing replicates (>0.5 Cq difference) removal and conversion to mean relative quantities. An Excel based BestKeeper (Version 1.0) software determines the most stable reference genes based on Pearson correlation coefficient (r), coefficient of variance (CV) and standard deviation[42]. The ΔCq approach bypasses the need to accurately quantify input RNA and instead uses ΔCq comparisons between genes[43]. As BestKeeper and ΔCq calculations are performed in Excel, there is no option in these algorithms to pre-process the data for analyses. A web based comprehensive tool (RefFinder)[45] developed for evaluating and ranking reference genes[44], is used for overall ranking of the reference genes. RefFinder integrates the currently available major computational programmes (geNorm, NormFinder, BestKeeper and ΔCq method) to compare and rank the tested candidate reference genes[44,45]. Based on the rankings from each programme, it assigns an appropriate weight to an individual gene and calculates the geometric mean of their weights for the overall final ranking. The current study investigated the expression stability of ten commonly used reference genes in laying hens infected with IBV T and Vic S strains. Furthermore, different candidate target genes involved in calcium transportation (C*ALB1*) across cell membrane[46] and protoporphyrin synthesis (*ABCB6*)[47] in the shell gland and genes (*IFNγ* and *IL7*) involved in immune system in spleen of laying hens were used for the validation of the reference genes. The outcome of the study provided a set of reference genes that

can be used for gene expression data normalisation in chicken involving the IBV infection model.

7.3 Results

7.3.1 Efficiency and specificity of primers

All primers amplified a single PCR product of the expected size confirmed by Agilent 2100 Bioanalyzer gel (Figure 7.1). The melting curve analysis of all primer pairs further confirmed primer specificity and minimal primer dimers as shown by single peak melting curves for individual genes (Figure 7.2). The amplification efficiency of all ten candidate reference genes was between 94% and 105%. The amplification efficiencies were 101% for *18S rRNA*, 97% for each of *ACTB, HMBS* and *TBP*, 105% for each of *ALB* and *GAPDH*, 100% for *HPRT1*, 93% for *RPL4*, 94% for *SDHA* and 104% for *YWHAZ*. The correlation coefficient (R^2) of all the standard curves performed in 6-point dilutions of RNA, ranged from 0.99253 to 0.99980. The overall expression patterns (Cq values) for these ten reference genes in the shell gland and spleen are shown in Figure 7.3a, b, respectively. In the shell gland, most of the reference genes were highly expressed, with average Cq values between 15 and 21 cycles, except *18S rRNA* and *ALB*, which showed average Cq values around 6 and 26 cycles, respectively (Figure 7.3a). In the spleen, the average Cq values of the genes ranged from 12 to 21 cycles except for *18S rRNA* that showed average Cq values around 4 (Figure 7.3b). Both in the shell gland and in the spleen, the expression pattern of the ten reference genes was calculated in the combined data set of control, IBV T and Vic S strains challenged groups.

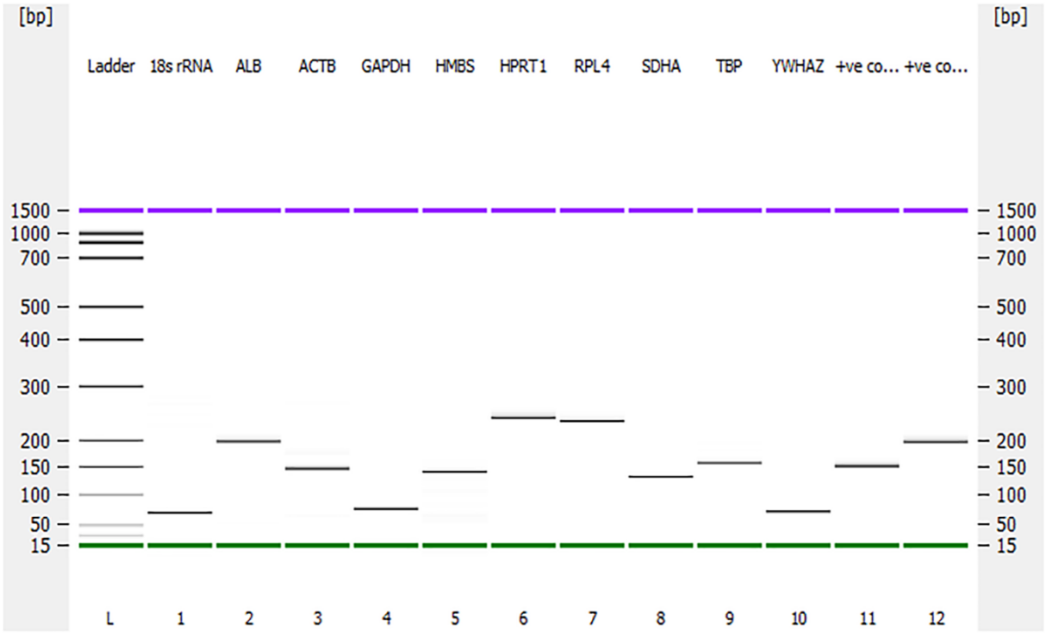

Figure 7.1 Amplification of the genes fragments from the shell gland tissue of chicken to assess the specificities of the primers used in the current study

(**L**) DNA ladder (bp); (**1**) *18S rRNA* (63 bp); (**2**) *ALB* (197 bp); (**3**) *ACTB* (139 bp); (**4**) *GAPDH* (66 bp); (**5**) *HMBS* (131 bp); (**6**) *HPRT1* (245 bp); (**7**) *RPL4* (235 bp); (**8**) *SDHA* (126 bp); (**9**) *TBP* (147 bp); (**10**) *YWHAZ* (61 bp); (**11**) *ND4*-positive control (137 bp); (**12**) *TLR7*-positive control (200 bp). The upper (purple) and lower (green) markers act as internal standards and are used to align the ladder analysis with the individual DNA sample analysis. The standard curve (plotting migration time against DNA amplicon size), in conjunction with the markers, is then used to calculate DNA fragment sizes for each well from the migration times measured (see Agilent 2100 Bioanalyzer Users Guide for Molecular Assays). The DNA gel

in Agilent 2100 Bioanalyzer was performed as per manufacturer's instructions of Agilent DNA 1000 Kit.

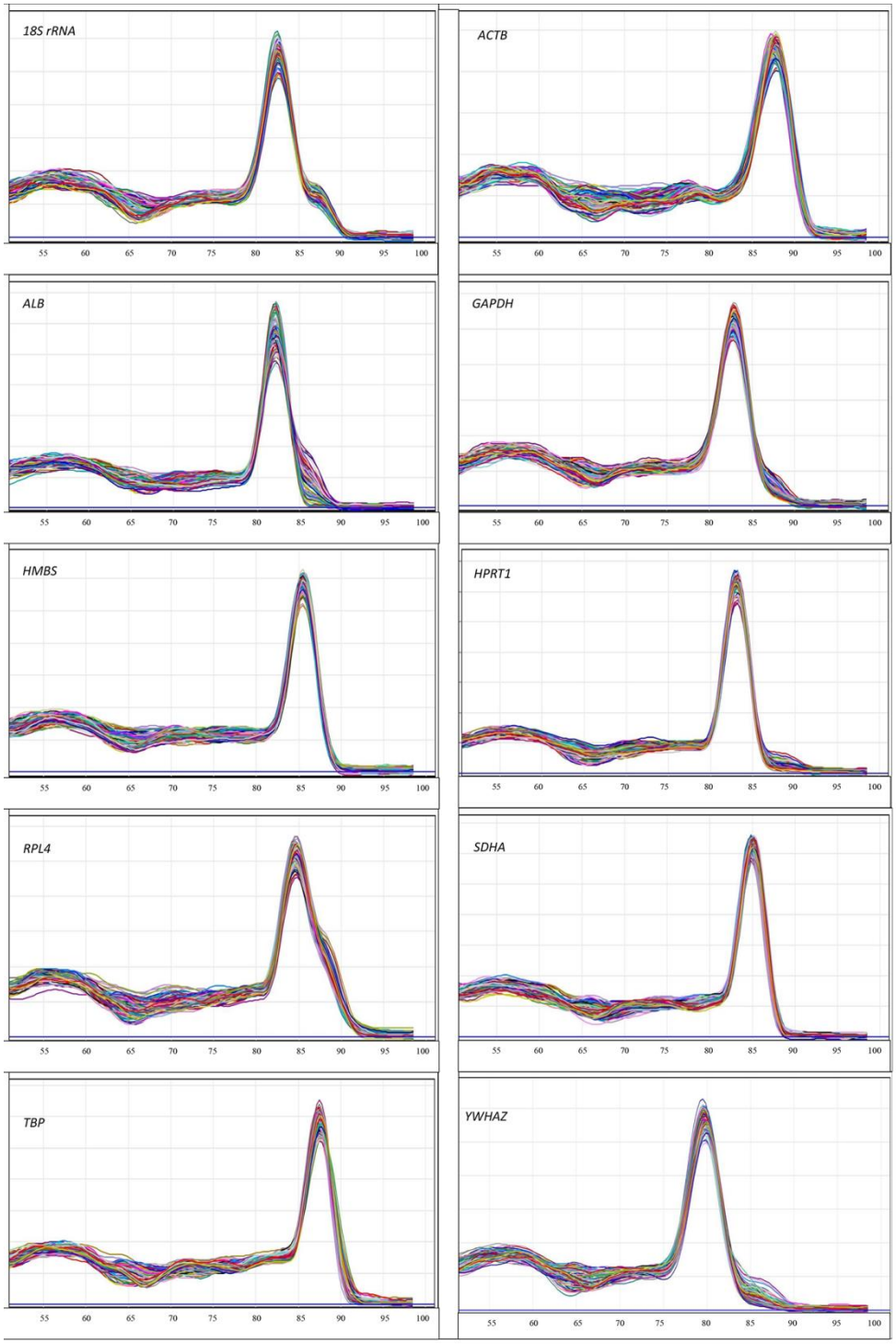

Figure 7.2 Melting curves of 10 reference genes in the shell gland samples

All melting curves showing a single peak indicated that all primers were specific in amplifying fragments of the genes and chances for primer dimers were minimum in the qPCR products. A melting phase at a ramp from 50°C to 99°C at 1°C increments in Rotor-Gene Q was performed to assess the specificity of PCR amplification.

7.3.2 Reference gene expression stability in shell gland and spleen

In the shell gland, in the combined data set of control, IBV T and Vic S strain challenge groups, the two most stable reference genes in geNorm, NormFinder, ΔCq method and RefFinder were *TBP* and *YWHAZ* (Table 7.1). In the same data set, BestKeeper ranked *HMBS* and *RPL4* as the two most stable genes. Despite slight variations in gene ranking in different software, the average expression stabilities (geNorm M) of the ten reference genes in the combined data set were within the acceptable range (<0.50) and varied from 0.159 (*YWHAZ*) to 0.373 (*ALB*) (Table 7.1). The two least stable genes across all the software except BestKeeper and RefFinder were *ACTB* and *ALB* (Table 7.1). The pairwise variation (geNorm V) recommended *TBP* and *YWHAZ* as the best set of genes with geNorm V (V2/3) value as 0.048 (Figure 7.3c). A geNorm V value <0.2 for the combination of first two genes showed that there was no need to combine the third gene to be used as set of reference genes for expression data analysis.

In the spleen, with the combined data set of control, IBV T and Vic S strain challenge groups, the two most stable genes were *TBP* and *YWHAZ* with slight variations in the ranking obtained in NormFinder and ΔCq method (Table 7.1). The two least stable genes across all the statistical software were *RPL4* and *ALB* (Table 7.1). The pairwise variation recommended *TBP* and *YWHAZ* as the two most stable genes with geNorm V value as 0.089 (Figure 7.3c). Based on the data combined from the shell gland and spleen, *TBP* and *YWHAZ* were ranked as the two most stable genes in geNorm, BestKeeper and RefFinder. In the same data set, NormFinder ranked *ACTB* and *HPRT1*, and ΔCq method ranked *GAPDH* and *HPRT1* as the two most stable genes. The two least stable genes varied in different software (Table 7.1). The pairwise variation recommended *TBP* and *YWHAZ* as the two most stable genes with geNorm V value as 0.05 (Figure 7.3c).

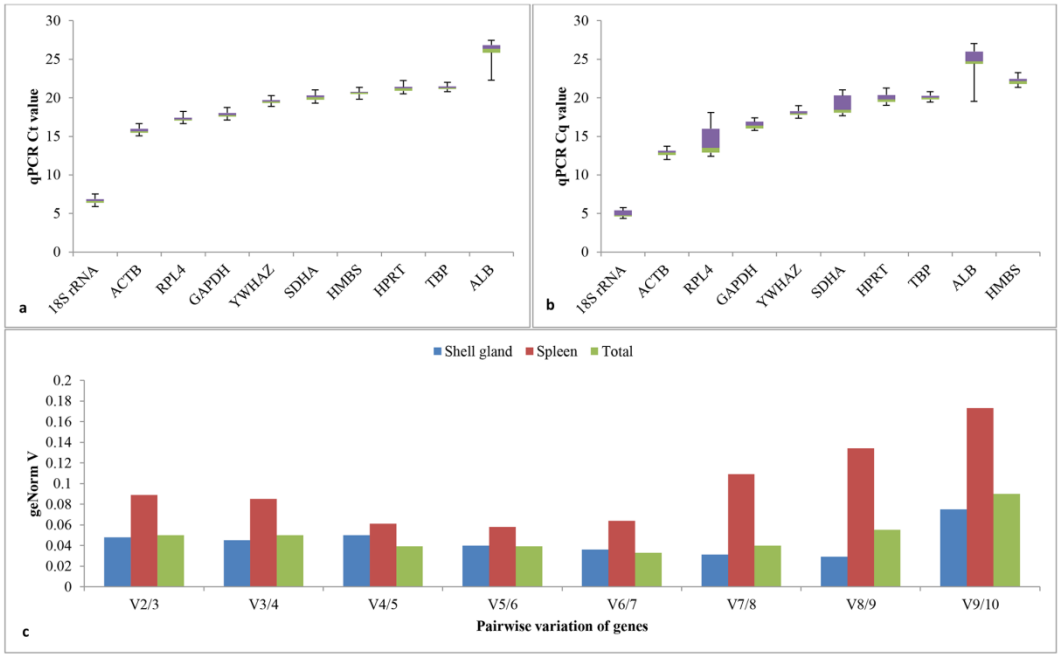

Figure 7.3 Effect of IBV challenge on the expression stability of 10 reference genes in the shell gland and spleen

(**a**) Mean Cq values of the control, IBV T and Vic S strains challenged groups in the shell gland. A square across the box is depicted as the median. The box indicates the 25th and 75th percentiles and the whiskers caps represent the maximum and minimum values. (**b**) Mean Cq values of the control, IBV T and Vic S strains challenged groups in the spleen. A square across the box is depicted as the median. The box indicates the 25th and 75th percentiles and the whiskers caps represent the maximum and minimum values. (**c**) Pairwise variation (geNorm V) of genes in the shell gland (control, IBV T and Vic S strains challenge groups together), in the spleen (control, IBV T and Vic S strains challenge groups together) and in the combined data set of the shell gland and spleen. In qbase+ software, geNorm V was calculated as standard deviation of the $\log_2$ transformed relative quantities between those two genes. The geNorm V analysis started with the two most stably expressed genes being compared to the pair including the third (V2/3), and the process continued until the least stable gene was added (i.e. V9/10).

Group	Rank	geNorm		NormFinder		BestKeeper		ΔCq method		RefFinder	
		Gene	M value	Gene	SD	Gene	SD	Gene	SD	Gene	Geomean
Shell gland	1	*YWHAZ*	0.159	*TBP*	0.071	*HMBS*	0.156	*TBP*	0.294	*TBP*	1.32
	2	*TBP*	0.161	*YWHAZ*	0.111	*RPL4*	0.176	*YWHAZ*	0.313	*YWHAZ*	3.25
	3	*18S*	0.162	*RPL4*	0.115	*TBP*	0.179	18S	0.325	*HMBS*	3.46
	4	*HPRT1*	0.180	*HMBS*	0.118	*ACTB*	0.207	*RPL4*	0.335	*RPL4*	3.56
	5	*RPL4*	0.216	18S	0.133	*GAPDH*	0.211	*HPRT1*	0.344	*HPRT1*	3.66
	6	*GAPDH*	0.235	*GAPDH*	0.154	*HPRT1*	0.216	*HMBS*	0.349	18S	4.49
	7	*SDHA*	0.250	*HPRT1*	0.166	*YWHAZ*	0.224	*GAPDH*	0.353	*GAPDH*	6.19
	8	*HMBS*	0.262	*SDHA*	0.166	*18S*	0.242	*SDHA*	0.373	*ACTB*	7.14
	9	*ACTB*	0.274	*ACTB*	0.186	*SDHA*	0.246	*ACTB*	0.379	*SDHA*	7.97
	10	*ALB*	0.373	*ALB*	0.787	*ALB*	0.537	*ALB*	0.779	*ALB*	10.0
Spleen	1	*TBP*	0.233	*HMBS*	0.088	*YWHAZ*	0.227	*HMBS*	0.669	*TBP*	1.50
	2	*YWHAZ*	0.248	*ACTB*	0.088	*TBP*	0.256	*GAPDH*	0.676	*YWHAZ*	2.74
	3	*ACTB*	0.260	*GAPDH*	0.190	*ACTB*	0.279	*ACTB*	0.679	*GAPDH*	3.22
	4	*HMBS*	0.312	*TBP*	0.246	18S	0.304	*HPRT1*	0.686	*ACTB*	3.46
	5	*GAPDH*	0.331	*HPRT1*	0.252	*HMBS*	0.406	*YWHAZ*	0.765	*HPRT1*	3.83
	6	*HPRT1*	0.352	*YWHAZ*	0.364	*GAPDH*	0.417	*TBP*	0.863	*HMBS*	3.98
	7	*18S*	0.390	18S	0.441	*HPRT1*	0.517	18S	0.870	18S	6.09
	8	*SDHA*	0.516	*SDHA*	0.457	*SDHA*	1.049	*SDHA*	0.988	*SDHA*	8.00
	9	*RPL4*	0.673	*RPL4*	0.694	*ALB*	1.218	*RPL4*	1.365	*RPL4*	9.24
	10	*ALB*	0.900	*ALB*	7.130	*RPL4*	1.442	*ALB*	1.833	*ALB*	9.74
All together (shell gland and spleen)	1	*TBP*	0.154	*ACTB*	0.450	*YWHAZ*	0.557	*GAPDH*	0.842	*TBP*	1.57
	2	*YWHAZ*	0.159	*HPRT1*	0.944	*TBP*	0.623	*HPRT1*	0.844	*YWHAZ*	2.28
	3	*GAPDH*	0.161	*YWHAZ*	1.017	*GAPDH*	0.630	*TBP*	0.857	*HPRT1*	2.83
	4	*ACTB*	0.191	*SDHA*	1.027	*HPRT1*	0.720	*YWHAZ*	0.883	*GAPDH*	2.99
	5	*HMBS*	0.203	*GAPDH*	1.076	18S	0.746	*SDHA*	0.988	18S	4.74
	6	*18S*	0.217	*TBP*	1.105	*HMBS*	0.757	*ACTB*	1.230	*SDHA*	5.44
	7	*HPRT1*	0.231	*RPL4*	1.725	*SDHA*	0.856	*RPL4*	1.458	*ACTB*	6.64
	8	*SDHA*	0.261	*HMBS*	2.300	*RPL4*	1.286	18S	1.460	*RPL4*	7.91
	9	*RPL4*	0.317	18S	3.020	*ACTB*	1.483	*HMBS*	1.516	*HMBS*	8.49
	10	*ALB*	0.439	*ALB*	9.984	*ALB*	1.742	*ALB*	1.618	*ALB*	8.80

Table 7.1 Overall stability values of reference genes in the combined data set of shell gland and spleen affected by IBV T and Vic S strain challenge

The Cq values were analysed in geNorm, NormFinder, BestKeeper and ΔCq and a comprehensive ranking was obtained in RefFinder.

7.3.3 Reference gene validation in shell gland and spleen

The relative expression levels of candidate target genes *CALB1* and *ABCB6* in the shell gland of laying hens challenged with IBV T strain were analysed with the two most stable (*TBP*, *YWHAZ*) and the two least stable reference genes (*SDHA*, *ALB*), according to the comprehensive ranking (RefFinder) applied in the study. The relative expression levels of *CALB1*, normalized with each of the two most stable and the least stable genes, were not different from each other (Figure 7.4a, b). However, the P values showed variation when the expression level of *CALB1* was normalised with the two most and two least stable genes. The expression level of *ABCB6* was significantly affected when the data were normalized with the two least stable reference genes (Figure 7.4c, d). The normalisation with the two least stable reference genes led to erroneous interpretation of the data and the level of significance was changed from P=0.0152 to P=0.0713. In the spleen, the relative expression levels of *IFNγ* and *IL7* were analysed with the two most stable (*TBP*, *YWHAZ*) and the two least stable reference genes (*RPL4*, *ALB*). The relative expression levels of *IFNγ* were quite different from each other and the level of significance (P value increased) decreased between the control and IBV T groups by applying the two least stable reference genes for normalisation (Figure 7.4e, f). The relative expression levels of *IL7* normalised with the two most stable genes were significantly different between the IBV T and control groups, while the expression level of *IL7* became non-significant when the two least stable genes were used for normalisation (Figure 7.4g, h).

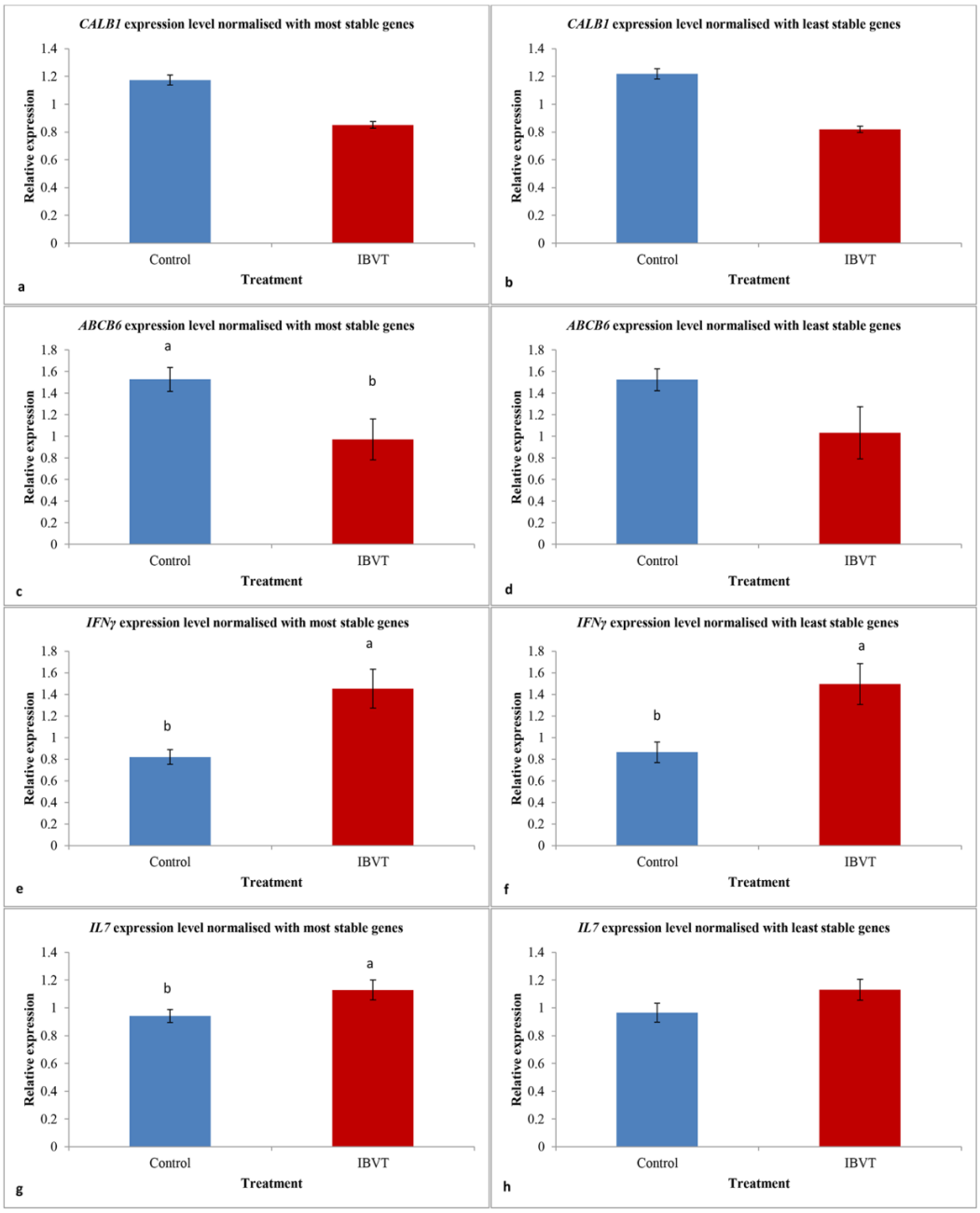

Figure 7.4 Relative expression levels of the candidate target genes affected by IBV T challenge in the shell gland and spleen of laying hens

(**a**) *CALB1* expression level in the shell gland normalized with the most stable genes *YWHAZ* and *TBP* (P=0.6783). (**b**) *CALB1* expression level in the shell gland normalized with the least stable genes *SDHA* and *ALB* (P=0.7788). (**c**) *ABCB6* expression level in the shell gland normalized with the most stable genes *YWHAZ* and *TBP* (P=0.0152). (**d**) *ABCB6* expression level in the shell gland normalized with the least stable genes *SDHA* and *ALB* (P=0.0713). (**e**) *IFNγ* expression level in the spleen normalized with the most stable genes *YWHAZ* and *TBP* (P=0.0021). (**f**) *IFNγ* expression level in the spleen normalized with the least stable

genes *RPL4* and *ALB* (P=0.0050). (**g**) *IL7* expression level in the spleen normalized with the most stable genes *YWHAZ* and *TBP* (P=0.0333). (**h**) IL7 expression level in the spleen normalized with the least stable genes *RPL4* and *ALB* (P=0.1130). Values are relative expression quantities. Error bars show standard error. Across the treatment, [a,b] show significant difference (P < 0.05). For the candidate target genes, normalised relative quantities (NRQ) were calculated in qbase+ based on ($2^{\wedge -\Delta\Delta Cq}$) approach with gene amplification specific efficiencies to show the relative expression of Cq levels in folds to the mean Cq of all samples of the genes. NRQ values were further analysed in Statview software (SAS) and Tukey-Kramer test was used to differentiate level of significance (P < 0.05) between means.

7.4 Discussion

We investigated the stability of ten reference genes in the shell gland region of the oviduct in laying hens when the egg was in the isthmus (5 hr postoviposition time-point) region of oviduct in IBV T and Vic S strains challenged groups. The same set of genes was also investigated in spleen under the same IBV model. The current study provides information on the expression stability of these candidate reference genes and most stably expressed reference genes are suggested for the normalisation of gene expression data in the chicken shell gland and spleen in infectious bronchitis study models. In our previous study, *HPRT1* and *HMBS* were chosen as the two most stable reference genes in relation to three or four time-points of eggshell formation and nicarbazin challenge (to be published). In the current study, the *HMBS* and *HPRT1* fell in the middle of the ranking order among the 10 reference genes ranked with the combination of data from both the shell gland and spleen. This study suggests that *YWHAZ* and *TBP* express more stably in the shell gland and spleen of laying hens compared with *HPRT1* and *HMBS*. As a general guideline, with geNorm ranking, it is stated that the benefit of using an extra $(n+1)^{th}$ reference gene is limited as soon as the Vn/n+1 value drops below the 0.15 threshold. Therefore, in the current study, the geNorm V for the two most stably expressed genes was <0.5 and adding the third most stable gene for expression data normalisation was not necessary. In gene expression studies performed on different tissues of chicken, *TBP*, *HPRT1* and *HMBS* have been reported to be among the

most stable genes[48-50]. *RPL13* and *TBP* were ranked to be the most stable reference genes in chickens and turkeys infected with *Histomonas meleagridis* and fowl aviadenovirus[51]. However, in many other avian studies, differences in the stability of genes between the control and infected, among multiple avian species and between different tissues of the same species, were observed[48,51,52]. Similarly, in non-avian species, differences in the stability of reference genes raking in different tissues of the same species or organ developmental stages have been established[53-56]. Nevertheless, in the current study, the overall higher stability of *YWHAZ* and *TBP* across most of the software in the combination of different data sets indicated that these two genes can be used as reference genes for the normalisation of expression data in laying hen in IBV infection models. In the current study, in the combined data set of the shell gland samples, all ten reference genes were in the acceptable range as stable reference genes with geNorm M value <0.5 and SD <1.0. In the spleen samples, all genes but *SDHA*, *RPL4* and *ALB* showed SD <1.0. This demonstrated that most of the genes analysed had relatively high stability both in the shell gland and spleen tissues in response to IBV challenge. A better stability value of *ACTB* in the spleen might indicate that this gene is more stable in spleen than in shell gland tissue. Recently, *ALB* and *ACTB* have been shown to be the least stable reference gene in various tissues of wild duck challenged with low pathogenic avian influenza A virus[57]. Similarly, *ACTB* has been reported as an unsuitable reference gene in *in vitro* studies of primary mouse fibroblasts treated with tumour extract[58]. In different vertebrate species, different reference genes under different treatments have been validated in the reproductive system. *GAPDH* and *HPRT1* were ranked as the two most stable reference genes in the ovary of geese[59]. In bovines, the two most stable reference genes in the uterus were *GAPDH* and *YWHAZ*[60]. In the ovary of a mouse, under various toxicological treatments, the two most stable reference genes were *GAPDH* and *RPL13a*[61]. *GAPDH* is involved in the glycolytic pathway and its expression depends on tissue type[62,63] and certain conditions, such as deprivation of glucose and stress induction[64]. Recently, *GAPDH* was found the least stable gene in the inguinal white adipose tissue and skeletal muscle of caloric restricted mice[56]. In the current study, both in the shell gland and spleen, the *GAPDH* ranking was in the middle order across most of the statistical tools. Thus, it is recommended not to use *GAPDH* as a reference gene for expression

data normalisation until it has been tested under the prevailing experimental conditions, as MIQE guidelines recommend that the validation of reference genes should be performed before their use in expression data normalisation[65].

The present study has demonstrated that the rankings of the expression stability of 10 candidate reference genes had similar trends but discrepancies were observed among different statistical programmes used. Differences in gene ranking were also observed between shell gland and spleen. Similar discrepancies have been observed in our previous study (to be published) and elsewhere with different species and treatments[50,59,66]. With different algorithms in different programs, slight change of gene stability orders can be expected by the analyses using these programs. Furthermore, the reference gene validation with the two most stable and two least stable genes showed that the least stable genes significantly affect the outcome of expression data normalisation and may lead to erroneous interpretation of such data.

In summary, we have performed optimisation of reference genes in samples collected from the shell gland and spleen tissues in IBV challenged laying hens. Two most stably expressed genes, *YWHAZ* and *TBP* have been chosen for the normalisation of gene expression data in the shell gland and spleen of chickens under IBV infection models in poultry and other avian species. The validation study has confirmed that the use of these two genes as reference genes led to discrimination between the expression levels of two candidate target genes upon different treatments, while the use of two least stable candidate reference genes may lead to incorrect interpretation of data.

7.5 Methods

7.5.1 Ethics statement

The experimental setup was approved by the University of New England, Animal Ethics Approval Committee under Authority No. AEC15-118. The protocol was carried out in accordance with the guidelines specified in Australian Code for the Care and Use of Animals for Scientific Purposes 8th edition 2013.

7.5.2 Rearing of IBV free laying hens and virus challenge

Day old Isa-Brown laying chickens were obtained from the Baiada Hatchery at Tamworth, NSW, Australia. At day-old, all the chickens received vaccine (Rispens) against Marek's disease at the hatchery but were not vaccinated against infectious bronchitis (IB). The chickens were raised in isolation sheds at the University of New England under a strict biosecurity system. All chickens were fed commercial starter mash up to 4 weeks of age, pullet grower to 18 weeks of age and layer mash until the termination of the experiment. Pullets were moved from the isolation sheds at 18 weeks of age to individual cages in an isolated poultry house. There was no morbidity or mortality from the rearing period until challenge by IBV T and Vic S strains. Before challenge, an ELISA was performed to confirm that all birds were negative for IBV antibody titre in the blood. At 35 weeks of age, eggs were collected and processed for traditional egg quality measurements. Hens were divided into 2×3 factorial design (Table 7.2) in such a way that the egg weight and eggshell colour (L*) were not significantly different among the groups. The hens selected for IBV T and Vic S strain challenge were moved to a separate poultry house one week prior to challenge in order to settle down and recover from the trans-location stress. From the control hens, eggs were analysed until the hens were euthanised for shell gland and spleen tissues collection. At the time of euthanasia, the egg in individual hens was in the distal magnum/isthmus (5 hr post-oviposition time). At this oviposition time, the egg is getting ready to enter to shell gland tissue and thus it is assumed that the secretory activities in the shell gland will be commencing. From the challenged hens, eggs were analysed for 2 days prior to challenge and daily collection of eggs for analysis continued until individual hens were euthanised. In the challenged groups, 5 hens from each group at a time were intra-occularly inoculated with 10^7 embryo infective dose (EID_{50}) and closely monitored for the development of clinical signs of IB and loss in eggshell colour until days 9-10 post-infection (p.i.). The EID_{50} dose was determined in embryonated SPF eggs infected at 9 days of incubation with 10-times serial dilutions (10^{-3} to 10^{-8} dilutions) of IBV T strain. Eggs were opened at 16 days of incubation and the number of live, dead or virus affected (dwarfed, curled) embryos recorded. The 10^7 EID_{50} dose for IBV Vic S strain was calculated from the dose on

the vial of commercial freeze-dried vaccine (Poulvac Bron Vic S, Zoetis Australia). The infection in challenged birds was confirmed through RT-qPCR (shell gland and spleen tissues) and ELISA (ELISA kit, IDEXX Laboratories, Inc., Westbrook, MA, USA).

Variable	No. of hens (n=10)	Shell gland	Spleen
Control	+	+	+
IBV T challenge	+	+	+
IBV Vic S challenge	+	+	+

Table 7.2 Grouping of laying hens for tissues collection for reference genes study

The control group was the same for both the IBV T and Vic S strains challenge groups.

7.5.3 Selection of primers sequence and validation

In the current study, all ten reference genes were selected from the literature published for chickens (Table 7.3). Specific amplifications of the primers were assessed by generation of a single peak of melting curve using uMelt web based tool for predicting DNA melting curves and denaturation profiles of PCR products[67]. Furthermore, primer specificity was confirmed by obtaining a single band of appropriate size in Agilent 2100 Bioanalyzer using Agilent DNA 1000 kit per manufacturer's instructions. PCR amplification efficiencies and correlation coefficients (R^2) were determined with the amplifications of a series of six 10-fold dilutions based on the following equation[68-71]; $E = (10 - ^{(\frac{1}{-slope})} - 1) \times 100$

The qPCR was performed on the reference genes when the PCR amplification efficiency was in a range of 93 to 105%, and linear correlation coefficient $R^2 >$ 0.980 were considered of high standard[65,70].

Gene name	**Gene symbol**	**Primer sequence (5′-3′)**	**Amplicon size (bp)**	**Ta °C**	**PCR efficiency (%)**	**R^2**	**Slope**	**Accession No.**	**Reference**
Nuclear ribosomal RNA small subunit	*18S rRNA*	F: TGTGCCGCTAGAGGTGAAATT R: TGGCAAATGCTTTCGCTTT	63	60	101	0.99873	-3.288	AF173612.1	Kuchipudi *et al.*, 2014[72]
β-actin	*ACTB*	F: CTGTGCCCATCTATGAAGGCTA R: ATTTCTCTCTCGGCTGTGGTG	139	60	97	0.99980	-3.387	NM_205518.1	Yang *et al.*, 2013[73]
Albumin	*ALB*	F: CCTGGACACCAAGGAAAT R: TGTGGACGCCGATAGAAT	197	60	105	0.99253	-3.009	NM_205261.2	Yang *et al.*, 2013[73]
Glyceraldehyde 3-phosphate dehydrogenase	*GAPDH*	F: GAAGCTTACTGGAATGGCTTTCC R: CGGCAGGTCAGGTCAACAA	66	60	105	0.99874	-3.217	NM_204305.1	Kuchipudi et al., 2012[74]
Hydroxymethylbilane synthase	*HMBS*	F: GGCTGGGAGAATCGCATAGG R: TCCTGCAGGGCAGATACCAT	131	60	97	0.99953	-3.397	XM_417846.2	Yin *et al.*, 2011[75]
Hypoxanthine Phosphoribosyltransferase	*HPRT1*	F: ACTGGCTGCTTCTTGTG R: GGTTGGGTTGTGCTGTT	245	63	100	0.99870	-3.322	NM_204848.1	Yang et al., 2013[73]
Ribosomal protein L4	*RPL4*	F: TTATGCCATCTGTTCTGCC R: GCGATTCCTCATCTTACCCT	235	60	93	0.99785	-3.502	NM_001007479.1	Yang *et al.*, 2013[73]
Succinate dehydrogenase complex flavoprotein subunit A	*SDHA*	F: TCTGTCCATGGTGCTAATCG R: TGGTTTAATGGAGGGGACTG	126	60	94	0.99790	-3.484	NM_001277398.1	Bages et al., 2015[48]
TATA-Box Binding Protein	*TBP*	F: TAGCCCGATGATGCCGTAT R: GTTCCCTGTGTCGCTTGC	147	61	97	0.99676	-3.407	NM_205103	Li et al., 2005[76]
Tyrosine 3-monooxygenase/tryptophan 5-monooxygenase activation protein, zeta polypeptide	*YWHAZ*	F- TTGCTGCTGGAGATGACAAG R- CTTCTTGATACGCCTGTTG	61	60	104	0.99912	-3.222	NM_001031343.1	Bages et al., 2015[48]
Calbindin 1	C*ALB1*	F: TTGGCACTGAAATCCCACTGA R: CATGCCAAGACCAAGGCTGA	116	60	100	0.99873	-3.322	NM_205513.1	Qi et al., 2016[77]
ATP binding cassette subfamily C member 6	*ABCB6*	F: CTCAACTGGTTCGGCACCTA R: TTCACTGCATCCTTCACCTCC	107	60	105	0.99761	-3.150	XM_015290086.1	this study
Interferon gamma	*IFNγ*	F-GTGAAGAAGGTGAAAGATATCATGGA R- GCTTTGCGCTGGATTCTCA	71	60	99	0.99878	-3.180	NM_205149.1	this study
Interleukin 7	IL7	F- GGTTCTGCCACTTCTCCTTG R- CTTGCAGCATCTGTCACGATA	160	60	103	0.99554	-3.255	NM_001037833.1	this study

Table 7.3 Candidate reference and target genes in expression studies by qPCR in the shell gland and spleen of laying hens challenged with infectious bronchitis virus T and Vic S strains

For calculating amplification efficiency, a standard curve was generated using a 10-fold dilution of RNA amplified on the Rotor-Gene Q thermocycler real-time system. Standard curve was obtained by plotting the Cq values against the log of the starting quantity of template for each dilution.

7.5.4 Tissue collection for RNA extraction

Hens were humanley euthanised with CO_2 gas and the shell gland was aseptically retracted through the abdominal incision. The shell gland was opened from the anterior-ventral side and an approximately 500 mg sample tissue was cut from the centre of the shell gland and directly transferred to RNALater (Sigma Aldrich, Australia) in 2 mL Eppendorf tubes. The samples were stored at -20°C and were processed for total RNA extraction within one day of collection. At the same time of shell gland tissue collection, an approximately 500 mg sample of spleen was cut in such a way that it contained both red and white pulp and was directly transferred into RNALater and processed as described earlier.

7.5.5 Total RNA extraction and purification

Total RNA was extracted using TRIsure (Bioline, Australia), according to the manufacturer's instructions. Briefly, an approximately 100 mg of tissue (wet weight) was homogenized in 1 mL of TRIsure using an IKA T10 basic Homogenizer (Wilmington, NC, USA). After the RNA pellets were washed with 1 mL ethanol (75%), 50 µL of UltraPure™ DEPC-Treated water (Ambion, USA) was used to dissolve RNA pellets. The total RNA was further purified using RNeasy Mini Kit (Qiagen, GmbH, Hilden, Germany) as per the manufacturer's instructions. A DNase-I step was included to get rid of the genomic DNA. The elution of RNA from the spin column with 50 µL of RNase-free water was repeated twice and the eluted RNA solutions were mixed thoroughly. The purified RNA was analysed in a NANODROP-8000 spectrophotometer (ThermoFisher Scientific, Wilmington, DE, USA) to measure its quantity and purity. RNA integrity and purity were also examined in Agilent 2100 Bioanalyzer (Agilent Technologies, Waldbronn, Germany) using Agilent RNA 6000 Nano Kit as per the manufacturer's instructions. All the RNA showed distinct 18S and 28S bands with an average RNA integrity number (RIN) >9.1.

7.5.6 Quantitative PCR

qPCR was performed with the SensiFAST SYBR® Lo-ROX One-Step RT-PCR Kit (Bioline, Australia). Master mix was prepared as per manufacturer's protocol and 4 µL of RNA template from 1:100 dilutions was added to the reaction wells using QIAgility robotic (Qiagen, Australia). The reaction was run in triplicates of 20 µL in a Gene Rotor Disc 100 (Qiagen, Australia) with a Rotor-Gene Q thermocycler (Qiagen, Australia). No template control (NTC) and no reverse transcriptase (-RT) control were also included to detect possible contamination. Thermocycling conditions for a 2-step PCR were: reverse transcription at 45°C for 10 minutes, first denaturation at 95°C for 2 minutes, then 40 cycles of denaturation at 95°C for 5s and annealing at 60°C, 61°C or 63°C for 20s.The fluorescent data were acquired at the end of each annealing step during PCR cycles. A melting step was conducted to assess the specificity of PCR amplification. The qPCR products were examined in the Bioanalyzer using Agilent DNA 1000 Kit to determine the amplification specificity by the size of the amplicons estimated.

7.6 Statistical analysis

The geNorm module in qbase+ software (version 3.0) was used to calculate the gene expression stability measure (geNorm M)[34,39]. The input data for qbase+ were generated using the relative quantities based on comparative quantification cycle (Cq). In addition, the raw Cq values were analysed in NormFinder (GenEx version 6.0.1)[40,41] for reference gene expression stabilities. NormFinder calculates the standard deviation (SD) of the genes relative to the mean expression of all the genes in the panel. An Excel based BestKeeper (Version 1.0) software was used to determine the most stable reference genes based on Pearson correlation coefficient (r), coefficient of variance (CV) and standard deviation[42]. A ΔCq method was used to compare the ranking of 10 reference genes by calculating the mean SD of individual gene from all the genes in the panel[43]. The overall ranking of the 10 reference genes was obtained in the RefFinder online tool[44,45]. The principles of individual software (algorithms) have been detailed in the introduction section.

For reference gene validation, relative expression levels of candidate target genes *CALB1*, *ABCB6*, *IFNγ* and *IL7* genes were calculated by the comparative $2^{-\Delta\Delta Cq}$ approach[68,78] in qbase+ software (version 3.0)[39], using the two most stable (*YWHAZ* and *TBP*) and the two least (*ALB* and *SDHA*/*RPL4*) stable reference genes. From the qbase+, normalized relative quantities (NRQ) values were further analysed with One-way ANOVA in Statview Version 5.0.1.0 (SAS Institute Inc., 1998) and Tukey-Kramer test was used to differentiate level of significance ($P < 0.05$) between means.

7.7 Acknowledgements

This study was funded by Australian Egg Corporation Limited, Australia under grant number AECL 1UN121.

7.8 Authors' contributions

S.S. developed the hypotheses, designed and performed the experiments, analysed and interpreted data, and drafted the manuscript; J.R. oversaw the animal trials, administrated the overall research project, assisted with the experiments, analysis and interpretation of data and critically revised the manuscript; S-B.W. designed gene expression experiments, analysed and interpreted the data, and drafted the manuscript.

7.9 Competing interests

The authors declare that they have no competing interests.

7.10 Competing financial interests

The authors declare no competing financial interests.

7.11 References

1 Nys, Y. Relationships between age, shell quality and individual rate and duration of shell formation in domestic hens. *Br. Poult. Sci.* **27**, 253-259 (1986).

2 Bar, A. Calcium transport in strongly calcifying laying birds: mechanisms and regulation. *Comp. Biochem. Physiol. A Mol. Integr. Physiol.* **152**, 447-469 (2009).

3 Liu, Z., Zheng, Q., Zhang, X. & Lu, L. Microarray analysis of genes involved with shell strength in layer shell gland at the early stage of active calcification. *Asian-Australas. J. Anim. Sci.* **26**, 609-624 (2013).

4 Jonchère, V. *et al.* Gene expression profiling to identify eggshell proteins involved in physical defense of the chicken egg. *BMC Genomics* **11**, 57 (2010).

5 Cavanagh, D., Mawditt, K., Britton, P. & Naylor, C. J. Longitudinal field studies of infectious bronchitis virus and avian pneumovirus in broilers using type-specific polymerase chain reactions. *Avian Pathol.* **28**, 593-605 (1999).

6 Jackwood, M. W. & de Wit, S. Infectious bronchitis in *Diseases of Poultry* (ed David E. Swayne) 139-160 (2013).

7 Boursnell, M. E. G. *et al.* Completion of the sequence of the genome of the coronavirus avian infectious bronchitis virus. *J. Gen. Virol.* **68**, 57-77 (1987).

8 Boursnell, M. E. G., Binns, M. M., Brown, T. D. K., Cavanagh, D. & Tomley, F. M. Molecular biology of avian infectious bronchitis virus. *Prog. Vet. Microbiol. Immunol.* **5**, 65-82 (1989).

9 Cavanagh, D. Coronavirus avian infectious bronchitis virus. *Vet. Res.* **38**, 281-297 (2007).

10 Sevoian, M. & Levine, P. P. Effects of infectious bronchitis on the reproductive tracts, egg production, and egg quality of laying chickens. *Avian Dis.* **1**, 136-164 (1957).

11 Chhabra, R., Chantrey, J. & Ganapathy, K. Immune responses to virulent and vaccine strains of infectious bronchitis viruses in chickens. *Viral Immunol.* **28**, 478-488 (2015).

12 Liu, S. *et al.* Identification of a newly isolated avian infectious bronchitis coronavirus variant in China exhibiting affinity for the respiratory tract. *Avian Dis.* **52**, 306-314 (2008).

13 Cook, J. K. A., Darbyshire, J. H. & Peters, R. W. The use of chicken tracheal organ cultures for the isolation and assay of avian infectious bronchitis virus. *Arch. Virol.* **50**, 109-118 (1976).

14 Ghetas, A. M., Thaxton, G. E., Breedlove, C., van Santen, V. L. & Toro, H. Effects of adaptation of infectious bronchitis virus Arkansas attenuated vaccine to embryonic kidney cells. *Avian Dis.* **59**, 106-113 (2014).

15 Bhattacharjee, P. S. & Jones, R. C. Susceptibility of organ cultures from chicken tissues for strains of infectious bronchitis virus isolated from the intestine. *Avian Pathol.* **26**, 553-563 (1997).

16 Maiti, N. K., Sharma, S. N. & Sambyal, D. S. Isolation of infectious bronchitis virus from intestine and reproductive organs of laying hens with dropped egg production. *Avian Dis.* **29**, 509-513 (1985).

17 Hamzić, E. *et al.* RNA sequencing-based analysis of the spleen transcriptome following infectious bronchitis virus infection of chickens selected for different mannose-binding lectin serum concentrations. *BMC Genomics* **17**, 82 (2016).

18 Raj, G. D. & Jones, R. C. An *in vitro* comparison of the virulence of seven strains of infectious bronchitis virus using tracheal and oviduct organ cultures. *Avian Pathol.* **25**, 649-662 (1996).

19 Chousalkar, K. K. & Roberts, J. R. Ultrastructural study of infectious bronchitis virus infection in infundibulum and magnum of commercial laying hens. *Vet. Microbiol.* **122**, 223-236 (2007).

20 Chousalkar, K. K. & Roberts, J. R. Ultrastructural observations on effects of infectious bronchitis virus in eggshell-forming regions of the oviduct of the commercial laying hen. *Poult. Sci.* **86**, 1915-1919 (2007).

21 Cook, J. K. A. The classification of new serotypes of infectious bronchitis virus isolated from poultry flocks in Britain between 1981 and 1983. *Avian Pathol.* **13**, 733-741 (1984).

22 Crinion, R. A. P., Ball, R. A. & Hofstad, M. S. Abnormalities in laying chickens following exposure to infectious bronchitis virus at one day old. *Avian Dis.* **15**, 42-48 (1971).

23 Nii, T., Isobe, N. & Yoshimura, Y. Effects of avian infectious bronchitis virus antigen on eggshell formation and immunoreaction in hen oviduct. *Theriogenology* **81**, 1129-1138 (2014).

24 Rahman, S. A. E., El-Kenawy, A., Neumann, U., Herrler, G. & Winter, C. Comparative analysis of the sialic acid binding activity and the tropism for the respiratory epithelium of four different strains of avian infectious bronchitis virus. *Avian Pathol.* **38**, 41-45 (2009).

25 Guo, X., Rosa, A. J., Chen, D.-G. & Wang, X. Molecular mechanisms of primary and secondary mucosal immunity using avian infectious bronchitis virus as a model system. *Vet. Immunol. Immunopathol.* **121**, 332-343 (2008).

26 Seo, S. H. & Collisson, E. W. Specific cytotoxic T lymphocytes are involved in *in vivo* clearance of infectious bronchitis virus. *J. Virol.* **71**, 5173-5177 (1997).

27 Valosky, J., Hishiki, H., Zaoutis, T. E. & Coffin, S. E. Induction of mucosal B-cell memory by intranasal immunization of mice with respiratory syncytial virus. *Clin. Diagn. Lab. Immunol.* **12**, 171-179 (2005).

28 Zhang, Y. *et al.* Immunoglobulin A-deficient mice exhibit altered T helper 1-type immune responses but retain mucosal immunity to influenza virus. *Immunology* **105**, 286-294 (2002).

29 Animas, S. B., Otsuki, K., Hanayama, M., Sanekata, T. & Tsubokura, M. Experimental infection with avian infectious bronchitis virus (Kagoshima-34 strain) in chicks at different ages. *J. Vet. Med. Sci.* **56**, 443-447 (1994).

30 Animas, S. B., Otsuki, K., Tsubokura, M. & Jane, K. A. Comparison of the susceptibility of chicks of different ages to infection with

nephrosis/nephritis-causing strain of infectious bronchitis virus. *J. Vet. Med. Sci.* **56**, 449-453 (1994).

31 Jeurissen, S. H. M. Structure and function of the chicken spleen. *Res. Immunol.* **142**, 352-355 (1991).

32 Romppanen, T. & Sorvari, T. E. A morphometrical study of chicken spleen with special reference to the bursa dependence of the white pulp. *Int. Arch. Allergy Immunol.* **65**, 349-358 (1981).

33 Dhanasekaran, S., Doherty, T. M. & Kenneth, J. Comparison of different standards for real-time PCR-based absolute quantification. *J. Immunol. Methods* **354**, 34-39 (2010).

34 Vandesompele, J. *et al.* Accurate normalization of real-time quantitative RT-PCR data by geometric averaging of multiple internal control genes. *Genome Biol.* **3**, research0034 (2002).

35 Wong, M. L. & Medrano, J. F. Real-time PCR for mRNA quantitation. *Biotechniques* **39**, 75 (2005).

36 Lee, P. D., Sladek, R., Greenwood, C. M. & Hudson, T. J. Control genes and variability: absence of ubiquitous reference transcripts in diverse mammalian expression studies. *Genome Res.* **12**, 292-297 (2002).

37 Greer, S., Honeywell, R., Geletu, M., Arulanandam, R. & Raptis, L. Housekeeping genes; expression levels may change with density of cultured cells. *J. Immunol. Methods* **355**, 76-79 (2010).

38 Thellin, O. *et al.* Housekeeping genes as internal standards: use and limits. *J. Biotechnol.* **75**, 291-295 (1999).

39 *qbase+ version 3.0 Biogazelle, Belgium. https://www.qbaseplus.com/sites/default/files/public_file/qbaseplus_manual.pdf.*

40 Andersen, C. L., Jensen, J. L. & Ørntoft, T. F. Normalization of real-time quantitative reverse transcription-PCR data: a model-based variance estimation approach to identify genes suited for normalization, applied to bladder and colon cancer data sets. *Cancer Res.* **64**, 5245-5250 (2004).

41 *GenEx version 6.0.1. http://genex.gene-quantification.info/.*

42 Pfaffl, M. W., Tichopad, A., Prgomet, C. & Neuvians, T. P. Determination of stable housekeeping genes, differentially regulated target genes and sample integrity: BestKeeper–Excel-based tool using pair-wise correlations. *Biotechnol. Lett.* **26**, 509-515 (2004).

43 Silver, N., Best, S., Jiang, J. & Thein, S. L. Selection of housekeeping genes for gene expression studies in human reticulocytes using real-time PCR. *BMC Mol. Biol.* **7**, 33 (2006).

44 Xie, F., Xiao, P., Chen, D., Xu, L. & Zhang, B. miRDeepFinder: a miRNA analysis tool for deep sequencing of plant small RNAs. *Plant Mol. Biol.* **80**, 75-84 (2012).

45 *RefFinder online tool. http://150.216.56.64/referencegene.php*.

46 Bar, A., Vax, E. & Striem, S. Relationships between calbindin (Mr 28,000) and calcium transport by the eggshell gland. *Comp. Biochem. Physiol. A Physiol.* **101**, 845-848 (1992).

47 Krishnamurthy, P. C. *et al.* Identification of a mammalian mitochondrial porphyrin transporter. *Nature* **443**, 586-589 (2006).

48 Bagés, S., Estany, J., Tor, M. & Pena, R. N. Investigating reference genes for quantitative real-time PCR analysis across four chicken tissues. *Gene* **561**, 82-87 (2015).

49 Borowska, D., Rothwell, L., Bailey, R., Watson, K. & Kaiser, P. Identification of stable reference genes for quantitative PCR in cells derived from chicken lymphoid organs. *Vet. Immunol. Immunopathol.* **170**, 20-24 (2016).

50 Nascimento, C. S. *et al.* Identification of suitable reference genes for real time quantitative polymerase chain reaction assays on Pectoralis major muscle in chicken (*Gallus gallus*). *PLoS ONE* **10**, e0127935 (2015).

51 Mitra, T., Bilic, I., Hess, M. & Liebhart, D. The 60S ribosomal protein L13 is the most preferable reference gene to investigate gene expression in selected organs from turkeys and chickens, in context of different infection models. *Vet. Res.* **47**, 105 (2016).

52 Olias, P., Adam, I., Meyer, A., Scharff, C. & Gruber, A. D. Reference genes for quantitative gene expression studies in multiple avian species. *PLoS ONE* **9**, e99678 (2014).

53 Nakamura, A. M. *et al.* Reference genes for accessing differential expression among developmental stages and analysis of differential expression of OBP genes in *Anastrepha obliqua*. *Sci. Rep.* **6**, 17480 (2016).

54 van de Moosdijk, A. A. A. & van Amerongen, R. Identification of reliable reference genes for qRT-PCR studies of the developing mouse mammary gland. *Sci. Rep.* **6**, 35595 (2016).

55 Zhang, Q.-L. *et al.* Selection of reliable reference genes for normalization of quantitative RT-PCR from different developmental stages and tissues in amphioxus. *Sci. Rep.* **6**, 37549 (2016).

56 Gong, H. *et al.* Evaluation of candidate reference genes for RT-qPCR studies in three metabolism related tissues of mice after caloric restriction. *Sci. Rep.* **6**, 37549 (2016).

57 Chapman, J. R. *et al.* A panel of stably expressed reference genes for real-time qPCR gene expression studies of mallards (*Anas platyrhynchos*). *PLoS ONE* **11**, e0149454 (2016).

58 Selvey, S. *et al.* β-Actin-an unsuitable internal control for RT-PCR. *Mol. Cell. Probes* **15**, 307-311 (2001).

59 Ji, H. *et al.* Selection of reliable reference genes for real-time qRT-PCR analysis of Zi geese (Anser anser domestica) gene expression. *Asian-Australas. J. Anim. Sci.* **26**, 423-432 (2013).

60 Goossens, K. *et al.* Selection of reference genes for quantitative real-time PCR in bovine preimplantation embryos. *BMC Dev. Biol.* **5**, 27 (2005).

61 Svingen, T., Letting, H., Hadrup, N., Hass, U. & Vinggaard, A. M. Selection of reference genes for quantitative RT-PCR (RT-qPCR) analysis of rat tissues under physiological and toxicological conditions. *PeerJ* **3**, e855 (2015).

62 Barber, R. D., Harmer, D. W., Coleman, R. A. & Clark, B. J. GAPDH as a housekeeping gene: analysis of GAPDH mRNA expression in a panel of 72 human tissues. *Physiol. Genomics* **21**, 389-395 (2005).

63 Zhang, Z. & Hu, J. Development and validation of endogenous reference genes for expression profiling of medaka (*Oryzias latipes*) exposed to endocrine disrupting chemicals by quantitative real-time RT-PCR. *Toxicol. Sci.* **95**, 356-368 (2007).

64 Fink, T. *et al.* Instability of standard PCR reference genes in adipose-derived stem cells during propagation, differentiation and hypoxic exposure. *BMC Mol. Biol.* **9**, 98 (2008).

65 Bustin, S. A. *et al.* The MIQE guidelines: minimum information for publication of quantitative real-time PCR experiments. *Clin. Chem.* **55**, 611-622 (2009).

66 Cinar, M. U. *et al.* Evaluation of suitable reference genes for gene expression studies in porcine PBMCs in response to LPS and LTA. *BMC Res. Notes* **6**, 56 (2013).

67 Dwight, Z., Palais, R. & Wittwer, C. T. uMELT: prediction of high-resolution melting curves and dynamic melting profiles of PCR products in a rich web application. *Bioinformatics* **27**, 1019-1020 (2011).

68 Hellemans, J., Mortier, G., De Paepe, A., Speleman, F. & Vandesompele, J. qBase relative quantification framework and software for management and automated analysis of real-time quantitative PCR data. *Genome Biol.* **8**, R19 (2007).

69 Pfaffl, M. W. & Hageleit, M. Validities of mRNA quantification using recombinant RNA and recombinant DNA external calibration curves in real-time RT-PCR. *Biotechnol. Lett.* **23**, 275-282 (2001).

70 *Bio-Rad Application User Guide. http://www.bio-rad.com/webroot/web/pdf/lsr/literature/Bulletin_5279.pdf.*

71 Rasmussen, R. Quantification on the LightCycler in *Rapid cycle real-time PCR* 21-34 (Springer, 2001).

72 Kuchipudi, S. V. *et al.* Highly pathogenic avian influenza virus infection in chickens but not ducks is associated with elevated host immune and pro-inflammatory responses. *Vet. Res.* **45**, 118 (2014).

73 Yang, F., Lei, X., Rodriguez-Palacios, A., Tang, C. & Yue, H. Selection of reference genes for quantitative real-time PCR analysis in chicken embryo

fibroblasts infected with avian leukosis virus subgroup J. *BMC Res. Notes* **6**, 402 (2013).

74 Kuchipudi, S. V. *et al.* 18S rRNA is a reliable normalisation gene for real time PCR based on influenza virus infected cells. *Virol. J.* **9**, 230 (2012).

75 Yin, R. *et al.* Systematic selection of housekeeping genes for gene expression normalization in chicken embryo fibroblasts infected with Newcastle disease virus. *Biochem. Biophys. Res. Commun.* **413**, 537-540 (2011).

76 Li, Y. P., Bang, D. D., Handberg, K. J., Jorgensen, P. H. & Zhang, M. F. Evaluation of the suitability of six host genes as internal control in real-time RT-PCR assays in chicken embryo cell cultures infected with infectious bursal disease virus. *Vet. Microbiol.* **110**, 155-165 (2005).

77 Qi, X. *et al.* Deterioration of eggshell quality in laying hens experimentally infected with H9N2 avian influenza virus. *Vet. Res.* **47**, 35 (2016).

78 Pfaffl, M. W. A new mathematical model for relative quantification in real-time RT–PCR. *Nucleic Acids Res.* **29**, e45-e45 (2001).

Higher Degree Research Thesis by Publication
University of New England

STATEMENT OF AUTHORS' CONTRIBUTION

(To appear at the end of each thesis chapter submitted as an article/paper)

We, the Research Master/PhD candidate and the candidate's Principal Supervisor, certify that all co-authors have consented to their work being included in the thesis and they have accepted the candidate's contribution as indicated in the *Statement of Originality*.

	Author's Name (please print clearly)	% of contribution
Candidate	**Sami Samiullah**	60
Other Authors	**Juliet Roberts**	15
	Shu-Biao Wu	25

Name of Candidate: **Samiullah**

Name/title of Principal Supervisor: **Associate Professor Juliet Roberts**



Candidate Date 09/06/2017



Principal Supervisor Date 09/06/2017

Higher Degree Research Thesis by Publication
University of New England

STATEMENT OF ORIGINALITY

(To appear at the end of each thesis chapter submitted as an article/paper)

We, the Research Master/PhD candidate and the candidate's Principal Supervisor, certify that the following text, figures and diagrams are the candidate's original work.

Type of work	**Page number/s**
Figure 7.1	190
Figure 7.2	191
Figure 7.3	193
Figure 7.4	196
Text and tables	185-213

Name of Candidate: **Samiullah**

Name/title of Principal Supervisor: **Associate Professor Juliet Roberts**

[redacted]

Candidate Date 09/06/2017

[redacted]

Principal Supervisor Date 09/06/2017

Chapter 8 RNA-Sequencing analysis of shell gland of laying hens in relation to time-points of eggshell formation and infectious bronchitis virus challenge

Sami Samiullah[1], Shu-Biao Wu[1] and Juliet Roberts[1]

[1]Animal Science, School of Environmental and Rural Science, University of New England, Armidale, New South Wales, 2351, Australia

To be submitted to: BMC Genomics

8.1 Abstract

Background: Eggshell formation takes place in the shell gland of the oviduct of the laying hen. The eggshell is rich in calcium and many glycoproteins synthesised in the shell gland. Infectious bronchitis virus (IBV) multiplies in the upper respiratory tract, kidney and oviduct of infected birds and causes deterioration of egg quality. The current study investigated the effect of IBV infection on global gene expression in the shell gland at different stages of eggshell formation using transcriptomic analysis.

Results: There were no differentially expressed genes (DEGs) (adjusted P value >0.05; fold change >1.5) between the challenged and control birds. However, gene expression profiles of the shell gland at 5 and 15 hr time-points were clearly separated from each other and there were 1608 and 1806 DEGs at 5 and 15 hrs, respectively. Validation of RNA-Sequencing results through qPCR showed a positive correlation. The putative functions of genes identified ranged from calcium binding to receptor activity. The five most enriched GO terms appearing at the 5 hr time-point were anion transport, synaptic vesicle localisation, organic anion transport, secretion and signal release. The five most enriched GO terms appearing at the 15 hr time-point were regulation of phospholipase activities, alanine transport, transmembrane receptor protein tyrosine kinase signalling pathway,

regulation of blood vessels diameter and 3, 5-cyclic nucleotide phosphodiesterase activity.

Conclusions: The lack of difference between the challenged and non-challenged shell gland samples for the genes involved in shell formation and mucosal immune system could be due to a number of factors including sampling time post infection. The DEGs at the 5 hr time-point were most likely involved in the transport of molecules and synthesis activities, initiating the formation of eggshell. The DEGs at the 15 hr time-point were most likely involved in synthesis and secretory activities, reflecting the peak stage of eggshell formation. These findings broaden our understanding of eggshell formation at the molecular level and provide a foundation for further studies of RNA and possibly microRNA regulation involved in eggshell formation in the shell gland of laying hens. However, the time post-infection of sample collection needs to be carefully determined in order to capture the changes under investigation.

Keywords: infectious bronchitis, oviduct, next generation sequencing, ions transport

8.2 Background

In laying hens, eggshell formation takes place in the shell gland region of the oviduct over an 18 hr period. The eggshell is composed of six distinct layers having calcite as a main component [1]. The calcium and bicarbonate ions contributing to the calcite (calcium carbonate) are secreted from the epithelial cells of the mucosa of the shell gland (reviewed in Hincke et al.) [2]. In addition to other regulators and transporters, the calbindin (*CALB1*) gene is involved in Ca^{2+} transportation across the cell membrane for eggshell formation [3]. The eggshell matrix contains proteins such as ovocalyxin-36 [4, 5], ovocleidin-17 [6], ovocalyxin-32 [7] and ovocalyxin-25 [8] that possess antimicrobial functions. The metallo-proteinase family of proteins has been shown to play a role in reproductive tract remodelling [9]. The synthesis of brown eggshell pigment known as protoporphyrin IX (PP IX) occurs in the shell gland region of the oviduct. The PP IX biosynthetic pathway occurs in mitochondria and cytosol through multi-enzymatic steps; however, the exact location of PP IX synthesis in the shell gland has not been established. The

concentration of PP IX in brown eggshells is affected by various factors such as hen age, strain, stress level, drugs and diseases. Infectious bronchitis virus (IBV) can have negative effects on egg shell quality and egg internal quality [10-12]. IBV is a gammacoronavirus with enveloped positive-sense, single stranded RNA (27.6 kbp) [13-15] that is the etiological agent of an acute highly contagious infectious bronchitis in layers and broilers. The incubation period is relatively short [16] and the virions spread quickly to kidney [17, 18] and reproductive tract [19-22] after initial multiplication in the upper respiratory tract [23]. *In vitro* studies have shown that different strains have the ability to multiply in various organs [24] and the variation in multiplication in different organs is also affected by viral dosage [25]. A high mutation rate in the spike-protein of IBV results in the emergence of new variants [26-29]. The Australian field strain, IBV T (N1/62), is primarily nephropathogenic [30-32] but also multiplies in the upper respiratory tract [31] and the oviduct [21, 22]. Laying hens infected with the M41 strain showed glandular hyperplasia in oviducal epithelium and reduction in secretory function of the oviduct [12] and the viral antigen was demonstrated in the oviduct between 6 and 9 days post-infection (p.i.). Many strains of IBV adversely affect egg production in laying hens [11, 33-36]. The presence of blood and/or meat spots in eggs laid by infected hens has also been reported [37, 38]. Other egg quality defects reported as being caused by IBV include corrugated eggs, change in egg shape index and decline in albumen height and Haugh unit. Microscopic changes in the oviduct include reduction in the height of the epithelial cells, reduction in number or complete absence of cilia, dilation of glandular cells, lymphocytic foci and cellular infiltration in the lamina propria and intertubular stroma [11]. In an *in vitro* study with oviduct organ culture, virulent strains of IBV caused complete stasis of cilia at three weeks post-infection [39]. Immunogenic components of IBV are mainly S (spike) and N (nucleoprotein) proteins [40]. IBV-induced IgA and IgG have been demonstrated in tracheal washes [41] and oviduct [42] of infected chickens with an increase in antibody secreting cells [43, 44]. Immune cells such as CD^{+8} T cells, αβ T lymphocytes [45] and cytotoxic T-lymphocyte [46], interferons [47-49] and proinflammatory cytokines [50] play an important role in controlling IBV infection. IBV infects different chicken strains at different levels of pathogenicity and, in one study, brown Leghorns were more resistant to infection than White Leghorns strains

[51]. All age groups are susceptible; however, the clinical disease is more severe in young chicks compared with older birds [52, 53], with older birds being less susceptible to IBV induced mortality [54] as well as lesions in the oviduct [55] and kidney [56]. We hypothesised that IBV infection may disrupt the mechanism of eggshell formation and PP IX synthesis through changing the expression level of the genes involved. To test this hypothesis, we developed an *in vivo* IBV infection model in brown-egg laying hens. IBV T strain was used as it causes IB in Australia and is considered the most pathogenic in the Australian layer industry. The main objective of the current study was to acquire a comprehensive picture of the transcriptional changes in the shell gland of brown-egg laying hens challenged with IBV T strain. We also aimed to identify unknown candidate genes involved in eggshell formation.

8.3 Materials and Methods

8.3.1 Ethics statement

The experimental setup was approved by the University of New England, Animal Ethics Approval Committee under Authority No. AEC15-118. The protocol was carried out in accordance with the guidelines specified in Australian Code for the Care and Use of Animals for Scientific Purposes 8th edition 2013.

8.3.2 Rearing of IBV free laying hens and virus challenge

Day old Isa-Brown laying chickens were obtained from the Baiada Hatchery at Tamworth, NSW, Australia. At the hatchery, at day-old, all chickens received Rispens vaccine against Marek's disease but were not vaccinated for infectious bronchitis (IB). The chickens were raised in isolation sheds at the University of New England under strict biosecurity protocols. All chickens were fed commercial starter to 4 weeks of age, pullet grower to 18 weeks of age and layer mash until the termination of the experiment. From the isolation sheds, pullets were moved at 18 weeks of age to individual cages in an isolated poultry house. Before challenge, an ELISA was performed to confirm that all birds were negative for IBV antibody titre in the blood plasma. At 35 weeks of age, eggs were collected and processed for traditional egg quality measurements. Hens were then divided into a 2×2 factorial

design in such a way that the egg weight and eggshell colour (L*) were not significantly different among the groups. The hens selected for IBV challenge were moved to a separate poultry house one week prior to challenge in order to settle down and recover from the trans-location stress. From the control hens, eggs were analysed until the hens were euthanised for shell gland tissue collection. At the time of euthanasia, the egg in individual hens was either in the distal magnum/isthmus (5 hr post-oviposition time-point) or in the shell gland (15 hr time-point). From the challenged hens, eggs were analysed for 2 days prior to challenge and daily collection of eggs for analysis continued until individual hens were euthanised. In the challenged groups, 5 hens from each group at a time were intra-occularly inoculated with 10^7 embryo infective dose (EID_{50}) and closely monitored for the development of clinical signs of IB [16] and loss in eggshell colour until days 9-10 p.i. This time p.i. was selected on the basis of loss of shell colour in response to IBV challenge reported from previous study [10]. The EID_{50} dose was determined in embryonated SPF eggs infected at 9 days of incubation with 10-times serial dilutions (10^{-3} to 10^{-8}) of IBV T strain [57, 58] according to the method of Reed and Muench [59]. Eggs were opened at 16 days of incubation and the number of live, dead or virus affected (dwarfed, curled) embryos recorded. The infection in challenged birds was confirmed through RT-qPCR (in mucosal scrapings from the shell gland) and ELISA (blood plasma - ELISA kit, IDEXX Laboratories, Inc., Westbrook, MA, USA). The ELISA procedure was per the manufacturer's instructions and the microtiter plates were read on a SpectraMax M2e microplate reader (Molecular Devices; Sunnyvale, CA, 94089, USA). The absorbance values were calculated as a sample/positive ratio from which the positive/negative titre endpoint was calculated for each plate assayed.

8.3.3 Tissue collection

Hens were euthanised with CO_2 gas and the shell gland was aseptically retracted through the abdominal incision. An approximately 500 mg sample tissue was cut from the centre of the shell gland and directly transferred to RNALater (Sigma Aldrich, Australia). The samples were stored at -20°C and were processed for total RNA extraction within one day of collection. For total RNA extraction, a whole

piece of shell gland tissue (all tissue layers) was processed based on the uncertainty of which cells in the shell gland are involved in PP IX synthesis.

8.3.4 Total RNA extraction and purification

Total RNA was extracted using TRIsure (Bioline, Australia), according to the manufacturer's instructions. Briefly, an approximately 100 mg of tissue (wet weight) was homogenized in 1 mL of TRIsure using an IKA T10 basic Homogenizer (Wilmington, NC, USA). After the RNA pellets were washed with 1.5 mL ethanol (75%), 50 µL of UltraPure™ DEPC-treated water (Ambion, USA) was used to dissolve RNA pellets. The total RNA was further purified using RNeasy Mini Kit (Qiagen, GmbH, Hilden, Germany) as per the manufacturer's instructions. A DNase-I step was performed to remove traces of genomic DNA from the extracted total RNA. The elution of RNA from the spin column with 50 µL of RNase-free water was repeated twice and the eluted RNA solutions were mixed thoroughly. The purified RNA was analysed in a NANODROP-8000 spectrophotometer (ThermoFisher Scientific, Wilmington, DE, USA) to measure its quantity and purity. RNA integrity and purity were further examined in Agilent 2100 Bioanalyzer as per manufacturer's instructions of an Agilent RNA 6000 Nano Kit. All the RNA showed distinct 18S and 28S bands with an average RNA integrity number (RIN) >9.1. Representative shell gland purified total RNA samples (Figure 8.1) were processed by Australian Genome Research Facility (AGRF) for RNA-Sequencing analysis and basic bioinformatics.

8.3.5 RNA-Sequencing of selected shell gland samples

8.3.5.1 cDNA libraries preparation

Illumina's TruSeq Stranded mRNA Prep Kit was used for processing the RNA samples. The process included mRNA purification via oligo(dT) beads, fragmentation of mRNA with divalent cations and heat, 1st strand cDNA and 2nd strand cDNA syntheses. cDNA libraries were prepared by DNA fragment end repair, 3' Adenylation of DNA fragments, sequence adaptor ligation and amplification of library via PCR. In total, 12 cDNA libraries (i.e. one library for

each sample) were constructed for sequencing. Sequencing of libraries using 100 bp single read was performed on an Illumina HiSeq 2500 sequencing system.

8.3.5.2 Sequence quality control and sequence data evaluation

The primary sequence data was generated using the Illumina bcl2fastq 2.17.1.14 pipeline. Initial quality control of the RNA sequences was evaluated by the FastQC v0.11.5 [60]. The raw reads were also screened for the presence of any Illumina adaptor/overrepresented sequences, low quality sequences, empty reads and cross species contamination. Illumina adaptors and contaminated sequences were removed through trim_galore and Fastq_clean (http://ieeexplore.ieee.org/document/6999309/).

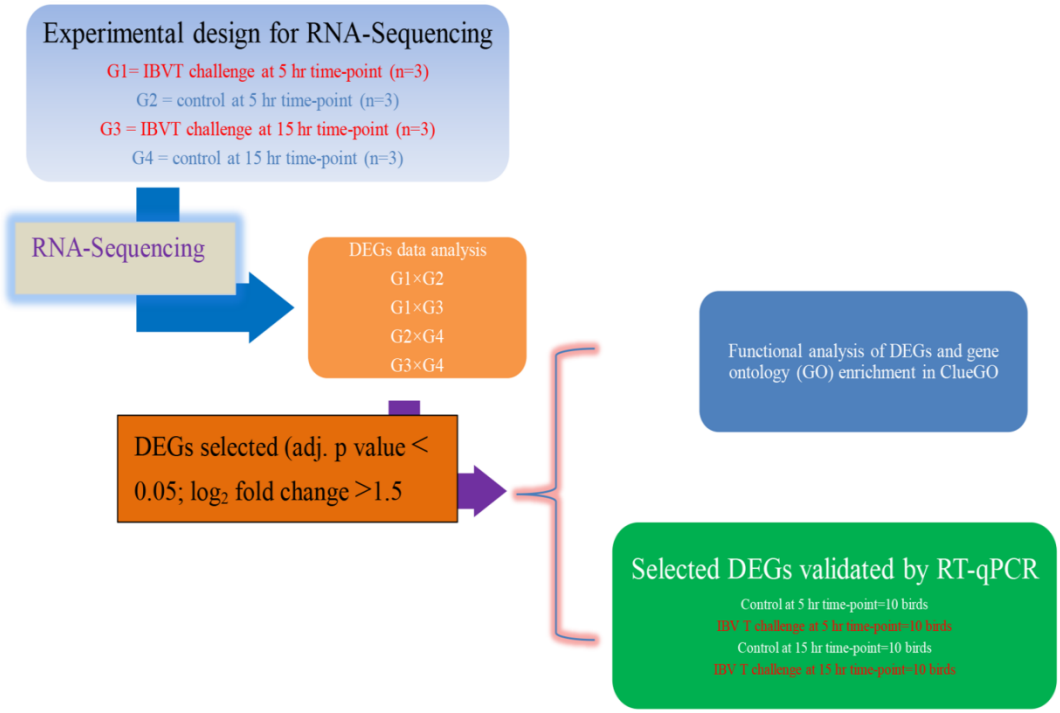

Figure 8.1 Schematic diagram explaining the selection of samples for RNA-Sequencing and DEGs data analysis

To validate the results of RNA-Sequencing, qPCR was performed on all 40 RNA samples and the data was analysed in qbase+ software for gene expression study.

8.3.5.3 Reads mapping and raw gene counts

Gene expression was calculated in Fragments Per Kilobase of Exon Per Million Fragments Mapped (FPKM). The cleaned sequence reads were further normalised into FPKM values and then aligned against the *Gallus gallus* genome (Built version 5 Ensembl release 86) [61]. The Tophat aligner (v2.0.14) [62] was used to map reads to the genomic sequences. The counts of reads mapping to each known gene were summarised at gene level using the featureCounts v1.4.6-p5 utility of the subread package (http://subread.sourceforge.net/).

8.3.5.4 Reference guided transcript assembly

The transcripts were assembled with Stringtie tool v1.2.4 (http://ccb.jhu.edu/software/stringtie/) utilising the reads alignment and reference annotation based assembly option (RABT). This option generated assembly for known and potentially novel transcripts. The Ensembl annotations (Gallus_gallus.Gallus_gallus-5.0.86.gtf) for genome were used as a guide.

8.3.6 Differential gene expression data analysis

The read counts were used to estimate gene expression and identify differentially expressed genes (DEGs) using R packages (R version 3.3.1) 'edgeR' (v3.14.0) [63] and 'limma' (3.28.21) [64]. To obtain further insight on the functions of the DEGs encoding hypothetical (unknown) proteins, Ensembl BLAST/BLAT searches were performed with nucleotide and protein sequences queries using a cut-off e value $10E^{-20}$.

8.3.7 Hierarchical clustering analysis

Hierarchical clustering analysis (HCA) was performed in Genesis [65]. In HCA, each sample begins as a separate cluster and the algorithm proceeds to combine them until all of the samples belong to one cluster. Average gene counts for the top 50 up or down-regulated DEGs in individual groups (G1-G4) were considered when performing hierarchical clustering. The HCA results were presented as heatmaps.

8.3.8 Functional annotation of DEGs

The DEGs (log_2 fold change >1.5; adjusted P value <0.05) were subjected to functional analysis using ClueGO version 2.2.6 [66, 67] + CluePedia version 1.2.6 [68] plugins in Cytoscape version 3.4.0 [69] as has previously been used in similar studies [70]. The DEGs were enriched for terms specific to biological process (BP), molecular functions (MF) and cellular component (CC). The annotation enrichment of the DEGs was performed for two groups (G2 and G4; Figure 8.1). To create the annotation network, ClueGO investigates the distribution of the target genes across the Gene Ontology (GO) terms and pathways. CluePedia is a Cytoscape plugin for pathway insights using integrated experimental and *in silico* data [68]. CluePedia extends the functionality of ClueGO down to gene level [68]. In ClueGO analysis, P value was calculated using the right-sided hypergeometric tests with Benjamini-Hochberg adjustment for multiple test correction [71]. An adjusted $P \leq 0.001$ indicated a statistically significant deviation from the expected distribution, and that the corresponding GO terms and pathways were enriched for the target genes. The association strength between the terms was calculated using a corrected kappa statistic score of 0.4, in ClueGO [67, 72]. The relationship between the selected terms was defined based on their shared genes in a similar way. The created network showed the GO terms as nodes and size of the nodes reflected the enrichment significance. The network was automatically laid out using the organic layout algorithm supported by the Cytoscape software [69]. Functional groups represented by their most significant term were visualized in the network providing an insightful view of their interrelations [66].

8.3.9 Primers sequence for candidate genes and validation

Primers for the candidate target genes were designed in NCBI software by choosing an option for exon-intron spanning (Table 8.1). Primers for the reference and *CALB1* genes were sourced from published literature. Specific amplifications of the primers were confirmed by a single peak of melting curve analysis and a single amplicon band of appropriate size in Agilent 2100 Bioanalyzer gel electrophoresis using DNA 1000 Kit (Agilent Technologies, Waldbronn, Germany). PCR amplification efficiencies and correlation coefficients (R^2) were determined with

the amplifications of a series of six 10-fold RNA dilutions based on the following equation [73-75]; $E = (10 - ^{(\frac{1}{-slope})} - 1) \times 100$

The qPCR was performed on the genes when the amplification efficiency was in a range of 90 to 105%, and linear correlation coefficient R^2 >0.980 were considered of high standard [75-77].

Table 8.1 Candidate target and reference* genes in expression studies by qPCR in the shell gland of laying hens challenged with infectious bronchitis virus T strain

Gene Name	Gene Symbol	Primer sequence (5′-3′)	Amplicon size (bp)	Ta (°C)	PCR Efficiency (%)	Accession No	Reference
Secreted phosphoprotein 1	*SPP1*	F-CCAGGAAGCTCATTGAGGATG R-GCTGTCGTTCTCTACGCTCT	134	60	101	NM_204535 4	this study
proopiomelanocortin	*POMC*	F-TGGTGTTTTGGCGTGTGC R-CATCACGTACTTGCGGATGC	115	65	105	NM_001031098 1	this study
Calbindin	*CALB1*	F: TTGGCACTGAAATCCCACTGA R: CATGCCAAGACCAAGGCTGA	116	60	100	NM_205513 1	Qi et al , 2016
Claudin 16	*CLDN16*	F- TACCTTGCTCATTGCAGGTCT R- GTGAGCAGGGACCCAGATAAG	186	63	105	XM_426702 3	this study
G protein subunit gamma 4	*GNG4*	F- CAGACCAATGCACAAGTTTCA R- GCCTCAAGTGGAAAGGTCAC	243	63	97	XM_004935468 2	this study
Potassium voltage-gated channel subfamily H member 1	*KCNH1*	F- AGAGGCAGAGATCCAGACGA R- GGTCTGATGTCCCAGACGTT	160	63	93	XM_015283863 1	this study
BPI fold containing family B, member 3	*BPIFB3*	F- CCATGCAACAAGTGCTGTCC R- AGCAGTTGCCACTGAGATCC	234	63	94	NM_001030861	this study
Rho related BTB domain containing 3	*RHOBTB3*	F- GACGTCGCATCTGTGATCC R- TCTTCCTTAGCTCGGCGTTA	171	63	95	ENSGALG00000014675	this study
Somatostatin II	*SS2*	F- GCTCTTGGAGAGCTCAGACG R- GCACTAGCAGGAGGTGAAGG	160	65	97	NM_204455 1	this study
Otopetrin 2	*OTOP2*	F- GGAGCAAGCAATTGCCCAAA R- CGCTGCTTTGCTGCCTG	202	63	99	XM_003642368 3	this study
Klotho beta	*KLB*	F- GAGCAATACGGGGGATGGAA R- GCATGAGCCTTGATCAGATTGT	224	61	101	XM_003641245 3	this study
glycoprotein hormones, alpha polypeptide	*CGA*	F- GTCCAGAGTGCAAGCTAGGG R- GCTACACAGCACGTTGCTTC	166	63	105	:NM_001278021	this study
GATA-binding factor 3	*GATA3*	F- CAGAAGGCAGGGAGTGTGTAA R- GCTGCAGACAGCCTTCTCT	157	63	100	NM_001008444	this study
TYRO3 protein tyrosine kinase	*TYRO3*	F- GTGCAGTGCAGCAATGAGAT R- CAGCCTGTATCCCAGGACAT	186	61	98	NM_204627	this study
Matrix metallopeptidase 13	*MMP13*	F-AGCTCTATGGTGCTGGAGAC R-CCTGTCCTTGAAGACCAGCAT	128	63	100	NM_001293090	this study
Gap junction protein, alpha 8	*GJA8*	F- CTGCTATGATGAGGCCTTCC R- GGCAGCTTCTCTTCATCCAC	186	63	98	NM_204997 1	this study
Carbonic anhydrase 9	*CA9*	F- CTCAGTGACAGCAGCAGGA R- TGGCAAAGAGCACTCCGAAT	80	63	99	XM_004937157 2	this study
Cytochrome P450 family 7 subfamily A member 1	*CYP7A1*	F- AGGAGGCAATGAGGCTATCG R- TGAGTGTCAAGGGATCAGCA	171	63	96	NM_001001753 1	this study
Galactose-3-O-sulfotransferase	*GAL3ST2*	F- TGCTTCGAGGACTACCAAAAA R- TGGGTCTTGAGGAACATGACG	177	61	96	NM_001277431 1	This study
IBV T strain S1 glycoprotein	*S1*	F- TCAGGTGGTTGGCATTTACA R- ATTGCGAACTTGACCATTCC	181	60	98	U29522 1	This study
TATA-Box Binding Protein	*TBP**	F: TAGCCCGATGATGCCGTAT R: GTTCCCTGTGTCGCTTGC	147	61	97	NM_205103 D83127	Li et al , 2005 [78]
Tyrosine 3-monooxygenase/tryptophan 5-monooxygenase activation protein, zeta polypeptide	*YWHAZ**	F- TTGCTGCTGGAGATGACAAG R- CTTCTTGATACGCCTGTTG	61	60	104	NM_001031343 1	Bages et al , 2015 [79]

The candidate target genes were selected from the DEGs either in G2 (5 hr time-point) or G4 (15 hr time-point) of eggshell formation

8.3.10 Validation of RNA-Seq results by qPCR

qPCR was performed with the SensiFAST SYBR® Lo-ROX One-Step RT-PCR Kit (Bioline, Australia). Master mix was prepared as per the manufacturer's protocol and 4 µL of RNA template from 1:100 dilutions was added to the reaction wells using QIAgility robotic (Qiagen, Australia). The reaction was run in duplicates of 20 µL in a Rotor-gene Disc 100 (Qiagen, Hilden, Germany) with a Rotor-Gene Q thermocycler (Qiagen, Australia). No template control (NTC) and no reverse transcriptase (-RT) control were also included to detect possible contamination. Thermocycling conditions for a 2-step PCR were: reverse transcription at 45°C for 10 minutes, first denaturation at 95°C for 2 minutes, then 40 cycles of denaturation at 95°C for 5s and annealing at 60°C, 61°C, 63°C or 65°C for 20s depending on the primers used. The fluorescent data were acquired at the end of each annealing step during PCR cycles. A melting step was conducted to assess the specificity of PCR amplification.

8.3.11 Viral quantification from shell gland of challenged hens

IBV T strain (kindly provided by CSIRO, Geelong, Australia) was cultured in 11 day old SPF embryonated eggs and allantoic fluid harvested at 16 days. Viral RNA was extracted from the allantoic fluid using TRIsure as per the manufacturer's protocol. A 181 bp fragment of viral RNA was reversely transcribed using SensiFAST SYBR® Lo-ROX One-Step RT-PCR Kit and the PCR product was cloned into a plasmid vector using TOPO® TA Cloning® Kit for sequencing (ThermoFisher Scientific, Australia) as per the manufacturer's protocol. The recombinant plasmid was transfected into *Escherichia coli* that was grown overnight on Difco™ LB agar (Bacto Laboratories, Australia) and then a single colony was enriched in LB broth. Recombinant plasmid DNA from overnight cultured *Escherichia coli* in LB broth was extracted using the PureLink® Quick Plasmid Miniprep Kit (ThermoFisher Scientific, Australia) as per the manufacturer's instructions. The viral insert into plasmid was confirmed by PCR and the size of the amplicon determined using Agilent 2100 Bioanalyzer (Agilent Technologies, Waldbronn, Germany). The protocol for running the gel was per

manufacturer's instructions of Agilent DNA 1000 Kit. A standard curve was constructed from 10-times serial dilutions (10^{-2}~10^{-9}). Approximately 1 µg RNA from individual samples extracted from the shell gland (whole tissue) and shell gland mucosal scrapings was reversely transcribed into cDNA using the QuantiTect Reverse Transcription Kit (Qiagen, Australia) as per the manufacturer's instructions. Quantitative PCR was performed with SYBR green method by using the SensiFAST™ SYBR® No-ROX Kit (Bioline, Australia). PCR reaction was performed in a total volume of 20 µL in duplicate with a Rotor-Gene Q thermocycler and cloned plasmid DNA was included in the same run for standard curve construction. The cloned plasmid DNA with insert was converted into plasmid DNA copies/µL in six different dilutions for analysis. Plasmid copy number was calculated based on the concentration of plasmid DNA and its molecular weight. Amplicons from all 40 samples were run in a Bioanalyzer as described earlier, to assess the specificity and size of IBV T RNA.

8.4 Statistical analysis

Egg quality data were analysed by Statview software (SAS Institute Inc., Version 5.0.1.0). To calculate the relative expression of the candidate target genes, Cq values were analysed in qbase+ software version 3.0 [80]. The Cq values of target genes were normalized against reference genes (*TBP* and *YWHAZ*) Cq values to obtain normalized relative quantities of individual genes. Candidate target genes specific amplification efficiencies were used based on the method of pfaffl [81]. The normalized relative quantities were further analysed in Statview software by taking time-point as main effect. Significant differences between the treatments were separated by Tukey-Kramer test at probability < 0.05.

8.5 Results

8.5.1 IBV detection in shell gland of challenged laying hens

IBV T RNA was not detectable in the shell gland samples processed for RT-qPCR or RNA-Sequencing. However, virus was detected when total RNA was extracted from the shell gland epithelial scrapings following the method of Chousalkar et al.

[82]. All samples from challenged birds were positive with a mean viral load of approximately 3.5×10^7 copies per gram of shell gland tissue. A significantly higher titre of antibodies for the challenged birds in the ELISA test confirmed that the virus multiplied and caused a significant immune response in the challenged birds (Figure 8.2). During the post-challenge period, all infected birds showed characteristic clinical signs of IB [16]. No virus was isolated from the control birds.

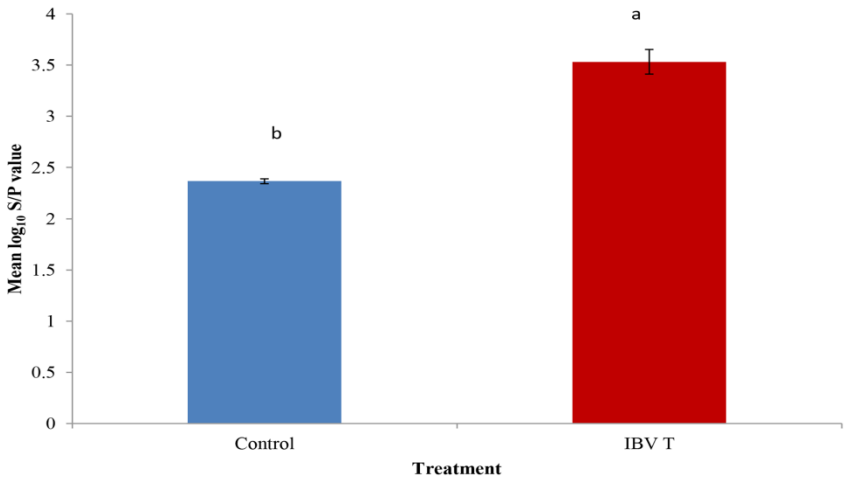

Figure 8.2 Antibody titre of the control and challenged hens on days 9-10 post-infection

The antibody titre was calculated as per protocol of Infectious Bronchitis Virus Antibody Test Kit (IDEXX Laboratories). Bars represent standard deviation. Superscripts (^{a,b}) show significant difference

8.5.2 Global gene response to virus challenge and differential gene expression at different stages of eggshell formation

A total of 261,684,549 (26.17 Gb of data bulk) clean reads with an average length of 100 bp were generated from the twelve libraries divided into four groups (G1-G4; Figure 8.1). The reads feature summary is depicted in Table 8.2. The feature summary shows that the percentage of reads mapped to *Gallus gallus* genome was ≥ 80%. A multivariate analysis was performed on the raw and normalized gene count data to identify any discrepancies. Multi-dimensional scaling (MDS) plot showed that there was no significant effect of virus but a significant effect of time-point on the expressed genes. The lack of significant differences in DEGs between G1 and G2 and G3 and G4 indicated no significant effect of viral infection on either

the mucosal immune system or the genes involved in eggshell formation including PP IX synthesis according to the data analysis utilised (Figure 8.3a-d). Therefore, data presented hereafter focused on the DEGs between time-points of eggshell formation and the data for comparison between G2 (5 hr time-point) and G4 (15 hr time-point) are presented. The top 30 up- regulated genes at 5 and 15 hrs time-points are depicted in Tables 8.3 and 8.4, respectively.

Table 8.2 Summary statistics of sequence quality and alignment information of 12 shell gland samples in four groups (G1-G4)

Sample name	**Total reads**	**Number of reads mapped to chicken genome**	**Percentage of reads mapped to chicken genome**	**Number of reads mapped to one feature**	**Percentage of reads mapped to one feature**	**Number of mapped reads not mapped to any feature**	**Percentage of total reads that mapped to the genome but not to any known features**
G1a	23419963	18942266	80.88	12137770	51.83	5855006	25.00
G1b	22633784	18410799	81.34	11944759	52.77	5541424	24.48
G1c	22478580	18055302	80.32	11646051	51.81	5503560	24.48
G2a	21759465	17607983	80.92	11461812	52.68	5268439	24.21
G2b	22657131	18480220	81.56	12031069	53.10	5536020	24.43
G2c	21832656	17675184	80.96	11615956	53.20	5182041	23.74
G3a	21033600	17095487	81.28	11393823	54.17	4839852	23.01
G3b	20845746	16707543	80.15	11030858	52.92	4836757	23.20
G3c	20784865	16624745	79.98	11034132	53.09	4745972	22.83
G4a	21073856	17140851	81.34	11265366	53.46	5021572	23.83
G4b	21309212	17398557	81.65	11516521	54.04%	5014414	23.53
G4c	21828196	17648497	80.85	11763767	53.89	4986438	22.84

There were 3 shell gland samples (a-c) in each individual group.

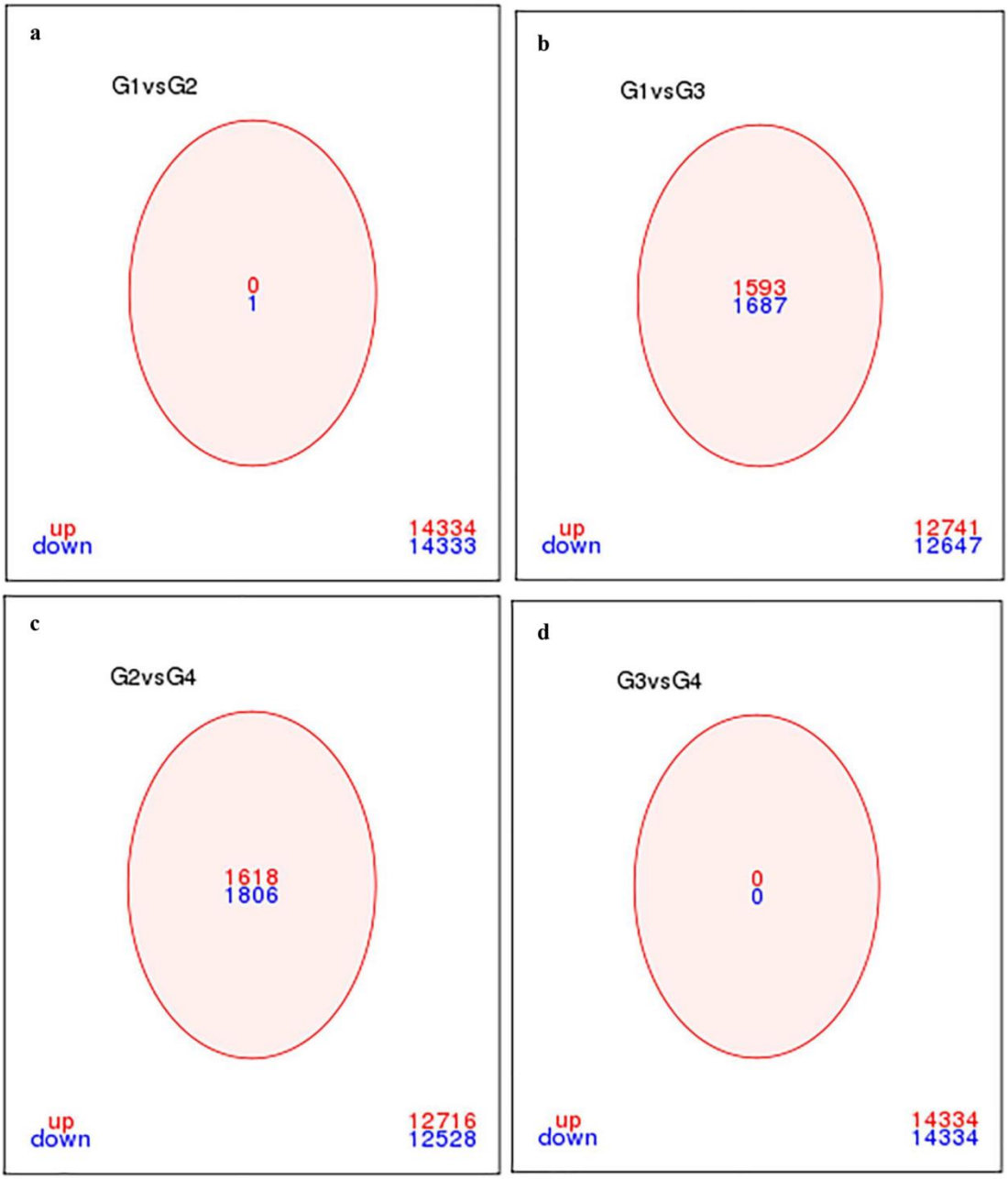

Figure 8.3 Ven diagram of differentially expressed genes between different groups

G1 and G2 show samples collected from challenged and control birds (respectively) at 5 hr time-point of eggshell formation. G3 and G4 show samples collected from challenged and control birds (respectively) at 15 hr time-point of eggshell formation.

Table 8.3 Top 30 DEGs in G2 (5 hr time-point) vs G4 (15 hr time-point)

Gene symbol	Gene name	FC	Adjusted P value
SLC13A5	Solute carrier family 13 member 5	6.516	1.99E-07
KLB	Klotho beta	5.998	0.00079
XAF1	XIAP associated factor 1	5.316	9.26E-05
FIBIN	Fin bud initiation factor homolog (zebrafish)	4.894	1.40E-07
POMGNT1	Protein O-linked mannose N-acetylglucosaminyltransferase 1 (Beta 1,2-)	4.828	0.00026
MMP13	Matrix metallopeptidase 13	4.673	0.00089
CTNNA3	Catenin alpha 3	4.625	0.00239
GJA8	Gap junction protein alpha 8	4.522	0.00089
CA9	Carbonic anhydrase 9	4.519	0.00042
HABP2	Hyaluronan binding protein 2	4.464	0.00119
ARHGAP25	Rho GTPase-activating protein 25	4.284	1.18E-06
SEMA3G	Semaphorin 3G	4.254	3.39E-06
Fibrinogen	Fibrinogen beta chain	4.199	0.00057
CYP7A1	Cytochrome P450 family 7 subfamily A member 1	4.17	0.00081
ADPRHL1	ADP-ribosylhydrolase like 1	4.103	0.00035
GHRHR	Growth hormone releasing hormone receptor	4.075	0.0037
TCERG1L	Transcription elongation regulator 1 like	3.925	4.38E-05
FREM2	FRAS1 related extracellular matrix protein 2	3.835	0.00608
NR1D1	nuclear receptor subfamily 1, group D, member 1	3.785	0.00235
EVPL	Envoplakin	3.749	1.20E-05
ODZ1	Teneurin transmembrane protein 1	3.732	0.00339
TDT	DNA nucleotidylexotransferase	3.714	0.00241
SAMD7	Sterile alpha motif domain containing 7	3.62	0.00405
HAS2	Hyaluronan synthase 2	3.564	0.00034
PCBP2	Poly(RC) binding protein 2	3.548	0.00125
SLC25A15	solute carrier family 25 (mitochondrial carrier; ornithine transporter) member 15	3.545	4.48E-05
ADRA2A	Adrenoceptor alpha 2A	3.512	0.00042
CBX2	Chromobox 2	3.484	0.00497
TNFSF10	Tumor necrosis factor superfamily member 10	3.475	5.95E-05
SLC26A4	Solute carrier family 26 member 4	3.467	0.03297

Fold change (FC) was calculated in log_2 value. The table shows the genes that were up-regulated at 5 hr time-point when direcntly compared with the 15 hr time-point of eggshell formation

Table 8.4 Top 30 DEGs in G4 (15 hr time-point) vs G2 (5 hr time-point)

Gene symbol	Gene name	FC	Adjusted P value
POMC	Proopiomelanocortin	9.17902	0.0005
CALB1	Calbindin	8.08124	3E-08
SPP1	secreted phosphoprotein 1	7.99306	2E-07
NEU4	Neuraminidase 4	7.68189	0.0021
CEMIP	Cell migration inducing hyaluronan binding protein	7.55532	9E-06
GAL3ST2	Galactose-3-O-sulfotransferase 2	6.99921	0.0005
SLC6A17	Solute carrier family 6 member 17	6.64264	0.0271
GNG4	G protein subunit gamma 4	6.58638	0.0416
BPIFB3	BPI fold containing family B, member 3	6.41396	3E-06
ECEL1	Endothelin converting enzyme Like 1	6.40797	0.0312
REG4	Regenerating family member 4	6.27187	0.0017
ANGPTL3	Angiopoietin like 3	6.19877	0.0002
LOC415478	transmembrane protein 2-like	6.06208	6E-06
KCNH1	potassium voltage-gated channel, subfamily H (eag-related), member 1	5.95599	0.0009
GNRHR	gonadotropin-releasing hormone receptor	5.94954	0.0122
MKI67	Marker of proliferation Ki-67	5.81474	0.0127
BPIL3	bactericidal/permeability-increasing protein-like 3	5.25023	0.0004
SLC29A4	Solute carrier family 29 member 4	5.18251	8E-05
WNT11	Wnt family member 11	4.79905	4E-05
CHRD	Chordin	4.69082	3E-05
OFCC1	Orofacial cleft 1 candidate gene 1 protein homolog	4.33034	0.0005
GPR183	G Protein-coupled receptor 183	4.32869	0.0001
ETV4	ETS variant 4	4.30918	0.0264
RHOBTB3	Rho related BTB domain containing 3	4.30487	0.0036
OTOP2	Otopetrin 2	4.22581	1E-05
MFSD13A	Major facilitator superfamily domain containing 13A	4.19013	2E-08
TNFRSF6B	TNF receptor superfamily member 6b	4.18184	0.0005
PLPPR4	Phospholipid phosphatase related 4	4.16077	8E-05
B3GNT7	betaGal beta-1,3-N-acetylglucosaminyltransferase 7	4.13978	9E-05
SEMA3D	Semaphorin 3D	4.12623	0.0206

Fold change (FC) was calculated in $\log_2$ value. The table shows the genes that were up-regulated at 15 hr time-point when direcntly compared with the 5 hr time-point of eggshell formation

8.5.3 DEGs analysis for hypothetical functions

Most of the DEGs with hypothetical functions appeared to possess domains that function in diverse cellular activities (Table 8.5). The associated GO terms showed that the functions of the unknown genes may be correlated with the synthesis and secretory activities in the shell gland during an eggshell formation (Table 8.5).

Table 8.5 Putative functions of mRNA sequences that did not annotate to any known gene functions during alignment

Group	Sequence ID	Gene ID	*Associated GO term*	Log FC	Adjusted P value
[a]G2	ENSGALG00000039411	*COL25A1*	*Heparin binding* and *beta-amyloid binding*	4.8987	0.0031
	ENSGALG00000032113	*NAT8L*	*N-acetyltransferase activity* and *aspartate N-acetyltransferase activity*	4.0380	9E-05
	ENSGALG00000029321	*NAT8L*	*N-acetyltransferase activity* and *aspartate N-acetyltransferase activity*	3.8569	0.0009
	ENSGALG00000030322	*TMEM163*	*No associated GO term found*	3.3488	0.0003
	ENSGALG00000038759	*PARD6B*	*No associated GO term found*	2.8674	0.0007
[b]G4	ENSGALG00000037163	*SLC6A4*	*Protein homodimerization activity* and *Rab GTPase binding*	6.4017	0.0004
	ENSGALG00000006393	*ADGRG6*	*G-protein coupled receptor activity* and *transmembrane 236ignalling receptor activity*	5.2435	0.0306
	ENSGALG00000039812	*GPR6*	*G-protein coupled receptor activity* and *sphingosine-1-phosphate receptor activity*	5.1541	0.0014
	ENSGALG00000029410	*NR1D1*	*Transcription factor activity, sequence-specific DNA binding* and *RNA polymerase II core promoter proximal region sequence-specific DNA binding*	4.5779	0.0031
	ENSGALG00000041414	*BHLHE41*	*Protein homodimerization activity* and *RNA polymerase II core promoter proximal region sequence-specific DNA binding*	4.4199	0.0003
	ENSGALG00000042845	*PDE3A*	*3,5-cyclic-nucleotide phosphodiesterase activity* and *3,5-cyclic-AMP phosphodiesterase activity*	3.8851	0.0039
	ENSGALG00000035935	*UNC13C*	*Diacylglycerol binding*	3.7014	7E-06
	ENSGALG00000033066	*UBE2E2*	*Ligase activity* and *acid-amino acid ligase activity*	3.6725	0.0166
	ENSGALG00000033883	*PCDH7*	*Calcium ion binding*	3.1249	0.0042
	ENSGALG00000031565	*ZNF277*	*RNA polymerase II core promoter sequence-specific DNA binding*	3.0054	0.0399
	ENSGALG00000037545	*GRIP2*	*Protein C-terminus binding* and *receptor 236ignalling complex scaffold activity*	2.9367	0.0009
	ENSGALG00000008047	*TP53I11*	*Ligase activity* and *ubiquitin protein ligase activity*	2.9031	0.0216
	ENSGALG00000011860	*MYO16*	*Actin binding* and *actin filament binding*	2.5957	0.0036
	ENSGALG00000042801	*NT5DC4*	*Hydrolase activity* and *5-nucleotidase activity*	2.3957	0.0298
	ENSGALG00000039716	*HPCA*	*Calcium ion binding* and *actin binding*	2.3035	1E-05
	ENSGALG00000041604	*NPTXR*	*No associated GO term found*	2.2953	0.0051
	ENSGALG00000030673	*KCTD14*	*NADH dehydrogenase (ubiquinone) activity*	2.0963	0.0076
	ENSGALG00000042104	*ROBO1*	*Identical protein binding* and *LRR domain binding*	2.0438	0.0119
	ENSGALG00000038532	*ESPN*	*Actin binding* and *SH3 domain binding*	1.8782	0.0086
	ENSGALG00000038993	*NEGR1*	*No associated GO term found*	1.8417	3E-06
	ENSGALG00000041238	*SEMA3B*	*Receptor activity*	1.7979	3E-05
	ENSGALG00000042411	*FAM198B*	*No associated GO term found*	1.7650	0.0009
	ENSGALG00000043703	*ELN*	*Extracellular matrix structural constituent* and *extracellular matrix constituent conferring elasticity*	1.6303	0.0034
	ENSGALG00000043198	*DNPEP*	*Metallopeptidase activity* and *aminopeptidase activity*	1.6094	0.0021
	ENSGALG00000043209	*ADGRB2*	*G-protein coupled receptor activity* and *transmembrane 236ignalling receptor activity*	1.5730	0.0267

To retrieve the best homology hit, the sequence IDs were blasted against chicken, duck, turkey and human reference genomes in Ensembl BLAT database. The cut off criterion was established as e value $<10E^{-20}$. [a]Represents genes up-regulated at 5 hr time-point; [b]Represents genes up-regulated 15 hr time-point

8.5.4 Functional annotation of DEGs

An enrichment gene set analysis was performed to identify over expressed GO terms specific to Biological Process (BP), Cellular Component (CC) and Molecular Functions (MM) between G2 and G4. The most enriched GO terms between the two groups are depicted in Figure 8.4. Out of 14 GO terms revealed, the five major GO terms associated with genes that were differentially expressed in G2, were anion transport (GO:0006820), synaptic vesicle localization (GO:0097479), organic anion transport (GO:0015711), secretion (GO:0046903) and signal release (GO:0023061) (Figure 8.4a). However, it should be noted that all of the 14 GO terms were significantly enriched (enrichment pathway P value <0.05) (Figure 8.4a). In G2, a total of 278 DEGs (fold change >1.5; adjusted P value <0.05) were mapped to the GO BP, CC and MF pathways. Among the DEGs, *SLC13A5* (Solute carrier family 13 member 5), *KLB* (Klotho beta), *XAF1* (XIAP associated factor 1), *FIBIN* (Fin bud initiation factor homolog (zebrafish)) and *POMGNT1* (Protein O-linked mannose N-acetylglucosaminyltransferase 1 (Beta 1,2-) were the top five highly expressed genes. Network representation of the enriched GO terms and their associated genes in G2 is included in Appendix A.

In G4, all of the terms enriched were significant at an enrichment pathway P value <0.05 (Figure 8.4b). Out of the total 10 GO terms, the five major terms were: regulation of phospholipase activity (GO:0010517), alanine transport (GO:0032328), transmembrane receptor protein tyrosine kinase 237ignalling pathway (GO:0007169), regulation of blood vessel diameter (GO:0097746) and 3',5'-cyclic-nucleotide phosphodiesterase activity (GO:0004114). For the functional analysis of DEGs (Fold change >1.5; adjusted P value <0.05) in G4, a total of 413 genes were mapped to the GO BP, CC and MF pathways.

Among the DEGs, the top five highly expressed genes were POMC (Proopiomelanocortin5), *CALB1* (Calbindin), *SPP1* (secreted phosphoprotein 1), *NEU4* (Neuraminidase 4) and *CEMIP* (Cell migration inducing hyaluronan binding protein). Network representation of the enriched GO terms and their associated genes in G4 is included in Appendix A.

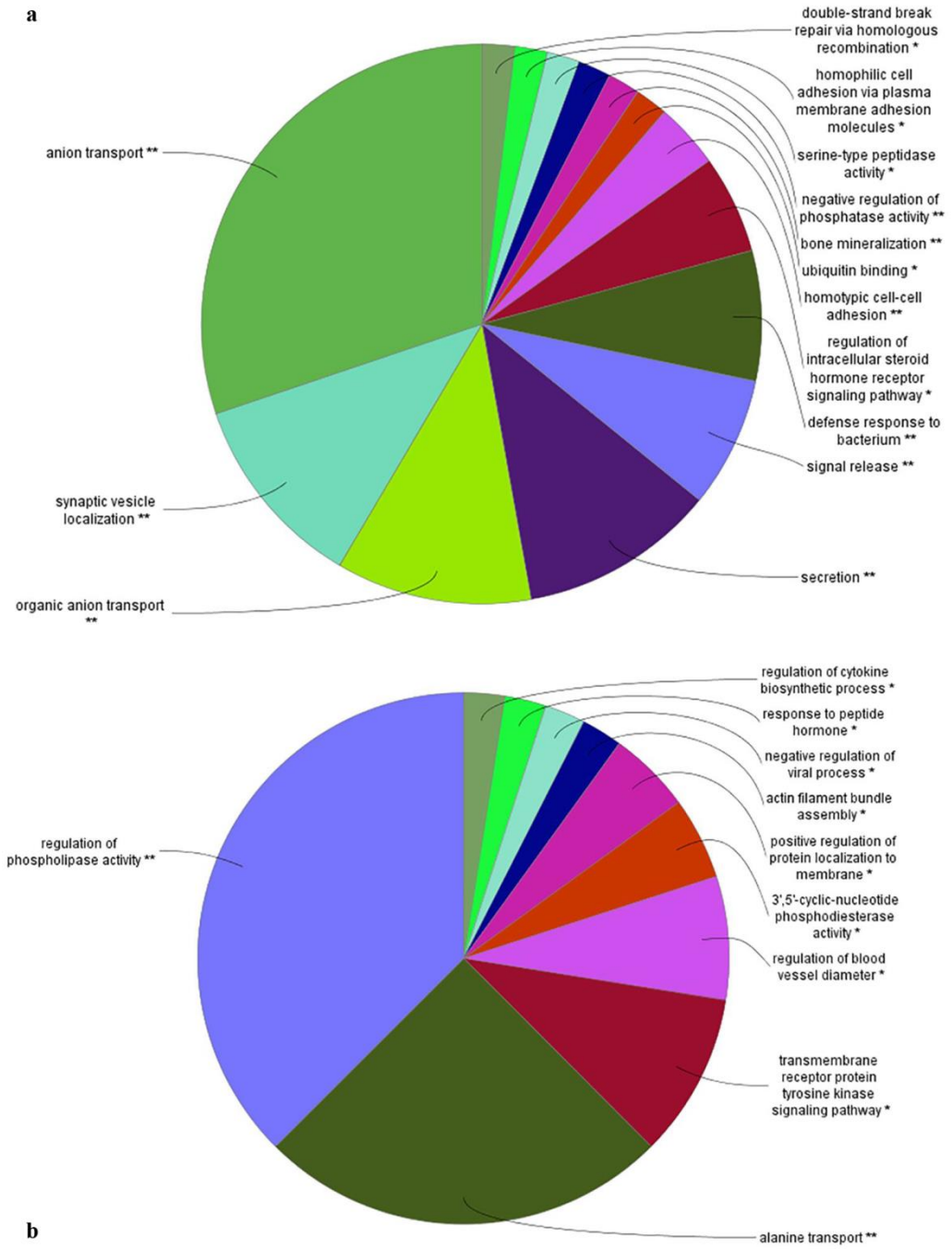

Figure 8.4 Functional map of differentially expressed genes (adjusted P value <0.05; fold change >1.5) enriched for GO biological process, cellular component and molecular functions terms

The chart fragments represent the number of genes associated with the terms as a proportion with the total number of genes within the GO term. **A**) GO terms significantly up-regulated at 5 hr time-point of eggshell formation. **B**) GO terms significantly up-regulated at 15 hr time-point of eggshell formation. **P<0.001; *P<0.01

The enriched GO terms (P value <0.05) that were common between G2 (5 hr time-point) and G4 (15 hr time-point) were also calculated. Among these terms, the five most significantly enriched GO terms were anion transport (GO:0006820), positive regulation of MAP kinase activity (GO:0043406), cyclic nucleotide metabolic process (GO:0009187), carboxylic acid transport (GO:0046942) and neurotransmitter transport (GO:0006836) (Figure 8.5).

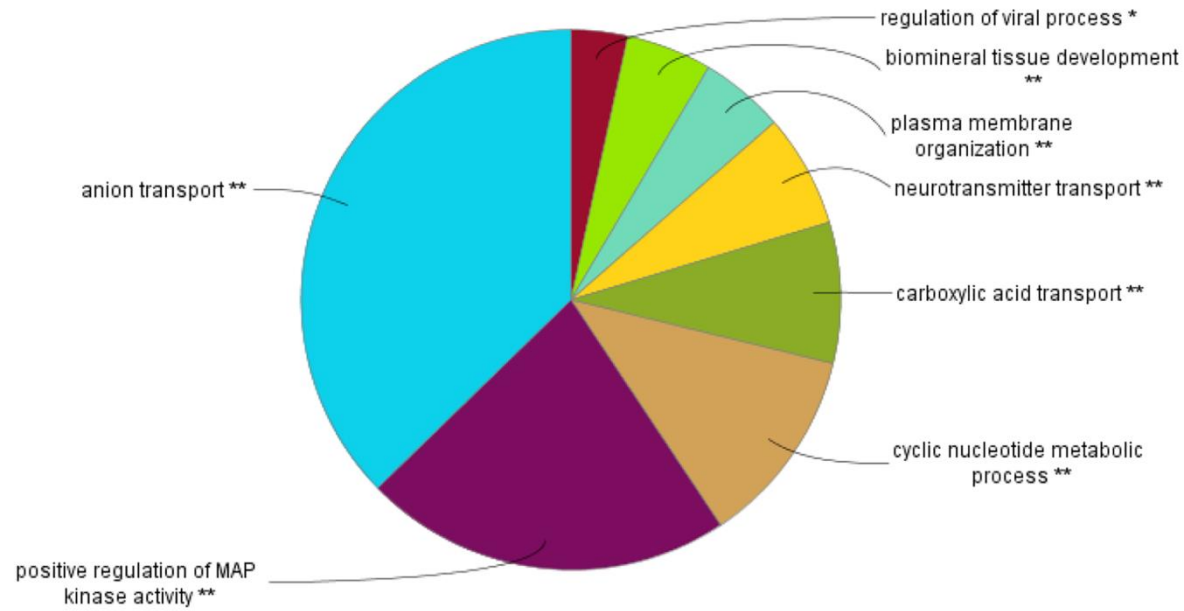

Figure 8.5 GO terms that were common between 5 and 15 hrs time-points

Functional map of differentially expressed genes (adjusted P value <0.05; fold change >1.5) enriched for GO biological process, cellular component and molecular functions terms. The chart fragments represent the number of genes associated with the terms as a proportion with the total number of genes within the GO term.

8.5.5 Hierarchical clustering analysis

Hierarchical clustering analysis (HCA) was performed using the DEGs obtained by RNA-Sequencing. For the HCA, DEGs counts among all the four groups (G1-G4) were visualised; however, our main focus was on the visualisation of the gene expression pattern between G2 and G4. The pattern of expression for the top 50 DEGs either in G2 or in G4 are presented in Figure 8.6a, b. A clear difference for the pattern of DEGs at the two time-points has been visualised.

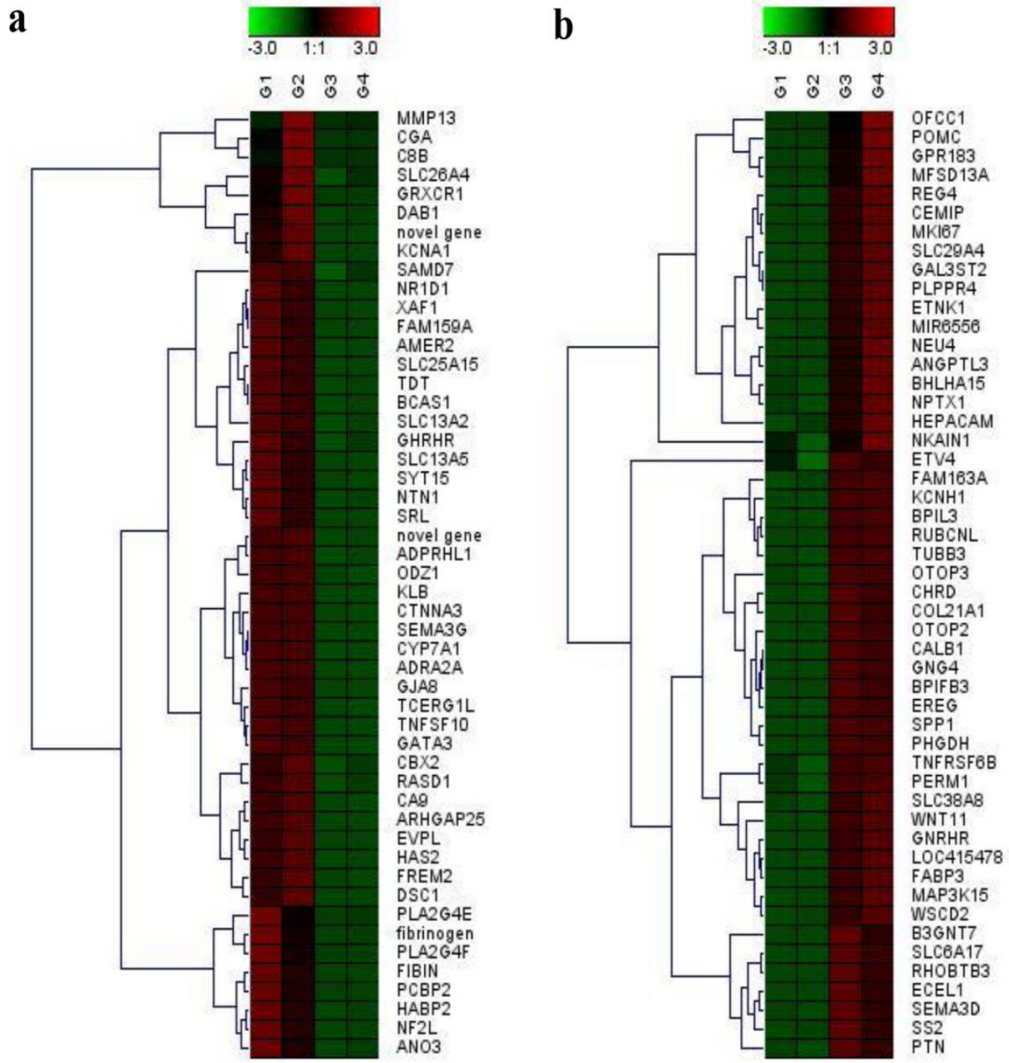

Figure 8.6 Hierarchical clustering analysis of the top 50 DEGs

(**a**) Top 50 DEGs selected for visualisation in G2 compared with G1, G3 and G4. (**b**) Top 50 DEGs selected for visualisation in G4 compared with G1, G2 and G3. G1 and G2 represent samples collected at 5 hr time-point, while G3 and G4 represent samples collected at 15 hr time-point. A clear pattern of expression is shown either between G1 and G3 or G2 and G4. The heatmap was generated in Genesis software.

8.5.6 Validation of RNA-Seq data by qPCR

All primers used for RNA-Seq data validation by qPCR were specific in amplifications (Figure 8.7a, b). The amplification efficiencies of individual primers have been depicted in Table 8.1. The expression levels of nineteen genes selected for validation of RNA-Seq data showed a positive linear relationship (Table 8.6).

The results suggested that the RNA-Seq is a good reference for expression profiling study and the assembly quality of the sequences was desirable. Although the magnitude of fold change obtained by qPCR and RNA-Sequencing was slightly different, the qPCR results demonstrated a similar trend (positive correlation) compared with the RNA-Sequencing for the 19 genes being tested (Table 8.6).

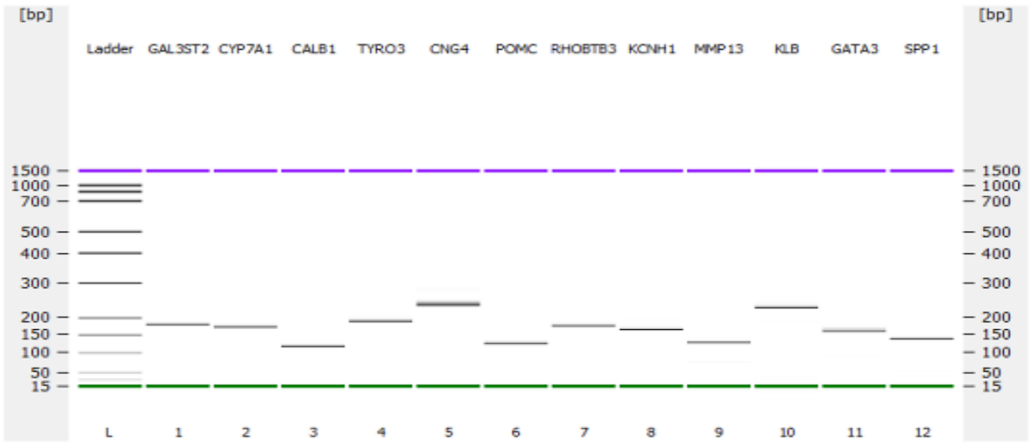

a

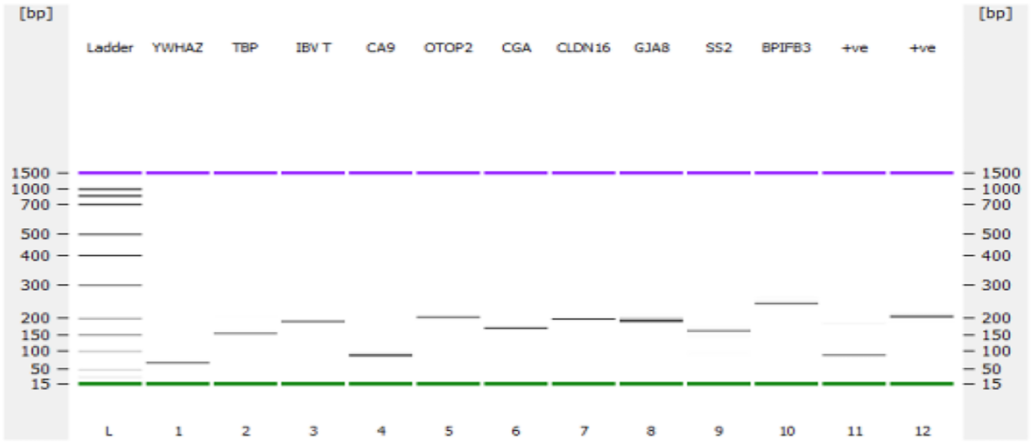

b

Figure 8.7 DNA gel electrophoresis of the qPCR products showing that the primers were specific in amplification

The upper (purple) and lower markers (green) act as internal standards and are used to align the ladder analysis with the individual DNA sample analysis. The standard curve (plotting migration time against DNA amplicon size), in conjunction with the markers, is then used to calculate DNA fragment sizes for each well from the migration times measured (see Agilent 2100 Bioanalyzer Users Guide for Molecular Assays). The DNA gel in Agilent 2100 Bioanalyzer was performed as per the manufacturer's instructions of Agilent DNA 1000 Kit.

Table 8.6 Comparison of the gene expression changes between G2 (5 hr time-point) vs G4 (15 hr time-point)

Group	Expression in respective group	Gene	Fold change	
			qPCR	RNA-Seq
G2	Up-regulated at 5 hr time-point	*CGA*	2.335	3.078
		CYP7A1	10.374	4.170
		GATA3	7.331	3.036
		GJA8	19.366	4.522
		MMP13	4.320	4.673
		TYRO3	4.249	1.942
		CA9	10.377	4.519
		KLB	38.019	5.998
G4	Up-regulated at 15 hr time-point	*GNG4*	5.427	6.586
		KCNH1	32.199	5.956
		BPIFB3	30.038	6.414
		POMC	316.268	9.179
		SPP1	306.140	7.993
		GAL3ST2	68.867	6.999
		OTOP2	12.366	4.226
		CALB1	74.817	8.081
		SS2	13.025	5.434
		CLDN16	5.378	3.212
		RHOBTB3	14.644	4.305

For qPCR, the relative expression level of genes was calculated between the G2 and G4 in qbase+ software based on $2^{\wedge\text{-}\Delta\Delta Cq}$ with genes amplification specific 242ignalling. *TBP* and *YWHAZ* were used as reference genes. All the genes tested were significantly expressed ($P < 0.05$) between the two groups (G2 vs G4). qPCR was performed to validate the DEGs between the two groups obtained in RNA-Seq analysis. Regression analysis showed a positive correlation ($R^2=0.526$; P value 0.004) between the qPCR and RNA-Seq data.

8.6 Discussion

Significant advances have been made in understanding the morphological and biochemical aspects of eggshell biogenesis, the molecular mechanism underpinning the formation of various layers of the eggshell formation is still not well understood. The present study focused on the effect of infectious bronchitis virus (IBV) challenge on the transcriptome of shell gland of brown-egg laying hens, aiming to shed further light on the regulation of genes in the presence of viral infection. As there were no DEGs found between the challenged and non-challenged laying hens, we focused further on the understanding of the expression of genes involved in eggshell formation when the egg was either in the distal magnum or isthmus (5 hr time-point, post oviposition time) or in the shell gland (15 hr time-point). Therefore, discussion is focussed on the data obtained from the RNA-Seq of the shell gland at

5 and 15 hr time-points. qPCR was also performed to validate the results of RNA-Seq. The results showed that the RNA-Seq data were comparable with the qPCR data and thus RNA-Seq was a reliable mechanism for obtaining expression data of the shell gland in an IBV infection model. The failure to detect of IBV virus in the samples from challenged birds (based on pieces of whole shell gland tissue) through RNA-Seq and qPCR might indicate that the levels of viral RNA in the isolated samples was low due to dilution of RNA from the cells of the muscle layers. However, the presence of viral RNA in the shell gland mucosal scrapings confirmed that the laying hens were successfully challenged and that virus was replicating in the shell gland tissue at days 9-10 p.i. Isolation of IBV RNA from the oviduct of laying hens at different post-infection times has yielded a variety of outcomes with virus being re-isolated at days 10-12 p.i, [83], 6-20 p.i. [82], one week p.i [84] and from the eggs laid up to 6 weeks post-infection and even from a small number of hatched chicks [85].

The lack of significant effect of IBV challenge on genes involved in eggshell formation, including the synthesis of PP IX, could be due to a combination of factors such as flock age, use of a whole piece of shell gland tissue as opposed to mucosal scrapings, genotype of bird and using an adjusted P value (cut-off <0.05) for RNA-Sequencing data analysis as opposed to using the raw P value. The egg quality analysis showed that the viral challenge significantly affected shell reflectivity, shell colour (L*), shell deformation, albumen height and Haugh unit at days 4-9 p.i. when compared with values at days 0 and 1 p.i. Shell colour was at its palest at days 5 and 6 p.i., which is earlier than has been reported in previous study [10]. From these findings, it appears that the viral load in the shell gland may have decreased by days 9-10 p.i. A better understanding of the effect of IBV challenge on eggshell formation including PP IX synthesis would have been obtained if the samples had been collected at days 5-6 p.i.; however, this information was available only after the analysis of the egg quality data at the end of the experiment. The lack of significant difference between the control and challenged groups for the expression of genes involved in the synthesis of PP IX was further confirmed by the quantification of PP IX from the shell gland tissue, which was not significantly different between the two groups (0.0877 and 0.0895 nMoles/g of tissue in the control and challenged groups, respectively). Hen age could be a contributing factor

as IB has more severe effects in young birds as compared with older flocks [20, 52, 53]. We did not compare the pathogenicity of IBV T with other strains; however, studies have shown that strains such as Arkansas [37] and Massachusetts are highly pathogenic for the oviduct [55] as compared with T strain. In Australia, studies with such pathogenic strains could not be performed for quarantine reasons. A severe decline in egg quality is not necessarily a feature of infection with IBV T. An adjusted P value (<0.05) was used for comparison of RNA-Sequencing data between the control and challenged groups; this could also have been a contributing factor to the lack of significant difference between the challenged and control groups. When the data between the control and challenged groups were separated on the basis of P value (<0.05), there were 57 DEGs genes between the two groups with a major GO terms as negative regulation of viral process (GO:0048525) and defence response to virus (GO:0051607) (Appendix A). This confirms that viral challenge affected the expression level of some genes but not to a great extent. If birds had been sampled at 5-6 days p.i., the outcome may have been different.

The RNA-Seq analysis revealed a number of DEGs between the two time-points (5 and 15 hrs; post-oviposition time) of eggshell formation. The GO term anion transport (GO:0006820) may indicate that the genes involved in transport of ions across cell membrane were significantly up-regulated. This would indicate that the synthesis and secretory activities in the shell gland cells were already initiated while the egg was still forming in the distal magnum or isthmus. Among those, *SLC13A5* plays an important role in transporting ions and/or molecules across cell membranes. A significantly higher fold change (6.516) of *SLC13A5* at 5 hr time-point compared with 15 hr time-point might reflect its role in transportation of ions for the initiation of synthesis of molecules involved in eggshell formation. The genes *SLC13A5* and *SLC13A2* belong to solute carrier family 13 group of proteins and are sodium-dependent citrate cotransporters in regulating metabolic processes. Among its related pathways are transport of various sugars, bile salts and organic acids, metal ions and amine compounds. In the GO term synaptic vesicle localisation, most of the genes involved function in transportation of synaptic vesicles across cell membrane. It seems that the genes in this pathway mainly performed activities in neurotransmission necessary for the transport and synthesis of various molecules including hormones. Organic anion transport was the third

most enriched GO term. Some of the genes that were annotated to anion transport also served as transporters for organic anions across cell membrane. Organic anions contain molecules that are negatively charged and contain carbon in covalent linkage. The significantly enriched GO term secretion may indicate the synthesis of substances that were either directly involved in eggshell formation or served a role in transportation of other molecules such as hormones. The enriched GO term signal release indicates that signal secretion to the extracellular medium from a cellular source was occurring around 5 hr time-point. This may indicate that the shell gland cells were actively involved in the synthesis of molecules necessary for either cellular function or eggshell formation.

In G4 (15 hr time-point), the GO term regulation of phospholipase activity (GO:0010517) shows that the hydrolysis of lipids was higher in order to produce energy for the synthetic processes of eggshell formation. Among these genes, *CEMIP, ANGPTL3, WNT11, EREG, MAP3K15* and *SLC20A1* were highly expressed with fold changes of 7.555, 6.198, 4.799, 3.867, 3.736 and 3.302, respectively. *CEMIP* is mainly involved in metabolism and glycosaminoglycan metabolism pathways. The N terminal chain of *ANGPTL3* is important for lipid metabolism. The *WNT11* gene functions in developmental processes and its higher expression may reflect its direct role in eggshell formation. Significantly higher expression of *CALB1* at 15 vs 5 hr time-point confirms a higher rate of calcium transportation across the cell membrane during the peak stage of eggshell formation. A higher expression of *CALB1* during eggshell calcification has been reported [86-88]. Low free Ca^{+} in cell is maintained by calcium uptake in the endoplasmic reticulum through ATP dependent calcium pumps [86]. ATP2A3 appears to be playing role in this Ca^{+} balance, which is confirmed by its up-regulation (log fold change 3.484) at 15 hr vs 5 hr time-point. Significantly higher expression of *BPIFB3* (*OCX-36*) at 15 vs 5 hr time-point indicates the importance of OCX-36 protein in the shell matrix. OCX-36 is lipopolysaccharide-binding protein that is present in various layers of the eggshell and possesses antibacterial activity [5]. In addition, the second most enriched GO term, alanine transport (GO:0032328) indicated that the alanine, 2-aminopropanoic acid transport across the cell was higher, which might be involved in energy generation during eggshell formation. Significantly up-regulated *SLC6A17* (log fold change 6.642) at 15 vs 5

hr time-point indicates its role in the analine transport pathway. The transmembrane receptor protein tyrosine kinase 246ignalling pathway (GO:0007169) is usually initiated by the binding of an extracellular ligand to a receptor on the surface of the target cell where the receptor possesses tyrosine kinase activity to regulate transcription. The most enriched GO:0007169 might indicate higher transcriptional activities of the cells being involved in the synthesis and secretion of macromolecules needed for eggshell formation. The GO enriched term regulation of blood vessel diameter (GO:0097746) might indicate that the blood flow to the shell gland at 15 hr time-point was significantly affected by the eggshell formation as has been shown previously [89]. The GO term 3',5'-cyclic-nucleotide phosphodiesterase activity (GO:0004114) indicates that these genes were mainly involved in the catalysis of the reaction: nucleoside 3',5'-cyclic phosphate + H2O = nucleoside 5'-phosphate. The genes involved in GO:0004114 encode enzymes that degrade the phosphodiester bond in cAMP and cGMP molecules. The up-regulation of these genes in the shell gland may indicate their role in energy production during the synthesis of various molecules.

The common GO terms between 5 and 15 hrs time-points indicate that the metabolic activities in the shell gland were already initiated when the egg was forming in the distal magnum and/or isthmus. It appears that activities in the shell gland might have increased significantly when egg formation was passing through a peak formation stage (15 hr time-point). Furthermore, the common GO terms also indicate that such activities are necessary for the normal metabolic processes happening in cells at all times.

The alignment of the sequences with unknown gene/protein functions suggests that these genes are vital to shell gland function. The majority of the DEGs with unknown functions were from the 15 hr time-point, further confirming that these genes were significantly up-regulated while eggshell formation was at its peak in the shell gland. The associated GO terms ranged from calcium ion binding to receptor activity. A large number of novel linc RNA might indicate their role as regulators in the shell gland of laying hens. Further studies are recommended to investigate the spatio-temporal expression of genes involved in the synthesis of various eggshell layers and role of microRNA and lincRNA in the regulation of genes involved in the eggshell formation.

8.7 Conclusions

Overall, between the control and challenged groups, a lack of significant differences in the expression level of the genes involved in eggshell formation and the mucosal immune system could be due to the time interval between the day of challenge and sampling time. Other contributing factors to these findings could be taking a whole piece of shell gland tissue and bird age. The DEGs at the 5 hr time-point may indicate that the synthesis activities were already initiated in the shell gland when the egg was still forming in the distal magnum or isthmus regions of the oviduct. The DEGs at the 15 time-point reflect the phospholipid activities and synthesis or transport of molecules for the peak period of eggshell formation. The findings in the current study improve our understanding of eggshell formation at molecular level.

8.8 References

1. Bain M. Egg composition and chemistry. In: Edited by Roberts J, Achieving sustainable production of eggs. vol. 1. UK: Burleigh Dodds Science Publishing Limited; 2017: 3-23.
2. Hincke MT, Nys Y, Gautron J, Mann K, Rodriguez-Navarro AB, McKee MD: The eggshell: structure, composition and mineralization. Front Biosci. 2012;17:1266-1280.
3. Nys Y, Mayel-Afshar S, Bouillon R, Van Baelen H, Lawson DEM: Increases in calbindin D 28K mRNA in the uterus of the domestic fowl induced by sexual maturity and shell formation. Gen Comp Endocrinol. 1989;76:322-329.
4. Kovacs-Nolan J, Cordeiro C, Young D, Mine Y, Hincke M: Ovocalyxin-36 is an effector protein modulating the production of proinflammatory mediators. Vet Immunol Immunopathol. 2014;160:1-11.
5. Gautron J, Murayama E, Vignal A, Morisson M, McKee MD, Réhault S, Labas V, Belghazi M, Vidal M-L, Nys Y *et al*: Cloning of ovocalyxin-36, a novel chicken eggshell protein related to lipopolysaccharide-binding

proteins, bactericidal permeability-increasing proteins, and plunc family proteins. J Biol Chem. 2007;282:5273-5286.

6. Mann K, Siedler F: The amino acid sequence of ovocleidin 17, a major protein of the avian eggshell calcified layer. Biochem Mol Biol Int. 1999;47:997-1007.

7. Gautron J, Hincke MT, Mann K, Panhéleux M, Bain M, McKee MD, Solomon SE, Nys Y: Ovocalyxin-32, a novel chicken eggshell matrix protein isolation, amino acid sequencing, cloning, and immunocytochemical localization. J Biol Chem. 2001;276:39243-39252.

8. Marie P, Labas V, Brionne A, Harichaux G, Hennequet-Antier C, Nys Y, Gautron J: Quantitative proteomics and bioinformatic analysis provide new insight into protein function during avian eggshell biomineralization. J Proteomics. 2015;113:178-193.

9. Huh M-I, Jung J-C: Expression of matrix metalloproteinase-13 (MMP-13) in the testes of growing and adult chicken. Acta Histochem. 2013;115:475-480.

10. Chousalkar KK, Roberts JR: Effects of Australian strains of infectious bronchitis virus on internal and external quality of hen eggs. Animal Production Science. 2009;49:162-169.

11. Sevoian M, Levine PP: Effects of infectious bronchitis on the reproductive tracts, egg production, and egg quality of laying chickens. Avian Dis. 1957;1:136-164.

12. Butler EJ, Curtis MJ, Pearson AW, McDougall JS: Effect of infectious bronchitis on the structure and composition of egg albumen. J Sci Food Agric. 1972;23:359-369.

13. Boursnell ME, Brown TDK, Foulds IJ, Green PF, Tomley FM, Binns MM: Completion of the sequence of the genome of the coronavirus avian infectious bronchitis virus. J Gen Virol. 1987;68:57-77.

14. Boursnell MEG, Binns MM, Brown TDK, Cavanagh D, Tomley FM: Molecular biology of avian infectious bronchitis virus. Prog Vet Microbiol Immunol. 1989;5:65-82.

15. Cavanagh D: Coronavirus avian infectious bronchitis virus. Vet Res. 2007;38:281-297.

16. Jackwood MW, de Wit S. Infectious bronchitis. In: Edited by Swayne DE, Diseases of poultry. 13 edn. Wiley-Blackwell; 2013: 139-160.

17. Chong KT, Apostolov K: The pathogenesis of nephritis in chickens induced by infectious bronchitis virus. J Comp Pathol. 1982;92:199-211.

18. Cumming RB: Infectious avian nephrosis (uraemia) in Australia. Aust Vet J. 1963;39:145-147.

19. Chew PH, Wakenell PS, Farver TB: Pathogenicity of attenuated infectious bronchitis viruses for oviducts of chickens exposed *in ovo*. Avian Dis. 1997;41:598-603.

20. Crinion RAP, Hofstad MS: Pathogenicity of two embryo-passage levels of avian infectious bronchitis virus for the oviduct of young chickens of various ages. Avian Dis. 1972;16:967-973.

21. Chousalkar KK, Roberts JR: Ultrastructural study of infectious bronchitis virus infection in infundibulum and magnum of commercial laying hens. Vet Microbiol. 2007;122:223-236.

22. Chousalkar KK, Roberts JR: Ultrastructural observations on effects of infectious bronchitis virus in eggshell-forming regions of the oviduct of the commercial laying hen. Poult Sci. 2007;86:1915-1919.

23. Hofstad MS, Yoder HW: Avian infectious bronchitis: Virus distribution in tissues of chicks. Avian Dis. 1966;10:230-239.

24. Darbyshire JH, Cook JKA, Peters RW: Growth comparisons of avian infectious bronchitis virus strains in organ cultures of chicken tissues. Arch Virol. 1978;56:317-325.

25. Darbyshire JH, Cook JK, Peters RW: Organ culture studies on the efficiency of infection of chicken tissues with avian infectious bronchitis virus. Br J Exp Pathol. 1976;57:443-454.

26. Cavanagh D: A nomenclature for avian coronavirus isolates and the question of species status. Avian Pathol. 2001;30:109-115.

27. Kottier SA, Cavanagh D, Britton P: Experimental evidence of recombination in coronavirus infectious bronchitis virus. Virology. 1995;213:569-580.

28. Brooks JE, Rainer AC, Parr RL, Woolcock P, Hoerr F, Collisson EW: Comparisons of envelope through 5B sequences of infectious bronchitis coronaviruses indicates recombination occurs in the envelope and membrane genes. Virus Res. 2004;100:191-198.

29. Cavanagh D, Davis PJ, Cook JKA, Li D, Kant A, Koch G: Location of the amino acid differences in the S1 spike glycoprotein subunit of closely related serotypes of infectious bronchitis virus. Avian Pathol. 1992;21:33-43.

30. Winterfield RW, Albassam MA: Nephropathogenicity of infectious bronchitis virus. Poult Sci. 1984;63:2358-2363.

31. Ignjatovic J, Ashton D, Reece R, Scott P, Hooper P: Pathogenicity of Australian strains of avian infectious bronchitis virus. J Comp Pathol. 2002;126:115-123.

32. Chandra M: Comparative nephropathogenicity of different strains of infectious bronchitis virus in chickens. Poult Sci. 1987;66:954-959.

33. Box PG, Holmes HC, Finney PM, Froymann R: Infectious bronchitis in laying hens: The relationship between haemagglutination inhibition antibody levels and resistance to experimental challenge. Avian Pathol. 1988;17:349-361.

34. Raj GD, Jones RC: An *in vitro* comparison of the virulence of seven strains of infectious bronchitis virus using tracheal and oviduct organ cultures. Avian Pathol. 1996;25:649-662.

35. Cook JKA: The classification of new serotypes of infectious bronchitis virus isolated from poultry flocks in Britain between 1981 and 1983. Avian Pathol. 1984;13:733-741.

36. Broadfoot DI, Smith WM: Effects of infectious bronchitis in laying hens on egg production, percent unsettable eggs and hatchability. Poult Sci. 1954;33:653-654.

37. Muneer MA, Newman JA, Halvorson DA, Sivanandan V, Coon CN: Effects of avian infectious bronchitis virus (Arkansas strain) on vaccinated laying chickens. Avian Dis. 1987;31:820-828.

38. Mcdougal JS: Infectious bronchitis in laying fowls-its effect upon egg production and subsequent egg quality. Vet Rec. 1968;83:84-86.

39. Raj GD, Jones RC: Protectotypic differentiation of avian infectious bronchitis viruses using an *in vitro* challenge model. Vet Microbiol. 1996;53:239-252.

40. Ignjatovic J, Galli U: Immune responses to structural proteins of avian infectious bronchitis virus. Avian Pathol. 1995;24:313-332.

41. Hawkes RA, Darbyshire JH, Peters RW, Mockett APA, Cavanagh D: Presence of viral antigens and antibody in the trachea of chickens infected with avian infectious bronchitis virus. Avian Pathol. 1983;12:331-340.

42. Raj GD, Jones RC: Local antibody production in the oviduct and gut of hens infected with a variant strain of infectious bronchitis virus. Vet Immunol Immunopathol. 1996;53:147-161.

43. Lohr JE, Hinze V, Kaleta EF: Immunological relationship between the New Zealand A and the Australian T strains of infectious bronchitis virus as measured by cross-immunisation tests in tracheal organ cultures from immunised birds. N Z Vet J. 1991;39:113-114.

44. Nakamura K, Cook JKA, Otsuki K, Huggins MB, Frazier JA: Comparative study of respiratory lesions in two chicken lines of different susceptibility infected with infectious bronchitis virus: histology, ultrastructure and immunohistochemistry. Avian Pathol. 1991;20:241-257.

45. Collisson EW, Pei J, Dzielawa J, Seo SH: Cytotoxic T lymphocytes are critical in the control of infectious bronchitis virus in poultry. Dev Comp Immunol. 2000;24:187-200.

46. Seo SH, Collisson EW: Specific cytotoxic T lymphocytes are involved in *in vivo* clearance of infectious bronchitis virus. J Virol. 1997;71:5173-5177.

47. Ariaans MP, van de Haar PM, Hensen EJ, Vervelde L: Infectious Bronchitis Virus induces acute interferon-gamma production through polyclonal stimulation of chicken leukocytes. Virology. 2009;385:68-73.

48. Hackney K, Cavanagh D, Kaiser P, Britton P: *In vitro* and *in ovo* expression of chicken gamma interferon by a defective RNA of avian coronavirus infectious bronchitis virus. J Virol. 2003;77:5694-5702.

49. Otsuki K, Nakamura T, Kawaoka Y, Tsubokura M: Interferon induction by several strains of avian infectious bronchitis virus, a coronavirus, in chickens. Acta Virol. 1988;32:55-59.

50. Asif M, Lowenthal JW, Ford ME, Schat KA, Kimpton WG, Bean AGD: Interleukin-6 expression after infectious bronchitis virus infection in chickens. Viral Immunol. 2007;20:479-486.

51. Bumstead N, Huggins MB, Cook JKA: Genetic differences in susceptibility to a mixture of avian infectious bronchitis virus and *Escherichia coli.* Br Poult Sci. 1989;30:39-48.

52. Animas SB, Otsuki K, Hanayama M, Sanekata T, Tsubokura M: Experimental infection with avian infectious bronchitis virus (Kagoshima-34 strain) in chicks at different ages. J Vet Med Sci. 1994;56:443-447.

53. Animas SB, Otsuki K, Tsubokura M, Jane KA: Comparison of the susceptibility of chicks of different ages to infection with nephrosis/nephritis-causing strain of infectious bronchitis virus. J Vet Med Sci. 1994;56:449-453.

54. Smith WH, Cook JK, Parsell ZE: The experimental infection of chickens with mixtures of infectious bronchitis virus and *Escherichia coli*. J Gen Virol. 1985;66:777-786.

55. Crinion RAP, Hofstad MS: Pathogenicity of four serotypes of avian infectious bronchitis virus for the oviduct of young chickens of various ages. Avian Dis. 1972;16:351-363.

56. Albassam MA, Winterfield RW, Thacker HL: Comparison of the nephropathogenicity of four strains of infectious bronchitis virus. Avian Dis. 1986;30:468-476.

57. Villegas P, Purchase HG: Titration of biological suspensions. A laboratory manual for the isolation and identification of avian pathogens, 4th ed DE Swayne, JR Glisson, MW Jackwood, JE Pearson, and WM Reed, eds

American Association of Avian Pathologists, Kennett Square, PA. 1998:248-253.

58. Senne DA: Virus propagation in embryonating eggs. A laboratory manual for the isolation and identification of avian pathogens. 1998:235-240.

59. Reed LJ, Muench H: A simple method of estimating fifty per cent endpoints. American Journal of Epidemiology. 1938;27:493-497.

60. FastQC: a quality control tool for high throughput sequence data. Available online at: http://www.bioinformatics.babraham.ac.uk/projects/fastqc

61. Hillier LW, Miller W, Birney E, Warren W, Hardison RC, Ponting CP, Bork P, Burt DW, Groenen MA, Delany ME: Sequence and comparative analysis of the chicken genome provide unique perspectives on vertebrate evolution. Nature. 2004;432:695-716.

62. Kim D, Pertea G, Trapnell C, Pimentel H, Kelley R, Salzberg SL: TopHat2: accurate alignment of transcriptomes in the presence of insertions, deletions and gene fusions. Genome Biol. 2013;14:R36.

63. Robinson MD, McCarthy DJ, Smyth GK: edgeR: a Bioconductor package for differential expression analysis of digital gene expression data. Bioinformatics. 2010;26:139-140.

64. Ritchie ME, Phipson B, Wu D, Hu Y, Law CW, Shi W, Smyth GK: limma powers differential expression analyses for RNA-sequencing and microarray studies. Nucleic Acids Res. 2015;43:e47.

65. Sturn A, Quackenbush J, Trajanoski Z: Genesis: cluster analysis of microarray data. Bioinformatics. 2002;18:207-208.

66. Bindea G, Mlecnik B, Hackl H, Charoentong P, Tosolini M, Kirilovsky A, Fridman W-H, Pagès F, Trajanoski Z, Galon J: ClueGO: a Cytoscape plug-in to decipher functionally grouped gene ontology and pathway annotation networks. Bioinformatics. 2009;25:1091-1093.

67. Mlecnik B, Galon J, Bindea G: Comprehensive functional analysis of large lists of genes and proteins: *J Proteomics.* 2017; DOI: 10.1016/j.jprot.2017.03.016.

68. Bindea G, Galon J, Mlecnik B: CluePedia Cytoscape plugin: pathway insights using integrated experimental and in silico data. Bioinformatics. 2013;29:661-663.

69. Cline MS, Smoot M, Cerami E, Kuchinsky A, Landys N, Workman C, Christmas R, Avila-Campilo I, Creech M, Gross B: Integration of biological networks and gene expression data using Cytoscape. Nat Protoc. 2007;2:2366-2382.

70. Hamzić E, Kjærup RB, Mach N, Minozzi G, Strozzi F, Gualdi V, Williams JL, Chen J, Wattrang E, Buitenhuis B: RNA sequencing-based analysis of the spleen transcriptome following infectious bronchitis virus infection of chickens selected for different mannose-binding lectin serum concentrations. BMC Genomics. 2016;17:82.

71. Benjamini Y, Hochberg Y: Controlling the false discovery rate: a practical and powerful approach to multiple testing. Journal of the royal statistical society Series B (Methodological). 1995:289-300.

72. ClueGO documentation [http://www.ici.upmc.fr/cluego/ClueGODocumentation.pdf]

73. Rasmussen R. Quantification on the LightCycler. In, Rapid cycle real-time PCR. Springer; 2001: 21-34.

74. Hellemans J, Mortier G, De Paepe A, Speleman F, Vandesompele J: qBase relative quantification framework and software for management and automated analysis of real-time quantitative PCR data. Genome Biol. 2007;8:R19.

75. Bio-Rad Application User Guide. http://www.bio-rad.com/webroot/web/pdf/lsr/literature/Bulletin_5279.pdf

76. Bustin SA, Benes V, Garson JA, Hellemans J, Huggett J, Kubista M, Mueller R, Nolan T, Pfaffl MW, Shipley GL: The MIQE guidelines: minimum information for publication of quantitative real-time PCR experiments. Clin Chem. 2009;55:611-622.

77. Ginzinger DG: Gene quantification using real-time quantitative PCR: An emerging technology hits the mainstream. Exp Hematol. 2002;30:503-512.

78. Li YP, Bang DD, Handberg KJ, Jorgensen PH, Zhang MF: Evaluation of the suitability of six host genes as internal control in real-time RT-PCR assays in chicken embryo cell cultures infected with infectious bursal disease virus. Vet Microbiol. 2005;110:155-165.

79. Bagés S, Estany J, Tor M, Pena RN: Investigating reference genes for quantitative real-time PCR analysis across four chicken tissues. Gene. 2015;561:82-87.

80. qbase+ qPCR data analysis software version 3.0: https://www.qbaseplus.com/

81. Pfaffl MW: A new mathematical model for relative quantification in real-time RT–PCR. Nucleic Acids Res. 2001;29:e45-e45.

82. Chousalkar KK, Cheetham BF, Roberts JR: LNA probe-based real-time RT-PCR for the detection of infectious bronchitis virus from the oviduct of unvaccinated and vaccinated laying hens. J Virol Methods. 2009;155:67-71.

83. Chousalkar KK, Cheetham BF, Roberts JR: Detection of infectious bronchitis virus strain N1/88 from the oviduct and feces of experimentally infected vaccinated and unvaccinated hens. Poult Sci. 2010;89:1603-1608.

84. Gough RE, Alexander DJ: Comparison of duration of immunity in chickens infected with a live infectious bronchitis vaccine by three different routes. Res Vet Sci. 1979;26:329-332.

85. Cook JKA: Recovery of infectious bronchitis virus from eggs and chicks produced by experimentally inoculated hens. J Comp Pathol. 1971;81:203-211.

86. Brionne A, Nys Y, Hennequet-Antier C, Gautron J: Hen uterine gene expression profiling during eggshell formation reveals putative proteins involved in the supply of minerals or in the shell mineralization process. BMC Genomics. 2014;15:220.

87. Bar A, Striem S, Mayel-Afshar S, Lawson DEM: Differential regulation of calbindin-D28K mRNA in the intestine and eggshell gland of the laying hen. J Mol Endocrinol. 1990;4:93-99.

88. Jeong W, Lim W, Kim J, Ahn SE, Lee HC, Jeong J-W, Han JY, Song G, Bazer FW: Cell-specific and temporal aspects of gene expression in the

chicken oviduct at different stages of the laying cycle. Biol Reprod. 2012;86:172.

89. Wolfenson D, Frei YF, Berman A: Responses of the reproductive vascular system during the egg-formation cycle of unanaesthetised laying hens. Br Poult Sci. 1982;23:425-431.

Higher Degree Research Thesis by Publication
University of New England

STATEMENT OF AUTHORS' CONTRIBUTION

(To appear at the end of each thesis chapter submitted as an article/paper)

We, the Research Master/PhD candidate and the candidate's Principal Supervisor, certify that all co-authors have consented to their work being included in the thesis and they have accepted the candidate's contribution as indicated in the *Statement of Originality*.

	Author's Name (please print clearly)	% of contribution
Candidate	**Sami Samiullah**	60
Other Authors	**Shu-Biao Wu**	25
	Juliet Roberts	15

Name of Candidate: **Samiullah**

Name/title of Principal Supervisor: **Associate Professor Juliet Roberts**



Candidate Date 09/06/2017



Principal Supervisor Date 09/06/2017

Higher Degree Research Thesis by Publication
University of New England

STATEMENT OF ORIGINALITY

(To appear at the end of each thesis chapter submitted as an article/paper)

We, the Research Master/PhD candidate and the candidate's Principal Supervisor, certify that the following text, figures and diagrams are the candidate's original work.

Type of work	**Page number/s**
Figure 8.1	223
Figure 8.2	230
Figure 8.3	232
Figure 8.4	238
Figure 8.5	239
Figure 8.6	240
Figure 8.7	241
Text and tables	217-256

Name of Candidate: **Samiullah**

Name/title of Principal Supervisor: **Associate Professor Juliet Roberts**

[redacted]

Candidate Date 09/06/2017

[redacted]

PrincipalSupervisor Date 09/06/2017

Chapter 9 Mitochondrial count in oviduct of laying hens challenged with infectious bronchitis virus

Sami Samiullah[1], Shu-Biao Wu[1] and Juliet Roberts[1]

[1]Animal Science, School of Environmental and Rural Science, University of New England, Armidale, New South Wales, 2351, Australia

To be submitted to: Biology of Reproduction

9.1 Abstract

Mitochondrial count per cell was determined in relation to time-points post-oviposition of egg formation in three different segments of the oviduct of laying hens 9-10 days following challenge with infectious bronchitis virus (IBV) T and Vic S strains. In the shell gland, the mitochondrial count per cell was significantly lower ($P < 0.05$) in the IBV T strain group compared with the control group; however, there was no difference for the Vic S strain challenged group. The mitochondrial count per cell did not vary significantly between the control and IBV challenged groups in the isthmus and magnum regions of the oviduct. The relative expression levels of nuclear DNA encoding genes involved in mitochondrial biogenesis and fission were studied in the shell gland tissue of IBV challenged and control groups at different time-points of eggshell formation. There were no significant differences in expression level of any of the genes between the control and IBV challenged groups. The expression levels of *CS* and *Drp1* genes were significantly lower at 5 hr compared with the 15 hr time-point. The expression level of *SDHA* and *CYC, S* genes were significantly higher at 15 hr compared with the 5 hr time-point. The expression level of *PGC-1α*, a master regulator of mitochondrial biogenesis, was not significantly affected by time-point.

It can be concluded that IBV T strain infection in laying hens reduced the mean mitochondrial count per cell only in the shell gland region of the oviduct. The genes involved in mitochondrial biogenesis or function showed no clear pattern of

expression that correlates with the mean mitochondrial count per cell in the shell gland of oviduct of hens challenged with T strain infectious bronchitis virus.

9.2 Introduction

The four main segments of the oviduct of the laying hen that are involved in egg formation are infundibulum, magnum, isthmus and shell gland (uterus). The isthmus and shell gland are involved primarily in eggshell formation. Egg formation is regulated by steroid hormones, which regulate the proliferation and growth of oviducal epithelial cells. The administration of estrogen and/or progesterone leads to massive growth of the epithelia in the oviduct of juvenile hens [1-3]. An egg is composed of egg internal contents and eggshell. Among the internal contents, albumen is secreted by the magnum, which is composed mainly of ovalbumin, muco-proteins and globulins [4]. The shell membranes are synthesized in the isthmus region of the oviduct and are mainly composed of fibrous proteins, such as collagen [5]. However, eggshell membranes also contain glycosaminoglycans, such as dermatan sulphate and chondroitin sulphate and sulphated glycoproteins including hexosamines, such as glucosamine [5]. Eggshell formation takes place in the shell gland region of the oviduct and is composed mainly of calcium carbonate [6] and shell matrix proteins, such as the ovocalyxin family [5].

Mitochondria play a vital role in cellular metabolism, calcium handling, heme biosynthesis, cell differentiation, apoptosis and aging [7-9]. Chicken mitochondrial DNA (mtDNA) consists of 16775 bp that encode genes for 13 polypeptides, 2 rRNA, 22 tRNA, non-coding regions of light-strand replication point and a displacement-loop (D-loop) [10-14]. Previously, it has been shown that mitochondrial count varies depending on energy demands of a cell, as well as the age and sex of an organism, the organ and patho-physiological conditions [15-19]. A higher mitochondrial respiratory capacity and count has been recorded in physically active human beings [20, 21]. Similarly, in the rat, increases in mitochondrial mass (mtDNA) have been observed during muscle development [22] and in brown adipose tissue of various mammals in response to low temperature [23]. Throughout the cell cycle, mitochondria undergo changes in number, shape and location; however, it is not known how quickly mitochondria divide in

metabolically active and inactive cells. Also, it is not clear for the oviduct of laying hens, if the need for ATP increases, how mitochondria respond by either inducing mitochondrial division or accelerating mitochondrial function without undergoing division. A type of retrograde communication may also occur in which cells can respond to changes in mitochondrial activity with changes in nuclear gene expression (reviewed in [24]). mtDNA replication is independent of the cell cycle and is controlled by the nuclear DNA encoded polymerase γ (POLγA) and mitochondrial transcription factor A [25, 26]. mtDNA replication machinery synthesizes different proteins that include the catalytic subunit of DNA POLγA and processivity factor (POLγB), the mitochondrial single-stranded DNA binding protein (mtSSB), the replicative helicase TWINKLE and the mitochondrial RNA polymerase (POLYRMT) [27, 28]. The main regulator of mitochondrial division is the dynamin-related protein Drp1 (DNM1L), which is recruited and stimulated to oligomerize by Mdv1 bound to the outer mitochondrial membrane via Fis1 [29-32]. All proteins essential for mtDNA maintenance and expression are encoded by the nuclear genome and imported into the mitochondria after protein synthesis in the cytosol [28]. Therefore, expression of the mtDNA and nuclear genomes must be coordinated in order to regulate oxidative phosphorylation capacity in response to changes in physiological demands of cells [33]. Studies in human HeLa cells, the yeast *Candida albicans* and algae showed that increase in mitochondrial count occurs continuously during the cell cycle and is well correlated with the increase in cell volume [34-36]. In human HeLa and *Candida albicans* cells, the mitochondrial volume makes up about 10% of the total cell volume at any time during the cell cycle, while in algae this value is much lower (3%) but also constant throughout cell division [34-36]. To study the mitochondrial activity in the chicken, such information needs to be established. Citrate synthase (CS) is a nuclear encoded enzyme synthesized in cytoplasmic ribosomes and is localized in the mitochondrial matrix [37]. In mammals, the *CS* gene has been extensively used as a marker for intact mitochondrial density [38-40]; however, its role has been questioned in developmental stages [41], age related [42] and physical activity studies [43]. *CS* has been shown to be positively correlated with acute exercise activities in mammalian muscles [44, 45]. Succinate dehydrogenase complex, subunit A (*SDHA*) gene, encodes a major catalytic subunit of succinate-ubiquinone

oxidoreductase, a complex of the mitochondrial respiratory chain. SDHA gene provides instructions for making one of four parts (subunits) of the succinate dehydrogenase (SDH) enzyme. SDH then participates in both the citric acid cycle and the electron transport chain. Peroxisome proliferator-activated receptor gamma coactivator 1-alpha **(***PGC-1α/PPARGC1A*) is the master regulator in mitochondrial biogenesis [46]. Overexpression studies in mammalian cells in culture or in transgenic mice have shown that PGC-1α is capable of activating the expression of a cascade of genes involved in mitochondrial biogenesis and respiratory function in adipocytes, cardiac myocytes and myogenic cells [47-49]. Thus, *PGC-1α* is mainly involved in mitochondrial energy metabolism and mitochondrial biogenesis. Cytochrome C somatic (*CYC, S*) gene encodes cytochrome C enzyme that plays a role in the electron transport chain in mitochondria and during apoptosis. Na^+-K^+ *ATPase* gene encodes an enzyme that is an integral membrane protein which consists of α and β subunits [50]. This enzyme plays an essential role in maintaining the transmembrane gradient of Na^+ and K^+ ions in cells [51].

Infectious bronchitis virus (IBV) is a highly contagious mucosal pathogen of both broiler and layer chickens worldwide [52]. Similar to other coronaviruses, the lipid envelope of IBV contains at least three proteins: the small membrane protein (E), the integral membrane protein (M) and the spike glycoprotein (S) [53]. The S protein is composed of two subunits, the S1 (head) and the S2 (stalk) that is responsible for binding to the target cell receptor and fusion of the viral and cellular membranes [54, 55]. The N protein induces cell mediated immunity [56]. There is not much information about whether IBV entry and fusion occur following endocytosis or at the cell membrane [55, 57] and thus the nature of IBV fusion during entry into host cells remains ambiguous. Studies have shown that fusion does not occur at neutral pH and fusion activation is a direct low pH dependent process occurring within acidic endosomes [58]. Among other host cell surface receptors, sialic acid has been shown to act as a receptor for binding of IBV spike proteins in respiratory, kidney and oviduct epithelia [59-62]. Although all ages are susceptible, very young chicks exhibit more severe respiratory signs and much higher mortality compared with older birds [63]. Mortality rates depend upon viral strain, age and immune status of the bird [64]. Among all the field strains of Australian IBV, T (N1/62) is considered the most virulent in inducing pathological changes in the

tracheal, kidney and oviduct epithelia of laying hens. Infection with IBV in the oviduct leads to various degree pathogenesis in the oviduct and reduction in egg production [65-70].

The present study determined mean mitochondrial count per cell in different segments of the oviduct of laying hens. An IBV *in vivo* infection model using T (N1/62) and Vic S strains was employed to study any possible variation in mitochondrial count. Furthermore, nuclear DNA encoded genes were studied in the shell gland to gain insights into any variation of mitochondrial count in the shell gland region of the oviduct in response to IBV infection.

9.3 Materials and Methods

9.3.1 Rearing of IBV free laying hens and IBV challenge

The experimental setup was approved by the University of New England, Animal Ethics Approval Committee under Authority No. AEC15-118. The protocol was carried out in accordance with the guidelines specified in the Australian Code for the Care and Use of Animals for Scientific Purposes 8th edition 2013. Day-old Isa-Brown laying chickens (n=61) were obtained from the Baiada Hatchery at Tamworth, NSW, Australia. At the hatchery, at day-old, all chickens received Rispens vaccine against Marek's disease but were not vaccinated for infectious bronchitis. The chickens were raised in isolation sheds at the University of New England under strict biosecurity protocols. All experimental chickens were fed commercial starter to 4 weeks of age, pullet grower to 18 weeks of age and layer mash until the termination of the experiment. From the isolation sheds, pullets were moved at 18 weeks of age to individual cages in an isolated poultry house. There was no morbidity or mortality from the rearing period until birds were challenged by IBV T and Vic S strains. Before challenge, an ELISA was performed to confirm that all birds were negative for IBV antibody titre in the blood. At 35 weeks of age, eggs were collected and processed for traditional egg quality measurements. Hens were divided into groups (Table 9.1) in such a way that the egg weight and eggshell colour (L*) were not significantly different among the groups (data not shown).

Table 9.1 Allocation of birds into various groups for IBV challenge study in the oviduct of laying hens

Group	Time-point (hr)	
	5	15
Experiment 1 IBV T strain (20 birds)	+	+
Control (20 birds)	+	+
Experiment 2 IBV Vic S strain (11 birds)	+	-
Control (10 Birds)	+	-

In Experiment 1, in each group, there were 10 birds in each time-point. Experiment 2 utilised birds remaining from Experiment 1 and, as the number of birds was sufficient for only one time-point, the 5 hr time-point postoviposition of eggshell formation was selected.

The hens selected for IBV T and Vic S strain challenge were moved to a separate poultry house one week prior to challenge in order to settle down and recover from the trans-location stress. In the challenged groups, 5 hens from each group at a time were intra-occularly inoculated with 10^7 embryo infective dose (EID_{50}) and closely monitored for the development of clinical signs of IB [65] and loss in eggshell colour until days 9-10 post-infection (p.i.). The EID_{50} dose was determined in embryonated SPF eggs infected at 9 days of incubation [71] with 10-times serial dilutions (10^{-3} to 10^{-8} dilutions) of IBV T strain. Eggs were opened at 16 days of incubation and the number of live, dead or virus affected (dwarfed, curled) embryos recorded after the method of Reed and Muench [72]. The 10^7 EID_{50} dose for IBV Vic S strain was calculated as per the dose on the vial of commercial freeze-dried vaccine (Poulvac Bron Vic S, Zoetis Australia). The infection in challenged birds was confirmed through RT-qPCR (in oviduct tissue) and by ELISA of plasma samples (ELISA kit, IDEXX Laboratories, Inc., Westbrook, MA, USA).

9.3.2 Oviduct tissue collection

For both experiments, individual hen oviposition times were recorded by video camera, and each hen was processed at a specific post-oviposition time (5 and 15 hrs Experiment 1; 5 hr Experiment 2). Hens were humanley euthanized with CO_2 gas and approximately 500 mg pieces of tissue from each of the shell gland, isthmus

and distal magnum were aseptically collected in RNALater (Sigma Aldrich, Australia) in 2mL Eppendorf tubes. The samples were stored at -20°C and were processed for DNA/RNA extraction within one day of collection.

9.3.3 Total DNA extraction

Total DNA was extracted from a piece of whole oviduct tissue (all tissue layers) that had been stored in RNALater at -20°C. The TRIsure (Bioline, Australia) protocol was followed with slight modifications. Briefly, approximately 100 mg of tissue (wet weight) was homogenized in 1 mL of TRIsure, using an IKA T10 basic Homogenizer (Wilmington, NC, USA). After chloroform treatment and centrifugation, the upper layer that contained total RNA was removed. The middle and bottom layers were mixed and processed for total DNA extraction. Next, 0.3 mL absolute ethanol was added to precipitate DNA and samples incubated for 3 minutes at room temperature. The precipitated DNA was centrifuged at 2000 ×g for 5 minutes at 4°C to obtain a DNA pellet. The pellet was washed with 1 mL of 0.8 M sodium citrate in 10% ethanol and the process was repeated for a total of three times. Next, the pellet was washed with 1.5 mL ethanol (75%) and centrifuged as described earlier. After ethanol removal, the pellet was dissolved in 100 µL TE buffer (10 mM Tris-HCl, 1 mM disodium EDTA, pH 8.0) and centrifuged at 12000 ×g for 10 minutes at 4°C to remove any insoluble material. The quantity and purity of total DNA in 2 µL of each sample was determined in a spectrophotometer (NANODROP-8000, ThermoFisher Scientific, Wilmington, DE, USA). The pure extracted DNA was stored at -20°C until used for downstream applications.

9.3.4 Total RNA extraction and purification

During DNA extraction, the upper layer after chloroform treatment was processed for total RNA extraction according to the manufacturer's instructions. After the RNA pellet was washed with 1 mL ethanol (75%), 50 µL of UltraPure™ DEPC-treated water (Ambion, USA) was added to dissolve RNA pellets. The total RNA was further purified using RNeasy Mini Kit (Qiagen, GmbH, Hilden, Germany) as per the manufacturer's instructions. The elution of RNA from the spin column with 50 µL of RNase-free water was repeated twice and the eluted RNA solutions were

mixed thoroughly. The extracted RNA was analysed in a NANODROP-8000 spectrophotometer as described earlier. RNA integrity and purity were further examined in Agilent 2100 Bioanalyzer (Agilent Technologies, Waldbronn, Germany) using Agilent RNA 6000 Nano Kit as per the manufacturer's protocol. All RNA showed distinct 18S and 28S bands with an average RNA integrity number (RIN) >9.1.

9.3.5 Primer design for oligonucleotides

The primer sequences were designed using NCBI primer and BLAST options (Table 9.2). Primer quality was checked in "Beacon Designer" software (http://www.premierbiosoft.com/qOligo/Oligo.jsp?PID=1) for possible self and cross secondary structures. To check the sequence specificity, primers were aligned against the NCBI database using BLASTN, Ensembl Chicken Galgal4 and UCSC's Chicken (*Gallus gallus*) Genome Browser Gateway. Prior to real-time qPCR, the primer amplification efficiency and specificity for each primer pair were analysed by using five 10-fold series dilutions of the purified total DNA/RNA to construct a standard curve. The amplification efficiency was calculated by the equation [73]:

$E = 10^{(1/slope)} - 1$

Table 9.2 Forward (F) and reverse (R) sequence of the primers used in the study

Gene names	Abbreviation used	Primer sequence (5' – 3')	Amplicon size (bp)	Annealing temperature C	Amplification efficiency (%)	R^2	Slope	Accession No.
NADH dehydrogenase subunit 4	*ND4*[a]	F:CGCAGGCTCCATACTACTCG R:TTAGGGCACCTCATAGGGCT	137	60	99	0.99944	-3.341	NC_001323.1
Glyceraldehyde-3-phosphate dehydrogenase	*GAPDH*[b]	F: GGTCACCAAGAAGGTGGAGA R: GACAGTGCCCTTGAAGTGTC	137	63	96	0.99888	-3.434	NC_006088.3
Citrate synthase	*CS*	F-TACTACACGGTGCTCTTCGG R-CGGATCCTGCCGGATTTGTAG	152	60	96	0.99943	-3.089	XM_015300287.1
Succinate dehydrogenase complex flavoprotein subunit A	*SDHA*	F: TCTGTCCATGGTGCTAATCG R: TGGTTTAATGGAGGGGACTG	126	60	94	0.99790	-3.484	NM_001277398.1
Dynamin-1-like protein	*Drp1/DNM1L*	F- TGTGACCCGAAGACCCCTTA R- AGCATCTATCTCATTTTCATCTCCA	91	60	99	0.99861	-3.345	NM_001079722.1
Cytochrome C, somatic	*CYC, S*	F- CCCAGTGCCATACGGTTGAA R- CTCACCCCAAGTGATACCTTTGT	140	60	96	0.9930	-3.430	NM_001079478.1
PPARG coactivator 1 alpha	*PGC-1α /PPARGC1A*	F- AGTGACATCGAGTGTGCTGCT R- GGTCAAGTTCTGGGAGATCTGGG	70	63	100	0.99472	-3.331	NM_001006457.1
(Na^+-K^+) ATPase	*(Na^+-K^+) ATPase*	F-GTCAACCCGAGGGATGCTAA R-ACTGCTACAATGGCACCCTG	179	60	99	0.99663	-3.338	J03230.1
Infectious bronchitis virus T strain	IBV T	F-TCAGGTGGTTGGCATTTACA R-ATTGCGAACTTGACCATTCC	181	60	99	0.99982	-3.323	U29522.1
Infectious bronchitis virus Vic S strain	IBV Vic S	F-GATAGGCATGTAGCTTGATTACCTACA R-CGTTTCCAGGCTACTAAGTAGACAGA	78	60	98	0.99873	-3.281	DQ059623 1
TATA-Box Binding Protein	*TBP**	F: TAGCCCGATGATGCCGTAT R: GTTCCCTGTGTCGCTTGC	147	61	97	0.99676	-3.407	NM_205103 D83127
Tyrosine 3-monooxygenase/tryptophan 5-monooxygenase activation protein, zeta polypeptide	*YWHAZ**	F- TTGCTGCTGGAGATGACAAG R- CTTCTTGATACGCCTGTTG	61	60	104	0.99912	-3.222	NM_001031343.1

[a]Gene was used to amplify fragment of mtDNA; [b]Gene was used to amplify fragment of gDNA

*The primers sequences for reference genes *TBP* [74] and *YWHAZ* [75] were sourced from literature.

9.3.6 Mitochondrial DNA quantification

9.3.6.1 DNA cloning

In order to quantify the copy number of mtDNA, a recombinant plasmid vector was constructed by cloning 137 bp fragments of each of the *ND4* and *GAPDH* genes, using TOPO® TA Cloning® Kit for sequencing (ThermoFisher Scientific, Australia) as per the manufacturer's protocol. The recombinant plasmid was transfected into *Escherichia coli* that was grown overnight on Difco™ LB Agar (Bacto Laboratories, Australia) and then a single colony was enriched in LB broth. Recombinant plasmid DNA from overnight cultured *Escherichia coli* in LB broth was extracted using the PureLink® Quick Plasmid Miniprep Kit (ThermoFisher Scientific, Australia). The procedure was as per the manufacturer's protocol with 75 µL pre-heated (65°C) TE buffer used for elution. The eluted recombinant plasmid DNA quality and quantity were checked with the NANODROP-8000 spectrophotometer and stored at -20°C until used for downstream applications. For viral RNA detection in the oviduct of challenged hens, 181 bp and 78 bp nucleotide fragments of IBV T and Vic S strains, respectively, were cloned into plasmid by following the procedure mentioned above.

qPCR was performed on the recombinant plasmid DNA at six different dilutions (10^{-2}~10^{-8}) in a 20 µL reaction to check the cloned chicken mtDNA and the gDNA amplification efficiencies alongside plasmid DNA amplification. The master-mix preparation and cycling conditions were as per the protocol of the SensiFAST™ SYBR® No-ROX Kit (Bioline, Australia). To construct the standard curve, eight 10-fold serial dilutions (10^{-2}~10^{-9}) were prepared from the recombinant plasmid DNA, and qPCR was performed on all the samples as described earlier. A standard curve was constructed by plotting the quantification cycles (Cq) against $\log_{10}$ counts of plasmids. All recombinant plasmid constructs were analysed by PCR to confirm that accurate cloning of target DNA fragments was executed.

9.3.6.2 Mitochondrial DNA copy number quantification by qPCR

Mitochondria were enumerated by the quantification of their DNA copies in a cell and genomic DNA copies were used to represent cell numbers in the samples [76]. Quantitative PCR (qPCR) to quantify mitochondrial DNA counts in a cell was performed with SYBR green method using the SensiFAST™ SYBR® No-ROX Kit (Bioline, Australia). qPCR reaction was performed in a total volume of 20 µL with a Rotor-Gene 6000 thermocycler (Corbett Research, Sydney, Australia). The reaction consisted of 10 µL 2× SensiFAST™ SYBR® No-ROX mix, 400 nM each of the primers, 6.4 µL RNase-free water and 2 µL of diluted DNA (10^{-2} of extracted DNA samples). Reaction without DNA template was included as a negative control (NTC). qPCR was conducted following a 2-step protocol: polymerase activation and DNA denaturation at 95°C for 3 minutes, and 40 cycles of denaturation at 95°C for 5 seconds and annealing and extension at 60°C or 63°C for 30 seconds. Fluorescent signals were acquired at the end of each annealing/extension step during qPCR cycles (40). A melting phase at a ramp from 50ºC to 99ºC at 1ºC increment was conducted to assess the specificity of qPCR amplification. The qPCR products were also examined in Bioanalyzer using DNA 1000 Kit as per the manufacturer's instructions to determine the amplification specificity by the size of the amplicons estimated.

9.3.6.3 Calculation of mitochondria per cell

The cloned plasmid DNA with ND4 and GAPDH gene inserts were converted into plasmid DNA copies/µL in six different dilutions for analysis. Plasmid count was calculated based on the concentration of plasmid DNA and its molecular weight. The cloned plasmid DNA amplification cycle (Cq) values were then used to construct a standard curve to calculate the mtDNA and gDNA copies per diploid cell. The absolute count of mtDNA per cell was calculated according to the equation: (count of mtDNA)/(count of gDNA/2).

9.3.7 Gene expression analysis by qPCR

For the gene expression studies, RNA samples were run in duplicate with the inclusion of NTC and no reverse transcriptase (-RT) controls. Master-mix was prepared as per the manufacturer's protocol using the SensiFAST SYBR® Lo-ROX One-Step RT-PCR Kit (Bioline, Australia). The reaction in a volume of 20 µL contained 10 µL of 2× SensiFAST SYBR low Rox one-step mix, 400 nMoles primers, 0.2 µL of reverse transcriptase, 0.4 µL of RiboSafe RNase inhibitor, 3.8 µL RNase-free water and 4 µL of RNA template (diluted 100 times). Reverse transcription and amplification were conducted following the thermal cycling protocol in Rotor-Gene 6000: reverse transcription at 45°C for 10 minutes, polymerase activation and denaturation at 95°C for 2 minutes, then 40 cycles of denaturation at 95°C for 5 seconds and annealing and extension at 60°C, 61°C or 63°C for 20 seconds. The fluorescent data collection, melting analysis, and amplification efficiency calculation were performed as described previously.

9.4 Statistical analysis

To determine the mitochondrial count, the mtDNA copies per cell data were analysed in Statview software (SAS Institute Inc., Version 5.0.1.0) taking the time-point and virus challenge as main effects. Tukey test was used to differentiate the level of significance ($P < 0.05$) between mean values. For gene expression data analysis, raw Cq values were analysed in qbase+ software version 3.0 against *TBP* and *YWHAZ* as reference genes. The analysis was based on relative expression ($2^{-\Delta\Delta Cq}$) using genes specific amplification efficiencies [77-79]. To determine the effect of time-point and IBV challenge, from the qbase+, normalised relative quantities (NRQ) were exported and analysed in Statview using one-way ANOVA.

9.5 Results

All the primers used in the current study were specific in amplifications (Figure 9.1). The amplification efficiency of the primers ranged from 94-104% (Table 9.2).

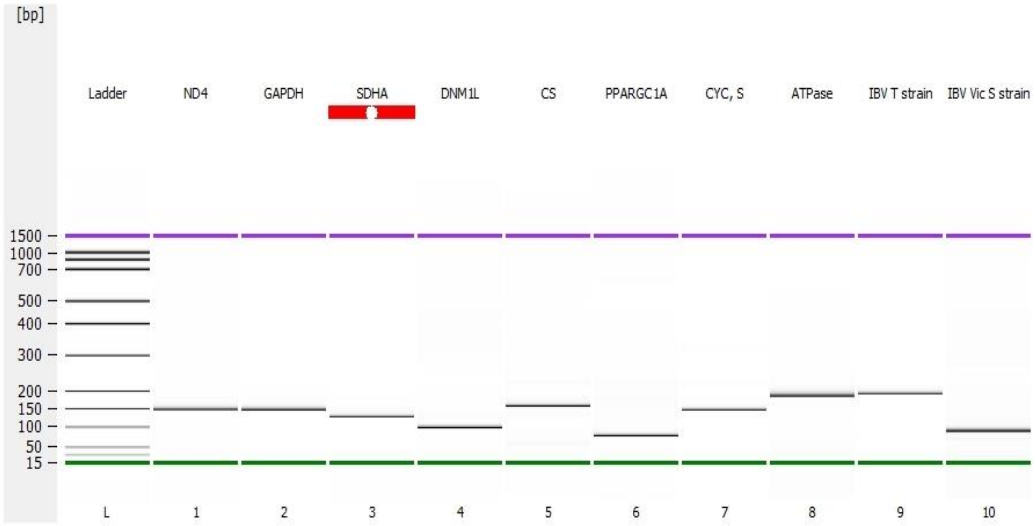

Figure 9.1 Amplification of the genes fragments to assess the specificities of the primers

L) DNA ladder; **1**) *ND4* (137 bp); **2**) *GAPDH* (137 bp); **3**) *SDHA* (126 bp); **4**) *Drp1/DNM1L* (91 bp); **5**) *CS* (152 bp); **6**) *PGC-1α/PPARGC1A* (70 bp); **7**) *CYC, S* (140 bp); **8**) *Na^+-K^+ ATPase* (179 bp); **9**) IBV T strain (181 bp); **10**) IBV Vic S strain (78 bp). The upper (purple) and lower (green) markers act as internal standards and are used to align the ladder analysis with the individual DNA sample analysis. The standard curve (plotting migration time against DNA amplicon size), in conjunction with the markers, is then used to calculate DNA fragment sizes for each well from the migration times measured (see Agilent 2100 Bioanalyzer Users Guide for Molecular Assays). The DNA gel in Agilent 2100 Bioanalyzer was performed as per the manufacturer's instructions of Agilent DNA 1000 Kit.

9.5.1 Mitochondrial count per cell

The mean mitochondrial count per cell was not significantly affected ($P > 0.05$) by time-points of egg formation in any of the three segments of the oviduct (Figure 9.2). There was no significant interaction between the time-point and IBV T strain challenge for mitochondrial count per cell in the shell gland, isthmus and magnum regions of the oviduct. The mean mitochondrial count per cell in the shell gland region of oviduct was significantly lower ($P < 0.05$) in the IBV T strain challenged hens compared with the control group (Figure 9.2A). The IBV T strain challenge did not significantly affect the mean mitochondrial count per cell in isthmus and magnum regions of the oviduct (Figure 9.2C, E). Similarly, the mitochondrial count

per cell between the control and IBV Vic S strain challenged groups was not significantly different in all three segments of the oviduct (Figure 9.2B, D, F).

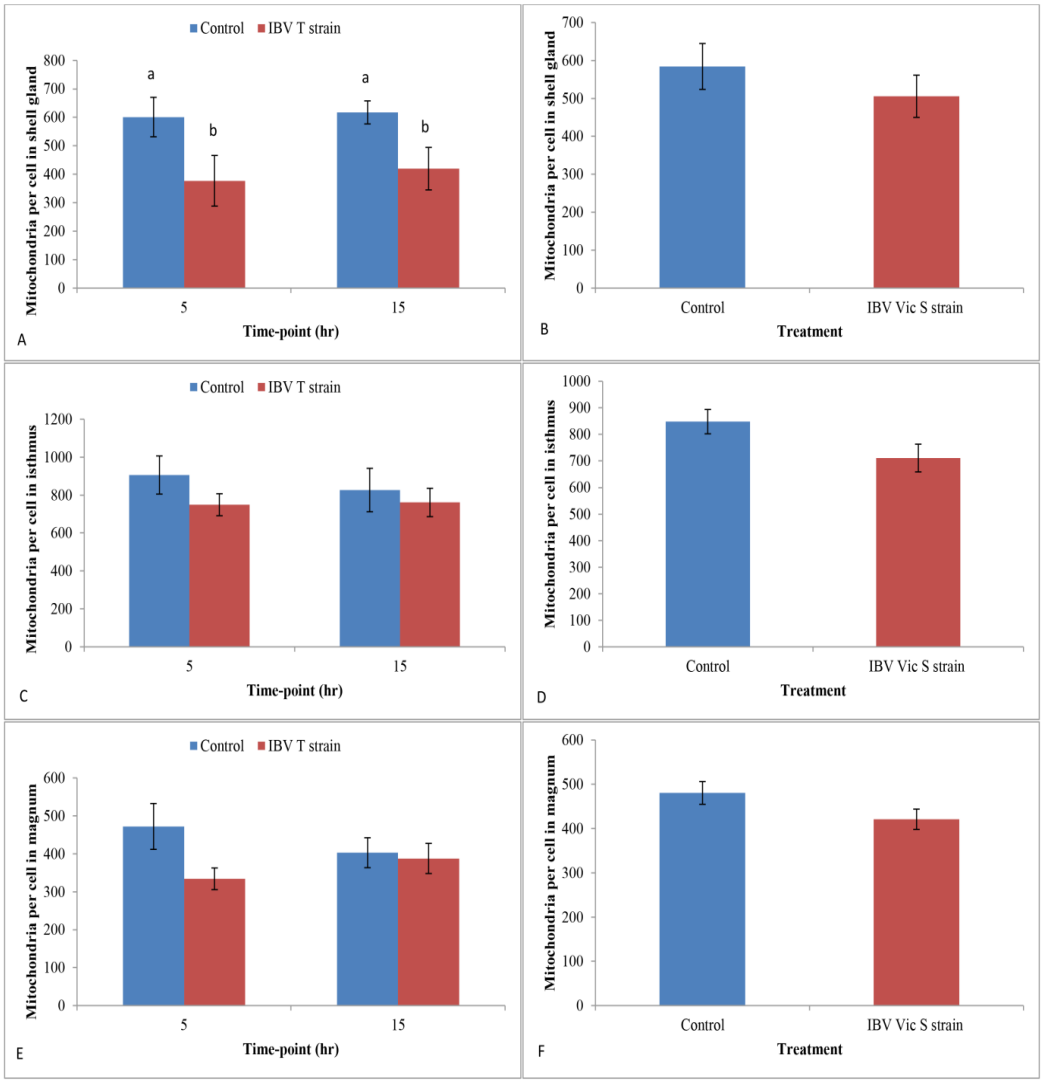

Figure 9.2 Mean mitochondrial count per cell in different segments of oviduct of laying hens challenged with IBV T and Vic S strains

A) Mitochondrial count per cell in the shell gland region of the oviduct at two time-points of eggshell formation and in response to IBV T strain challenge. **B**) Mitochondrial count per cell in the shell gland region of oviduct between the control and IBV Vic S challenged groups. **C**) Mitochondrial count per cell in the isthmus region of the oviduct at two time-points of eggshell formation and in response to IBV T strain challenge. **D**) Mitochondrial count per cell in the isthmus region of oviduct between the control and IBV Vic S challenged groups. **E**) Mitochondrial count per cell in the magnum region of the oviduct at two time-points of eggshell formation and in response to IBV T strain challenge. **F**) Mitochondrial count per cell

in the magnum regions of oviduct between the control and IBV Vic S challenged groups. Bars represent standard error. Superscripts (^{a,b}) show significant difference between the control and IBV T strain challenged groups.

9.5.2 Effect of IBV and time-point on gene expression in the shell gland tissue

The relative expression level of all of the genes studied was not significantly affected ($P > 0.05$) by IBV challenge (Table 9.3). The expression levels of all the genes except *PGC-1α* were significantly affected ($P < 0.05$) by time-point of eggshell formation (Figure 9.3A-F). The expression levels of *CS*, *CYC*, *S* and *Na^+-K^+ ATPase* genes were significantly higher at 15 hr compared with 5 hr time-point (Figure 9.3A, C, F). The expression levels of *SDHA* and *Drp1* genes were significantly higher at 5 hr compared with 15 hr time-point (Figure 9.3B, E).

Table 9.3 Relative expression stabilities of genes in the shell gland of laying hens challenged with IBV

Gene	IBVT Strain		P value	Gene	IBV Vic S strain		P value
	Challenged	Control			Challenged	Control	
CS	1.043±0.097	0.959±0.097	0.5468	***CS***	0.608±0.369	0.926±0.102	0.3143
SDHA	0.956±0.037	1.045±0.054	0.2422	*SDHA*	0.890±0.045	0.920±0.018	0.2512
Drp1	1.033±0.033	0.967±0.020	0.2619	*Drp1*	0.975±0.038	0.956±0.037	0.5572
PGC-1α	1.002±0.026	0.997±0.033	0.9273	*PGC-1α*	0.934±0.019	0.881±0.039	0.5240
CYC, S	0.959±0.025	1.041±0.021	0.1900	*CYC, S*	0.993±0.028	1.061±0.016	0.1618
Na^+-K^+ ATPase	0.981±0.052	1.019±0.032	0.9254	*Na^+-K^+ ATPase*	0.985±0.032	1.014±0.020	0.8632

Values are normalised relative quantities (NRQ) to the mean expression level of all the samples±S.E.

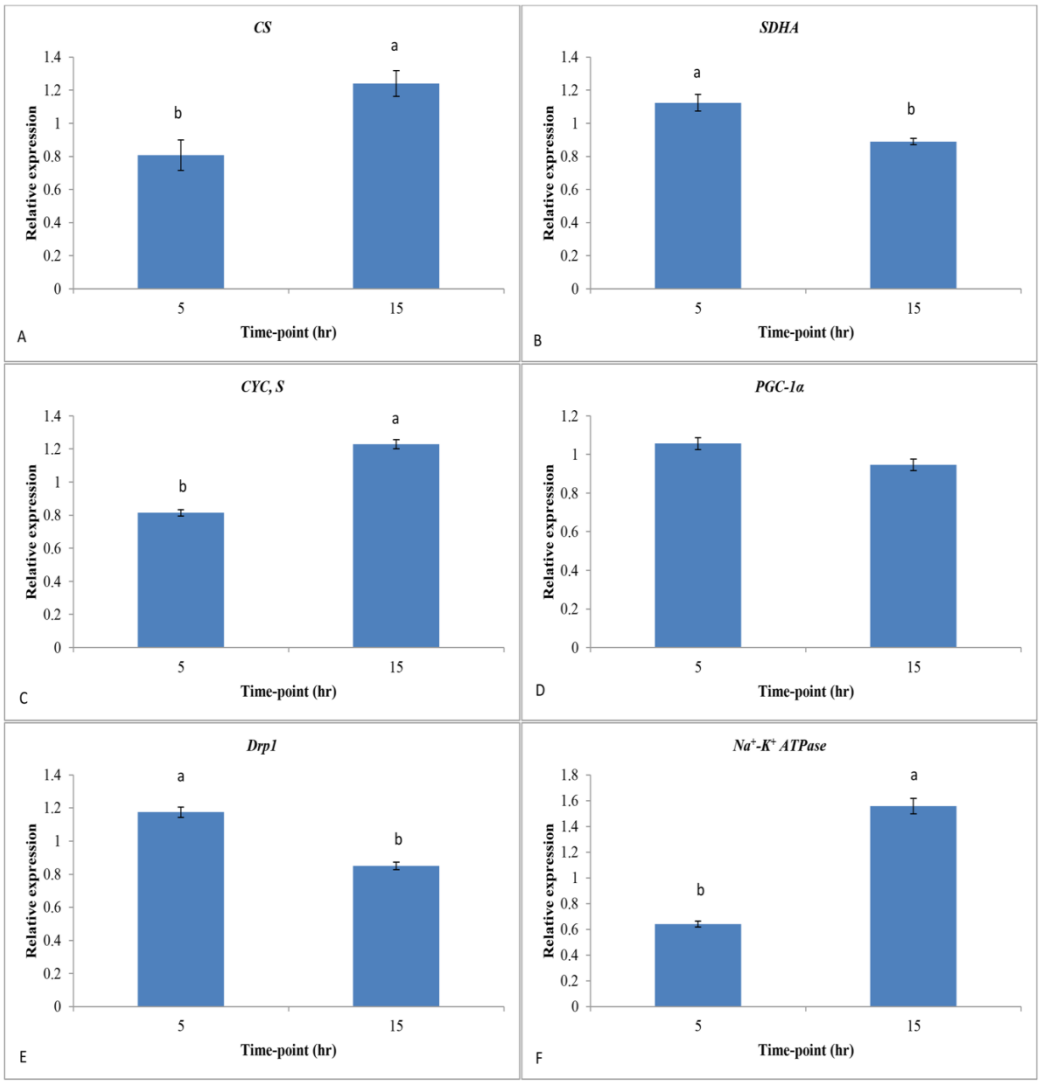

Figure 9.3 Relative expression levels of nuclear DNA encoded genes involved in mitochondrial biogenesis and fission

The genes were quantified from shell gland tissue collected at two different time-points of eggshell formation in IBV T strain challenged study. **A**) *CS* gene (P=0.0007). **B**) *SDHA* gene (P<0.0001). **C**) *CYC, S* gene (P<0.0001). **D**) *PGC-1α* gene (P=0.1080). **E**) *Drp1* gene (P<0.0001). **F**) *Na^+-K^+ ATPase* gene (P<0.0001). Values are mean and bars represent standard error. Suprescripts (^{a,b}) across the graph indicate significant difference.

9.6 Discussion

We investigated the mitochondrial count per cell in three different segments of the oviduct of laying hens challenged with IBV T and Vic S strains. A significantly lower mitochondrial number in the shell gland of IBV T challenged hens suggests

that the virus had a greater effect on this region, as compared with the isthmus and magnum regions of the oviduct. A greater severity of pathological lesions caused by IBV T in the isthmus and shell gland regions, compared with the magnum, has been reported [80]. From the current study, it seems that IBV T infection reduced the mean mitochondrial count per cell without reducing the actual number of cells as the gDNA count did not change. Generally, viral replication alters oxidative balance, mitochondrial permeability transition pore, mitochondrial membrane potential, electron transport and energy production at the cellular level [81]. It is not clear how mitochondria are degenerated by IBV T; however, in previous studies, degenerated mitochondria in IBV infected cells have been recorded [82]. Viral RNA of IBV T strain was detected through qPCR in the epithelial mucosa (epithelial scrapings) of the shell gland region of the oviduct but was not detected in isthmus and magnum regions of the oviduct. Similarly, viral RNA of IBV Vic S strain was not detected in any of the samples collected from challenged hens.

Based on the lack of significant differences in mean mitochondrial count per cell between the challenged and control groups for the magnum and isthmus, we focused further on shell gland tissue and studied the expression level of genes involved in mitochondrial density, biogenesis and fission. The lack of any significant difference in the relative expression levels of the genes between the control and IBV T challenged groups may indicate that mitochondrial function may have been enhanced and thus the overall eggshell quality may have not been affected by fewer mitochondria in the IBV T infected hens. CS enzyme activity has been widely used as a marker for intact mitochondrial density. In one study, the activity of CS was 42% higher in the leg muscle of dominant compared with subordinate male red jungle fowl, with no differences with overall muscle mass [83]. In the current study, the *CS* mRNA level was significantly higher at the 15 hr time-point indicating that mitochondrial density was higher at this time-point; however, the mtDNA content showed no significant difference between the 5 and 15 hr time-points of eggshell formation. The protein encoded by the *CS* gene is a Krebs tricarboxylic acid cycle enzyme that catalyses the synthesis of citrate from oxaloacetate and acetyl coenzyme A. The role of *SDHA* in the current study could not be explained clearly as its expression level was significantly higher at 5 hr compared with the 15 hr time-point of eggshell formation. *SDHA* functions in

mitochondrial complex II, a part of the citric acid cycle and electron transport chain. The lack of significant difference in the expression level of *PGC-1α* between the two time-points may correlate positively with mitochondrial count per cell. However, the finding of no significant difference in the expression level of *PGC-1α* between the control and IBV T challenged groups was not in agreement with mitochondrial count. The temporal relationship between mitochondrial biogenesis and the expression level of the genes involved in mitochondrial biogenesis are not clear and thus it is difficult to compare the expression level of such genes with mitochondrial count at different points of eggshell formation. *PGC-1α* protein is a nuclear encoded protein that is localised both in the cytoplasm and nucleus [84]. In mammals, the expression of *PGC-1α* is prominent in tissues with high demands of energy [85, 86] and the mRNA level is induced in conditions such as exposure to cold, fasting and physical exercise [86]. Increase in *PGC-1α* is sufficient to induce cellular pathways important for energy metabolism and mitochondrial biogenesis [87, 88]. Mitochondrial content and oxidative capacity are cell type specific and are regulated by energy demand of a cell [89]. In a study of adenovirus infected SAOS-2 cells, the *PGC-1α* mediated induction of mitochondrial proteins led to an increase in mitochondrial content [89] measured 48 hrs after infection. *Drp1* is a nuclear encoded protein that plays an important role in the fission of the outer mitochondrial membrane. In healthy cells, fission and fusion events occur to regulate mitochondrial morphology [90]. In the current study, the lack of significant difference in the levels of *Drp1* between the control and IBV T challenged groups might indicate that reduction in mitochondrial count did not influence mean cell number. The higher expression level of *Drp1* at 15 hr compared with the 5 hr time-point cannot be clearly linked with higher activities of mitochondrial fission and/or fusion as most of the genes studied did not show a clear pattern of change with lower mean mitochondrial count in IBV T challenged groups. The objective of *Na^+-K^+ ATPase* quantification was to understand cell membrane potential level in the control and IBV T challenged groups and at two different time-points of eggshell formation. *Na^+-K^+ ATPase* is involved in maintaining membrane excitation potential, tight junction polarity and vectorial transport in cells (reviewed in Rajasekaran et al. [91]). A lack of significant difference in the expression level of *Na^+-K^+ ATPase* between the control and IBV T challenged groups indicates that

viral multiplication in the cells did not alter the normal function of *Na^+-K^+ ATPase* and that the cells in both the groups were functioning similarly. A higher expression level of *Na^+-K^+ ATPase* at 15 hr compared with the 5 hr time-point is an indication of higher cellular activity of the shell gland tissue during the formation of the eggshell. The expression levels of the genes studied between the control and challenged groups of IBV Vic S followed a similar pattern to that observed in the IBV T challenged groups, and the expression level was not significantly different between the control and Vic S samples.

Taken together, the results of the current study show that the IBV T strain challenge in laying hens significantly lowered the mean mitochondrial count only in the shell gland part of oviduct. Furthermore, the expression level of the nuclear DNA encoded genes that are involved in mitochondrial biogenesis and/or function could not be correlated with lower mean mitochondrial count and mitochondrial biogenesis and/or function at different time-points of eggshell formation. Further investigation is required to determine the actual turnover of mitochondria in metabolically active organs, such as laying hen oviduct, in normal and pathological conditions.

9.7 References

1. Palmiter RD, Wrenn JT. Interaction of estrogen and progesterone in chick oviduct development III. Tubular gland cell cytodifferentiation. J Cell Biol 1971; 50:598-615.
2. Kohler PO, Grimley PM, O'malley BW. Estrogen-induced cytodifferentiation of the ovalbumin-secreting glands of the chick oviduct. J Cell Biol 1969; 40:8-27.
3. Oka T, Schimke RT. Interaction of estrogen and progesterone in chick oviduct development II. Effects of estrogen and progesterone on tubular gland cell function. J Cell Biol 1969; 43:123-137.
4. Majumder K. Composition and properties of egg white. In: Roberts JR (ed.) Achieving sustainable production of eggs, vol. 1. UK: Burleigh Dodds Science Publishing Limited; 2017: 25-48.

5. Bain M. Composition and properties of eggshell. In: Roberts JR (ed.) Achieving sustainable production of eggs, vol. 1. UK: Burleigh Dodds Science Publishing Limited; 2017: 3-24.

6. Bar A. Calcium transport in strongly calcifying laying birds: mechanisms and regulation. Comp Biochem Physiol Part A Mol Integr Physiol 2009; 152:447-469.

7. Mandal S, Lindgren AG, Srivastava AS, Clark AT, Banerjee U. Mitochondrial function controls proliferation and early differentiation potential of embryonic stem cells. Stem Cells 2011; 29:486-495.

8. Seo AY, Joseph A-M, Dutta D, Hwang JCY, Aris JP, Leeuwenburgh C. New insights into the role of mitochondria in aging: mitochondrial dynamics and more. J Cell Sci 2010; 123:2533-2542.

9. Mishra P, Chan DC. Metabolic regulation of mitochondrial dynamics. J Cell Biol 2016; 212:379-387.

10. Desjardins P, Morais R. Sequence and gene organization of the chicken mitochondrial genome: a novel gene order in higher vertebrates. J Mol Biol 1990; 212:599-634.

11. Mindell DP, Sorenson MD, Dimcheff DE. Multiple independent origins of mitochondrial gene order in birds. Proc Natl Acad Sci U S A 1998; 95:10693-10697.

12. Mindell DP, Sorenson MD, Dimcheff DE. An extra nucleotide is not translated in mitochondrial ND3 of some birds and turtles. Mol Biol Evol 1998; 15:1568-1571.

13. Bao H, Zhao C, Li J, Wu C. Sequencing and alignment of mitochondrial genomes of Tibetan chicken and two lowland chicken breeds. Sci China C Life Sci 2008; 51:47-51.

14. Clayton DA. Transcription and replication of animal mitochondrial DNAs. Int Rev Cytol 1992; 141:217-232.

15. Fuke S, Kubota-Sakashita M, Kasahara T, Shigeyoshi Y, Kato T. Regional variation in mitochondrial DNA copy number in mouse brain. Biochim Biophys Acta, Bioenerg 2011; 1807:270-274.

16. Guo W, Jiang L, Bhasin S, Khan SM, Swerdlow RH. DNA extraction procedures meaningfully influence qPCR-based mtDNA copy number determination. Mitochondrion 2009; 9:261-265.

17. Phillips NR, Sprouse ML, Roby RK. Simultaneous quantification of mitochondrial DNA copy number and deletion ratio: a multiplex real-time PCR assay. Sci Rep 2014; 4:3887.

18. Hartmann N, Reichwald K, Wittig I, Dröse S, Schmeisser S, Lück C, Hahn C, Graf M, Gausmann U, Terzibasi E. Mitochondrial DNA copy number and function decrease with age in the short-lived fish *Nothobranchius furzeri*. Aging Cell 2011; 10:824-831.

19. Navarro A, Boveris A. Rat brain and liver mitochondria develop oxidative stress and lose enzymatic activities on aging. Am J Physiol Regul Integr Comp Physiol 2004; 287:R1244-R1249.

20. Larsen RG, Callahan DM, Foulis SA, Kent-Braun JA. *In vivo* oxidative capacity varies with muscle and training status in young adults. J Appl Physiol 2009; 107:873-879.

21. Jacobs RA, Lundby C. Mitochondria express enhanced quality as well as quantity in association with aerobic fitness across recreationally active individuals up to elite athletes. J Appl Physiol 2013; 114:344-350.

22. Brunk CF. Mitochondrial proliferation during myogenesis. Exp Cell Res 1981; 136:305-309.

23. Klaus S, Casteilla L, Bouillaud F, Ricquier D. The uncoupling protein UCP: a membraneous mitochondrial ion carrier exclusively expressed in brown adipose tissue. Int J Biochem 1991; 23:791-801.

24. Poyton RO, McEwen JE. Crosstalk between nuclear and mitochondrial genomes. Annu Rev Biochem 1996; 65:563-607.

25. Bogenhagen D, Clayton DA. The number of mitochondrial deoxyribonucleic acid genomes in mouse L and human HeLa cells. Quantitative isolation of mitochondrial deoxyribonucleic acid. J Biol Chem 1974; 249:7991-7995.

26. Campbell CT, Kolesar JE, Kaufman BA. Mitochondrial transcription factor A regulates mitochondrial transcription initiation, DNA packaging, and

genome copy number. Biochim Biophys Acta, Gene Regul Mech 2012; 1819:921-929.

27. Fusté JM, Wanrooij S, Jemt E, Granycome CE, Cluett TJ, Shi Y, Atanassova N, Holt IJ, Gustafsson CM, Falkenberg M. Mitochondrial RNA polymerase is needed for activation of the origin of light-strand DNA replication. Mol Cell 2010; 37:67-78.

28. Jemt E, Persson Ö, Shi Y, Mehmedovic M, Uhler JP, López MD, Freyer C, Gustafsson CM, Samuelsson T, Falkenberg M. Regulation of DNA replication at the end of the mitochondrial D-loop involves the helicase TWINKLE and a conserved sequence element. Nucleic Acids Res 2015; 43:9262-9275.

29. Westermann B. Mitochondrial fusion and fission in cell life and death. Nat Rev Mol Cell Biol 2010; 11:872-884.

30. Smirnova E, Griparic L, Shurland D-L, Van Der Bliek AM. Dynamin-related protein Drp1 is required for mitochondrial division in mammalian cells. Mol Biol Cell 2001; 12:2245-2256.

31. Tieu Q, Nunnari J. Mdv1p is a WD repeat protein that interacts with the dynamin-related GTPase, Dnm1p, to trigger mitochondrial division. J Cell Biol 2000; 151:353-366.

32. Mozdy AD, McCaffery JM, Shaw JM. Dnm1p GTPase-mediated mitochondrial fission is a multi-step process requiring the novel integral membrane component Fis1p. J Cell Biol 2000; 151:367-380.

33. Falkenberg M, Larsson N-G, Gustafsson CM. DNA replication and transcription in mammalian mitochondria. Annu Rev Biochem 2007; 76:679-699.

34. Posakony JW, England JM, Attardi G. Mitochondrial growth and division during the cell cycle in HeLa cells. J Cell Biol 1977; 74:468-491.

35. Tanaka K, Kanbe T, Kuroiwa T. Three-dimensional behaviour of mitochondria during cell division and germ tube formation in the dimorphic yeast Candida albicans. J Cell Sci 1985; 73:207-220.

36. Atkinson AW, John PCL, Gunning BES. The growth and division of the single mitochondrion and other organelles during the cell cycle of Chlorella,

studied by quantitative stereology and three dimensional reconstruction. Protoplasma 1974; 81:77-109.

37. Holloszy JO, Oscai LB, Don IJ, Mole PA. Mitochondrial citric acid cycle and related enzymes: adaptive response to exercise. Biochem Biophys Res Commun 1970; 40:1368-1373.

38. Hood DA, Zak R, Pette D. Chronic stimulation of rat skeletal muscle induces coordinate increases in mitochondrial and nuclear mRNAs of cytochrome-c-oxidase subunits. Eur J Biochem 1989; 179:275-280.

39. Mogensen M, Bagger M, Pedersen PK, Fernström M, Sahlin K. Cycling efficiency in humans is related to low UCP3 content and to type I fibres but not to mitochondrial efficiency. J Physiol 2006; 571:669-681.

40. Boushel R, Gnaiger E, Schjerling P, Skovbro M, Kraunsøe R, Dela F. Patients with type 2 diabetes have normal mitochondrial function in skeletal muscle. Diabetologia 2007; 50:790-796.

41. Drahota Z, Milerova M, Stieglerova A, Houstek J, Ostadal B. Developmental changes of cytochrome c oxidase and citrate synthase in rat heart homogenate. Physiol Res 2004; 53:119-122.

42. Marin-Garcia J, Ananthakrishnan R, Goldenthal MJ. Human mitochondrial function during cardiac growth and development. Mol Cell Biochem 1998; 179:21-26.

43. Pesta D, Hoppel F, Macek C, Messner H, Faulhaber M, Kobel C, Parson W, Burtscher M, Schocke M, Gnaiger E. Similar qualitative and quantitative changes of mitochondrial respiration following strength and endurance training in normoxia and hypoxia in sedentary humans. Am J Physiol Regul Integr Comp Physiol 2011; 301:R1078-R1087.

44. Tonkonogi M, Harris B, Sahlin K. Increased activity of citrate synthase in human skeletal muscle after a single bout of prolonged exercise. Acta Physiol Scand 1997; 161:435-436.

45. Siu PM, Donley DA, Bryner RW, Alway SE. Citrate synthase expression and enzyme activity after endurance training in cardiac and skeletal muscles. J Appl Physiol 2003; 94:555-560.

46. Puigserver P, Wu Z, Park CW, Graves R, Wright M, Spiegelman BM. A cold-inducible coactivator of nuclear receptors linked to adaptive thermogenesis. Cell 1998; 92:829-839.

47. Wu Z, Puigserver P, Andersson U, Zhang C, Adelmant G, Mootha V, Troy A, Cinti S, Lowell B, Scarpulla RC, Spiegelman BM. Mechanisms Controlling Mitochondrial Biogenesis and Respiration through the Thermogenic Coactivator PGC-1. Cell 1999; 98:115-124.

48. Lehman JJ, Barger PM, Kovacs A, Saffitz JE, Medeiros DM, Kelly DP. Peroxisome proliferator-activated receptor gamma coactivator-1 promotes cardiac mitochondrial biogenesis. J Clin Invest 2000; 106:847-856.

49. St-Pierre J, Lin J, Krauss S, Tarr PT, Yang R, Newgard CB, Spiegelman BM. Bioenergetic analysis of peroxisome proliferator-activated receptor gamma coactivators 1alpha and 1beta (PGC-1alpha and PGC-1beta) in muscle cells. J Biol Chem 2003; 278:26597-26603.

50. Takeyasu K, Tamkun MM, Renaud KJ, Fambrough DM. Ouabain-sensitive (Na+ + K+)-ATPase activity expressed in mouse L cells by transfection with DNA encoding the alpha-subunit of an avian sodium pump. J Biol Chem 1988; 263:4347-4354.

51. Glynn IM. The Na+, K+-transporting adenosine triphosphatase. In: Martonosi AN (ed.) The Enzymes of Biological Membranes: Volume 3: Membrane Transport. Boston, MA: Springer US; 1985: 35-114.

52. de Wit JJ, Cook JKA, van der Heijden HMJF. Infectious bronchitis virus variants: a review of the history, current situation and control measures. Avian Pathol 2011; 40:223-235.

53. Spaan W, Cavanagh D, Horzinek MC. Coronaviruses: structure and genome expression. J Gen Virol 1988; 69:2939-2952.

54. Earp LJ, Delos SE, Park HE, White JM. The many mechanisms of viral membrane fusion proteins. In: Membrane Trafficking in Viral Replication: Springer; 2004: 25-66.

55. Gallagher TM, Buchmeier MJ. Coronavirus spike proteins in viral entry and pathogenesis. Virology 2001; 279:371-374.

56. Seo SH, Collisson EW. Specific cytotoxic T lymphocytes are involved in *in vivo* clearance of infectious bronchitis virus. J Virol 1997; 71:5173-5177.

57. Cavanagh D. The coronavirus surface glycoprotein. In: The Coronaviridae: Springer; 1995: 73-113.

58. Chu VC, McElroy LJ, Chu V, Bauman BE, Whittaker GR. The avian coronavirus infectious bronchitis virus undergoes direct low-pH-dependent fusion activation during entry into host cells. J Virol 2006; 80:3180-3188.

59. Winter C, Schwegmann-Weßels C, Cavanagh D, Neumann U, Herrler G. Sialic acid is a receptor determinant for infection of cells by avian Infectious bronchitis virus. J Gen Virol 2006; 87:1209-1216.

60. El Rahman SA, Winter C, El-Kenawy A, Neumann U, Herrler G. Differential sensitivity of well-differentiated avian respiratory epithelial cells to infection by different strains of infectious bronchitis virus. J Virol 2010; 84:8949-8952.

61. Rahman SAE, El-Kenawy A, Neumann U, Herrler G, Winter C. Comparative analysis of the sialic acid binding activity and the tropism for the respiratory epithelium of four different strains of avian infectious bronchitis virus. Avian Pathol 2009; 38:41-45.

62. Mork A-K, Hesse M, Abd El Rahman S, Rautenschlein S, Herrler G, Winter C. Differences in the tissue tropism to chicken oviduct epithelial cells between avian coronavirus IBV strains QX and B1648 are not related to the sialic acid binding properties of their spike proteins. Vet Res 2014; 45:67.

63. Raj GD, Jones RC. Infectious bronchitis virus: immunopathogenesis of infection in the chicken. Avian Pathol 1997; 26:677-706.

64. Jackwood MW, de Wit S. Infectious bronchitis. In: Swayne DE (ed.) Diseases of poultry. USA: John Wiley & Sons; 2013: 139-160.

65. Box PG, Holmes HC, Finney PM, Froymann R. Infectious bronchitis in laying hens: The relationship between haemagglutination inhibition antibody levels and resistance to experimental challenge. Avian Pathol 1988; 17:349-361.

66. Bisgaard M. The influence of infectious bronchitis virus on egg production, fertility, hatchability and mortality rate in chickens (author's transl). Nord Vet Med 1975; 28:368-376.

67. Broadfoot DI, Smith WM. Effects of infectious bronchitis in laying hens on egg production, percent unsettable eggs and hatchability. Poult Sci 1954; 33:653-654.

68. Chousalkar KK, Roberts JR, Reece R. Comparative histopathology of two serotypes of infectious bronchitis virus (T and N1/88) in laying hens and cockerels. Poult Sci 2007; 86:50-58.

69. Chousalkar KK, Roberts JR. Ultrastructural study of infectious bronchitis virus infection in infundibulum and magnum of commercial laying hens. Vet Microbiol 2007; 122:223-236.

70. Raj GD, Jones RC. An *in vitro* comparison of the virulence of seven strains of infectious bronchitis virus using tracheal and oviduct organ cultures. Avian Pathol 1996; 25:649-662.

71. Senne DA. Virus propagation in embryonating eggs. A laboratory manual for the isolation and identification of avian pathogens 1998:235-240.

72. Reed LJ, Muench H. A simple method of estimating fifty per cent endpoints. Am J Epidemiol 1938; 27:493-497.

73. Peirson SN, Butler JN, Foster RG. Experimental validation of novel and conventional approaches to quantitative real-time PCR data analysis. Nucleic Acids Res 2003; 31:e73-e73.

74. Li YP, Bang DD, Handberg KJ, Jorgensen PH, Zhang MF. Evaluation of the suitability of six host genes as internal control in real-time RT-PCR assays in chicken embryo cell cultures infected with infectious bursal disease virus. Vet Microbiol 2005; 110:155-165.

75. Bagés S, Estany J, Tor M, Pena RN. Investigating reference genes for quantitative real-time PCR analysis across four chicken tissues. Gene 2015; 561:82-87.

76. Miller FJ, Rosenfeldt FL, Zhang C, Linnane AW, Nagley P. Precise determination of mitochondrial DNA copy number in human skeletal and

cardiac muscle by a PCR-based assay: lack of change of copy number with age. Nucleic Acids Res 2003; 31:e61-e61.

77. Pfaffl MW, Horgan GW, Dempfle L. Relative expression software tool (REST©) for group-wise comparison and statistical analysis of relative expression results in real-time PCR. Nucleic Acids Res 2002; 30:e36-e36.

78. qbase+ user manual: https://www.qbaseplus.com/sites/default/files/public_file/qbaseplus_manual.pdf.

79. Hellemans J, Mortier G, De Paepe A, Speleman F, Vandesompele J. qBase relative quantification framework and software for management and automated analysis of real-time quantitative PCR data. Genome Biol 2007; 8:R19.

80. Chousalkar KK, Roberts JR, Reece R. Histopathology of two serotypes of infectious bronchitis virus in laying hens vaccinated in the rearing phase. Poult Sci 2007; 86:59-62.

81. Williamson CD, DeBiasi RL, Colberg-Poley AM. Viral product trafficking to mitochondria, mechanisms and roles in pathogenesis. Infect Disord Drug Targets 2012; 12:18-37.

82. Chousalkar KK, Roberts JR. Ultrastructural observations on effects of infectious bronchitis virus in eggshell-forming regions of the oviduct of the commercial laying hen. Poult Sci 2007; 86:1915-1919.

83. Hammond KA, Chappell MA, Cardullo RA, Lin R-S, Johnsen TS. The mechanistic basis of aerobic performance variation in red junglefowl. J Exp Biol 2000; 203:2053-2064.

84. Anderson RM, Barger JL, Edwards MG, Braun KH, O'Connor CE, Prolla TA, Weindruch R. Dynamic regulation of PGC-1α localization and turnover implicates mitochondrial adaptation in calorie restriction and the stress response. Aging Cell 2008; 7:101-111.

85. Schreiber SN, Knutti D, Brogli K, Uhlmann T, Kralli A. The transcriptional coactivator PGC-1 regulates the expression and activity of the orphan nuclear receptor estrogen-related receptor α (ERRα). J Biol Chem 2003; 278:9013-9018.

86. Puigserver P, Spiegelman BM. Peroxisome proliferator-activated receptor-γ coactivator 1α (PGC-1α): transcriptional coactivator and metabolic regulator. Endocr Rev 2003; 24:78-90.

87. Wu Z, Puigserver P, Andersson U, Zhang C, Adelmant G, Mootha V, Troy A, Cinti S, Lowell B, Scarpulla RC. Mechanisms controlling mitochondrial biogenesis and respiration through the thermogenic coactivator pgc-1. Cell 1999; 98:115-124.

88. Lehman JJ, Barger PM, Kovacs A, Saffitz JE, Medeiros DM, Kelly DP. Peroxisome proliferator–activated receptor γ coactivator-1 promotes cardiac mitochondrial biogenesis. The Journal of clinical investigation 2000; 106:847-856.

89. Schreiber SN, Emter R, Hock MB, Knutti D, Cardenas J, Podvinec M, Oakeley EJ, Kralli A. The estrogen-related receptor α (ERRα) functions in PPARγ coactivator 1α (PGC-1α)-induced mitochondrial biogenesis. Proc Natl Acad Sci U S A 2004; 101:6472-6477.

90. Frank S, Gaume B, Bergmann-Leitner ES, Leitner WW, Robert EG, Catez F, Smith CL, Youle RJ. The role of dynamin-related protein 1, a mediator of mitochondrial fission, in apoptosis. Dev Cell 2001; 1:515-525.

91. Rajasekaran SA, Barwe SP, Rajasekaran AK. Multiple functions of Na, K-ATPase in epithelial cells. In: Semin Nephrol, vol. 25: Elsevier; 2005: 328-334.

Higher Degree Research Thesis by Publication
University of New England

STATEMENT OF AUTHORS' CONTRIBUTION

(To appear at the end of each thesis chapter submitted as an article/paper)

We, the Research Master/PhD candidate and the candidate's Principal Supervisor, certify that all co-authors have consented to their work being included in the thesis and they have accepted the candidate's contribution as indicated in the *Statement of Originality*.

	Author's Name (please print clearly)	% of contribution
Candidate	**Sami Samiullah**	70
Other Authors	**Shu-Biao Wu**	15
	Juliet Roberts	15

Name of Candidate: **Samiullah**

Name/title of Principal Supervisor: **Associate Professor Juliet Roberts**



Candidate Date 09/06/2017



Principal Supervisor Date 09/06/2017

Higher Degree Research Thesis by Publication
University of New England

STATEMENT OF ORIGINALITY

(To appear at the end of each thesis chapter submitted as an article/paper)

We, the Research Master/PhD candidate and the candidate's Principal Supervisor, certify that the following text, figures and diagrams are the candidate's original work.

Type of work	**Page number/s**
Figure 9.1	271
Figure 9.2	272
Figure 9.3	274
Text and tables	259-286

Name of Candidate: **Samiullah**

Name/title of Principal Supervisor: **Associate Professor Juliet Roberts**

[redacted]

Candidate Date 09/06/2017

[redacted]

Principal Supervisor Date 09/06/2017

Chapter 10 Histological and immunohistological observations of shell gland of laying hens in relation to time-points of eggshell formation and nicarbazin treatment

10.1 Abstract

Shell gland tissue was collected from nicarbazin treated hens at three different time-points of eggshell formation and processed for immunohistochemical localisation of ALAS1, ALAD and FECH enzymes using commercially available antibodies. Shell gland tissue from the same treatment was fixed in 4% paraformaldehyde and processed for morphometric measurements of various layers of the shell gland tissue. A piece of tissue was fixed in Zenker Formol and processed for microscopy to view the autofluorescence of protoporphyrin IX (PP IX).

The immunohistochemical results showed that the antibodies did not recognise their respective proteins even though the amino sequence homology of the antibodies used with chicken was >90%. This was further confirmed by immunoblotting. Autofluorescence of PP IX was not detected in Zenker Formol tissue. There was no significant effect of time-point and nicarbazin treatment on the overall morphology of the shell gland tissue. The length and width of the various layers were not significantly different between the control and nicarbazin treated groups. Future studies with chicken specific antibodies should include positive controls from human tissue as the commercial antibodies available are based on the human amino acid sequence.

10.2 Introduction

A mature laying hen has only the left oviduct functional and involved in the formation of an egg. The shell gland is an expanded pouch-like part of the oviduct where an egg remains for approximately 18-20 hours, during which time shell formation takes place (Johnston *et al.*, 1963). Histologically, the shell gland consists of a mucosa, submucosa and a muscularis (Hodges, 1974). The peritoneal surface

of the shell gland is lined by a serosa and subjacent connective tissue (Figure 10.1, I). The mucosa is formed by a ciliated and a secretory epithelium resting on a cellular lamina propria (Figure 10.1, I). In humans and other animals, the number of ciliated and secretory cells varies along the oviduct (Abe, 1996; Hafez & Kanagawa, 1972; Kress & Morson, 2007). Similar findings have been observed in different segments of the oviduct of laying hens (Chousalkar & Roberts, 2008). The muscularis consists of an inner circular smooth muscle layer and an outer longitudinal layer (Figure 10.1, I). The mucosa consists of a richly vascularised lamina propria**, a** basement membrane and pseudostratified columnar epithelial cells (Figure 10.1, I, II)**.**

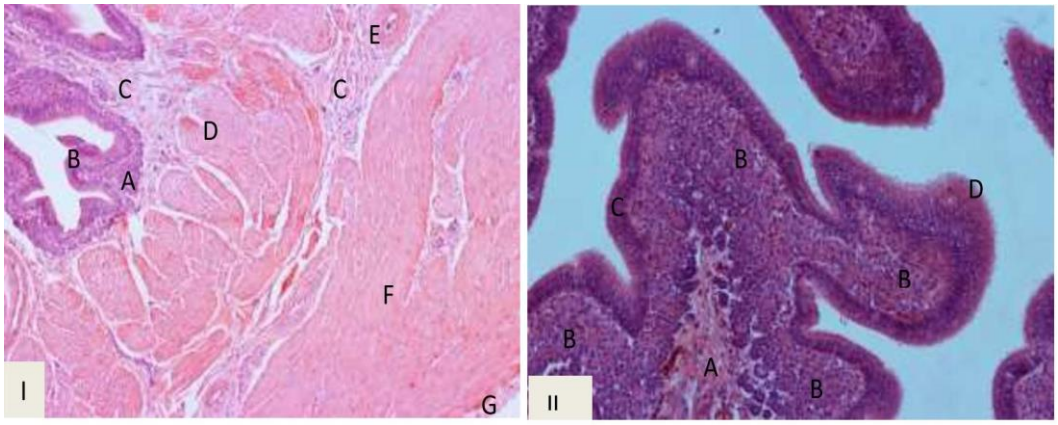

Figure 10.1 Histological structure of the cross section of shell gland tissue fixed in 4% paraformaldehyde

I) A. Lamina propria; **B**. Epithelium; **C**. Connective tissue ; **D**. Circular muscle; **E**. Blood vessel ; **F**. Tunica muscularis (longitudinal muscle); **G**. Tunica serosa. **II) A**. Connective tissue in the primary mucosal fold; **B**. Areas rich in secretory glands; **C**. Basal and apical cells in the epithelium; **D**. Cilia arising from epithelial cells (Hematoxylin & Eosin staining. I. x100; II. x200).

The surface epithelium consists of apical, ciliated and basal cells (Figure 10.1, II). The epithelial cells are mostly covered with motile cilia that help in transportation of egg components from the endometrium to the egg (Bradley, 1928). Epithelial height and proportion of ciliated to non-ciliated secretory cells vary and correlate with egg formation cycle changes (Richardson, 1935). The tubular glands are packed together below the epithelium (Figure 10.1, II). Microscopic studies have

been conducted on individual regions of the oviduct, such as the infundibulum (Aitken & Johnston, 1963; Wyburn *et al.*, 1970), magnum (Jung *et al.*, 2011; Wyburn et al., 1970), isthmus, tubular shell gland (Draper *et al.*, 1972) and shell gland pouch (Bakst & Howarth, 1975; Breen & De Bruyn, 1969; Wyburn *et al.*, 1973). Similarly, ultrastructural changes in individual segments of oviduct in relation to the laying cycle have also been demonstrated (Chousalkar & Roberts, 2008).

Calcification of the eggshell is associated with stimuli initiated by ovulation or by neuroendocrine factors that control and coordinate both ovulation and calcium secretion (Johnson, 2015). The hen's eggshell comprises six layers, formed in the acellular environment of the uterine fluid (Nys *et al.*, 2004), which is supersaturated with respect to calcium and bicarbonate and contains organic precursors of the shell matrix (Fernandez *et al.*, 2003; Hincke *et al.*, 2000; Nys et al., 2004; Parsons, 1982). The eggshell comprises: inner and outer shell membranes, mammillary layer (cone layer), palisade layer, vertical crystal layer and cuticle (Board, 1982; Cain & Heyn, 1964; Kusuda *et al.*, 2011; Lammie *et al.*, 2005; Rodriguez-Navarro *et al.*, 2002; Rose & Hincke, 2009; Simons, 1971; Wellman-Labadie *et al.*, 2010). Except for the shell membranes, all of these layers are formed in the shell gland lumen. In addition to the secretion of eggshell calcite and shell matrix molecules, the glandular epithelia of the shell gland also synthesize and deposit brown eggshell colour, protoporphyrin IX (PP IX), into various layers of the eggshell. PP IX is a fluorescent compound and its synthesis occurs through a multi-enzymatic pathway that takes place in mitochondria and cytosol (reviewed in (Samiullah *et al.*, 2015). PP IX concentration in the eggshell is affected by various factors such as stress levels, certain diseases and some drugs (reviewed in (Samiullah et al., 2015). It has been shown that PP IX fluoresces when either fixed or unfixed tissue is examined under a fluorescent microscope and the fluorescence signals were stronger in Zenker Formol fixed tissues compared with other fixatives (Tamura & Fujii, 1967). The enzyme delta-aminolevulinate synthase 1 (ALAS1) has a molecular weight of 69 kDa and catalyzes the reaction of succinyl co-enzyme A and glycine to form delta-aminolevulinic acid within the mitochondrial matrix (May *et al.*, 1995). Delta-aminolevulinic acid dehydratase (ALAD) has a molecular weight of 36 kDa and is involved in the conversion of delta-aminolevulinate to porphobilinogen (Moore *et*

al., 1987). The enzyme ferrocheletase (FECH) has a molecular weight of 45 kDa and catalyses the final step in converting PP IX into heme (Harbin & Dailey, 1985). In the current study, attempts were made initially to achieve immunofluorescence in the presence of PP IX as the commercially available antibodies (raised in rabbit from amino acids sequences from human) against ALAS1, ALAD and FECH enzymes showed 94, 91 and 91.4% immunogen similarities with chicken ALAS1, ALAD and FECH, respectively, through UniProt BLAST analysis. After obtaining no results for immunofluorescence, western blot was performed to investigate the affinity of the above mentioned antibodies for their respective proteins in the chicken shell gland. Furthermore, traditional histology was performed on paraformaldehyde fixed and paraffin embedded tissue to study any variations in tissue morphology at different time-points during eggshell formation and in the presence of nicarbazin treatment. Tissue pieces fixed in Zenker Formol were also viewed under a fluorescence microscope to localize PP IX. This study was intended to serve as a reference for future studies on the shell gland region of the oviduct of laying hens in relation to different stages of eggshell formation.

10.3 Materials and Methods

10.3.1 Preparation of frozen sections for immunofluorescence

Details of the complete experimental protocol and rearing of birds have been described in Chapters 5 and 6. Briefly, freshly collected pieces of unfixed shell gland tissue, taken at three different time-points during eggshell formation (5, 15, 23.5 hr) and with or without nicarbazin treatment (2×3, factorial design), were embedded in Optimal Cutting Temperature (OCT) compound (ProSciTech, Australia) in cryomolds, snap frozen in liquid nitrogen and stored at -80°C until used for sectioning. Tissue blocks were sectioned at 8-10 µm thickness using a Leica Cryostat (CM1850). Sections were collected on SuperFrost microscopic slides (ProSciTech, Australia) and allowed to dry for 3-5 minutes at room temperature. The sections were fixed in chilled 100% acetone for 5-10 minutes at room temperature and washed in PBS-T (Appendix B) for 3×5 min to remove tissue-freezing matrix. An antigenic retrieval step was performed by heating the section slides in sodium citrate buffer (10mM sodium citrate, 0.05% Tween 20, pH

6.0) (Appendix B) for 1-3 minutes in a microwave oven (Yamashita & Okada, 2005a, 2005b). The sections were washed in PBS-T for 3×5 min and encircled using a PAP pen (Sigma Aldrich, Australia). To block the non-specific binding of immunoglobulin, the sections were incubated with 1X PBS/5% normal serum/0.3% Triton™ X-100 (Appendix B) for 15 minutes at room temperature. The blocking serum was removed and the sections were incubated with 1 mL of unlabelled polyclonal primary antibody (ALAS1 from Novus Biological USA, Cat. No. NB100-56415, rabbit) at 1:200 dilutions (Appendix B) for 1 hour at room temperature. The sections were washed in PBS-T for 3×5 minutes and incubated in the dark with 1 mL of labelled goat polyclonal secondary antibody (Novus Biological USA, Goat anti- IgG Secondary Antibody [HiLyte Fluor 488] 0.5 mg (NB710-94932)) in 1:200 dilutions in PBS (Appendix B) for 30 minutes at room temperature. The sections were rinsed in PBS-T for 3×5 minutes. The sections were stained with DAPI (D9542-10MG; Appendix B) for 20 min in the dark. The sections were then rinsed in BPS-T for 3×5 min, mounted with DPX mountant (Sigma 06522) and viewed under a Nikon eclipse Ti fluorescent microscope with Imaging Software NIS Elements AR 3.10 installed. In this software, Filters UA 2A (Excitation 330-380 nm; Dichroic mirror 400 nm; Barrier filter 420 nm) and B 2A (Excitation 450-490 nm; Dichroic mirror 505 nm; Barrier filter 520 nm) options were used to detect DAPI counter stained nuclei and immunofluorescence of antibodies, respectively. The same procedure was performed for the ALAD (0.05 mg, NBP1-56506) and FECH primary antibodies (Antibody 0.1 mL, NBP2-33413, rabbit) Novus Biologicals USA). The details of the dilution preparation for ALAD and FECH are in Appendix B.

10.3.2 Western Blotting

10.3.2.1 Total protein extraction from shell gland tissue

A whole piece (with all tissue layers) of approximately 1 g of frozen shell gland tissue was homogenized using an IKA homogenizer in a 50 mL tube by adding 7 mL of cold extraction buffer (Appendix B). The homogenate was centrifuged at 3000 ×*g* for 15 min at 4°C. The fat layer floating on the surface was discarded and the supernatant was separated for soluble proteins extraction. For insoluble proteins

extraction, the remaining protein pellet in the tube was washed in extraction buffer, vortexed briefly (30 sec) and then centrifuged as mentioned earlier. The washing procedure was repeated for a total of 2-3 times to obtain a pure protein pellet. The pellet was resuspended in 2 mL extraction buffer and vortexed briefly. From both the soluble and insoluble proteins extraction, 0.75 mL was transferred to 2 mL Eppendorf tubes into which 0.75 mL sample buffer (Appendix B) was added. From the original concentration of extracted proteins, dilutions of 1:5 and 1:10 were prepared and heated at 60°C for 10 min. The tubes were stored at -20°C until used for downstream application.

10.3.2.2Total protein determination

The soluble and insoluble protein concentration of the chicken shell gland tissue samples was determined in triplicate using a Pierce™ BCA Protein Assay Kit (Frank *et al.*, 2017). The samples were stored at -20°C until used for sodium dodecyl sulfate polyacrylamide gel electrophoresis (SDS PAGE).

10.3.2.3SDS PAGE

A 12% separating gel (Appendix B) was prepared in a 50 mL sterile tube and poured into glass plates on the top of which a layer of water was added to avoid direct contact of the gel solution with air, which inhibits acrylamide polymerization. After polymerization of the separating gel, stacking gel (Appendix B) was prepared in a 5 mL sterile tube. The water was removed and stacking gel was immediately poured on the top of polymerized separating gel. The well comb was carefully inserted and allowed the stacking gel to be polymerized. The SDS PAGE gels were prepared in duplicate, one for protein bands staining and one for immunoblotting.

The protein samples were heated for 5 min at 95°C and mixed well before use. The electrophoresis apparatus (Bio-Rad, Australia) was set up and running buffer (Appendix B) was poured into the tank at appropriate level. All wells of the gel were washed by running buffer using an elongated 50 µL tip. To each of the wells, 25 µL of each of the protein samples were loaded. A 12 µL protein marker was loaded into first and last wells. The gel was run at 90V for 15 min and then 200V until the bromophenol blue reached the bottom of the gel (about 45 min). The gel

was carefully removed from the glass plates and the stacking gel was discarded. One gel was stained (about 30 min staining and 30 min de-staining) (Appendix B) for protein bands pattern and another was further processed for immunoblotting.

10.3.2.4Western Blotting (electro-transfer of the protein onto a membrane).

A transfer buffer (Appendix B) was prepared and poured into the immunoblot tank (Bio-Rad, Australia). A polyvinylidene difluoride (PVDF) membrane was equilibrated in methanol for 2 min before preparing the gel pad, as illustrated in Figure 10.2. To transfer the protein bands from the separating gel onto the PVDF membrane, the blot was run for 60 min at 60V in a gel tank.

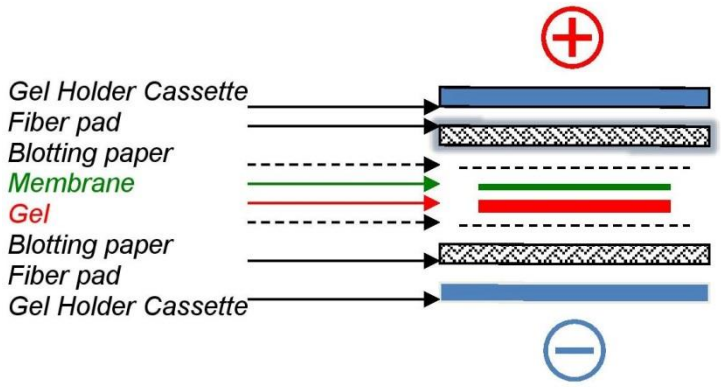

Figure 10.2 Gel pad preparation for transferring proteins bands from running gel (SDS-PAGE) to PVDF membrane

10.3.2.5Immuno-detection of protein

The blotted PVDF membrane was blocked for non-specific immunoglobulin binding with blocking buffer (Appendix B) for 30 min. The membrane was incubated with a 1:50 dilution of ALAS1 primary antibody (Novus Biologicals, Littleton, CO, USA, Cat# NB100-56415) for 1 hour and then washed 3×10 min in blocking buffer. The membrane was incubated with 1:5000 dilutions of secondary antibody (Novus Biologicals, Littleton, CO, USA, Cat# NB7160, goat anti-rabbit IgG antibody, HRP conjugated) for 30 min and washed as described earlier. For staining, the membrane was incubated with an avidin-biotin complex (ABC) staining kit (ThermoScientific, Australia) as per the manufacturer's protocol. The membrane was washed in TAE buffer (Appendix B) for 3×10 min and incubated in

DAB substrate (SIGMAFAST™ 3,3′-Diaminobenzidine tablets; Sigma Aldrich, Australia) until the development of brown colour (30 min to 1.0 hr). A negative control was processed in the same way except that it was incubated with blocking buffer rather than the primary antibody. The membrane was visually inspected for immune bands development. The same procedure was repeated when processing gels for detecting ALAD and FECH proteins (Novus Biologicals, USA, Cat# NBP1-56506; Cat#NBP2-33413, respectively). Based on the important role of ALAS1 in the PP IX biosynthetic pathway and the non-specific results of ALAS1 (Novus Biologicals, USA, Cat# NB100-56415), the procedure was repeated by using polyclonal ALAS1 antibody-N terminal region raised in rabbits (AVIVA Systems Biology, San Diego, CA, USA, Cat# ARP5454346_P050, M.W. 70 kDa). The molecular weight of migrated proteins relative to the protein (marker) ladder was measured by the following standard formula.

$$Rf = \frac{\text{migration distance of the protein}}{\text{Migration distance of the dye front}}$$

10.3.3 Paraffin embedded tissue preparation for histology

The shell gland tissue pieces, fixed in 4% paraformaldehyde solution (Appendix B) and stored in 70% ethanol at 4°C, were processed by standard histological procedures that included overnight processing and embedding in paraffin (Luna, 1968) (Appendix C). The tissues were sectioned in 6 µm and mounted on SuperFrost microscopic slides. All sections were stained with hematoxylin and eosin (H&E) (Sigma Aldrich, Australia) and examined under a light microscope for observing any structural and morphological changes in various layers of the tissue. Morphometric measurements were performed using a Nikon eclipse Ti fluorescent microscope with Imaging Software NIS Elements AR 3.10 installed. The plain filter was used for viewing H&E stained tissue. In the NIS elements software, Ti pad having option of Annotations and Measurements was used for the morphometric measurements of tissue sections. The primary, secondary and tertiary folds originating from the tunica mucosa were measured in terms of their height and width in five different regions of a single tissue section. Similarly, the height of tunica muscularis and serosa was also measured. In order to study the fluorescence

of PP IX in shell gland, shell gland tissue pieces were also fixed in Zenker Formol fixative (Appendices B and C), embedded in paraffin and processed for tissue sectioning as described earlier. The Zenker Formol fixed tissue sections (stained and unstained) were viewed in a Nikon microscope using a FITC filter that covers absorbance wavelength up to 495 nm. Similarly, the sections were also viewed in Nikon elicpse Ti fluorescent microscope with Filter B 2A that detects the absorbance wavelength of substances up to 515 nm.

10.4 Statistical analysis

Where appropriate, data analysis was performed in SPSS version 22 (IBM Corporation, Armonk, NY, USA) with the GLM module by taking the time-points of shell formation and nicarbazin treatment as main effects.

10.5 Results

10.5.1 Immunofluorescence microscopy of the shell gland tissue

None of the tissue sections showed staining for the antibodies used in the current study. As confirmation that the procedures performed were correct, all of the tissue sections examined under fluorescent microscope showed DAPI staining (Figure 10.3).

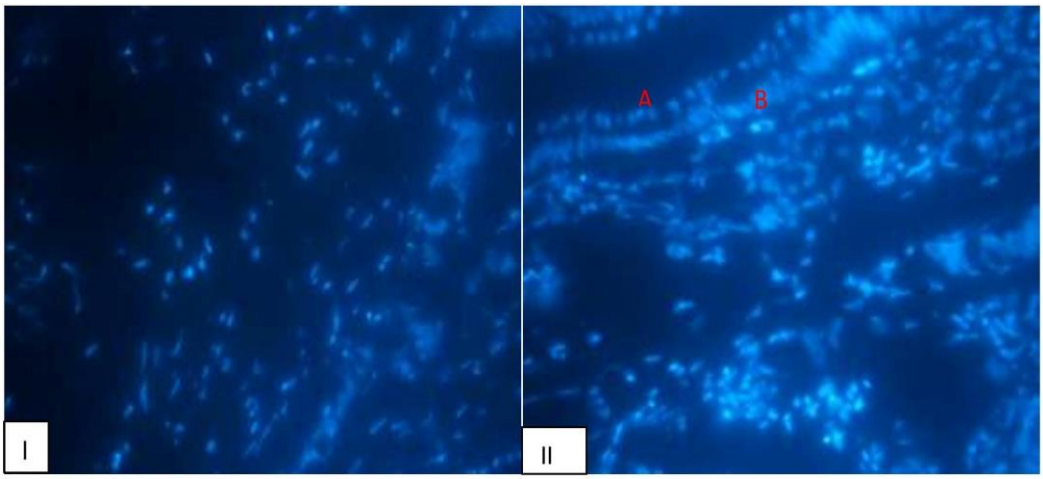

Figure 10.3 Immunofluorescence of nuclei in the sections of shell gland tissue of laying hens counter stained with DAPI for nuclear staining

I) Nuclei counter stained with DAPI in the muscular region of the shell gland tissue. **II**) Nuclei counter stained with DAPI in the epithelial region of the shell gland tissue. **A**) Apical cells nuclei counter stained with DAPI; **B**) Basal cells nuclei counter stained with DAPI

10.5.2 Western blotting

The results of the ALAS1 primary antibody (Cat# NB100-56415) were non-specific and the molecular weight of the band was in the range of 55 kDa. The ALAS1 primary antibody (Cat# ARP5454346_P050) did not identify any protein and thus no bands were developed on the membranes. Similarly, ALAD and FECH did not show any bands on the immunoblotted PVDF membrane. In the same experiment, we also quantified through qPCR the expression level of ALAS1 in shell gland tissue and found that its expression level was significantly affected by time-points of eggshell formation and nicarbazin treatment (data shown in Chapter 6). As shown in Figure 10.4, the transfer of protein bands to the PVDF membrane was successful and the procedure performed was correct. The two protein bands appearing on the PVDF membrane were due to non-specific binding of the secondary antibody (Figure 10.5). The bands that appeared from the ALAS1 antibody reactivity with insoluble proteins were in the range of 55 kDa migration distance and considered to be non-specific (Figure 10.5). Similarly, when the insoluble proteins relative to time-points and nicarbazin treated samples were immunoblotted, the band intensity was not visibly different between the nicarbazin

and control groups (Figure 10.6). These bands were in a similar range in migration distance (55 kDa) as observed in Figure 10.5.

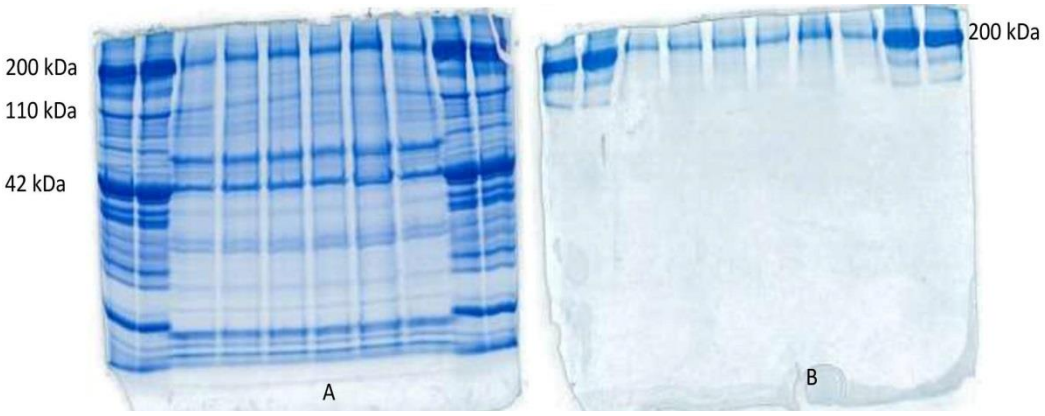

Figure 10.4 Total proteins separated on 12% SDS PAGE from shell gland tissue of laying hen

A) Proteins bands with two markers (bovine whole muscle extract) on each side of candidate protein bands. The first two lanes from the left and the last two lanes on the right show markers. The different lanes on the gel show extracted proteins from the shell gland tissue of the control nicarbazin treated laying hens collected at 5, 15 and 23.5 hr time-point. **B**) Stained gel is showing that the low molecular weight proteins were quantitatively transferred to the PVDF membrane

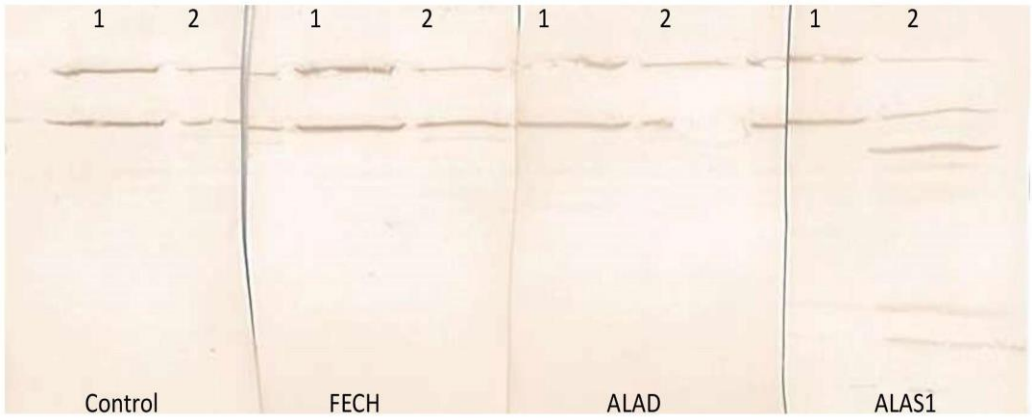

Figure 10.5 Protein immunoblotted from 12% SDS PAGE gel on PVDF membrane

1) Soluble protein immunoblotted with primary and secondary antibodies; **2**) Insoluble protein immunoblotted with primary and secondary antibodies; Control membrane was incubated with blocking buffer instead of primary antibody

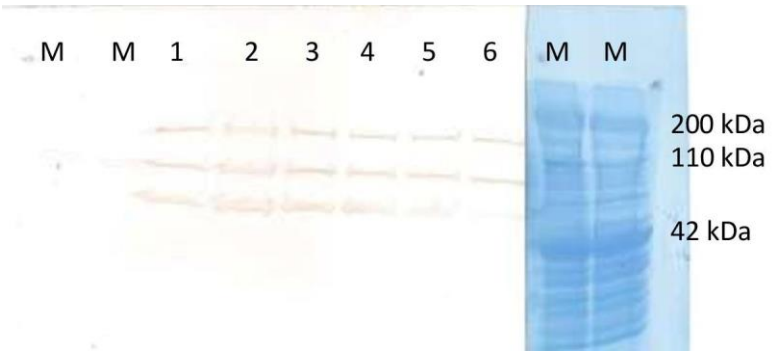

Figure 10.6 Protein bands on PVDF membrane

M is marker; **1**) Shell gland tissue sampled at 5 hr time-point from nicarbazin treated groups; **2**) Shell gland tissue sampled at 5 hr time-point from control groups; **3**) Shell gland tissue sampled at 15 hr time-point from nicarbazin treated groups; **4**) Shell gland tissue sampled at 15 hr time-point from control groups; **5**) Shell gland tissue sampled at 23.5 hr time-point from nicarbazin treated groups; **6**) Shell gland tissue sampled at 23.5 hr time-point from control groups

10.5.3 Histology of the shell gland tissue

There was no significant effect of time-point and nicarbazin treatment on the overall morphology of the shell gland tissue. The length and width of the various layers were not significantly different between the control and nicarbazin treated groups (Table 10.1). Examining the Zenker Formol fixed tissue under a fluorescence microscope, none of the tissue showed fluorescence for PP IX. However, it was noted that the tissue morphology in Zenker Formol was not as clear as observed in 4% paraformaldehyde fixed tissue sections.

Table 10.1 Morphometric measurements (µm) of various layers of shell gland tissue

Variable	Treatment		Time-points (hr)			P value		
	Control	Nicarbazin treatment	5	15	23.5	Treatment	Time-point	Treatment × Time-point
Serosa height (µ)	41.78±12.47	44.24±7.06	41.10±9.48	51.62±19.11	36.31±3.38	0.8701	0.6951	0.5407
Muscularis height (µ)	957.1±91.2	1087±114.7	1146.9±110.9	848.6±130.7	1071.8±129.5	0.3865	0.2512	0.7800
Mucosal primary folds height (µ)	2299.7±141.4	2461.1±254.8	2555.6±179.9	2311.3±228.2	2274.3±332.6	0.5955	0.7105	0.4269
[1]Mucosal primary fold width (µ)	186.4±17.5	257.4±32.9	201.7±33.1	252.8±37.7	211.2±37.7	0.0712	0.5079	0.3538
Mucosal secondary fold height(µ)	424.1±49.9	481.2±25.2	457.7±85.4	400.6±30.0	499.6±53.1	0.4387	0.5444	0.7884
Mucosal secondary fold width (µ)	212.8±18.8	184.3±11.1	195.1±9.3	208.7±14.4	191.8±29.1	0.2214	0.8119	0.6047

[1]Mucosal primary width was measured approximately in the middle section of the primary fold

10.6 Discussion

The results of this experiment showed that neither of the two different primary antibodies used against ALAS1 protein recognized the chicken form of the protein. The UniProt BLAST results showed that there was 92-94% sequence homology between the chicken form of the protein and the protein of the antibody (human); however, the present study showed that the antibodies did not recognize ALAS1 in chicken tissue. The antibodies used against ALAD and FECH proteins were predicted to have 91% sequence homology in chicken (per UniProt); nevertheless, these antibodies did not recognize the respective proteins in chicken. The reasons could be that the antibodies against the mentioned proteins were raised in rabbit on the basis of human peptide sequences. Future work should include human tissue as a positive control, if using the same antibodies in chicken tissue. The morphometric measurements of the 4% paraformaldehyde fixed tissue sections showed that the time-points of eggshell formation and nicarbazin treatment did not affect the mucosal height and width and muscularis layer height.

10.7 Conclusions

It can be concluded from the present work that the above antibodies despite showing >90 % sequence homology in chicken are not suitable antibodies for immunohistological localization of ALAS1, ALAD and FECH proteins in chicken oviduct tissue. It is recommended to develop and customise antibodies based on the chicken peptide amino acid sequences for similar studies in future.

10.8 References

Abe, H. (1996). The mammalian oviductal epithelium: regional variations in cytological and functional aspects of the oviductal secretory cells. *Histology and histopathology, 11*(3), 743-768.

Aitken, R. N. C., & Johnston, H. S. (1963). Observations on the fine structure of the infundibulum of the avian oviduct. *Journal of Anatomy, 97*(Pt 1), 87-99.

Bakst, M., & Howarth, B. (1975). SEM preparation and observations of the hen's oviduct. *The Anatomical Record, 181*(2), 211-225.

Board, R. G. (1982). Properties of avian egg shells and their adaptive value. *Biological Reviews, 57*(1), 1-28.

Bradley, O. C. (1928). Notes on the histology of the oviduct of the domestic hen. *Journal of Anatomy, 62*(Pt 3), 339-346.

Breen, P. C., & De Bruyn, P. P. H. (1969). The fine structure of the secretory cells of the uterus (shell gland) of the chicken. *Journal of Morphology, 128*(1), 35-65.

Cain, C. J., & Heyn, A. N. J. (1964). X-ray diffraction studies of the crystalline structure of the avian egg shell. *Biophysical Journal, 4*(1 Pt 1), 23-39.

Chousalkar, K. K., & Roberts, J. R. (2008). Ultrastructural changes in the oviduct of the laying hen during the laying cycle. *Cell and Tissue Research, 332*(2), 349-358.

Draper, M. H., Davidson, M. F., Wyburn, G. M., & Johnston, H. S. (1972). The fine structure of the fibrous membrane forming region of the isthmus of the oviduct of *Gallus domesticus*. *Quarterly Journal of Experimental Physiology and Cognate Medical Sciences, 57*(3), 297-310.

Fernandez, M. S., Escobar, C., Lavelin, I., Pines, M., & Arias, J. L. (2003). Localization of osteopontin in oviduct tissue and eggshell during different stages of the avian egg laying cycle. *Journal of Structural Biology, 143*(3), 171-180.

Frank, D. C., Geesink, G., Alvarenga, T. I. R. C., Polkinghorne, R., Stark, J., Lee, M., & Warner, R. (2017). Impact of high oxygen and vacuum retail ready packaging formats on lamb loin and topside eating quality. *Meat Science, 123*, 126-133.

Hafez, E. S. E., & Kanagawa, H. (1972). Ciliated epithelium in the uterine cervix of the macaque and rabbit. *Journal of Reproduction and Fertility, 28*(1), 91-94.

Harbin, B. M., & Dailey, H. A. (1985). Orientation of ferrochelatase in bovine liver mitochondria. *Biochemistry, 24*(2), 366-370.

Hincke, M. T., Gautron, J., Panheleux, M., Garcia-Ruiz, J., McKee, M. D., & Nys, Y. (2000). Identification and localization of lysozyme as a component of eggshell membranes and eggshell matrix. *Matrix Biology, 19*(5), 443-453.

Hodges, R. D. (1974). *The histology of the fowl*: Academic Press.

Johnson, A. L. (2015). Chapter 28 - Reproduction in the Female A2 - Scanes, Colin G *Sturkie's Avian Physiology (Sixth Edition)* (pp. 635-665). San Diego: Academic Press.

Johnston, H. S., Aitken, R. N. C., & Wyburn, G. M. (1963). The fine structure of the uterus of the domestic fowl. *Journal of Anatomy, 97*(Pt 3), 333-344.

Jung, J. G., Lim, W., Park, T. S., Kim, J. N., Han, B. K., Song, G., & Han, J. Y. (2011). Structural and histological characterization of oviductal magnum and lectin-binding patterns in *Gallus domesticus*. *Reproductive Biology and Endocrinology, 9*(1), 62.

Kress, A., & Morson, G. (2007). Changes in the oviducal epithelium during the estrous cycle in the marsupial *Monodelphis domestica*. *Journal of Anatomy, 211*(4), 503-517.

Kusuda, S., Iwasawa, A., Doi, O., Ohya, Y., & Yoshizaki, N. (2011). Diversity of the cuticle layer of avian eggshells. *The journal of Poultry Science, 48*(2), 119-124.

Lammie, D., Bain, M. M., & Wess, T. J. (2005). Microfocus X-ray scattering investigations of eggshell nanotexture. *Journal of Synchrotron Radiation, 12*(6), 721-726.

Luna, L. G. (1968). Manual of histologic staining methods of the Armed Forces Institute of Pathology.

May, B. K., Dogra, S. C., Sadlon, T. J., Bhasker, C. R., Cox, T. C., & Bottomley, S. S. (1995). Molecular regulation of heme biosynthesis in higher vertebrates. *Progress in Nucleic Acid Research and Molecular Biology, 51*, 1-51.

Moore, M. R., Mccoll, K. E., Rimington, C., & Goldberg, A. (1987). Porphyrins and enzymes of the heme biosynthetic pathway *Disorders of Porphyrin Metabolism* (pp. 21-72): Springer.

Nys, Y., Gautron, J., Garcia-Ruiz, J. M., & Hincke, M. T. (2004). Avian eggshell mineralization: biochemical and functional characterization of matrix proteins. *Comptes Rendus Palevol, 3*(6–7), 549-562.

Parsons, A. H. (1982). Structure of the eggshell. *Poultry Science, 61*(10), 2013-2021.

Richardson, K. C. (1935). The secretory phenomena in the oviduct of the fowl, including the process of shell formation examined by the microincineration technique. *Philosophical Transactions of the Royal Society of London. Series B, Biological Sciences, 225*(522), 149-195.

Rodriguez-Navarro, A., Kalin, O., Nys, Y., & Garcia-Ruiz, J. M. (2002). Influence of the microstructure on the shell strength of eggs laid by hens of different ages. *British Poultry Science, 43*(3), 395-403.

Rose, M. L. H., & Hincke, M. T. (2009). Protein constituents of the eggshell: eggshell-specific matrix proteins. *Cellular and Molecular Life Sciences, 66*(16), 2707-2719.

Samiullah, S., Roberts, J. R., & Chousalkar, K. (2015). Eggshell colour in brown-egg laying hens—a review. *Poultry Science, 94*(10), 2566-2575.

Simons, P. C. M. (1971). Ultrastructure of the hen eggshell and its physiological interpretation. Published by: Centre for Agricultural Pub. and Documentation.

Tamura, T., & Fujii, S. (1967). Comparative observations on the distribution of fluorescent pigments (porphyrins) in the chicken and quail uteri. *Journal of the Faculty of Fisheries and Animal Husbandry, Hiroshima University, 7*, 43-49.

Wellman-Labadie, O., Lemaire, S., Mann, K., Picman, J., & Hincke, M. T. (2010). Antimicrobial activity of lipophilic avian eggshell surface extracts. *Journal of Agricultural and Food Chemistry, 58*(18), 10156-10161.

Wyburn, G. M., Johnston, H. S., Draper, M. H., & Davidson, M. F. (1970). The fine structure of the infundibulum and magnum of the oviduct of *Gallus domesticus*. *Quarterly Journal of Experimental Physiology and Cognate Medical Sciences, 55*(3), 213-232.

Wyburn, G. M., Johnston, H. S., Draper, M. H., & Davidson, M. F. (1973). The ultrastructure of the shell forming region of the oviduct and the development of the shell of *Gallus domesticus*. *Quarterly Journal of Experimental Physiology and Cognate Medical Sciences, 58*(2), 143-151.

Yamashita, S., & Okada, Y. (2005a). Application of heat-induced antigen retrieval to aldehyde-fixed fresh frozen sections. *Journal of Histochemistry & Cytochemistry, 53*(11), 1421-1432.

Yamashita, S., & Okada, Y. (2005b). Mechanisms of heat-induced antigen retrieval: analyses *in vitro* employing SDS-PAGE and immunohistochemistry. *Journal of Histochemistry & Cytochemistry, 53*(1), 13-21.

Chapter 11 General conclusions

The current study investigated factors affecting the protoporphyrin IX (PP IX) level in shell gland tissue and eggshell in brown-egg laying hens. Molecular approaches were adapted to study how genes involved in the production of PP IX are regulated in relation to time-points (post-oviposition) of eggshell formation, nicarbazin treatment and infectious bronchitis virus (IBV) infection. An effect of mitochondrial count per cell on the synthesis of PP IX in relation to time-points of eggshell formation and nicarbazin treatment was elucidated. Attempts were made to localize three different enzymes involved in the PP IX synthesis in shell gland tissue at different time-points of eggshell formation and nicarbazin ingestion. Furthermore, mitochondrial count per cell was investigated in three different segments of the oviduct in relation to time-points of eggshell formation and IBV challenge. The outcome of the study contributes to an in-depth understanding of the PP IX synthesis at the molecular level and suggestions have been made for future research.

The findings in Chapter 2 showed that production system significantly affected shell reflectivity, egg weight and egg internal quality, while the flock age significantly affected most of the variables measured. A significantly higher amount of cuticle cover in barn eggs highlights the role of production system in cuticle formation. A higher amount of PP IX per gram of eggshell in cage eggs might indicate that eggshell colour is more uniform in eggs produced in the cage production system. A higher amount of cuticle in barn eggs and more PP IX in cage eggs indicates that PP IX deposition into eggshell is independent of the amount of cuticle present. A lower amount of cuticle cover and PP IX at 73 week flock age, compared with the 44 week flock, indicates that these traits are clearly affected by flock age and thus eggs produced by an aged flock may be less uniform in colour and have poorer cuticle cover. Taken together, the findings presented in Chapter 2 indicate that differences in egg quality existed when birds which were reared together were distributed into different production systems and sampled at different ages for egg quality analysis.

The findings reported in Chapter 3 indicate that the decreasing level of PP IX in eggshells as flocks age may be due to decreased synthesis of pigment in the shell

gland tissue. The genetic and/or hormonal mechanisms involved in darker brown coloured eggs being laid earlier in the morning are not completely understood. Further research is recommended to investigate the relationship between oviposition time and eggshell quality including shell colour. The egg position in-clutch study indicated that overall eggshell quality decreases as the egg position in a clutch increases and the effect is clearer in long clutches than in medium or short clutches. The mechanisms that contribute to these factors and how a hen returns to the quality of the first egg in-clutch following a one day pause in the laying cycle, requires further investigation at the molecular level.

The findings of Chapter 4 showed that IBV multiplication in the shell gland affected the synthesis level of PP IX resulting in, a lower amount of pigment appearing in eggshells for 7-12 days post infection (p.i.). It appears that viral multiplication in the shell gland tissue disrupted some aspect of the mechanism of PP IX synthesis. Significant differences in PP IX level in eggshells among flocks affected by various IBV strains indicate that different strains of IBV affect eggshell colour to different extents.

Experiments 4 and 5, reported in Chapters 5 and 6, investigated how the anticoccidial drug, nicarbazin, disrupts the molecular mechanism involved in the synthesis of PP IX at the cellular level. The findings of Chapter 5 showed that, despite the acceptable overall stability of the 10 reference genes, the expression stability was affected by time-points of eggshell formation and nicarbazin treatment. *HPRT1* and *HMBS* were the two most stably expressed reference genes both in the time-point and nicarbazin treatment model. A reference gene validation method further confirmed that the use of most stably expressed reference genes produced more robust and accurate results when compared with the results of expression level of genes being normalised with the two least stable reference genes (*CA2, B2M*). Therefore, *HPRT1* and *HMBS* were selected as reference genes for the normalisation of gene expression data obtained in Chapter 6. The findings reported in Chapter 6 showed that number of mitochondria per cell did not vary significantly with different time-points of eggshell formation, indicating that eggshell formation is independent of number of mitochondria per cell. However, it should be noted that there is a lack of information concerning the turnover rate of mitochondria in metabolically active tissue, such as the laying hen oviduct. Significantly different

differential expression levels of the genes selected from the biosynthetic pathway of PP IX, indicate that each of these genes is regulated in a different manner and their expression levels were generally up-regulated when shell formation was initiated. Feeding nicarbazin to laying hens disrupted the mechanism of PP IX synthesis by down-regulating the expression level of *ALAS1*, thus producing lower amount of PP IX in shell gland and eggshell. A molecular investigation of feeding nicarbazin to laying hens for longer period of time is suggested to understand the spatio-temporal regulation of genes involved in egg formation.

The findings reported in Chapter 7 (Experiment 6) showed that *YWHAZ* and *TBP* were the most two stably expressed reference genes in the shell gland and spleen of IBV challenged laying hens. The genes, *YWHAZ* and *TBP* were more stable in expression than *HPRT1* and *HMBS*, which were the two most stable reference genes in the nicarbazin model. These findings indicate that genes stable under one treatment may not be stably expressed in a different type of treatment. A clear difference in the results of the validation of reference gene data indicated that the data obtained from using the two most stable reference genes was more robust and accurate. Therefore, *YWHAZ* and *TBP* were used as reference genes for the normalisation of gene expression data obtained in Chapters 8 and 9. The findings of Chapter 8 reflect the whole transcriptomic analysis of shell gland tissue in an IBV T strain challenged model. The functional analysis of the Gene Ontology (GO) terms of the differentially expressed genes (DEGs) showed that the genes up-regulated at the 5 hr time-point were involved in the ion transport initiating the synthesis function of the shell gland. The DEGs at the 15 hr time-point were involved in energy metabolism and synthesis function, reflecting the peak synthesis stage of eggshell. Genes such as C*ALB*1 up-regulation at 15 hr time-point further confirms the role of such genes in the peak synthesis stage of eggshell. Findings in this study cannot completely rule out the effect of IBV on genes involved in the mucosal immune system and eggshell formation including PP IX synthesis, as it is likely that factors such as sampling time post infection, the nature of the tissue sampled (all tissue layers versus mucosal scrapings) used for RNA extraction and using an adjusted P value for RNA-sequencing data analysis affected the results. Other contributing factors include flock age and genotype of a hen as the disease is more severe in relatively younger birds and in White leghorn than Isa-brown strain.

The findings reported in Chapter 9 showed that IBV appeared to affect the shell gland to a greater extent than the isthmus and magnum; thus the mean mitochondrial count was significantly lower only in the shell gland of the challenged birds. The lack of a clear correlation between the expression levels of the nuclear DNA encoded genes and mitochondrial count in the shell gland tissue could not be clearly explained; however, it seems that the nuclear DNA encoded genes are regulated differently. The findings in this study also agreed with the findings reported in Chapter 6, which reported no significant difference in mean mitochondrial count per cell with different stages of egg and eggshell formation. Further studies are required to investigate how IBV infection causes degeneration of the mitochondria in cells of the shell gland.

Chapter 10 summarises the results of histology and immunofluorescence of shell gland tissue obtained in the nicarbazin treatment study. The findings showed that the commercially available antibodies applied in the study did not recognise their respective proteins due to the origin of the antibodies being based on human originated enzyme amino acids sequences. Therefore, a solid conclusion about the location of the synthesis of PP IX in shell gland tissue could not be made. However, it would be ideal to use human/mouse tissue as a positive control in future studies to confirm that the antibodies do recognise their respective proteins. The lack of auto-fluorescence in Zenker Formol fixed tissue suggests that this is not an ideal method for the localisation and quantification of PP IX in shell gland tissue. We recommend further studies using antibodies that have been obtained from enzyme amino acid sequences specific to the chicken. Such future studies will help to localize PP IX at a cellular level and confirm the nature of the cell(s) involved in PP IX synthesis in the shell gland of laying hens.

Appendices

Appendix A

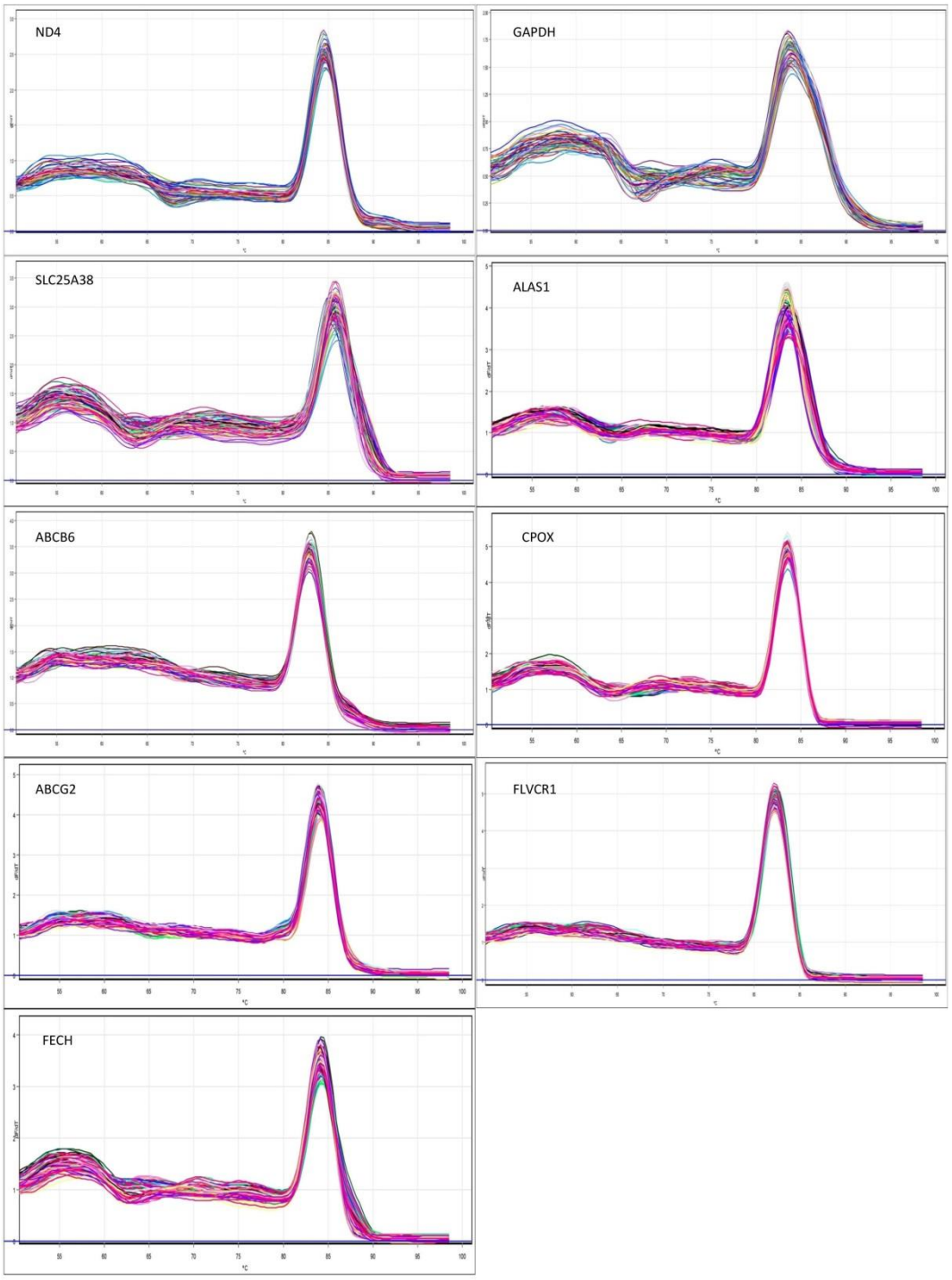

Melting curves of candidate target genes showing single peak indicated that all the primers were specific in amplifying fragment of the genes.

DEGs genes up-regulated in IBV T challenged vs control group at P value <0.05

Gene ID	Gene symbol	logFC	P value	Gene ID	Gene symbol	logFC	P value
ENSGALG00000017183	*MMP13*	3.4644	3E-05	ENSGALG00000023819	*LOC772158*	2.1777	0.0134
ENSGALG00000007651	*STAT1*	1.9059	7E-05	ENSGALG00000004243	*IFITM1*	2.1326	0.0143
ENSGALG00000014297	*IRF7*	2.1107	0.0003	ENSGALG00000010853	*C8B*	1.7324	0.0146
ENSGALG00000001558	*MOV10*	1.5327	0.0003	ENSGALG00000028982	*CMPK2*	2.432	0.0146
ENSGALG00000004859	*ZNFX1*	2.4065	0.0003	ENSGALG00000039970	*ENDOU*	2.3391	0.0153
ENSGALG00000041621	*LY6E*	2.1077	0.0004	ENSGALG00000042031	*GPX2*	1.528	0.0163
ENSGALG00000003217	*LITAF*	1.6226	0.0005	ENSGALG00000038140	*Unknown*	3.9407	0.0189
ENSGALG00000012072	*Unknown*	1.5316	0.0013	ENSGALG00000007257	*TEKT5*	1.8765	0.019
ENSGALG00000041380	*BF2*	1.6224	0.0017	ENSGALG00000037520	*Unknown*	1.6668	0.0209
ENSGALG00000011190	*Unknown*	1.9476	0.0022	ENSGALG00000036846	*KRT9L*	3.2301	0.0211
ENSGALG00000016142	*MX1*	3.0793	0.0024	ENSGALG00000013575	*IFI6*	3.1674	0.0214
ENSGALG00000042854	*Unknown*	2.0519	0.0027	ENSGALG00000040901	*LOC100859134*	2.1058	0.022
ENSGALG00000017378	*CRTAC1*	1.8992	0.0027	ENSGALG00000006106	*TNFRSF6B*	1.8164	0.0222
ENSGALG00000028424	*GJB3*	1.9204	0.0032	ENSGALG00000019061	*MMP1*	1.5008	0.0264
ENSGALG00000016964	*EPSTI1*	1.5152	0.0035	ENSGALG00000016400	*RSAD2*	2.9155	0.0278
ENSGALG00000030320	*YF6; MHCIA7*	1.9314	0.0039	ENSGALG00000016442	*RRM2*	2.0434	0.0295
ENSGALG00000029707	*LOC101751061*	3.8689	0.0042	ENSGALG00000011277	*Unknown*	2.6959	0.0362
ENSGALG00000033231	*RACGAP1*	2.4785	0.0048	ENSGALG00000038683	*Unknown*	2.3342	0.0371
ENSGALG00000026380	*Unknown*	2.662	0.0052	ENSGALG00000043176	*Unknown*	1.769	0.0385
ENSGALG00000042557	*LOC421238*	1.6572	0.0053	ENSGALG00000000619	*ANGPTL4*	2.4254	0.0389
ENSGALG00000023821	*DHX58*	1.5666	0.0057	ENSGALG00000008552	*MAL*	1.8658	0.0396
ENSGALG00000037408	*ADMP*	2.1076	0.0063	ENSGALG00000009639	*Unknown*	3.6235	0.0402
ENSGALG00000013057	*USP18*	2.6211	0.0079	ENSGALG00000027789	*Unknown*	1.5188	0.0411
ENSGALG00000013762	*LOC101749664*	2.9049	0.0089	ENSGALG00000000604	*NKAIN1*	1.8766	0.0417
ENSGALG00000042001	*Unknown*	1.9233	0.0105	ENSGALG00000001863	*VTG2*	1.6379	0.0424
ENSGALG00000002957	*SLC12A3*	2.844	0.0106	ENSGALG00000016154	*ARC*	3.7363	0.0481
ENSGALG00000034616	*INHBA*	2.5374	0.0109	ENSGALG00000004093	*TBX22*	1.9435	0.0498
ENSGALG00000041928	*Unknown*	3.0309	0.011	ENSGALG00000042065	*Unknown*	3.1022	0.0498
ENSGALG00000013723	*OASL*	3.5135	0.0126				

LogFC indicates fold change expressed in $\log_2$ value

DEGs genes down-regulated in IBV T challenged vs control group at P value <0.05

Gene ID	***Gene symbol***	**logFC**	**P value**	**Gene ID**	***Gene symbol***	**logFC**	**P value**
ENSGALG00000041008	*unknown*	3.6380	0.0037	ENSGALG00000007226	*OSTN*	2.1128	0.0112
ENSGALG00000030178	*unknown*	3.3552	0.0225	ENSGALG00000006318	*IL21R*	2.0837	0.0464
ENSGALG00000040044	*unknown*	3.3128	0.0006	ENSGALG00000040730	*RXRG*	2.0825	0.0021
ENSGALG00000004526	*TNR*	3.1824	0.0273	ENSGALG00000015835	*GRIK1*	2.0690	0.0452
ENSGALG00000038539	*unknown*	2.9522	0.0123	ENSGALG00000040815	*unknown*	2.0658	0.0197
ENSGALG00000004945	*SLC12A1*	2.9447	0.0083	ENSGALG00000041938	*unknown*	2.0257	0.0346
ENSGALG00000001252	*CREB3L3*	2.8982	0.0061	ENSGALG00000008283	*unknown*	2.0202	0.0124
ENSGALG00000028895	*LOC772096*	2.8959	0.0078	ENSGALG00000005458	*RPL3L*	1.9992	0.0105
ENSGALG00000035375	*LRTOMT*	2.8420	0.0149	ENSGALG00000011086	*ACTA1*	1.9945	0.0114
ENSGALG00000024136	*LOC408038*	2.8294	0.0003	ENSGALG00000035007	*unknown*	1.9854	0.0071
ENSGALG00000009266	*FGA*	2.7528	0.0024	ENSGALG00000017295	*PTHLH*	1.9845	0.0164
ENSGALG00000002993	*CA10*	2.7067	0.0001	ENSGALG00000038051	*unknown*	1.9831	0.0140
ENSGALG00000030405	*unknown*	2.6634	0.0013	ENSGALG00000003911	*CACNG5*	1.9825	0.0357
ENSGALG00000041805	*unknown*	2.6485	0.0225	ENSGALG00000036041	*unknown*	1.9636	0.0124
ENSGALG00000012869	*OVAL*	2.6331	0.0064	ENSGALG00000009107	*NRXN1*	1.9574	0.0067
ENSGALG00000034146	*unknown*	2.5422	0.0035	ENSGALG00000028415	*HES6*	1.9549	0.0009
ENSGALG00000005292	*KLHL40*	2.4441	0.0088	ENSGALG00000015028	*RLN3*	1.9129	0.0025
ENSGALG00000031693	*KCNB2*	2.3565	0.0047	ENSGALG00000043089	*VWCE*	1.9118	0.0214
ENSGALG00000007426	*MKX*	2.3378	0.0352	ENSGALG00000030905	*unknown*	1.9093	0.0497
ENSGALG00000040842	*HSPB2*	2.3116	0.0132	ENSGALG00000010293	*RBP*	1.8589	0.0138
ENSGALG00000005630	*CRYBB1*	2.2589	0.0273	ENSGALG00000005936	*AGTR2*	1.8513	0.0128
ENSGALG00000034388	*unknown*	2.2039	0.0258	ENSGALG00000015164	*unknown*	1.8412	0.0477
ENSGALG00000003025	*SLC19A3*	2.1993	0.0173	ENSGALG00000014455	*LPAR5*	1.8400	0.0310
ENSGALG00000025945	*LOC769899*	2.1849	0.0070	ENSGALG00000031615	*FAIM2*	1.8336	0.0378
ENSGALG00000010741	*MAP1LC3C*	2.1831	0.0196	ENSGALG00000032124	*unknown*	1.8080	0.0472
ENSGALG00000031866	*LOC423605*	2.1449	0.0393	ENSGALG00000011722	*STRA8*	1.7760	0.0308
ENSGALG00000032552	*unknown*	2.1382	0.0045	ENSGALG00000002840	*GRM4*	1.7428	0.0372
ENSGALG00000026754	*LOC769139*	2.1379	0.0378	ENSGALG00000028682	*CBLN2*	1.7229	0.0294
ENSGALG00000031628	*unknown*	2.1303	0.0054	ENSGALG00000037826	*unknown*	1.7142	0.0133

LogFC indicates fold change expressed in $\log_2$ value

Network representation of enriched GO terms at 5 hr tim-point of eggshell formation

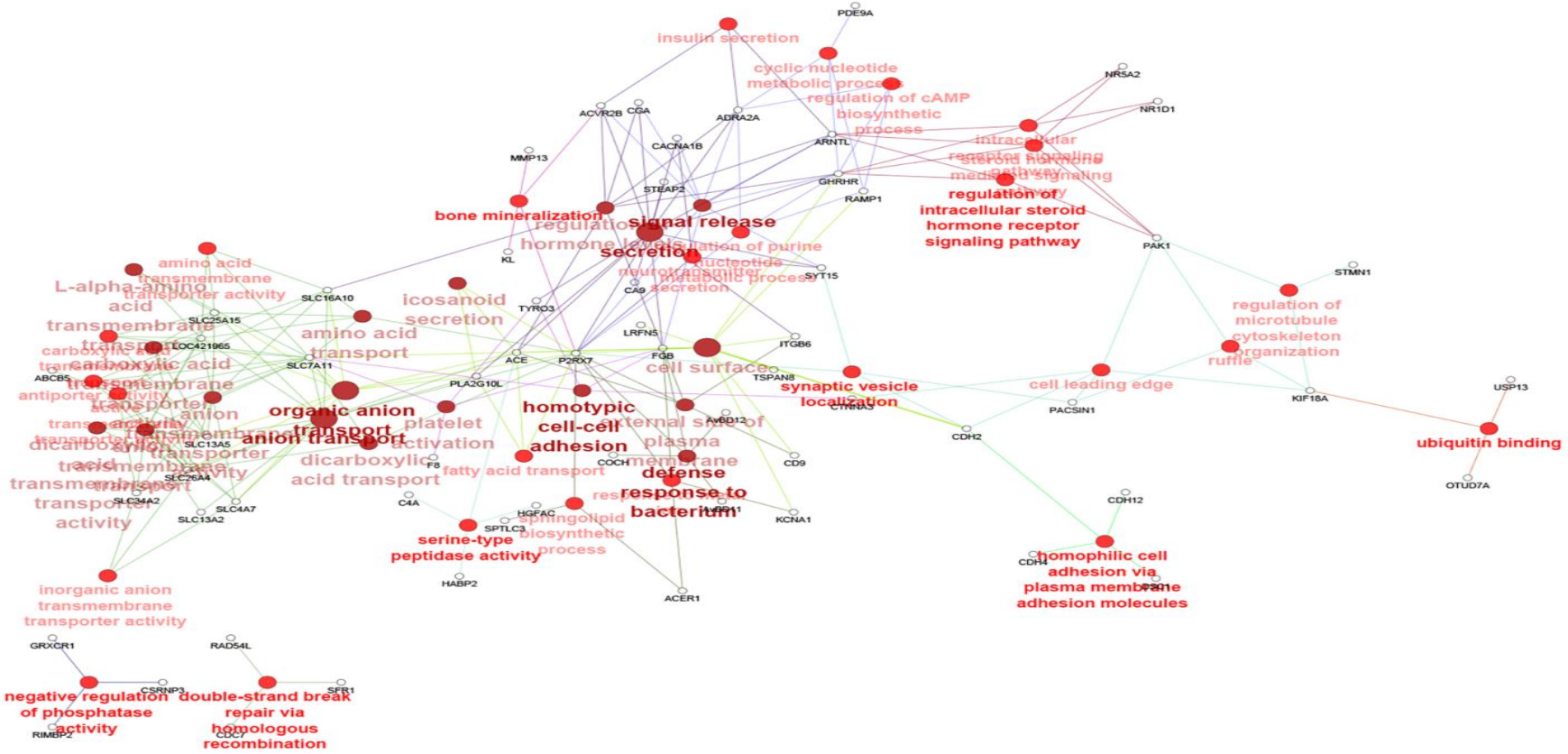

Network representation of enriched GO terms at 15 hr time-point of eggshell formation

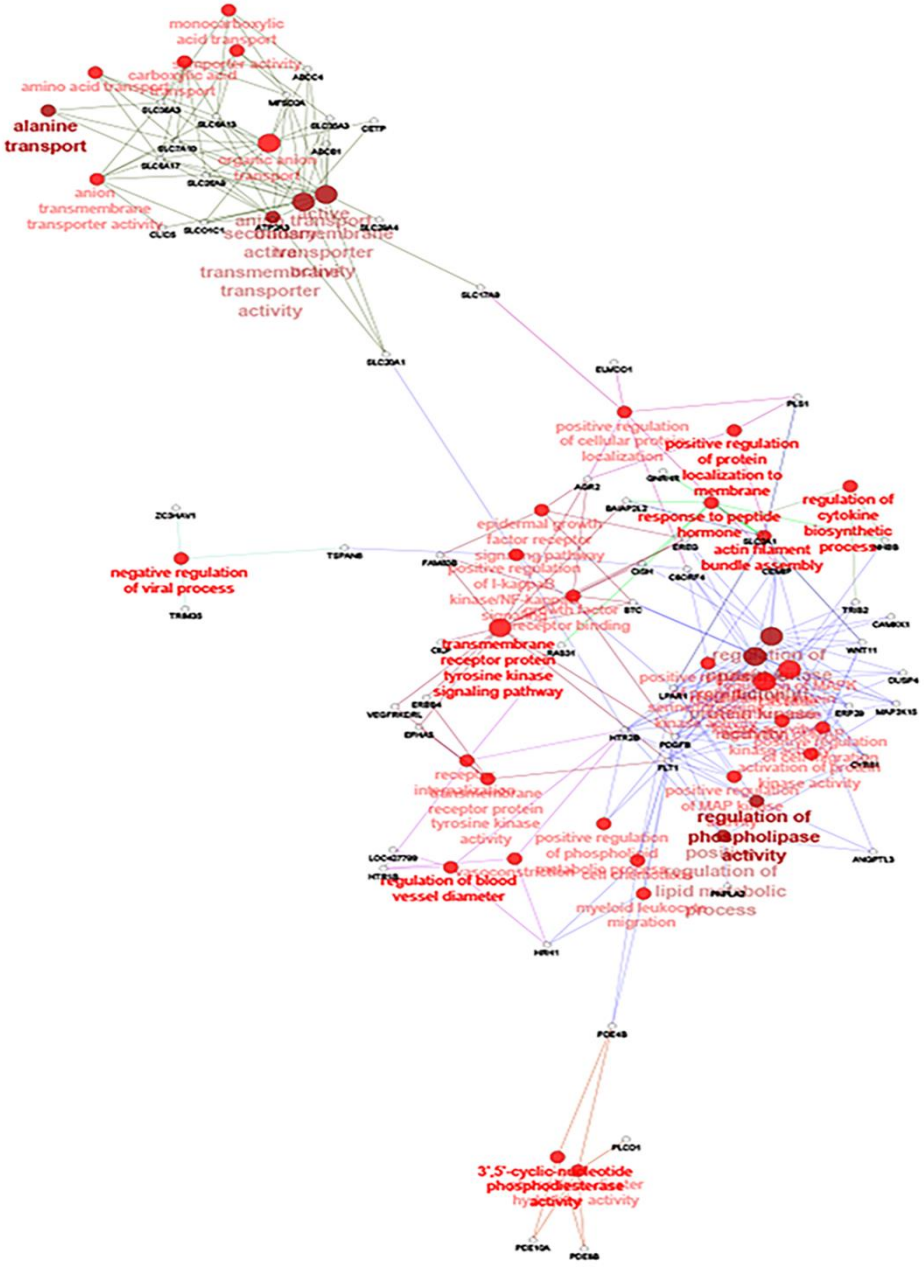

Appendix B

10X Phosphate buffer saline (PBS)

For preparing 10X stock solution of PBS (pH 7.5), dissolve 80 g of NaCl, 2 g of KCl, 14.4 g of Na_2HPO_4 and 2.4 g of KH_2PO_4 in 1 L distilled water, and autoclave at 121°C for 15 minutes. To prepare 1 L of working solution (1X PBS) from 10X BPS, add 100 mL of the 10X BPS to 900 mL autoclaved distilled water. Store the PBS solution at room temperature.

PBS-T solution

To prepare a working solution of PBS-T (BPS-Triton), add 0.4% Triton X-100 solution (Cat. No# **93443 SIGMA;** Sigma Aldrich, Australia) to 1X PBS. Store BPS-T at 4°C.

1X PBS/0.4% Triton X-100 (PBS/Triton)

To prepare 1 L of the solution, add 100 mL of 10X PBS to 900 mL dH_2O. Add 4 mL Triton X-100 and mix. Store the solution at 4°C.

***ALAS1* primary antibody dilution preparation**

ALAS1 (Novus Biological USA (Cat. No. NB100-56415) comes at 100 µg size and the suggested dilution for immunohistochemistry is 5 µg/mL. To prepare 5 mL of 1:200 dilution of *ALAS1*, take 5 µL of the original antibody and add into 4.995 mL of diluent (1X PBS). If not used, store at -20°C. Avoid freeze thaw cycles.

Secondary antibody (HRP conjugated) dilution preparation

To prepare 5 mL of 1:200 dilution of Goat anti-Rabbit IgG Antibody (Novus Biological USA; NB7160, concentration 1.0 mg/ml), add 25 µL of the original antibody into 4.975 mL 1X PBS. If not used, store at -20°C. Avoid freeze thaw cycles.

DAPI working solution

To prepare 100 mL of DAPI (**2-(4-Amidinophenyl)-6-indolecarbamidine dihydrochloride**) working solution, add 2 µL of DAPI stock solution (**D9542 SIGMA**) to 100 mL of 1X PBS. Store this working solution at 4 ºC, avoiding exposure to light.

ALAD primary antibody working dilution preparation

To prepare 5 mL of 1: 200 dilution of ALAD (polyclonal, NBP1-56506, concentration is 1 mg/ml), add 25 µL of the original antibody into 4.975 mL 1X PBS. If not used, store at -20°C. Avoid freeze thaw cycles.

FECH primary antibody working dilution preparation

To prepare 5 mL of 1:100 dilution of FECH (NBP2-33413), add 50 µL of the original antibody into 4.95 mL 1X BPS. If not used, store at -20°C. Avoid freeze thaw cycles.

Extraction buffer:

To prepare 1X extraction buffer, dissolve 6.06 g of 50 mM Tris and 3.72 g of 10 mM EDTA in 1L of dH_2O and adjust to pH 8.3. Store at 4°C.

Sample buffer

To prepare 200 mL of 1X sample buffer, add 50 mL of 0.5 M (pH 6.8) Tris, 80 mL of 10% SDS (sodium dodecyl sulphate), 40 mL of 20% glycerol into 10 mL of dH_2O. Store at room temperature.

Separating gel

To prepare 8 mL of 12% separating gel, add 1 µL of TEMED (Tetramethylethylenediamine; T7024-25mL Sigma), 1 µL APS, 2 mL of Tris-HCl (pH8.8), 2.4 mL of Acrylamide/Bis solution (37.5:1), 40 µL of SDS (20%) into 3.535 mL of dH_2O.

Stacking gel

To prepare 2 mL of stacking gel, add 625 µL Tris-HCl (pH6.8), 250 µL Acrylamide/Bis solution (37.5:1), 12.5 µL SDS (20%), 6.3 µL APS (Ammonium persulfate; A3678-25G Sigma) and 3.1 µL TEMED into 1.603 mL of dH_2O.

Transfer buffer

To prepare 800 mL of 1X transfer buffer, add 80 mL of 10X Running Buffer, 160 mL of ethanol, 2 mL of SDS (20%) into 558 mL of dH_2O.

TAE buffer

To prepare 1 L of 50X Tris-acetate-EDTA (TAE) buffer, add 242 g Tris base (M.W.=121.14) and dissolve in 800 mL distilled water. Carefully add 57.1 mL glacial acid and 100 mL of 0.5 M EDTA (pH 8.0). Gently mix and adjust the solution to a final volume of 1 L with distilled water. Adjust the pH of stock solution

of TAE to pH 8.5 with HCl and store at room temperature. For 1 L of working solution of TAE buffer (1X), add 20 mL of 50X TAE buffer to 980 mL distilled water. Final solute concentrations will be 40 mM Tris acetate, 20 mM acetic acid and 2 mM EDTA. Store at room temperature.

Staining solution

To prepare 100 mL of staining solution, add 40 mL of absolute ethanol and 7 mL of glacial acetic acid to 53 mL of dH_2O. To this solution add 0.1 g of Brilliant Blue G (**B5133 Sigma-Aldrich**). Mix well and store at room temperature.

De-staining solution

To prepare 100 mL of de-staining solution, add 40 mL of absolute ethanol and 7 mL of glacial acetic acid to 53 mL of dH_2O. Store at room temperature.

4% paraformaldehyde solution

For 1 L of 4% paraformaldehyde, add 800 mL of 1X PBS to a glass beaker on a stir plate in a ventilated hood. Heat the PBS while stirring to approximately 60°C and slowly add 40 g of paraformaldehyde powder. Slowly raise the pH by adding 1 N NaOH from a pipette until the paraformaldehyde solution clears. Adjust the volume of the solution to 1 L with 1X PBS. After cooling, filter the solution from a filter paper, and store at 4°C. This solution can be stored at 4°C for approximately 1 month.

Zenker Formol (Helly) fixative solution preparation

To prepare 50 mL of fresh solution of Zenker Formol, dissolve 1.25 g of potassium dichromate, 2.25g of mercuric chloride and 0.5 g of sodium sulfate in 45 mL distilled water.

Add 5 mL absolute formalin to the above just before use. The solution can be used for immediate fixation of tissue.

Appendix C

Formalin Fixed Paraffin Embedded (FFPE) Tissue processing for histology

The following steps were involved in processing FFPE tissue for traditional histology of shell gland tissue

- 70% alcohol 1 hour
- 90% alcohol 1 hour
- 90% alcohol 1 hour
- Absolute alcohol 1 hour
- Absolute alcohol 1 hour
- Absolute alcohol 2 hours
- Xylene 1 hour
- Xylene 1.5 hours
- Xylene 1.5 hours
- Paraffin wax 2 hours
- Paraffin wax (with vacuum) 1 hour

Acid alcohol

70% alcohol 99 ml

Hydrochloric acid (36% HCl) 1 ml

<u>Haematoxylin and Eosin staining protocol</u>

- Xylol I 5 minutes
- Xylol II 5 minutes
- Absolute alcohol I 3 minutes
- Absolute alcohol II 3 minutes
- 80% alcohol 2 minutes
- 50% alcohol 2 minutes
- Distilled water 1 minute
- Harris haematoxylin 15 minutes
- Rinse in tap water 5 minutes
- Acid-alcohol rinse 4 dips
- Running tap water 30 minutes
- 70% alcohol 2 minutes

- 90% alcohol 2 minutes
- Absolute alcohol II 2 minutes
- Eosin 3 minutes
- Absolute alcohol IV 3 minutes
- Absolute alcohol V 3 minutes
- Xylol III 2 minutes
- Xylol IV 3 minutes

Processing shell gland tissue for Zenker Formol fixative

Put the tissue in Zenker Formol fixative for 8 hours.

Wash the tissue cassette in running tap water for 20 hours

Dehydrate the tissue cassette for 45 min into 30% ethanol

Transfer the tissue cassette for 45 min into 50% ethanol

Transfer the tissue cassette for 45 min in 70% ethanol

Store the tissue cassette in 80% ethanol at 4°C until further processed for embedding. Further tissue processing for histology sections was the same as described for FFPE.